Automated Microscopic Analysis of Optical Fibre Transmission Surfaces

Author: Kieran Ryan, B.Eng

Date: 10th January 2005

Qualification: Submitted for Qualification of Masters by Research

Supervisor: Dr. Paul Young

School: Mechanical and Manufacturing Engineering

Volume: 1

Declaration

I hereby certify that this material, which I now submit for assessment on the programme of study leading to the award of masters by research is entirely my own work and has not been taken from the work of others save and to the extent that such work has been cited and acknowledged within the text of my work.

Signed: _____

ID No.: 97533483 .

Date: 10/01/05 .

Acknowledgements

I would like to acknowledge the following persons for helping me throughout the project:

- Dr. Paul Young for his supervision and guidance throughout the project.
- Mr Geoff Walsh for both technical and motivational assistance for the entire duration of the project.
- Mr David Mathews for his encouragement and assistance during the project.
- Ms Emma Leonard for agonisingly proof reading the entire document.

Abstract

Outlined in this thesis is the design of a prototype device for the inspection of optical fibre endfaces. The device designed uses lenses with different magnification's to acquire scaled microscopic images of the endfaces for analysis purposes. The design specifications for the device are established based on the optical transmission requirements of the fibres and the impact of defects on transmission losses in various regions of the optical fibre endface. The specifications of this device are as follows:

- Optical System
    - 3 lens automated changeover
- Imaging System:
    - Minimum Resolvable Object Size of 2.43μm
    - Maximum Field of View of 0.9mm
    - Resolution of 740 X 560 pixels
- Autofocus System with Focus Resolution of 1.25μm
- Coaxial Illumination System
- 12Mbits/sec USB video acquisition hardware

The device designed realises all the mechanical, optical and electronic functionality required to automate the inspection process of optical fibres. The hardware and software challenges involved in designing and building the prototype are discussed in detail in the thesis. A complete evaluation of the design is also carried out, difficulties and problems that occurred with the project are analysed, and recommendations for the improvement of the design are made.

Table of Contents

Chapter 1: Introduction

In the assembly of high value optical fibre network components, the quality of the fibre surface is crucial to the ability of the system to transfer large volumes of information at high speeds. With optical fibres the transmission medium is light. While light displays many advantages over other transmission mediums, such as high bandwidth and speed, the main disadvantage of this transmission medium is the high level of precision required when making connections. Unlike electrical connections, where simple conductor-conductor contact suffices, with optical fibres the surfaces have to be mated with high precision to ensure that no attenuation of the signal will occur. There are two primary factors, which affect how the fibres mate, the geometry and the condition of the fibre endface. Whilst the geometry is controlled and inspected at manufacture, the endface must be inspected before assembly as dust, dirt and other contaminants may have tainted the surface of the fibre during transport and storage. Any contaminate on the fibre endface will prevent the fibre from mating correctly and this will leave an airgap between the fibre surfaces, which will have a different refractive index to the glass. This will cause a change in the angle of reflection of the light signal and thus loss of the signal through back reflections or absorption into the cladding [1]. Therefore the fibre surface must be in perfect condition before being connected into the communications system or with another fibre.

At present each fibre is inspected by a skilled operator using a single magnification factor microscope, leading to a subjective analysis of the quality of the transmission surface. In addition to the time required to perform the inspection, cleaning and re-inspection if necessary, this process lacks the objectivity and repeatability of inspection using automated techniques. Additionally, as an alternative to using a

human dependent process, an automated process reduces costs and increases the reliability of the process. It also allows statistical analysis of a process, as automated processes by their nature are repeatable.

For the automation of such a process, machine vision is the only viable alternative. Other alternatives such as laser scanning, while reliable, are extremely costly and very slow relative to machine vision. Machine vision though costly allows for high-speed inspection, also there are a wide range of appropriate products both hardware and software designed specifically for machine vision inspection. This makes the design of any potential device easier and less expensive as it only requires the integration of specific parts. However, while machine vision can make precise measurements at high speeds, it lacks some of the key elements of human vision, such as pattern recognition that allow the identification of different classes of defect. This makes developing algorithms for interpretation and manipulation of images extremely complex in varying conditions, as some form of artificial intelligence is required. However, in one set environment where conditions such as illumination and shading can be controlled, complex information such as topology and depth can be extracted and this makes machine vision quite useful. Automated microscopic inspection will also reveal the characteristics of high loss. The characteristics will indicate corrective actions that might be required in connector installation and/or handling techniques, so the overall quality of the fibres can be increased.

1.1 Project Description

The overall aim of the project is to investigate the requirements of a machine vision system and build a prototype device that has the mechanical capability for the automated inspection of optical fibre endfaces. The approach taken was to limit the project's scope entirely to a vision based system. Little research was put into the potential alternatives such as laser scanning due to the costs and speed limitations of the potential systems. Only the hardware and software interfacing components of the vision system are designed. However, extensive research is carried out in the areas of machine vision imaging systems and image analysis, as it is necessary to have an understanding of these fields to properly design the hardware components of the system.

The system designed involves the use of optical microscopy to achieve a range of magnifications thereby allowing more complete examination of the fibre. The magnification required depends on the imaging sensor pixel size and area respectively. The relationship between the sensors, pixel size and the optical magnification is central to the design of the system, as it will determine the smallest detectable defect by the system. In order to make the system robust, lighting, focus, magnification, image acquisition are being integrated for automatic operation under PC control.

1.2 Chapter Contents

A brief breakdown of the chapters is as follows:

Chapter 2: Literature Review – A description of the field of optical fibre communications introduces the chapter. Imaging vision systems are then discussed which encapsulates the areas of optics, imaging sensors, autofocus systems, object illumination and image acquisition hardware. Finally, a theoretical introduction into defect detection using 2-D and 3-D image analysis is discussed in detail.

Chapter 3: Concept Design – Firstly requirements of the system are set out and the necessary components to fulfil these requirements detailed. Various concept designs are proposed, based on the system requirements. From an evaluation of the designs, the most adequate one is chosen based on its advantages and merits over the other concepts.

Chapter 4: Detail Design – Describes how the hardware and software was designed in detail. It discusses the relevant theory and implementation of the hardware designed namely the optics, electronics, image acquisition and software coding.

Chapter 5: Evaluation of Working Prototype – Describes the difficulties encountered in the design and implementation of the prototype. An alternative design based on what was learnt from the problems encountered with the original design, is set out in detail. Suggestions are made as to how it would overcome the problems of the original design and how it would be an improvement.

Chapter 6: Conclusions – Describes what was achieved and discusses the direction of possible future projects

Chapter 2: Literature Review

2.1 Introduction to Optical Fibres

Interest in the use of light as a carrier of information grew in the 1960's with the advent of the laser as a source of coherent light. Initially the transmission distances were very short, but as manufacturing techniques for very pure glass arrived in 1970, it became feasible to use optical fibres as a practical transmission medium [2]. At the same time, developments in semi-conductor light sources and detectors made optical fibre a commercially viable method of data communication. In recent times, due to the necessity for increased bandwidth and speed, optical fibre has become the standard for telecommunications transmission.

Optical fibres are fibres of glass, usually about 120 μm in diameter, which are used to carry signals in the form of pulses of light over large distances. The signals can be in the form of coded voice communications or digital data. Optical fibre communication has many advantages over standard copper transmission cables that it replaced, such as:

- Capacity - Optical fibres carry signals with much less energy loss than copper cable and with a much higher bandwidth. This means that fibres can carry more channels of information over longer distances and with fewer repeaters required.
- Size - Optical fibre cables are much lighter and thinner than copper cables with the same bandwidth. This means that much less space is required in underground cabling ducts.

- Security - Optical fibres are much more difficult to tap information from undetected. They are immune to electromagnetic interference from radio signals, car ignition systems, lightning etc.
- Maintenance Costs – Optical fibres use less power than traditional copper systems.

However, optical fibres have certain negative aspects:

- Price – With any new high-tech product the cost is going to be particular high. Optical fibres are no exception with their high manufacturing costs compared to copper cable. That said, however while fibres may be more expensive per metre than copper one fibre can carry many more signals than a single copper cable and the large transmission distances mean that fewer expensive repeaters are required.
- Connection - The main disadvantage with optical fibres is the difficulty in connecting them. Due to the transmission medium optical fibres use, i.e. light, it is difficult to get an adequate signal unless the fibres are precisely joined. There can therefore be no contamination or air gap between the fibres: otherwise an adequate signal will not be achieved.

It can be seen that the advantages of optical fibres far outweigh their disadvantages when compared to other transmission media. However, the difficulty in connecting them has limited their applications to industry, as it makes their use extremely specialised. They are most commonly used in the telecommunications industry. One of their most frequent uses is connecting high bandwidth routing lines for both voice and digital data. It is only the low bandwidth outer peripheral of the communications network that uses copper cables. Therefore the majority of the communications network uses optical fibres, which obviously means a significant number of optical

fibre connections. While the methods of connecting optical fibres have advanced in recent times, problems still remain in this area of the technology.

2.1.1 Connecting Optical Fibres

With any system for transmitting energy, there is always going to be some loss in the signal. In the case of optical fibres this loss is called attenuation, which is defined as the loss of output power with respect to optical input power [2]. Attenuation in an optical fibre is caused by several intrinsic and extrinsic factors. Intrinsic factors include:

- Scattering
- Absorption

They occur due to the nature of the transmission media and limitations of glass manufacturing techniques. Extrinsic factors include:

- Bending
- Fibre connections

This project concentrates on the attenuation caused by fibre endface connections. All modern connector designs involve physical contact between the two fibre ends. Most connector systems restrain two fibres to be coupled within precision ferrules, which in turn are held in place by a high quality mechanical housing or "plug". Figure 2-1 shows a typical LC connector plug. It is similar to a RJ45 Ethernet connector. A typical application for this connector would be in data and communication systems. The fibre ends are flush with the ferrule ends and are polished to reduce attenuation of the signal. The two plugs are

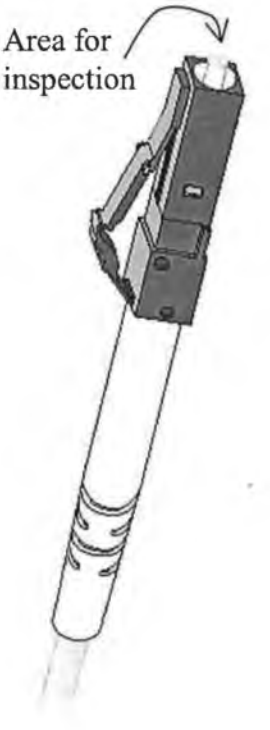

Figure 2-1 – LC fibre connector

mechanically joined using an adapter in which a precision alignment sleeve aligns the two ferrules and thus the two fibre ends.

Typically, attenuation for a mated pair of high quality connectors is 0.35 dB or less [3]; however in general insertion loss of up to 1dB may be tolerated [4]. This loss is greatly increased by defects on the fibre surface, ranging in size from 2 – 30μm, which prevent the fibres from mating correctly. Contaminants of this size are a problem in such optical connections because they interfere with the passage of light from one fibre to another. In addition, because the fibre cores make physical contact, if a connector is mated while contaminated ferrule end-face damage may occur, or the contaminant may get firmly bonded to the ferrule end-face. This can lead to permanent damage of the fibre or additional attenuation of the signal. For example a 1μm dust particle landing on the core can cause a 1db loss of signal [1]. Dust particles can be 20μm or larger and dust particles of 1μm can be suspended indefinitely in the air. To prevent these problems connector cleaning must be undertaken frequently. Also, prior to assembly in optical networks, fibres must be inspected to determine their endface quality. In order to understand how the fibre endfaces are inspected, there structure must firstly be explained.

2.1.2 Optical Fibre Endface Structure and Operation

It is important to understand the structure of fibres to be able to inspect them correctly. It would be understandable for one to think that it is only necessary to inspect the central core of the fibre. But when an understanding of how light is passed down fibre is explained it becomes clear why each area needs to be inspected.

There are three main regions to an optical fibre connector cross-section [2]:

- The Fibre - Dielectric material (glass) that guides light, it is composed of various concentric rings of glass, whose refractive indices decrease from the centre axis [2].
- The Ferrule - A mechanical fixture, usually a ceramic tube, used to confine and align the stripped end of a fibre
- The Connector body – this holds the ferrule in place

Figure 2-2 illustrates the three main areas. The total diameter of the connector is about 1mm. The fibre itself consists of two regions, the core and the cladding. The cladding surrounds the core and varies in diameter from 125μm to 140μm. The core can vary in size from 8μm to 62 μm depending on the type of fibre [2].

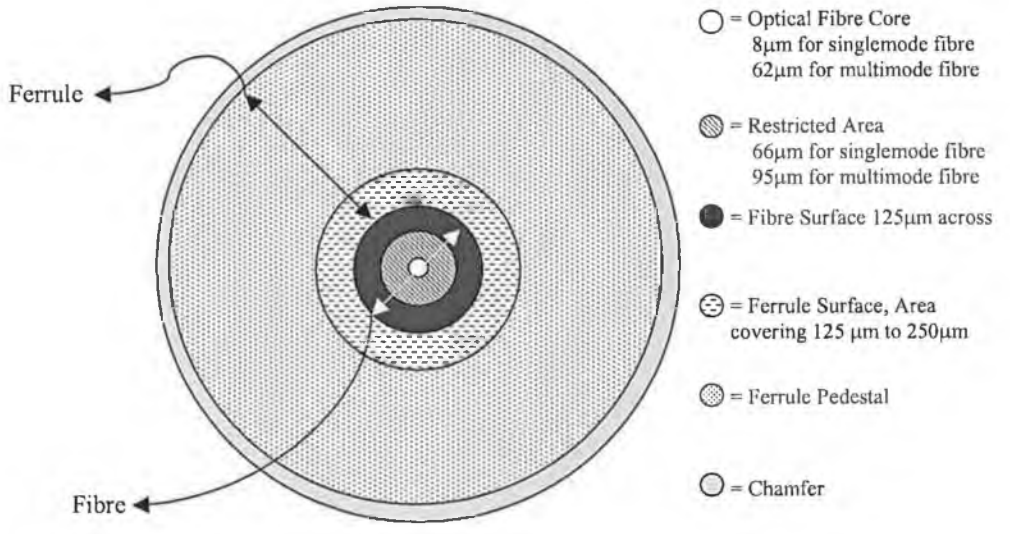

Figure 2-2 Fibre cross-section

The key design feature of all optical fibres is that the refractive index of the core is higher than the refractive index of the cladding. This allows total internal reflection to occur within the core where the signal is transmitted, which is the principle by which optical fibres operate. This is illustrated in Figure 2-3

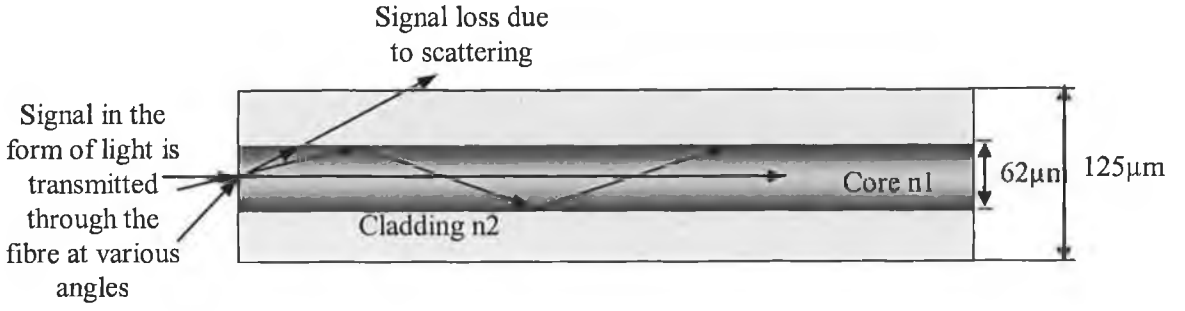

Figure 2-3-Light transmission through optical fibre

Three different modes of light are shown passing through the fibre. One mode passes through the centre of the fibre and travels straight down the fibre. Another mode is entered through the fibre at an angle greater than the critical angle of the fibre and is transmitted through the fibre. Light entering the fibre at an angle less than the critical angle is refracted into the cladding. The cladding is necessary to allow total internal reflection to occur. Since the fibre is made up of concentric rings of glass of different refractive indexes, the same process occurs at each interface. This has the effect of allowing some of the escaped light to re-enter the fibre and be transmitted. The light that is transmitted along the outer edge of the fibre has obviously to travel longer distances, so the transmitted signal will be out of phase. In reality the fibre shown in Figure 2-3 is made up of many layers of different refractive indexes. Light travelling through the centre of the core will travel at the slowest speed and the shortest distance while light being refracted off the outer edge will travel at the faster speed but the longest distance. Using concentric rings of glass of different reflective index helps overcome this problem as the light can travel faster in the outer layers than in the inner layers, and thus allows the light to reach the receiving end of the fibre at approximately the same time, reducing dispersion [2]. Most modern fibre cores are designed to have a parabolic index of refraction profile to prevent this disparity between the signals. [2]

2.2 Generic Vision System

The goal of this project is to design a vision based inspection system for the inspection of optical fibre surfaces. The system employs a vision-based approach to automate the inspection process. In order to determine the best approach for designing a vision system, research was carried out on the core components of a vision based inspection system. Below is the outline of a generic vision based system (Figure 2-4) and the components it encapsulates [5].

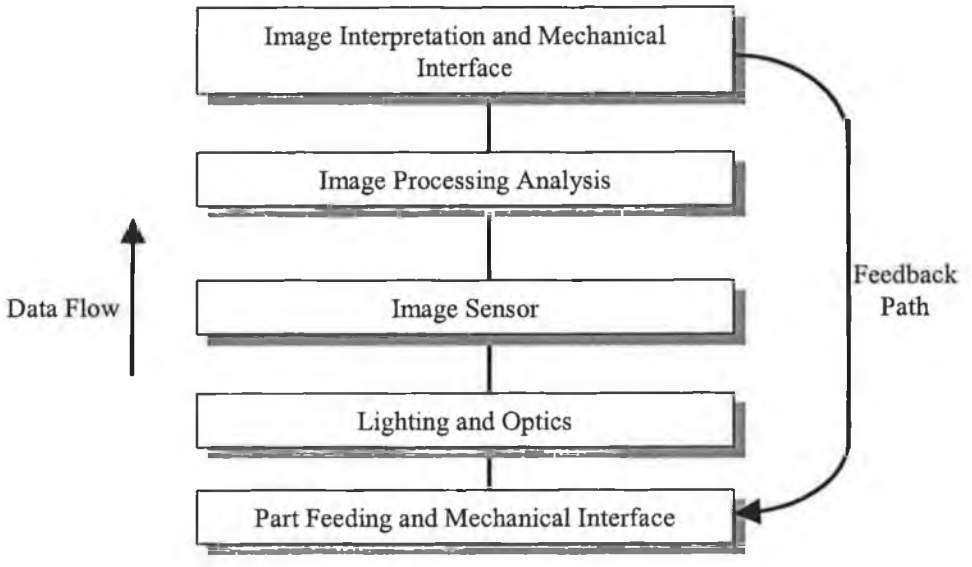

Figure 2-4 – Machine Vision System Components [5]

The purpose of its primary components is as follows:

- **Optics** – To magnify and focus the object onto the image sensor.
- **Lighting** – To adequately illuminate the object and if necessary provide additional information from illumination position and angle for image processing purposes.
- **Image Sensor** – To acquire an image of the object for digital processing and control feedback.
- **Image Processing/Analysis** - Alter the input image to produce an image that will make the analysis process simpler and more robust [5].

- **Image Interpretation and Mechanical Interface** – Determines the required information from the input image and prompts a mechanical response based on this information.

While the application itself determines the relevant importance of each of these tasks, successful implementation will have to take all the issues into consideration during the design. In order to achieve these aims, the keys areas of research are:

- Imaging Systems i.e. Optics and Image Sensors
- Illumination in Machine Vision
- Focus Control
- Image Acquisition
- Image Analysis

The following sections of this chapter discuss each of these areas individually, keeping their scope within the confines of the system requirements.

2.2.1 Imaging System

The primary purpose of any imaging system is to obtain enough image quality to allow for the extraction of necessary information [6]. In a machine vision system the quality of the image will be determined by the imaging system. The most basic imaging system consists of a lens and imaging sensor (Figure 2-5)

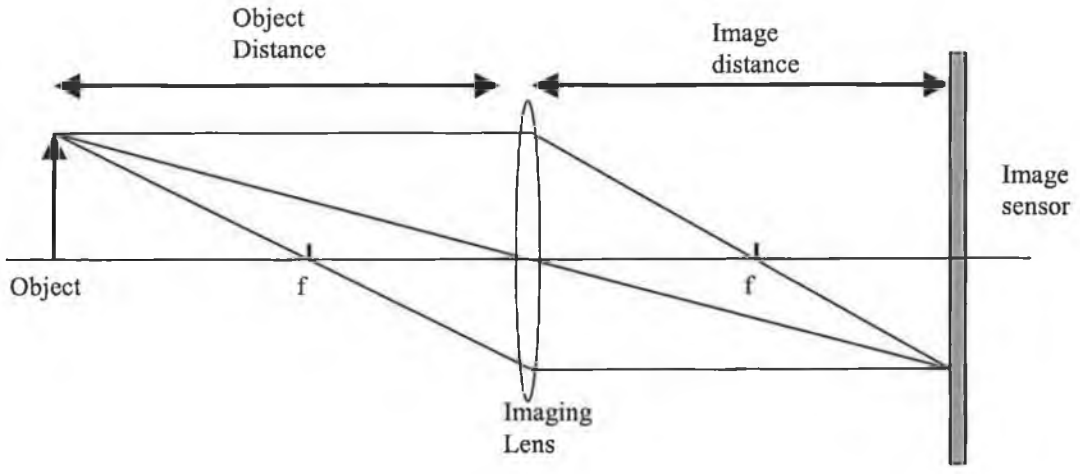

Figure 2-5 – Basic Imaging System

The basis of this system is to form an image of the object on the image sensor. The image system translates object points located on the object plane into image points on the image plane. The only variable in such a system, provided the system is in focus, is the scaling or magnification, which is determined by the lens focal length. The imaging system represented here is however, quite a simplistic representation of an imaging system. In reality, an imaging system is much more than an apparatus to magnify and focus an image onto an image sensor. There are many more important parameters that must be accounted for in the design. The five fundamental parameters of an imaging system are: (Figure 2-6) [7].

- **Field of View** - The viewable area of the object under inspection, or the area of the object that fills the imaging sensor.

- **Working Distance** - The distance from the front of the lens to the object under inspection. This parameter only affects the system when the object needs to be distant from the lens to allow room for manipulation.
- **Depth of Field** - The maximum object depth that can be maintained entirely in focus or alternatively the amount of object movement (in or out of best focus) allowable while maintaining a desired amount of focus.
- **Sensor Size** - The size of the sensor active area. This parameter is important in determining the correct lens magnification to obtain the required field of view.
- **Resolution/Pixel Size** - The pixel size determines the sensor's overall resolution. This parameter determines the minimum feature that can be resolved.

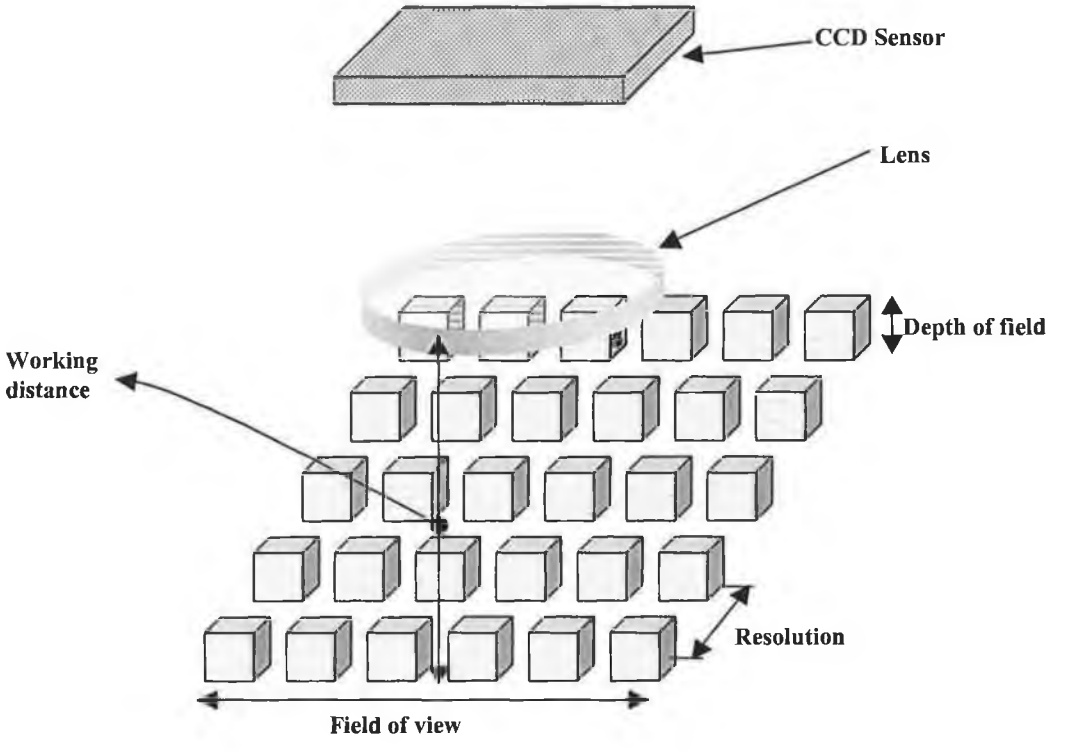

Figure 2-6– Fundamental Parameters of Imaging System

All these parameters are interlinked, so designing an imaging system is not a matter of satisfying each one but more a case of making trade offs between each to achieve the nearest satisfactory system. Consequently, when designing a system, each parameter must be carefully considered at each stage of the design, so as not to adversely affect any of the others. The fundamental parameters are determined by the two primary components of an imaging system:

- Optical System
- Imaging Sensor

The subsequent sections of this chapter discuss each one of these individually and the role of each in determining the overall capability of the system.

2.2.1.1 Optical System

An optical system is defined as a group of lenses, or lenses and prisms so constructed as to refract or reflect light to perform some definite optical function [8]. While this definition relates to all wavelengths of light an imaging system is only specific to the visible spectrum. An imaging optical system can therefore be more narrowly defined as a series of optical components combined in parallel or series to produce a required field of view and magnification.

In simple terms, the function of the optics is to focus the light received from an object onto an imaging sensor as demonstrated in Figure 2-7. The distance from the object to the lens and the lens focal length, determine the position where the lens focuses the light.

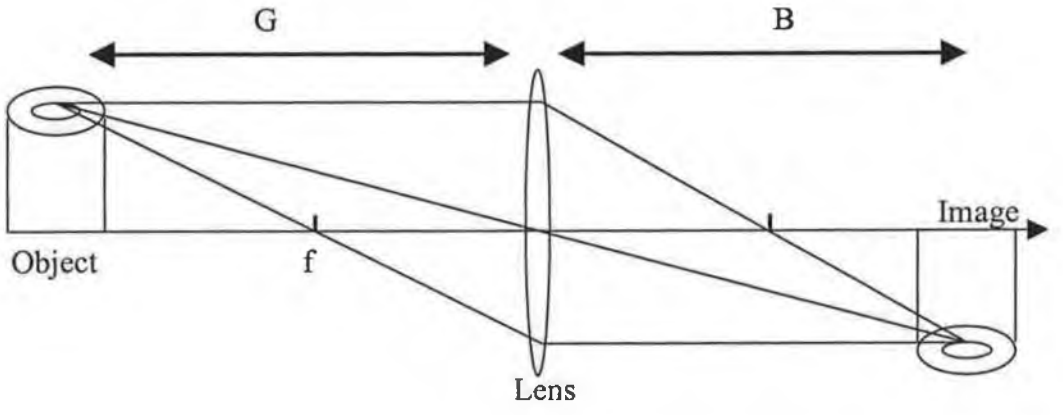

Figure 2-7 – Simple Optical System

The lens maker's formula defines the relationship between focal length object position and image position (Equation 2-1).

$$\frac{1}{f}=\frac{1}{G}+\frac{1}{B}\text{ [9]} \qquad \textbf{Equation 2-1}$$

f: focal length

B: Image Distance

G: Object Distance

The magnification of the lens is defined as the image distance (B) over the object distance (G).

$$M=\frac{B}{G} \qquad \textbf{Equation 2-2}$$

M: Optical Magnification

The Field of View is determined by the optical magnification and the size of the imaging sensor used [7].

$$\text{Field of View}=\frac{\text{SS}}{\text{M}} \qquad \textbf{Equation 2-3}$$

SS: Sensor size

It is therefore quite simple to determine the fundamental parameters of an imaging system once all the parameters are known. However, this simple approximation only works with extremely thin lenses that are free from aberrations and perfectly manufactured. In reality, optical systems are far more complex than the simple view presented. As well as the magnification and object distance the optical system determines the following parameters in an imaging system:

- Resolution
- Depth of field

Resolution

To understand the term resolution correctly the difference between system, optical, and camera resolution must be understood. Optical and camera resolution determine the overall system resolution. For now only the effect of the optical system on resolution is discussed. A later section discusses the effect of the camera on the system resolution. Resolution is determined by the systems ability to collect light, which is in turn determined by the optics. When light reflects off an object it is diffracted at various angles depending on its wavelength and the object medium (Figure 2-8)

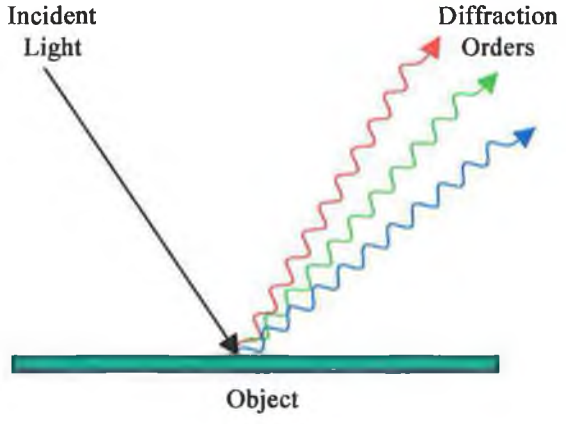

Figure 2-8 – Diffraction from an Object

So the image formed in an imaging system is formed from the diffraction orders reflected from the object. The more diffraction orders that can be collected by the lens, the greater the information present to form the resultant image [10]. In other words, the ability of the lens to gather light will directly influence the overall resolution of an image. The parameter that defines the light gathering ability of a lens is its numerical aperture. Numerical aperture is defined by the expression:

$$NA = i \sin q \qquad \textbf{Equation 2-4}$$

i = Refractive index

q = Maximum angle at which the lens can collect light

So, for example, if a lens has a numerical aperture of 0.6 it can collect all the light refracted at an angle less that 32^0, for i = 1 (Figure 2-9). However if the lens has a numerical aperture of 0.8 it will collect all the orders of light reflected at an angle less that 48^0 (for i = 1) and thus gather more information to form the image (Figure 2-9). Therefore the higher the numerical aperture of a lens the greater the resolution of the image formed.

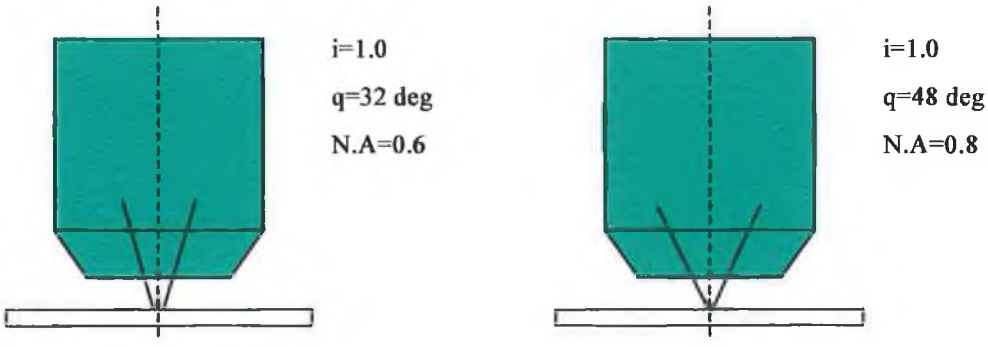

Figure 2-9 – Diffraction in microscope objectives at different NA. A wider cone of light is gathered by lenses with higher numerical apertures.

Depth of field

In an imaging system the depth of field refers to the distance in or out of best focus over which the system delivers an acceptably sharp image [11]. This definition, while accurate, leaves the description open to interpretation, as the meaning of acceptable sharp image is unclear and subjective. Therefore, to properly state the depth of field of an image, reference should be made to the displacement in and out of best focus and also to the minimum acceptable resolution of the image [12]. Figure 2-10 shows the light-forming path of an image and how it relates to the depth of field.

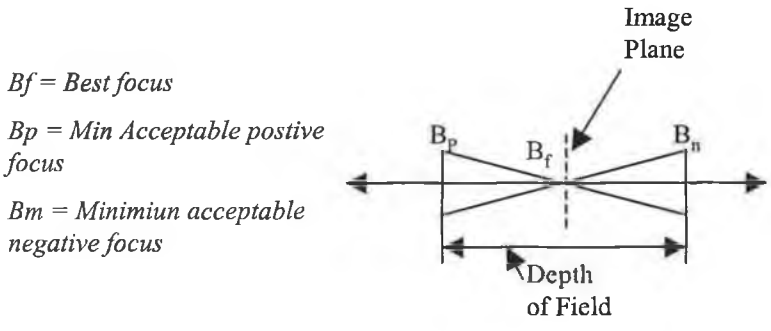

Figure 2-10– Depth of field

In an optical system the parameters that determine the depth of field are [13]:

- The Aperture - Depth of field increases as the lens aperture is closed down (i.e., the F-number increases).
- Focal Length - Depth of field increases as the focal length reduces.
- Object Distance - Depth of field increases with the subject distance.

In a lens systems the Numerical Aperture (NA) determines the overall depth of field, as it is a function of the lens aperture size and focal length. An expression for calculating the depth of field is shown below:

$$\text{Depth of Field} = \frac{\lambda}{NA^2} \qquad \textbf{Equation 2-5}$$

λ = *Wavelength*
NA = Numerical aperture

As demonstrated in this expression, the smaller the numerical aperture of a lens, the larger the depth of field. Therefore, when specifying an optical system for machine vision purposes, it is important to get a lens with an adequate numerical aperture so as to get the required depth of field for the object under examination.

Optical Aberrations

In addition to determining the fundamental parameters of the imaging system, the optics induce errors, called aberrations, in the final image. The term aberration encompasses many different optical errors that occur in an optical system. Aberrations that occur in imaging systems are:

- Chromatic
- Spherical
- Geometric Distortion
- Perspective Errors
- Astigmation

Optical aberrations occur in lenses due to manufacturing limitations and the wave nature of the light [13]. Most lenses can be manufactured to correct for these factors by using special coatings and/or a combination of lenses. However, no lens system is perfect and aberrations must be taken into account, especially in vision systems that are required for measurement purposes.

Following on from this introduction to optics theory, the next section discusses the various optical systems available for implementation of an imaging system and the advantages and disadvantages of each.

Optical System Concepts

In many cases optics for machine vision systems can be built using off-the-shelf components. The use of off-the-shelf products is usually the easiest option, as they are mass-produced, thus less expensive and they are usually aberration corrected. However, in some cases using off-the-shelf components may not be sufficient. For demanding machine vision applications, custom-designed optics may be required. Some particular instances in which a custom solution should be considered are as follows: [14]

- The field of view required to attain the necessary resolution cannot be achieved using standard lenses
- Variable magnification is required
- The required depth of field cannot be achieved with a standard lens

For the purpose of this project two optical systems were examined, a custom zoom lens system and microscope objectives.

Zoom lens

Zoom lens systems are a group of lenses arranged in such a way that when one of the optical components is moved relative to the other components the optical magnification is varied. The most basic zoom lens consists of a converging and a diverging lens (Figure 2-11). The first lens converges the light to form an intermediate image. Before reaching this image, however, the light is intercepted by the second lens so that an image is still formed but at much greater distance from the primary lens. The effect is to produce a system that has a long effective focal length (giving high magnification) but is physically compact. Furthermore, by adjusting the distance

between the two lenses, the effective focal length of the system can be continuously varied and thus the magnification can be changed [16].

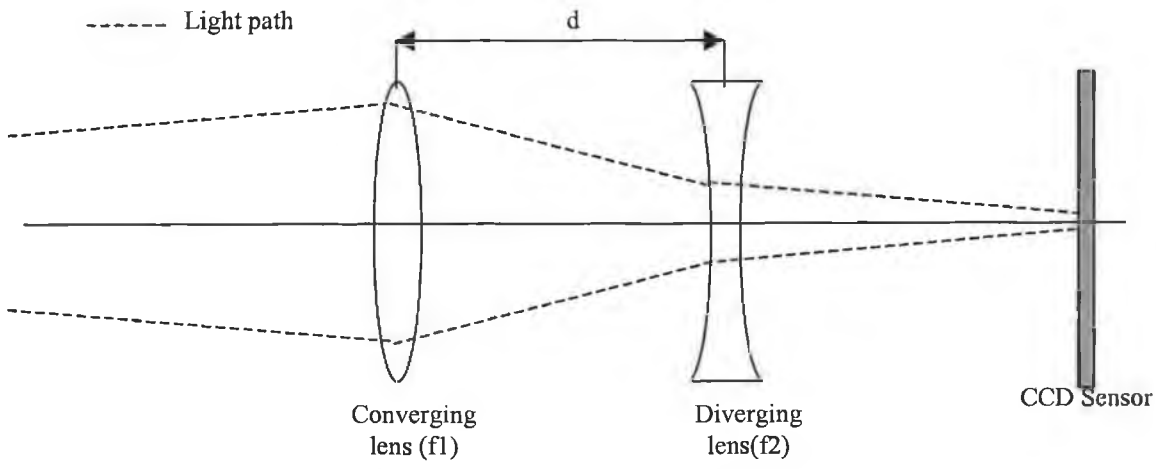

Figure 2-11-Zoom Lens Architecture

Equation 2-6 - Total Focal length (f) $= \frac{f_1 * f_2}{f_1 + f_2 - d}$

f_1 =focal length of converging lens
f_2 =focal length of diverging lens
d =distance between lenses

Advantages

- Variable magnifications can be achieved so there's no need to specify one exact magnification.
- Only one optical axis, no need to change the lens to achieve different magnification.

Disadvantages

- Zoom lens systems suffer from loss of image definition and less efficient light transmission due to the extra optical components required in their design [25].
- Can't buy specific product off-the-shelf, so lens arrangement must be designed. The design of such an optical system is quite complex. Any system designed would have to correct for both spherical and chromatic aberrations.

This would require a complicated multi–element system that would be costly and difficult to design.

Microscope Objectives

For machine vision applications that view small objects, microscope objectives provide a cheap, commercially available solution. There are a wide variety of objectives of different grades at correspondingly different price levels. Their cost and performance depends on their optical complexity, which is determined by how they correct for the dominant aberrations: chromatic, spherical and field curvature. There are three general classifications of objective [14]:

- Achromats
- Semi-Plan
- Plan

Achromats are the simplest objective lens as they only contain one lens element. They correct for colour in the red and blue spectrum, and for spherical aberration in the green. Semi-Plan are more complex objectives, which are colour corrected in the red, yellow, and blue spectrum, and corrected for spherical aberrations at 2-3 different wavelengths depending on their grade [14]. Plan objectives are identical to semi-plan lenses in the aberrations they correct, but unlike semi-plan lenses, plan lenses correct for field focus, which means approximately 95% of the field of view lies on the same plane. These lenses are used in applications that require good image quality across a wide field of view.

Microscope objectives are designed in such a way so as to give a specified magnification when setup at the standard image distance. The image distance is usually referred to as the tube length and is measured from the sensor to objective

mounting flange (Figure 2-12). This value is usually 160mm for most non-infinity corrected objectives [10]. When designing a system with objectives it is best to use the standard objective tube length as the lenses are aberration corrected at this distance and severe image distortion and field curvature can occur when using larger than the designated image distance [10].

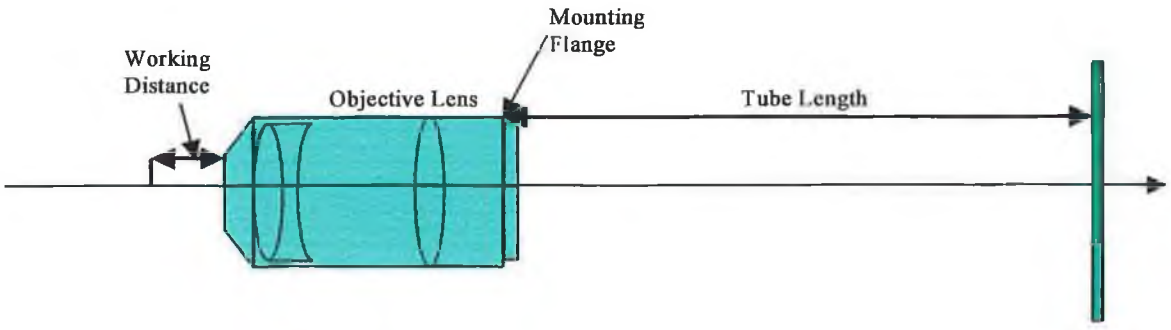

Figure 2-12– Microscope objective optical set-up

An alternative to standard focus objectives is "infinity corrected" lenses. These are optimised to provide collimated light on their image side. A separate decollimating or tube lens then forms the image (Figure 2-13). This design gives flexibility for inserting lighting and beamsplitters in the collimated space behind the objective and also for reducing the size of any device designed. The proper focal length tube lens is required to form an image at the objective nominal magnification.

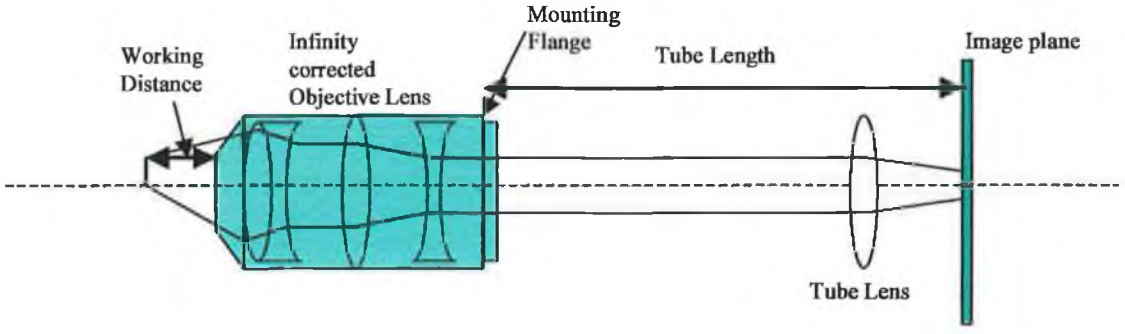

Figure 2-13 – Infinity Corrected Optical system

As a solution for imaging system optics, microscope objectives offer a relatively cheap, high quality option. However, when designing them into a system, due account must be taken for factors such as tube length and whether the lens is spherically corrected for all the primary colours or just one. The next section discusses the other component of an imaging system, the image sensor.

2.2.1.2 Imaging Sensors

The imaging sensor plays a significant role in the performance of an imaging system. The choice of sensor will determine certain parameters of an imaging system such as:

- Frame rate
- Resolution
- Digital magnification
- Pixel depth
- Aspect ratio

When choosing an imaging sensor, there are two different types to choose from:

- Charged coupled devices (CCD's)
- Complementary metal oxide sensors (CMOS)

Electronically, both sensor types have significant differences in how they are designed and built, but in operation they are quite similar. Both sensors are pixelated metal oxide semiconductors [17]. They both operate in a similar manner by accumulating charge in each pixel proportional to local illumination intensity. How they differ is the method used to transfer this charge to an output device. The CCD transfers each pocket charge sequentially to an external circuit, which converts charge to voltage. In a CMOS sensor the charge to voltage conversion takes place in each pixel, as the circuitry is inbuilt into the sensor chip [17]. With CMOS chips, due to the fabrication process used, most of the circuitry is inbuilt on the chip. This makes them faster and less expensive than CCD chips [18].

Due to the different manufacturing processes used, there are several noticeable differences between CCD and CMOS sensors [18].

- CCD sensors create high-quality, low-noise images, whereas CMOS sensors are more susceptible to noise.
- Each pixel on a CMOS sensor has several transistors located next to it, so the light sensitivity of a CMOS chip is lower. Many of the photons hitting the chip hit the transistors instead of the photodiode.
- CMOS sensors consume little power relative to CCDs due to the circuit fabrication process used to manufacture them. CCDs, on the other hand, use a process that consumes lots of power.
- CMOS chips can be fabricated on just about any standard silicon production line, so they tend to be extremely inexpensive compared to CCD sensors.

Since the use of CCD sensors is more widespread, the technical operation of image sensors will be discussed in relation to CCD sensors rather then to the less commonly used CMOS sensors.

CCD Imaging Sensor Operation

The CCD sensor works on the principle of transforming light of wavelength 400nm to 1000nm into a charge, which is then transformed into a voltage. This voltage is in turn transformed into a digital pixel value, which defines the image [21]. The architecture of a simple CCD sesnor is shown in Figure 2-14. The CCD device electronics can be divided into two areas:

- Image sensor/Acquisition unit
- Output unit

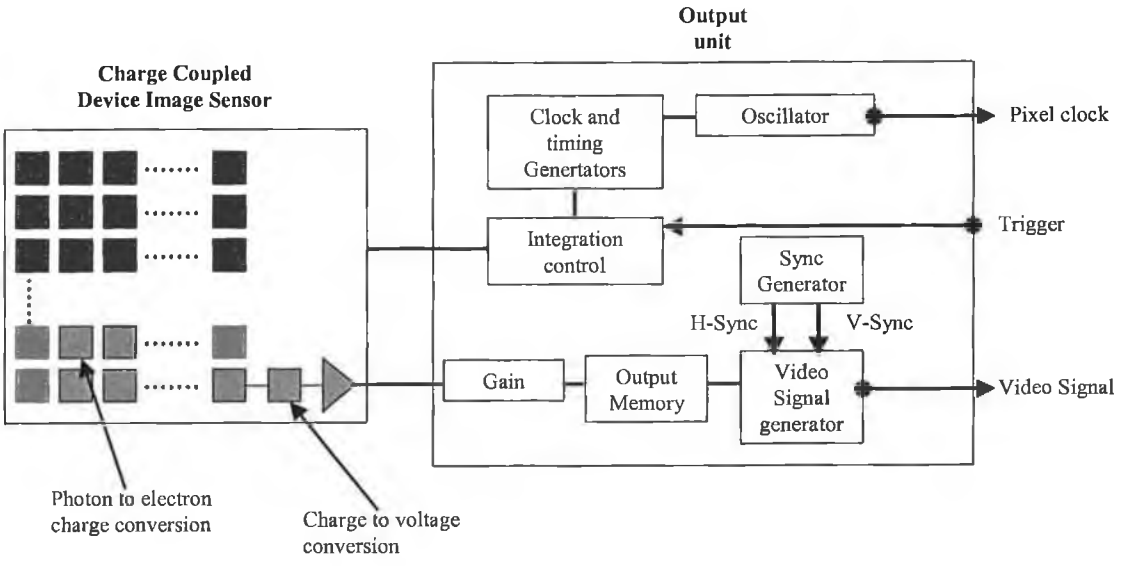

Figure 2-14 - CCD Sensor Architecture

The image sensor is a high-density 2D array of light sensitive photosites or pixels; these pixels change the incoming photons of light to electrons and thus accumulate charge. After a specific length of time, called the exposure time, the pixel charge is transferred to a read out buffer. The output charge is then converted to a voltage value and amplified. From here the output unit converts the electronic signal to a video signal based on a specific standard. This video signal can be in analog or digital form depending on the camera. In analog cameras, the signal is converted into a specific standard e.g. NTSC, PAL and sent to a display device. In the case of digital cameras, the video signal is converted to a digital format using an A/D converter. In a 12-bit camera the analog signal from the CCD is digitised with 12-bit depth. However, whether or not the output can be resolved into 12 bits – 4096 discrete levels depends on the camera noise [19]. This aspect is explained in more detail later in this chapter. The next section explains the various CCD architectures and how they are suited to various applications.

CCD Sensor Architecture

It is important to understand CCD sensor architecture, as the various methods employed produce different sensor performances and speeds. This is because they use different electronic circuit architecture to transfer the charge from the pixels to the output device. The two CCD designs that are most commonly used are:

- Interline Transfer
- Frame Transfer

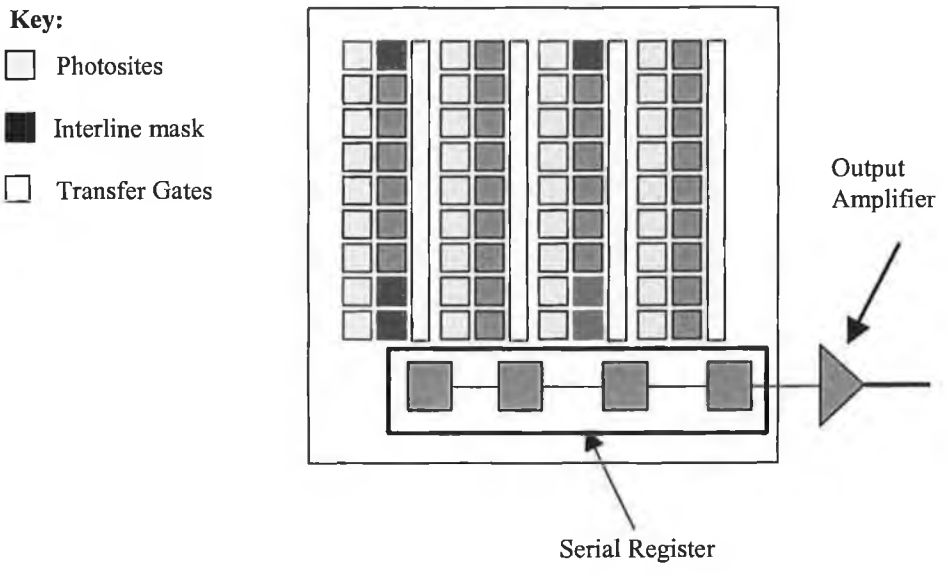

Figure 2-15 - Architecture of interline transfer CCD [22]

Interline-transfer CCDs incorporate charge transfer channels beside each photodiode so that the accumulated charge can be efficiently and rapidly shifted over to them (Figure 2-15). There are two different types of interline CCD:

- Interlaced Scan
- Progressive Scan

They differ in the methods they use to transfer charge off the pixel array to the serial register. Interlaced scanning works by transferring first the odd and then the even rows off the CCD array [23]. This type of scanning is better suited to video applications as the image can be formed after half the pixel values are read out. With

progressive scanning, the horizontal lines of the CCD are read out in order from top to bottom [23]. This CCD is best suited for machine vision applications as all the image information is required. All interline CCD devices use an electronic shuttering mechanism to control exposure time. This allows electronic shuttering off of a frame by dumping the stored charge instead of shifting it into the transfer channels.

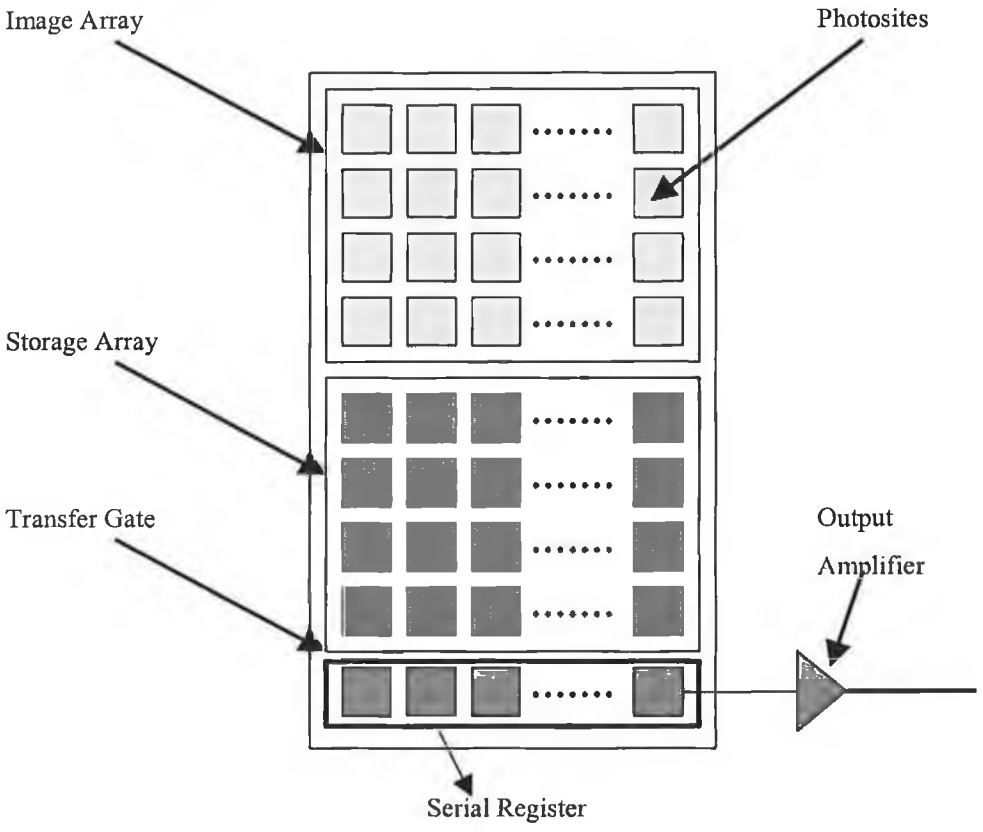

Figure 2-16-Frame transfer CCD

The frame-transfer CCD uses a two-part sensor in which the bottom half is covered by a light-tight mask and is used as a storage region. Light is allowed to fall on the uncovered portion, and the accumulated charge is then rapidly shifted into the storage array. While the signal is being integrated on the light sensitive portion of the sensor, the stored charge is read out. The pixel array illustrated in the full-frame CCD above consists of a parallel shift register, onto which images are optically projected by means of a sensor lens or microscope optical train. In this configuration, all of the photodiodes in the pixel array collectively act as the image plane and are available for

detecting photons during the exposure period. After photons composing the image have been collected by the pixel elements and converted into electrical potential, the CCD undergoes readout by shifting rows of image information in a parallel fashion, one row at a time, to the serial shift register. (Figure 2-16) The serial register then sequentially shifts each row of image information to an output amplifier as a serial data stream. The entire process is repeated until all rows of image data are transferred to the output amplifier and off the chip to an output device which converts the signal to a standard analog signal or digital signal depending on the sensor configuration.

CCD Specifications

In all CCD devices there are certain attributes that define the image sensor performance:

- Sensor size
- Exposure time
- Resolution
- Pixel Depth/Grayscale
- Signal to noise ratio
- Spectral Response-Quantum efficiency

These parameters determine the optical system's performance in terms of image quality and acquisition rate. They must therefore be understood when integrating a CCD into an optical system.

CCD Sensor Size

The size of the CCD sensor's active area will determine with the optical magnification the overall system field of view, so for a constant optical magnification, the larger the sensor area the greater the field of view. There are several standard CCD sensor sizes, ¼", ⅓", ½", ⅔" and 1" formats (Figure 2-17). The classifications of the CCD format do not reflect the actual sensor size. Historically, a one half-inch format is the size of the sensing area of a Vidicon tube, which is one half inch in Diameter [19]. The diagram below outlines the dimensions in millimetres of the various CCD sensors size formats.

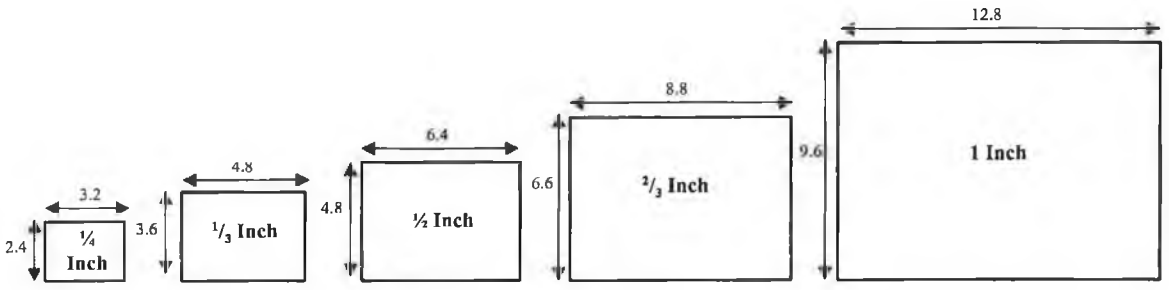

Figure 2-17 - Illustration of CCD chip formats (All dimensions in mm)

Exposure time

The exposure time, as the term suggests, is the length of time the CCD active area is exposed to the incoming light photons. The exposure time is controlled in two ways, via a mechanical shutter, which is the more traditional approach, or by means of an electronic shutter. The exposure control is a central parameter in a CCD sensor. If the frame is over exposed the image will appear too bright, and blooming will occur as shown in the image below (Figure 2-18). Blooming is where the pixel becomes over saturated and the electrons overflow to adjacent pixels [22]. Anti-blooming gates can be integrated onto a CCD; however, these reduce the CCD's active area, sensitivity and well depth [23]. On the other hand, if the image is under exposed, the image will appear too dark, as there will not be enough time for electron build-up on the pixels.

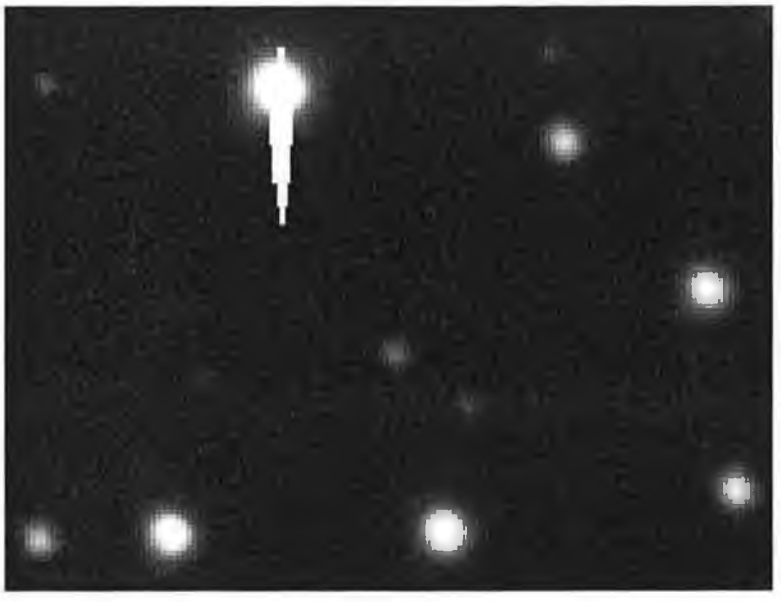

Figure 2-18 – Example of Image Blooming

Another requirement of exposure control is to dump the natural build up of electrons on the CCD. Additional electrons are generated on the pixels due to thermal effects when they are not illuminated. This effect is called "dark current" and is the cause of undesirable noise on the image [21].

CCD Resolution

Two factors determine the overall achievable resolution of an imaging system:

- Optics
- Imaging Sensor

The influence of the optics on a system's resolution has already been explained. This section demonstrates how the CCD device limits the system resolution and how the overall system resolution is determined.

The resolution of a CCD device is defined by two factors:

- The number of effective pixel elements in the array
- The size of these pixel elements

Mathematically, the CCD resolution is defined as twice the pixel size (Equation 2-7), as the maximum resolvable detail requires two pixels to define it. [19].

$$Camera\ Res.\ (\mu m) = 2 * Pixel\ Size\ (\mu m) \qquad \textbf{Equation 2-7}$$

The camera resolution can be specified as horizontal or vertical resolution depending on whether the horizontal or vertical pixel size is used (Figure 2-19).

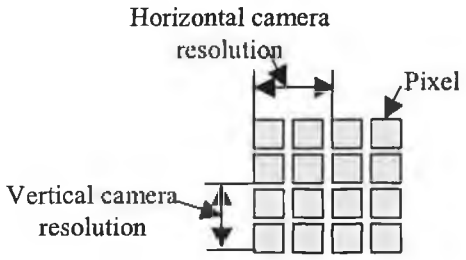

Figure 2-19 – CCD Resolution

Although it is the pixel size that defines the camera resolution to determine the entire resolution of the system, the optical magnification and effective area of the system must also be considered. Equation 2-8 below defines the system resolution or object resolution in terms of a camera's pixel size, effective area and field of view.

$$Object\ Res.\ (\mu m) = Camera\ Res.\ (\mu m)/Optical\ Magnification \qquad \textbf{Equation 2-8}$$

As shown in Equation 2-8 the limiting resolution of a CCD is dependent on two factors, the pixel size and the sensor size. The actual limiting resolution of a CCD is expressed as a ratio of these two factors and is called the Nyquist limit. This is defined as being one half of the number of pixels divided by horizontal sensor size [24].

$$Nyquist\ Limit = \tfrac{1}{2}(Number\ of\ pixels/Sensor\ size)(lp/mm) \qquad \textbf{Equation 2-9}$$

The Nyquist limit or system resolution is expressed in line-pair (lp/mm) where one line-pair is equivalent to two pixels (Figure 2-20).

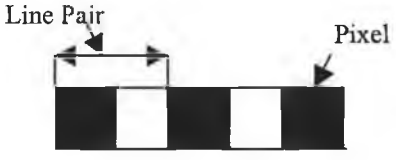

Figure 2-20 – A pair of imaging pixels are required to define a line pair

For example, in a standard monochrome high resolution CCD camera the sensors active area has 1024 horizontal pixels in 5 mm. This represents a horizontal sampling frequency of 205 pixels/mm. Therefore, in such an imaging system, the limiting

resolution or Nyquist limit is 103 lp/mm. This means that 103 objects or line pairs are resolvable per mm of the CCD sensor, which is the maximum achievable resolution of the system. It should, however, be noted that there are image-processing methods, such as sub-pixel sampling, which enable the user to statistically extrapolate higher resolution than the Nyquist limit [24].

While resolution has been explained in terms of a camera's pixel size and its effective area, other factors such as the image contrast influence the resolution of the imaging system. For example, if an image is blurry and lacking contrast due to optical limitations of a system, the resolution of the image will be reduced no matter what the CCD parameters. Therefore when expressing the resolution of a CCD, it is accurate to express it in terms of its Nyquist limits; however, when expressing the resolution of an imaging system it must be calculated as a factor of the optical resolution and the CCD resolution.

Pixel Depth/ Grayscale

Pixel depth or grayscale represents the number of steps of gray in an monochrome image. The most commonly used pixel depth is eight-bit as it represents a byte of information. Eight bits of data corresponds to 256 shades of gray in a monochrome image format. The pixel depth will therefore define the minimum amount of contrast achievable in the image, provided there isn't excessive noise on the input signal. If there is a lot of noise generated on the CCD itself, the output signal won't be able to resolve between each input change. So while a camera might have a specified pixel depth, if the noise on the signal is too high it will not be possible to achieve the specified pixel depth. The next section explains the effect of noise on a signal in more detail.

Signal to Noise Ratio (SNR)

Noise is obviously an unwanted property in any signal because it affects the quality of the signal and thus the final image. There are two sources of noise in CCD devices:

- Imperfections in the chip which cause dark current effects
- Thermal noise

The noise in the signal affects the image quality by limiting the maximum achievable pixel depth. The signal to noise ratio of a CCD device is the ratio of the noise component of a video signal to the signal itself. The signal to noise ratio is the parameter that details the effect of noise on a signal. It is expressed in terms of decibels (dB) in analog systems and bits in digital systems. In general, 6dB of analog SNR converts to 1-bit at 256 samples when digitised [19].

The higher the signal to noise ratio the better, as it will yield a higher number of steps in grayscale and thus a higher contrast image. So for example in an 8-bit system there are 256 grayscales so the signal is divided into 256 gray levels. For the noise not to adversely affect the image, the noise signal must be approximately half the value of each gray level signal, otherwise the electronics will not be able to distinguish between each gray level step (Figure 2-21).

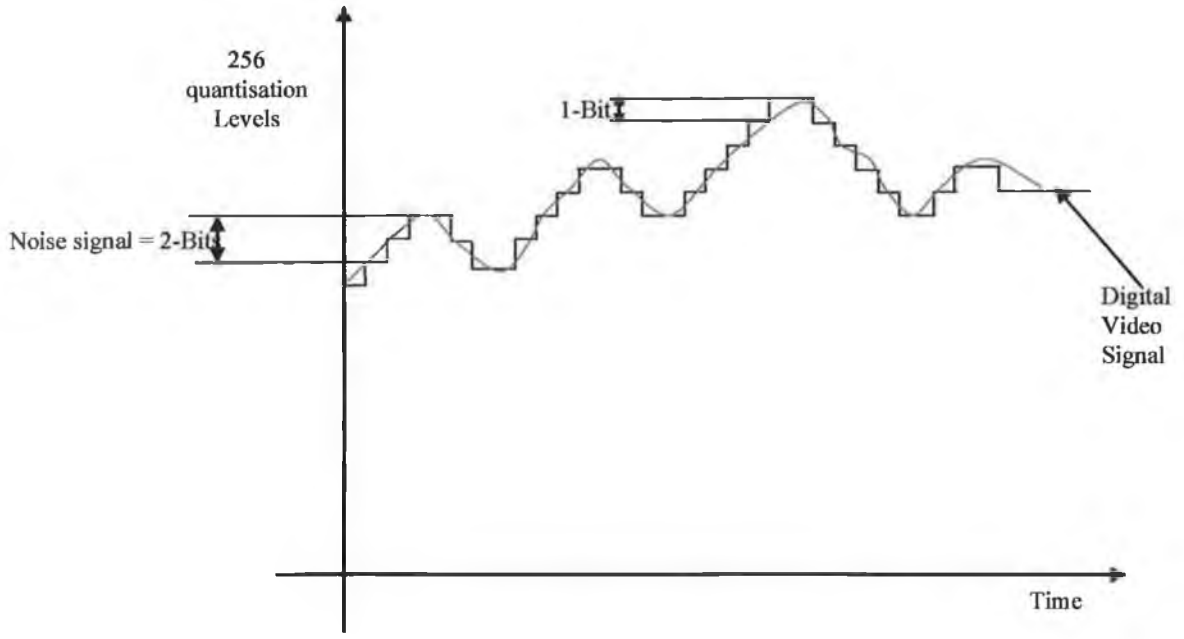

Figure 2-21 – 8 bit digital signal with 2-bit noise signal. Due to the noise signal the system can only decipher 128 quantisation levels so it would be more feasible to acquire the image with a 7-bit pixel depth

If this occurs, the image will have to be displayed with seven-bit pixel depth. Here there are 128 gray levels, so the signal to noise ratio will be higher and each gray level will be distinguishable; however, the contrast of the image will be reduced.

Spectral Response-Quantum efficiency

The quantum efficiency of a sensor describes its response to different wavelengths of light. Different sensors will have different performance levels depending on the CCD type and specifications. Standard front-illuminated sensors are more sensitive to green, red, and infrared wavelengths (in the 500 to 800 nm range) than they are to blue wavelengths (400 - 500 nm)[19]. Therefore, when illuminating the object, it is usually better to use a wavelength of light with a high spectral response for the CCD sensor being used. The spectral response describes the sensitivity of a photosensor to optical radiation of different wavelengths [20]. Figure 2-22 below shows a typical spectral response curve of a CCD sensor.

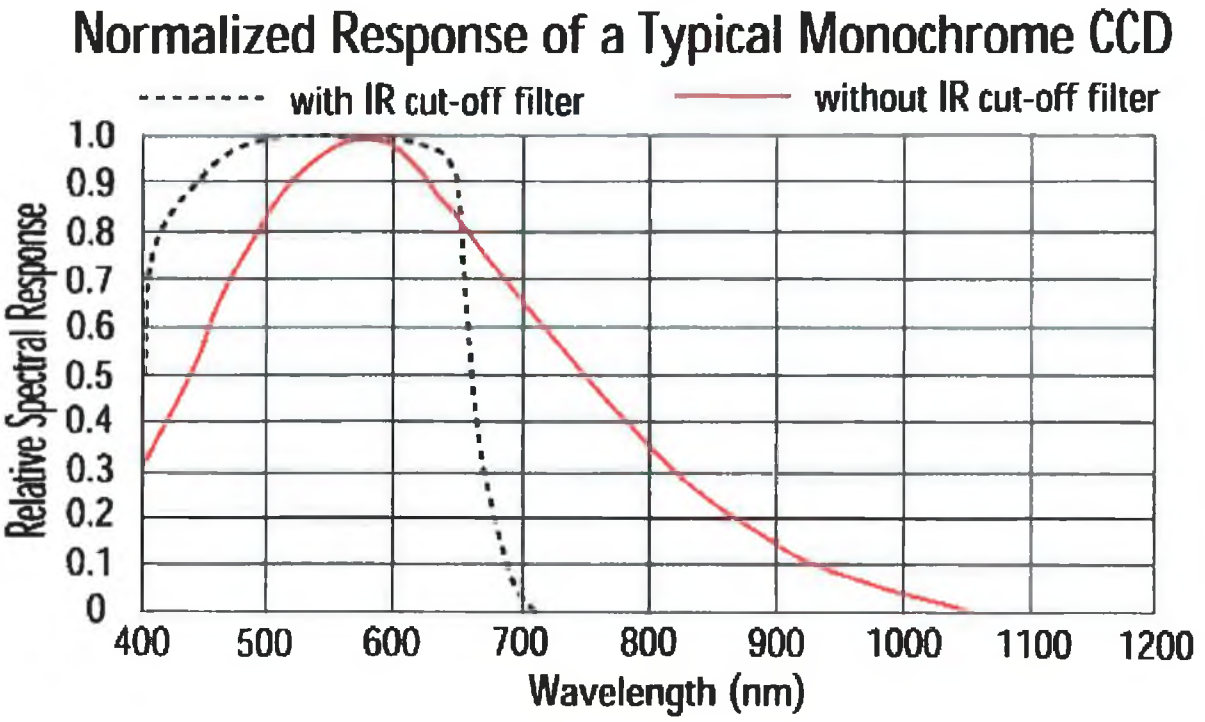

Figure 2-22 – Response curve of typical monochrome CCD [19]

Infrared light detected by the CCD will cause blurring of the image; some form of infrared blocking filter will therefore be required in the optical system to prevent this. Some CCD sensors have a built in cut-off filter which allows only the chip to detect wavelength in the visible region. A simpler and more effective solution is to enclose the entire optical system, thus removing the effect ambient light can have on the CCD.

2.2.2 Fibre Illumination

In any given machine vision system dedicated lighting is essential to produce a repeatable consistent image. The objectives of lighting are [25]:

- Optimise the contrast of the required image
- Normalise variances due to ambient conditions
- Simplify image processing and analysis.

Choosing the proper lighting scheme to achieve these objectives can result in:

- Increased accuracy
- Increased system reliability
- Improved response time

The basis of a vision system is its ability to collect light reflected from an object. The camera can control the amount, type and frequency at which light is collected but the image quality and aspect will be determined by the illumination used. Where aspect is defined as the 3-D orientation that can be interpreted from an image due to shadowing and shading effects.

The human vision system uses the illumination of an object when trying to determine its key features. It uses a wide range of cues, such as perspective, shadings, and parallax. These cues help to determine key features of an object, such as its topology and position. Using these cues in a machine vision system will enhance it's capability and reduce the complexity of the machine vision algorithms required. Simple problems, like determining top from bottom, finding a hole, or judging finer points, become a complicated task of definitions in machine vision. Certain vision problems cannot be resolved, no matter how complex the vision algorithm used, unless the correct lighting conditions are employed. To reduce the number of variables the

vision system must be provided with the best image for the particular inspection application. For example if the topology of the surface needs to be analysed, illuminating the object from an angle will cause shadowing of features, which will help highlight them. The diagram below illustrates the effectiveness of using different lighting techniques to determine feature characteristics. The image on the right uses front lighting (Figure 2-23), which highlights the top surface of the object. The image on the left uses backlighting (Figure 2-24), which produces a silhouette of the holes against a black background, thus determinng if the holes are drilled through or not.

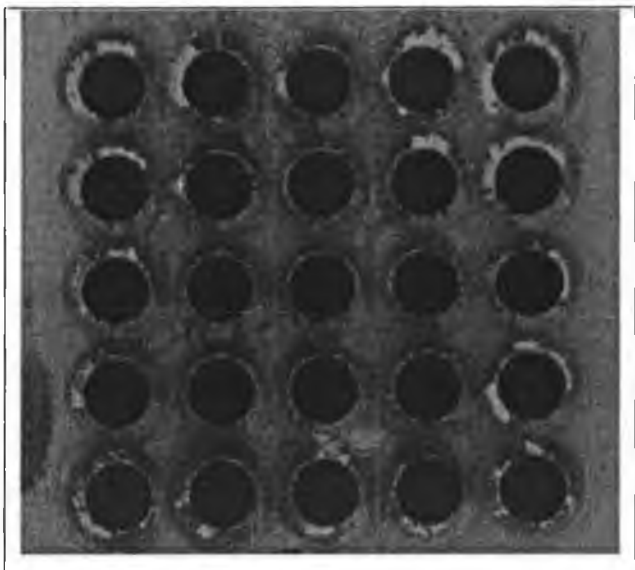

Figure 2-23 – Front lighting of through holes

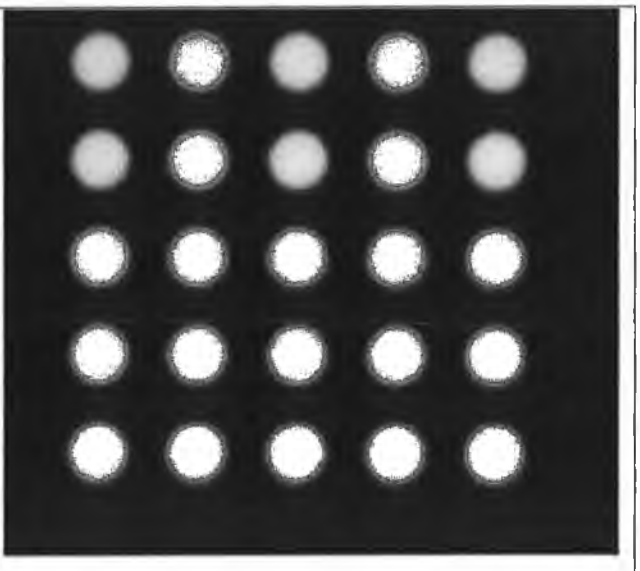

Figure 2-24 – Backlighting of through holes

Different applications require contrasting illumination solutions. For example some applications try to eliminate all glare. Other applications try to cause glare over a portion of the object. Some applications try to eliminate shadows; other applications rely on shadows. Yet other methods use multiple lighting techniques to determine feature characteristics. There is no such thing as a generic illumination method for all applications. Each individual application has to be assessed individually, with the selection of the most suitable form based on the parameters that are required from the

image to achieve the required solution. The next section discusses the different lighting methods available and the advantages involved in using each one.

2.2.2.1 Illumination Methods

Structured lighting: Structured Lighting is used in a front lighting mode for applications requiring surface feature extraction. Structured lighting is defined as the projection of a crisp line of light onto an object. One application of this lighting method is to determine the three dimensional characteristics of an object from the resulting reflections observed

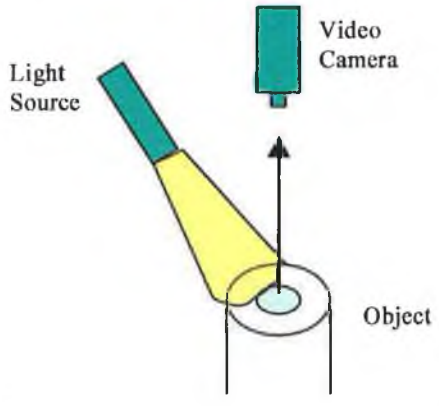

Figure 2-25 - Structured Lighting

Diffuse Back lighting: Backlighting provides the highest contrast and is relatively simple to set up. It produces a silhouette image and works best when a critical edge for dimensioning is desired. Diffuse backlighting places the target between the sensing lens and the light source. By illuminating the target from the rear with respect to the lens, the background appears uniformly white and the target is silhouetted producing a high contrast image. Figure 2-24 shows an example of backlighting where through holes are illuminated from the back.

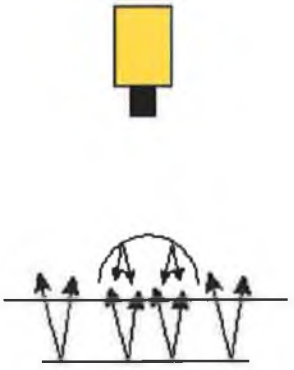

Figure 2-26 - Diffuse Back Lighting

Ring lighting: Ring lighting uses a ring of LEDs around the circumference of the object to illuminate it. Ring lights provide intense shadow-free on-axis lighting. A ring light solves the problem of diagonal shadow projection and thus is especially useful when imaging highly reflective objects [24].

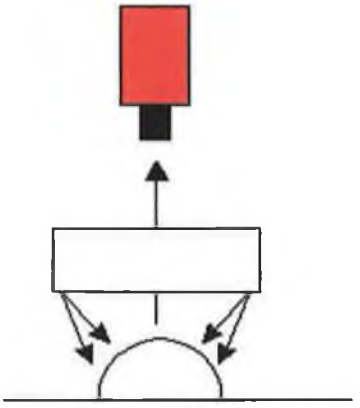

Figure 2-27 Ring Lighting

Dark Field Illumination: Many transparent objects are not readily visible using diffuse back lighting. One can improve image contrast by dark field illumination in which a transparent object's edges appear bright against a dark background. A dark field is achieved by projecting a cone of light from behind the transparent object. This cone of light would - if not obstructed by an object - diverge from the optical axis and not be imaged. Only the light scattered or reflected by the object will be directed into the optical axis and be imaged.

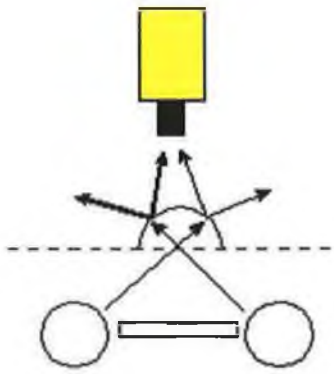

Figure 2-28 Dark Field Illumination

Diffused Axial Illumination [26]: Diffused axial illumination uses a half silvered mirror to illuminate the object from behind. Since the light is transmitted along the optical axis, it allows for shadow free illumination, which greatly improves the image quality and allows for increased measurement accuracy. There is also little specular reflection (glare) associated with this type of illumination, which helps highlight certain defects [27]. On the other hand, the fact that there is no shadowing means certain other defects will not be detected.

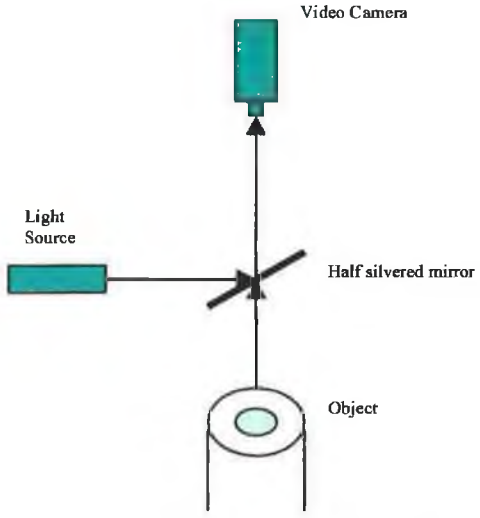

Figure 2-29 - Diffused Axial Illumination

Detailed explanations of the type of illumination used and the results achieved with this type of illumination are given in Chapter 4 – Detail design and Chapter 5 – Evaluation of working prototype.

2.2.3 Focusing Control System

Small variations in fibre movement with respect to the lens can cause substantial degradation of the image quality. This is due to the small depth of focus inherent in high magnification optics. As a result an autofocus system is essential in automated microscopy to overcome the problems of mechanical instability, the irregularities of the inspection surface and the use of various magnification lenses. The performance of an autofocus system in a microscopy system is much more critical than in many other optical systems because of the extremely narrow depth of fields. For example the numeric aperture (NA) of a 20X achromatic lens is in the region of 0.4, which gives a theoretical depth of field of 3.325μm [28].

The aim of any autofocus system is to achieve a repeatable feedback signal that can be fed to a controlling system. The feedback signal is almost always received from the image, which feeds into a control system. The control system then changes the distance between the lens and the object in order to focus the image. This loop is constantly repeated until the focus position is achieved. Figure 2-30 illustrates the signal flow.

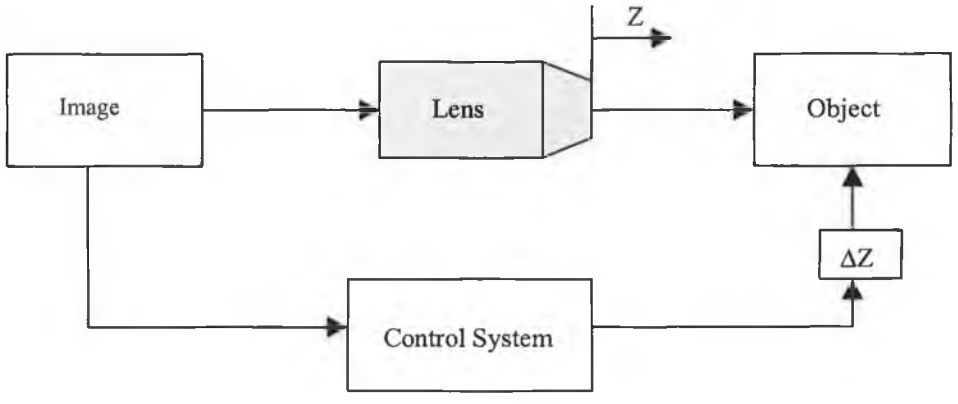

Figure 2-30 - Autofocus System Architecture

The difficulty in implementing an autofocus system lies in achieving an adequate feedback signal. There are a variety of methods available to achieve a feedback signal to autofocus an image [30].

- Fourier frequency methods
- Autofocus based on optical transfer function (OTF) and sampling
- Edge detection
- Autofocus based on image statistical properties

All the above methods are based on similar principles, which is to determine when the image has the highest level of contrast or resolution. A blurry unfocussed image will not contain any crisp well-defined edges, and any variation in image intensity will be gradual. A well-focused image will have well defined edges and variations in pixel intensity will be extreme along well-defined edges [29].

Fourier frequency methods look at the frequency components of an analogue image signal. The analogue signal of a focused image will have a high proportion of high frequency components as steep gradients or sharp edges are associated with high spatial frequencies within an image (Figure 2-31). This is because they introduce significant gray-level variations over a short distance. By analysing the Fourier frequency spectrum with highpass filters, these high frequencies can be isolated. This signal can then be used as feedback to focus the image. This method is commonly used for implementing autofocus systems using hardware components only to achieve a feedback signal.

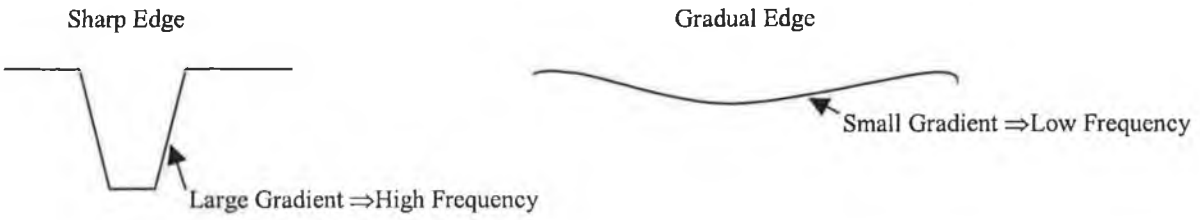

Figure 2-31 – Effect of object gradient on frequency response of image signal

Autofocus based on OTF takes into account the contributions of each element of the system to the focus quality of an image. It models the system as a linear shift invariant system and applies a band-pass filter on the image acquired by the CCD camera [31]. It looks for the image with highest signal power and calls this the focused image.

Autofocus using edge detection is an image specific method. This method examines the pixel intensity change across an edge. In a focused image, the edge will have a sharp intensity gradient change. For an unfocused image, the intensity gradient change is more gradual. The intensity gradient across an edge can thus be used as the feedback signal. However, this method can be subjective, because if the image is significantly out of focus the edge will not be detectable by the algorithm.

Autofocus based on image statistical properties measures a specific characteristic of an image pixel (intensity or contrast) that is analogous to focus. Calculating the spread of the image intensity will determine the contrast of the image and thus the focus. In an unfocused image the majority of the image pixels will lie within a small range of each other as features are undefined and the image is blurry. A focused image will be of higher contrast than an unfocused image and for this reason contains a wider spectrum of pixel intensities and therefore a larger pixel spread. Due to its simplicity in implementation, as well as its speed and accuracy, autofocus based on image statistical properties method is used in the development of the system. The

implementation of this system is discussed in further detail in Chapter 4 – Detail Design.

2.2.4 Image Acquisition Hardware

Image acquisition hardware acts as the interface between the camera and the PC. There are two categories of interfaces to choose from, analog and digital. In an analog camera, the signal from the sensor is turned into an analog voltage and sent to the frame-grabber board in the vision-system computer. NTSC, CCIR and PAL are all common analog interface standards [38]. Analog cameras are inexpensive when compared to digital cameras, but subject to noise and timing problems.

The majority of new machine vision cameras use a digital interface. The camera digitizes the signal from each pixel and the data is sent in digital form directly to the computer. CameraLink and Firewire are two popular digital interface standards. Digital signals are less susceptible to noise and there is a perfect correspondence between each pixel on the sensor and in the image. Digital cameras support a wide variety of image resolutions and frame rates. Since the signal is already digitized, a simple interface board replaces the frame-grabber. When choosing a method of acquiring digital image data into a PC there are only a small number of methods available:

- Frame grabbers
- Firewire
- USB port

Each one offers its own individual advantages and disadvantages. This section discusses the operation of each one and decides on the most beneficial for the project.

2.2.4.1 Frame Grabbers

Using a frame grabber is the more traditional approach to acquiring video data. The frame grabber became feasible with the development of the high bandwidth Peripheral Components Interface (PCI) bus as it became possible to acquire large amounts of digital data into a PC. The PCI bus allows for the acquisition of 127.2 Mbytes/sec that translates to an image of 1920 X 1024 resolution at 48 fps. This compares favourable to the previous maximum bandwidth of 15.9 Mbytes/sec via the ISA bus [32].

The overall architecture of frame grabbers is quite simple in theory although they are quite complex to implement due to timing issues. Figure 2-32 below shows the components of a basic frame grabber.

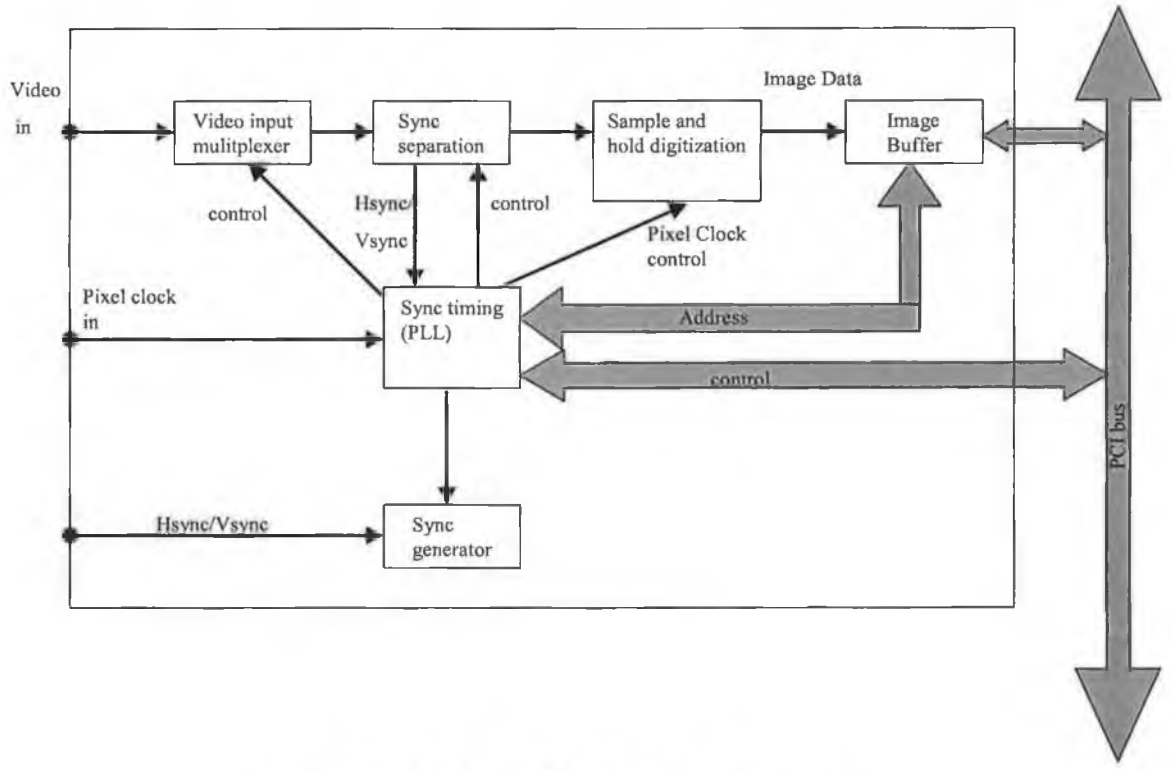

Figure 2-32 – Frame Grabber Architecture

The video is initially acquired through a video multiplexer, which controls the input signal. The first step in the acquisition is to pass the signal through a sync separator, which separates the synchronisation pulses from the incoming signal. The horizontal sync indicates the beginning of a new line and the vertical sync indicates the beginning of a new column or frame. This information is eventually used to address the digitised data. The next stage of the acquisition is to digitise the video data using an A/D converter. The digitisation process is controlled by an internal clock signal in the frame grabber. The clock signal can be also be obtained from the camera clock to achieve a more accurate digitised video signal. The digitised pixels are collected in an image buffer or FIFO buffer. The image buffer stores at least one completed frame and is used if the bandwidth of the bus is too small and all the data cannot be passed in real time. In most frame grabbers the size of the image buffer will be specified. Usually the image buffer is not critical as modern bus systems like the PCI are so fast only a small amount of memory is necessary to buffer irregularities of the data flow [33]. From the image buffer the image data can be accessed through software interfaces that can communicate with the frame grabbers via Application Programming Interfaces (API's).

This description of the frame grabber is quite simplistic, and most frame grabbers are far more complex as they contain on-board processors for image processing and compression. While frame grabbers are still the most common method of acquiring video their overall design has inherent flaws. They cannot be designed as simple I/O devices as they have to be installed internally into the PC through the PCI bus. This causes problems with connectors and in having to reboot the PC after installation and maintenance.

2.2.4.2 Firewire

Firewire is a video acquisition standard that was developed to communicate with multimedia devices, such as cameras and videos. Firewire is also known as IEEE 1394 as this is the standard that defines it [34]. The primary difference between IEEE-1394 and other interface standard is its peer-to-peer topology, which enables peripherals, such as cameras, to communicate between each other without the need for a master PC.

IEEE 1394 provides two types of data transfer: asynchronous and isochronous. Asynchronous is for traditional load-and-store applications, where data transfer can be initiated and an application interrupted as a given length of data arrives in a buffer. Isochronous data transfer ensures that data flows at a pre-set rate, so that an application can handle it in a timed way. For multimedia applications, this kind of data transfer reduces the need for buffering and helps ensure a continuous data display.

As a method of acquiring video Firewire has certain advantages over frame grabbers:

- Its hot-plugable
- Peer – to – peer

There are disadvantages to the standard as well.

- The standard is not as fast as frame grabber, operating at a maximum 50 Mbytes/sec compared to the 127 Mbytes/sec of frame grabbers
- Not all PCs have a port, as the standard is not royalty free, unlike USB 2.0
- The peer-to-peer feature does not provide any value in a system where the PC is doing your image capture, processing, display, storage and networking [36]

2.2.4.3 Universal Serial Bus (USB)

The Universal Serial Bus (USB) standard was originally developed to minimize the number of ports in the back of the PC. The major goal of USB was to define an external expansion bus, which makes adding peripherals to a PC low cost and easy to connect [37].

The first release of USB, USB 1.1 featured two different speeds [38]:

- Low speed – 1.5Mbits/sec
- Full speed – 12Mbits/sec

Low speed was designed for low bandwidth interrupts devices such as mice and keyboards. Full speed was for higher bandwidth devices such as printer's scanners and zip drives. The next release of USB, USB 2.0, was engineered to cater for high-speed devices as well as lower speed devices. It features a maximum bandwidth of 480 Mbps (60MBytes/sec). This makes the protocol ideal for video acquisition, as it enables the transfer of 1920x1080 images at 24fps (frames per second) for image processing or 320x240 images at 500fps for high-speed video motion analysis [36].

USB Protocol

USB employs a master slave hierarchy, where the PC is the master and the peripherals are slaves. The PC makes requests and peripherals respond. Unlike most serial interfaces where the format of data is not defined, USB is made up of several layers or protocols. So instead of using bits and bytes for serial transmission, USB uses packets for each transaction. A packet can consist of the following fields [37]:

- Sync - All packets must start with a sync field. The sync field is 8 bits long, which is used to synchronise the clock of the receiver with the transmitter. The last two bits indicate where the PID fields starts.

- PID - PID stands for Packet ID. This field is used to identify the type of packet that is being sent.
- ADDR- The address field specifies which device the packet is designated for. Being 7 bits in length allows for 127 devices to be supported. Address 0 is not valid, as any device which is not yet assigned an address, must respond to packets sent to address zero.
- ENDP - The endpoint field is made up of 4 bits, allowing 16 possible endpoints.
- CRC - Cyclic Redundancy Checks are performed on the data within the packet payload. All token packets have a 5-bit CRC, while data packets have a 16-bit CRC.
- EOP - End of packet.

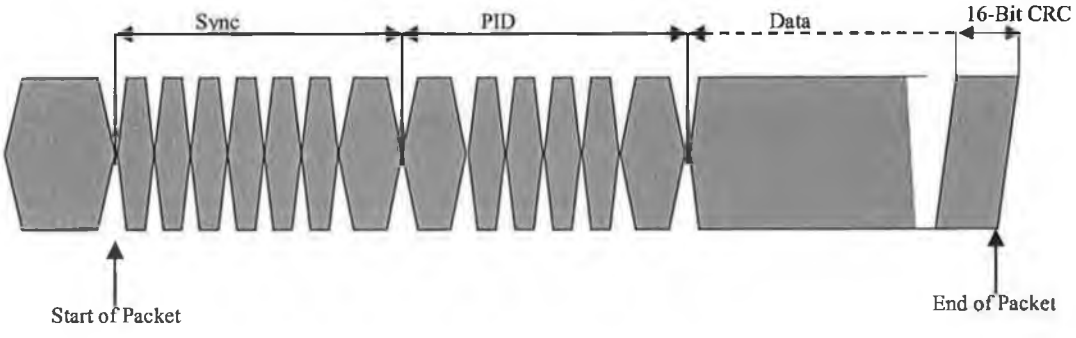

Figure 2-33 –Data packet [38]

Figure 2-33 details a typical data packet. The sync signal signifies the start of the packet. The PID defines the packet as a data packet. The remainder of the allocated bandwidth contains the transmitted data. The data packet is just one type of packet defined in the USB protocol; there are four different types of packet in all:

- Token
- Data
- Handshake

- Start of Frame Packets

Token packets indicate the type of transaction to follow, data packets contain the information, handshake packets are used for acknowledging data or reporting errors and start of frame packets indicate the start of a new frame. So a typical USB transaction for the transmission of data from a peripheral to the PC will require three different types of packets to be used:

- Token
- Data
- Handshake

Firstly, a Token packet is sent by the PC with the address of the device and an indication of the desired direction of data transfer. If data is being sent to the peripheral, such as camera setup commands, it is an OUT request. If data is being sent from the peripheral to the PC, such as image data input from a camera, it is an IN request. Next is the data packet transfer stage. A data packet can have up to 3072 bytes, along with a CRC value for error checking. The third stage is the handshake. Once the data has arrived successfully, a packet is sent to ACK or acknowledges it. For streaming data applications which do not require error checking or handshaking, isochronous mode is used. Isochronous mode is ideal for video transmission it allows a device to reserve a defined amount of bandwidth with guaranteed latency. This is ideal in audio or video applications where congestion may cause loss of data or frames to drop.

2.2.4.4 Choice of Hardware

When choosing image acquisition hardware, certain fundamental parameters must be taken into account:

- Bandwidth
- Reliability
- Accuracy of data transmission
- Costs

Table 2-1 compares each of the three acquisition methods.

Category	USB 2.0	IEEE-1394	Frame Grabber
Topology	Master - Slave	Peer - Peer	Master - Slave
Bandwidth (bits/s)	480 Megabits/s (60 Megabytes/s)	400 Megabits/s (50 Megabytes/s)	1 Gigabit/s (127 megabytes/s)
Transaction intervals	125 microseconds	125 microseconds	Synchronous
Cable Distance	5 M, Up to 30M with 5 hubs	4.5m	10M
No. Of Wires	4	6	26 or 52
Bus Power Consumption	Up to 500mA @ 5V	Up to 1.5A	None
Devices in network	127	63	1

Table 2-1

While frame grabbers have by far the highest bandwidth capability, and are designed solely for video acquisition, they still remain quite expensive when compared with USB and IEEE 1394. The real advantage of using USB and IEE1394 connection standards is their ability to allow acquisition peripherals to be designed to connect directly to desktop PC's. This gives a device an edge in the market, as the overall costs are cheaper compared to using a frame grabber. It also adds to the portability of the device, as it can be moved from PC to PC as long as the correct device drivers are present. Therefore, in choosing a hardware acquisition device, USB or IEEE 1394

would seem to be the better choices for an external peripheral, provided their bandwidth capabilities lie within the required spec. The next issue is which of these acquisition methods gives the best performance. USB 2.0 is the preferred connection method for PC peripherals as it achieves faster speeds and lower costs than IEEE-1394. The reduced cost arises from the fact the chipsets are cheaper to manufacture than IEEE-1394 chipsets, as 1394 peripheral controllers require four to five times more gates to implement the interface than a comparable USB 2.0 peripheral [37]. In addition, USB has remained royalty free, making inexpensive peripherals possible.

2.3 Image Analysis

There are two stages in the development of an image analysis algorithm:

- Image Processing
- Image Analysis

Image processing is an image-to-image process; it aims to produce images that will make the analysis stage simpler and more robust. Image analysis is defined as the process of extracting useful information from an image [5]. In the case of this application the useful information is defects and the location of the various regions of the optical fibre.

2.3.1 Image Processing

Digitized images are stored in data arrays. The most basic image format is the gray scale image. The pixels in this data format are represented by and integer value of intensity, in the case of an 8-bit image this intensity range is from 0 to 255, where 0 is black and 255 is white. This data is stored in an array that defines pixel location and intensity. Manipulation and analysis of the image is based on processing this array to achieve the required information.

Image processing can be divided into two major categories [5]:

- Image Enhancement and Restoration
- Measurement Extraction

Image enhancement and restoration involves improving the image contrast and brightness and/or eliminating noise from the image to make the analysis process easier. The type of enhancement algorithm used depends on the image quality and the data to be extracted at the analysis stage. Its works on the basis that neighbouring pixels in real images have essentially the same or similar intensity values [42]. So if a

distorted pixel can be picked out from an image it can usually be restored by averaging the neighbouring pixels.

Image measurement extraction aims to process the image so as to allow measurements to be made during the analysis process. An example of this is image thresholding, this involves setting the values of pixels above a certain threshold value to white, and all the others to black [5]. This helps to highlight various defects although the optimal threshold values must be carefully selected so as not to eliminate defects.

2.3.2 Defect Analysis

Two approaches can be taken when analysing defects in machine vision.

- Two dimensional analysis of an image to determine defect profile
- Three dimensional analysis of the of the object

2.3.2.1 Two Dimensional Analysis of Defects

The more traditional and most commonly used approach to defect detection in machine vision is 2-D analysis. There are two stages to defect analysis using the 2-D method:

- Analysis of the 2-D shape of a defect
- Analysis of the depth profile of the defect

Analysing the 2-D shape of a defect will distinguish whether it is circular, streaky, or irregularly clustered. Specialised 2-D shape descriptor algorithms are used to analyse the pixel orientation of a defect to determine its 2-D shape. An example of a shape descriptor is the circularity descriptor, which can be used to analyse the geometric shape of a defect. Equation 2-10 details the circularity descriptor mathematically:

$$Circularity = (Area/perimeter^2) \text{ [5]} \qquad \textbf{Equation 2-10}$$

The value obtained for circularity tends to a maximum value of $1/4\pi$ as the object becomes more circular and tends to zero and it becomes more irregular [5]. This method helps to differentiate between types of defects e.g. pinholes, scratches, and blemishes.

The second stage of 2-D defect detection is to analyse the depth profile of the defect. Analysis of the morphological gradient of a defect will tell us about its depth profile [5]. For example cracks can be detected by analysing their depth profile. The cross sectional area of a crack will have a sharp negative downslope followed by sharp positive upslope. This leads to a sharp variation in pixel intensity, which may be used to determine the character of the profile [43]. Scratches can be found in a similar way to cracks; however the change in intensity across the scratches is not as dramatic. Figure 2-34 shows a typical depth intensity profile for a crack and a scratch, which illustrates the differences in intensity change for each. Defects with a vertical profile such as pits, voids and pinholes are best imaged using side illumination, which produces shadows and therefore highlights depressions as dark spots in an image. Combining the information from both types of analysis will enable defects to be classified more accurately.

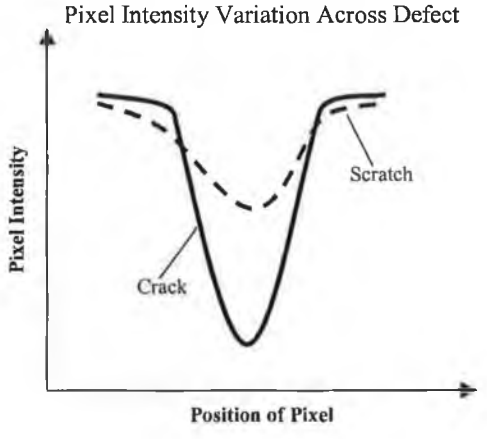

Figure 2-34 - Typical pixel intensity variation for a crack and a scratch

2.3.2.2 Three Dimensional Analysis of Defects

The main limitation of 2-D defect analysis is that it can only examine the cross section of the fibre surface in detail; it is therefore difficult to detect 3-D defects such as raised contamination and voids. Also, certain geometries such as the ferrule height and fibre radius of curvature cannot be determined. An alternative solution for the inspection of fibres is to reconstruct a 3-D mathematical model of the fibre surface. This method called 'photometric stereo' gives the ability to estimate local surface orientation by using several images of the same surface taken from the same viewpoint but under illumination from different directions [40]. The aim of photometric stereo is to determine the surface gradients of an object by using several images of the object taken from the same viewpoint but under illumination from different directions. The theory of photometric stereo can be more easily understood by examining the image produced of a sphere illuminated from one side (Figure 2-35).

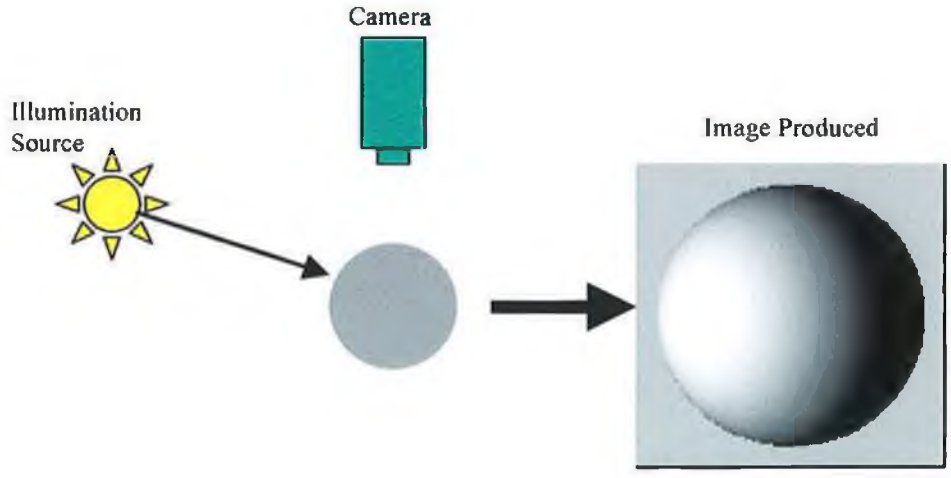

Figure 2-35 – Image produced when sphere is illuminated using directional illumination

While the image of the object produced is essentially 2-D, 3-D information can be extracted from it by examining the variations in surface brightness as the brightness of an object surface depends on two factors [41]:

- The surface orientation with respect to the camera
- The illumination intensity and orientation of the illumination relative to the surface being illuminated

This can be clearly seen in the image produced of the sphere. Where the surface is at right angles to the illumination source, the image intensity is highest. As the surface orientation changes, the image intensity reduces. Therefore it can be concluded that the image intensity will depend on two factors:

- The surface geometry relative to the camera and illumination source
- The amount of light that falls on the object being viewed

So if the position of the camera and illumination source is known relative to the object, the surface orientation can be extracted from a 2-D image of the object, this is the basis of photometric stereo.

To discuss photometric stereo reconstruction further would be to go beyond the scope of the project. Due to the complexity involved in implementing photometric stereo, the mechanical design of a prototype to implement 2-D image analysis of an optical fibre surface is pursued. However, for the benefit of future projects, that might propose to implement this approach, a detailed mathematical explanation of photometric stereo is given in *appendix 4*.

2.3.3 Image Analysis Summary

In order to adequately design a device for image processing and analysis it is necessary to review the type of analysis to be carried out, as the analysis required will determine the illumination technique(s) required, magnifications and lighting levels. The requirements to be meet when implementing a device for image processing and analysis are:

- Scaled focused images must be acquired
- Direct access to the images stored in the form of a pixel intensity array is required
- Information detailing the image pixel mapping must be acquired from the acquisition device.
- An adequate illumination system must be employed to assist the image analysis process.

2.4 Summary of Findings

A generic overview of the physics and technology involved in the implementation of an optical fibre inspection system has been given in the literature review. A brief introduction has been given to optical fibre technology and the issues involved in the connection of optical fibres. This overview leads to the formation of certain key of areas of research, the conclusions drawn from each of these areas is as follows:

- Imaging System – An imaging system consists of an optical system and an imaging sensor. The optical system focuses light onto the imaging sensor to form an image. The imaging sensor then converts this light into electronic format for storage and analysis
- Illumination - An illumination system consists of a light source or sources that can be oriented in many different ways to produce various illumination methods. Numerous illumination methods exist with contrasting solutions and applications. Choosing the proper lighting scheme is important as it will determine image quality and help simplify image processing and defect detection
- Focus Control – Focus control is necessary to overcome issues with mechanical irregularities and varying focal position between optics. Many autofocus methods exist, but the majority are based the analysing the frequency components of an image signal. The key aim in implementing an autofocus system is to achieve an adequate focus fedback signal.
- Image Acquisition – As a solution for image acquisition three methods were examined:
    - Frame grabbers
    - Firewire

- USB

While frame grabbers are the more traditional approach taken for image acquisition, USB and Firewire are becoming better alternatives as they use standard interface ports to the PC and are thus less expensive than frame grabbers. For the purpose of this project USB was found to be the best alternative as it can achieve faster speed than firewire and is royalty free.

- Image Analysis – Two methods of image analysis are presented:
  - 2-D analysis
  - 3-D analysis

While 3-D analysis has many advantages over 2-D analysis it is far more complicated to implement. Thus a system that employs 2-D analysis for inspection is to be designed.

The following chapter, sets out design concepts based on the research carried out in the literature review, from these the best approach for the design of the prototype is determined and a detailed specification for this set out.

Chapter 3: Concept Design

Having set out a generic area of research the next phase of the project was to develop a detailed product specification which leads to a conceptual design of a system for the analysis of optical fibre endfaces. However before moving onto this some background information on how fibres are presently inspected must be presented, as this is necessary to understand the system requirements set out in the product design specification.

The most common fibre inspection technique used in industry at present is human inspection. Here the fibre is viewed using a high magnification microscope. The operator searches for defects like dust, cracks, scratches and voids. Figure 3-1 details a typical image of a clean optical fibre endface under 200X magnification that would be viewed by an operator. The areas that can be observed in this image are the core, the fibre itself and the ferrule, which holds the fibre in place.

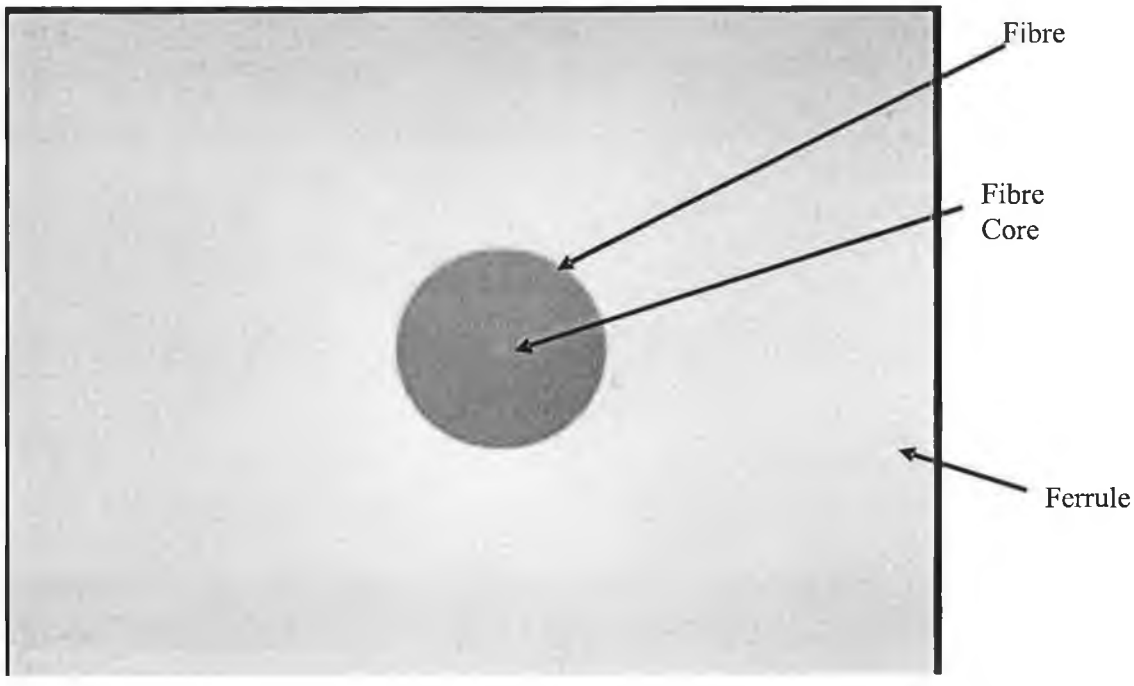

Figure 3-1– Clean Optical fibre endface under 200X magnification

The subjective nature of the process becomes apparent when a partially dirty fibre is viewed. Figure 3-2 provides such an example of one. While one operator might consider this fibre to be within spec another one might fail it.

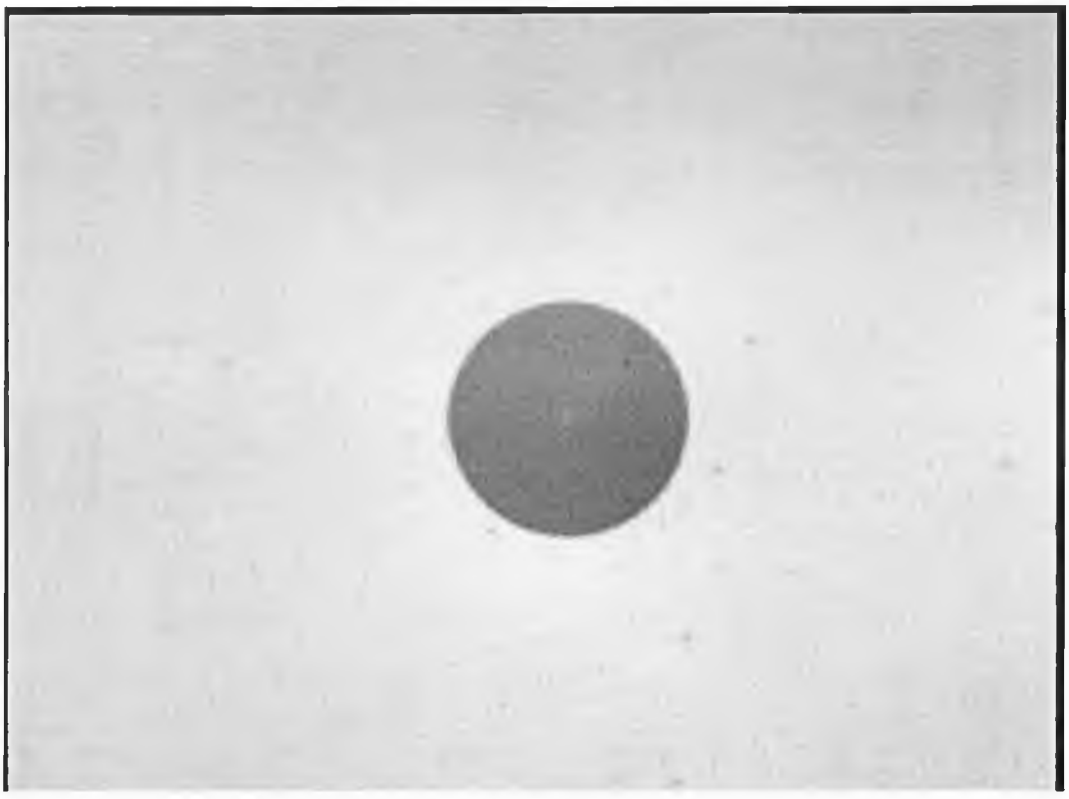

Figure 3-2 – Partially dirty fibre under 200X magnification

The method used to determine the pass/fail criteria is to reference predefined standards for the various regions of the fibre. There are presently no international standards for the inspection of optical fibres, as most companies draw up their own internal standards. Most standards are based on criteria devised from insertion loss testing of defective fibres. Table 3-1 gives an example of such a standard. Figure 3-3 shows the location of the various regions as referenced in Table 3-1.

Defect	A	B	C	D-F
Crack	Not Acceptable	No cracks such that when continued can intersect the core		N/A for polished end see ferrule spec
Chip	Not Acceptable	One defect up to 10 micron diameter is acceptable. Defects< 2 micron don't count	Multiple defects < 10 micron each are acceptable(can't touch fibre edge). Defects < 2 microns do not count. Sum of all defects types < 30 micron	N/A for polished end see ferrule spec
Pin holes/Voids			Multiple defects < 10 micron each are acceptable(can't touch fibre edge). Defects < 2 microns do not count. Sum of all defects types < 30 micron	N/A for polished end see ferrule spec
Scratches (Sm)	No scratches in core. Tangent to core acceptable if less than 2 micron width	Acceptable if they do not exceed 2 micron width		
Scratches (MM and APC)	Scratches in the core are acceptable if transmission requirements are met	Acceptable if they do not exceed 2 micron width		
Ferule Scratches			No Scratches >10 micron	Acceptable
Epoxy rings		Acceptable if width < 5 micron. No loose edge chipping		
Fixed contamination black spots	Not Acceptable	Not Acceptable	Multiple defects < 10 micron each are acceptable(can't touch fibre edge). Defects < 2 microns do not count. Sum of all defects types < 30 micron	Acceptable
Raised Contamination	Not Acceptable	Not Acceptable	Not Acceptable	Acceptable
Loose Contamination	Not Acceptable	Not Acceptable	Not Acceptable	Acceptable

Table 3-1 - Inspection Criteria for Optical Fibre Endface (Courtesy of Lucent Technologies Inc).

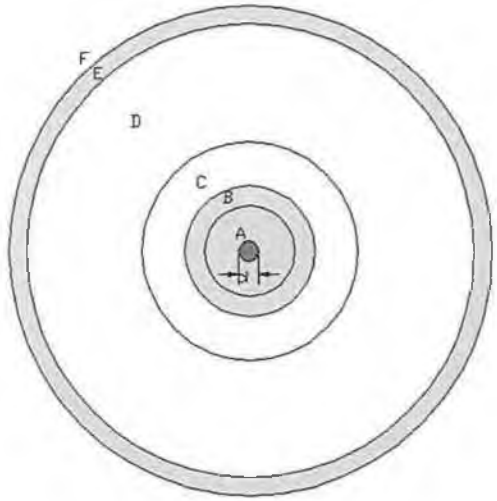

Key:

A = Restricted Area
B = Fibre surface
C = Ferrule Surface
D = Ferrule Pedestal
E = Chamfer
F = Outside Cylindrical Surface

F)igure 3-3 - Regions of an optical fibre endface

The system designed has to inspect fibre endfaces based on the criteria given in Table 3-1. The table details a variety of different defects that can be present on fibre endfaces, with the criteria becoming less stringent for the regions outside the fibre core, as these are less critical to the transmission abilities of the fibre. The size of the defects that must be detected range in scale from 2μm to 30μm. The types of defects that can be observed on the fibre surface vary from cracks and chips in the fibre glass to external contamination on the surface. Due to the variety of the defects that can be present on the surface, the only approach to implementing such a system is to use a vision based system. The system concept framework shown in *Section 3.2* of this chapter outlines the basis of a vision based inspection system. However, before discussing the design concepts a product design specification is set out, outlining the requirements of such a system in more detail.

3.1 Product Design Specification (PDS)

In detailing the design specifications, there are no rigorous standards set out for parameters like size and weight, ergonomics, maintenance or quality standards. This is because the device is designed with R&D in mind and not high volume production. Therefore, the product requirements are based on the device functionality and its ease of use as an R&D prototype. These requirements are outlined below.

3.1.1 Basic Functionality

- Optical microscopy to achieve a range of magnifications, thereby allowing more complete examination of the fibre
    - Imaging system must allow for a field of view of 1mm square across the sensors area, as this is the total size of the optical fibre.
    - Imaging system that allows for the detection of defects of down to 2μm in size.

- A specific illumination system to highlight defects
- An autofocus device to compensate for mechanical irregularities and the variation in focal position of the various lenses.
- High bandwidth image acquisition hardware to achieve full resolution images for processing
- PC based controller with interface via the USB and parallel ports to allow control of the fibre, optical magnification and focus of the microscope based on the acquired image
- Image processing software to identify any defects and ensure that the fibre meets the inspection criteria

3.1.2 Robustness

- The automated system must be able to accurately reproduce sharp focused images for machine vision image processing
- User interface that provides the user with interactive and real-time manual control

3.1.3 Assembly and Installation

- All optical devices must contain adjustment to allow the device to be aligned optically
- The device must be designed so it can be easily assembled and dissembled to allow for adjustment to be made to various components
- The device must be designed to to sit on a desktop

3.1.4 Materials

- Materials to be used to position optical devices must have good mechanical stability and not deform significantly with small variation in temperature ($\pm 10^0$ C)

3.1.5 Ergonomics

- All sharp edges/corners should be removed to avoid personal injury

3.1.6 Cost

- The device cost should be kept at as low as possible. However, cost is not a major factor in project

3.2 System Concept Outline

A generic vision system is outlined in *Chapter 2: Section 2.2.* Based on the information researched in the literature review, and the specifications outlined in the PDS, a more detailed concept design is outlined below.

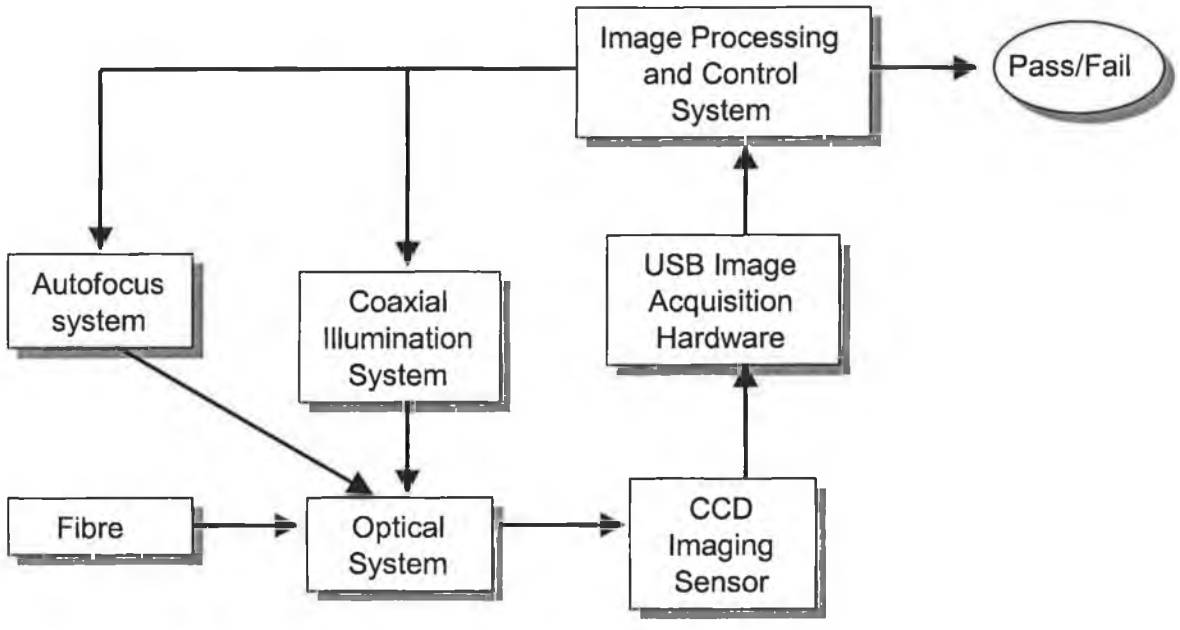

Figure 3-4 – Elements of an Automated Fibre Inspection System

Figure 3-4 details the various components of the proposed prototype and how they interact with each other.

- **Optical System** - optical system must be able to achieve a FOV of 1mm and detect objects 2μm in size
- **CCD camera** – ⅓ inch standard CCD camera with 6.5 μm square pixel size is to be integrated into the device
- **Image Acquisition Hardware** – USB acquisition hardware is to be used to provided an interface between the CCD camera and the PC
- **Illumination** – Coaxial illumination system

- **Autofocus** - Automated system that varies the distance between the optics and the optical fibre
- **Image processing and Control Software** –Software to interface between the PC and the device. Must allow bi directional control via the CCD camera and the autofocus system.

3.3 Design Concepts

Three different designs concepts were considered in order to achieve the specifications discussed in the PDS:

1. Single Magnification Lens System
2. Zoom Lens System
3. Three Lens System

3.3.1 Concept 1 – Single Magnification Lens System

Concept 1 was the first design envisaged for the optical fibre inspection system. The motivation behind the design of concept 1 was to make the device as simple as possible. By reducing the complexity of the device, the operational principles such as the optics and autofocus system could be understood more easily and there would be fewer difficulties in trying to implement such a system. A detailed diagram of concept 1 is shown in Figure 3-5. The main features of concept 1 are as follows:

- Stepper motor autofocus system with twin leadscrew guides
- Coaxial illumination system
- ⅓ inch, 6.5μm square pixel, CCD camera
- Single Magnification 20X microscope objective lens

While concept 1 contains the main features as required by the PDS, it is limited in certain aspects mainly in terms of the maximum feature size it can detect and the FOV achievable from the system. (**Note**: Calculations shown in *Appendix 1*)

- Maximum Feature size detectable: 0.65μm
- Maximum FOV achievable: 0.18mm

Concept 1 was therefore not considered a feasible option due to limitations of the imaging system.

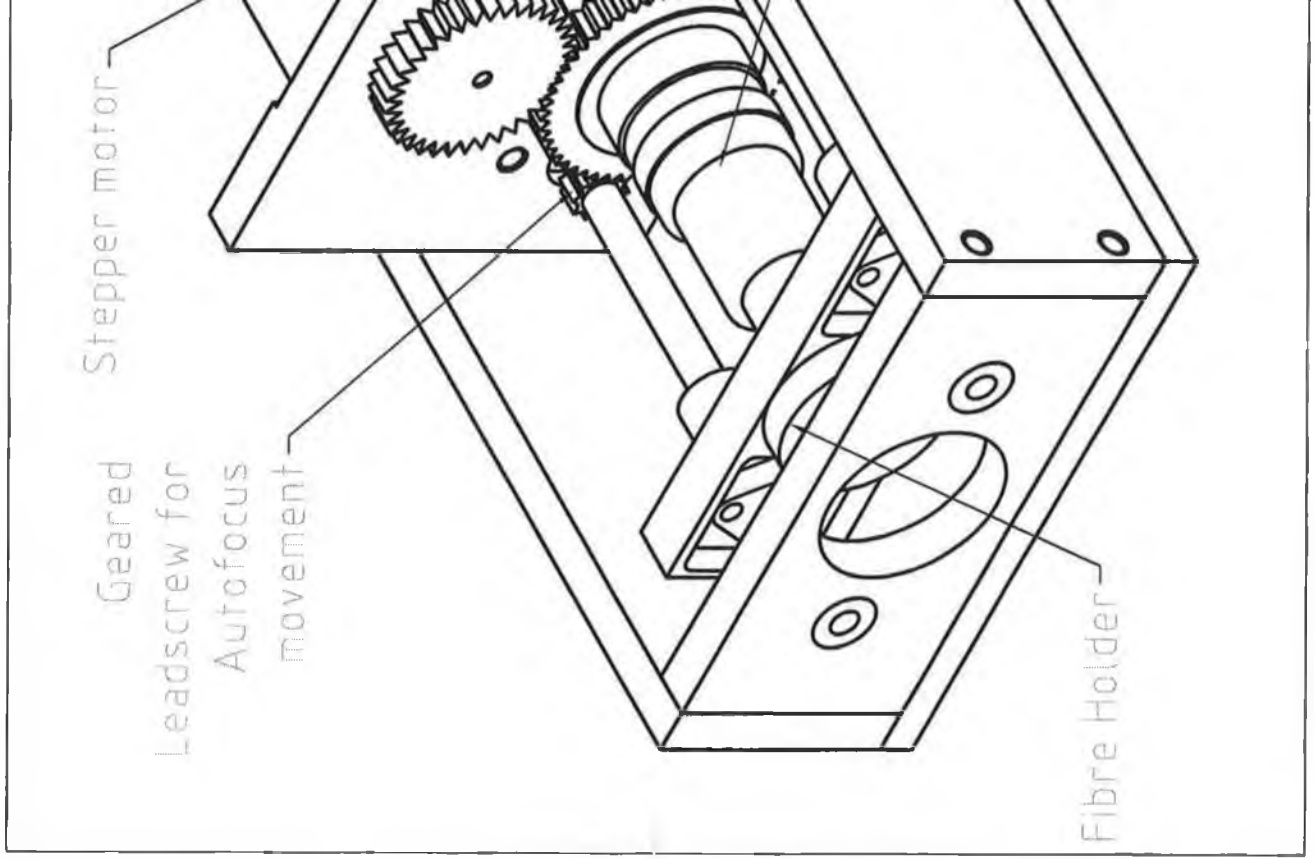

Figure 3-5 – Concept 1 Solid Model

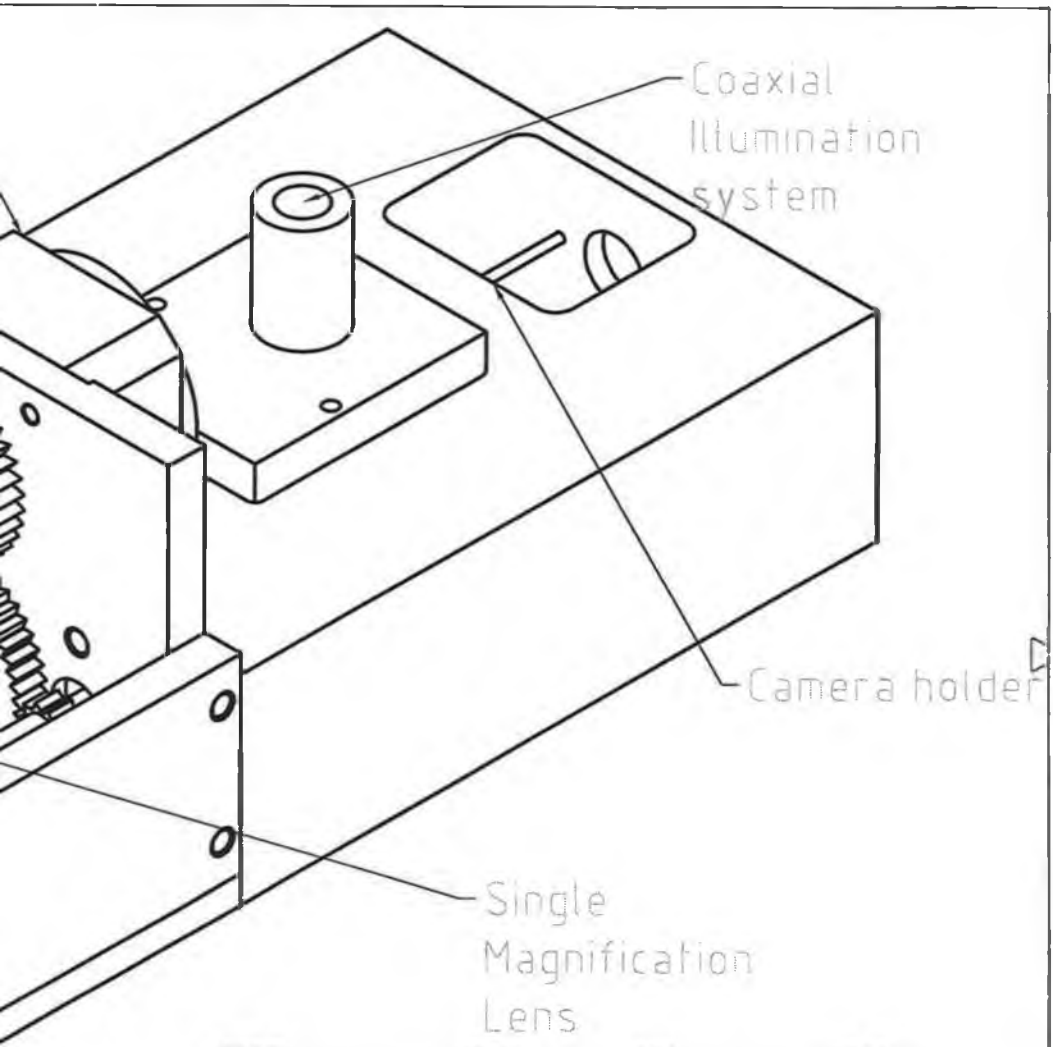

FILE NAME	FSCM NO	SHEET	SCALE
SIZE			
DRAWN			
CHECK			
APPR			
ISSUED			
REV		DWG NO	
CONTRACT NO		—	

3.3.2 Concept 2 – Zoom Lens System

Concept 2 took a more complex approach than concept 1 to the design of the system. The extra complexity was due to the optical system it required to achieve the necessary range of magnifications required. This entails the use of a zoom lens system with variable zoom from 1X – 20X magnifications. Figure 3-6 details a sketch of the system. Again, the system is a single optical axis system. Integrated into the system is a motorised zoom lens. This system moves one of the lenses, which in turn changes the focal length of the lens assembly and thus the magnification. A more detailed description of the operation of the zoom lens system is given in *Chapter 2: - Optical System Concepts- Zoom lens*. The main features of this system are:

- Stepper motor autofocus system with single leadscrew guide
- Coaxial illumination system
- ⅓ inch, 6.5μm square pixel CCD camera
- Motorised Zoom Lens System with range of 1X – 20X

The vision specifications for the system are:

- Minimum Feature size detectable: 0.65μm at 20X optical magnification
- Maximum FOV achievable: 3.6mm at 1X optical magnification

(**Note**: Calculations shown in *Appendix 1*)

These are well within specifications required from the PDS. But although the system achieves the main functionality as required from the PDS, there are certain disadvantages to such a system:

- Costs – Motorised zoom systems are expensive
- Zoom complexity – With any zoom system it is difficult to determine the actually magnification achieved each time without recalibrating the

system. Therefore precise measurements of defect size and fibre dimensions cannot be ascertained accurately.

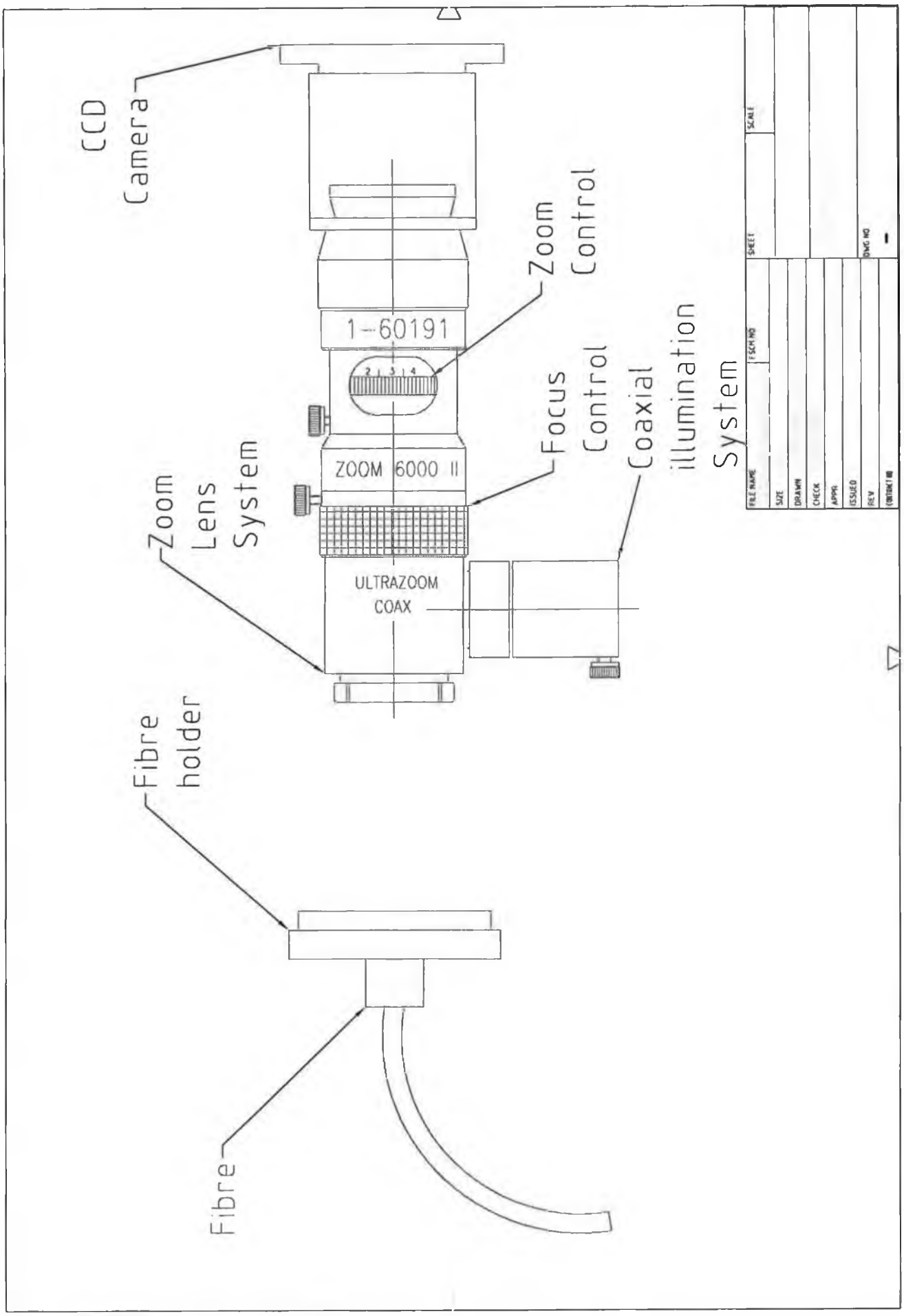

Figure 3-6 – Concept 2 Solid Model

3.3.3 Concept 3 – Three Lens System

Concept 3 is basically a trade off between the first two concepts. The basis of this concept is to use three microscope objectives to image different areas of the fibre. This method has the advantage of using set magnification lenses designed for microscopy and being able to achieve various magnifications to view the fibre area. The core of this design was to use low magnification lenses to image the outer area of the fibre and higher magnification lenses to image the inner regions of the fibre. As specified in Table 3-1, the smallest defect that needs to be detected in the outer regions of the fibre (Region C-F) is 10μm. Therefore the magnification required to achieve a resolution of 10μm is approximately 4X. To achieve the range of resolutions and fields of view required, a three-lens system was proposed, which uses various magnification lenses to view various areas of the fibre as specified below:

- Fibre Core (Region A) - High Magnification – 40X+
- Fibre (Region B) - Intermediate Magnification – 10X – 20X
- Ferrule and Outer Chamfer (Region C-F) - Low Magnification – 3X-5X

So using a 4X magnification lens would allow for the detection of 10μm objects and give the required field of view of 1mm, which is adequate for the outer areas of the fibre. The use of a 40X lens would allow for the system to detect features as small as 2μm while maintaining a field of view of approximately 90μm. This is adequate to image the fibre core, where it is necessary to detect this size of defect. A more detailed description of how the specific magnifications were decided upon is given in *Chapter 4: Detail Design- Section 4.1.1 Imaging System.* Figures 3-7 details a solid model of concept 3.

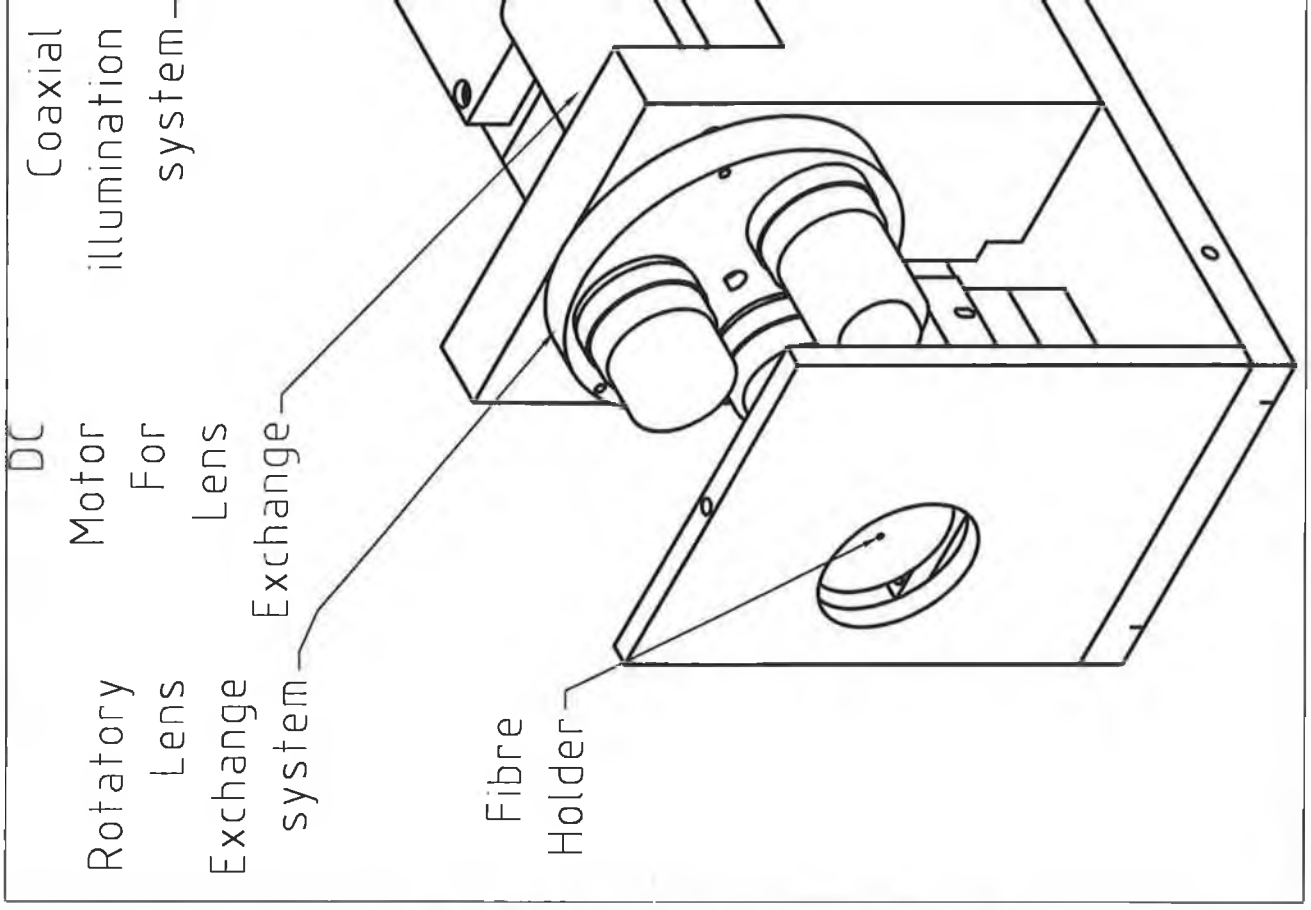

Figure 3-7 - Assembled Solid Model of Concept 3

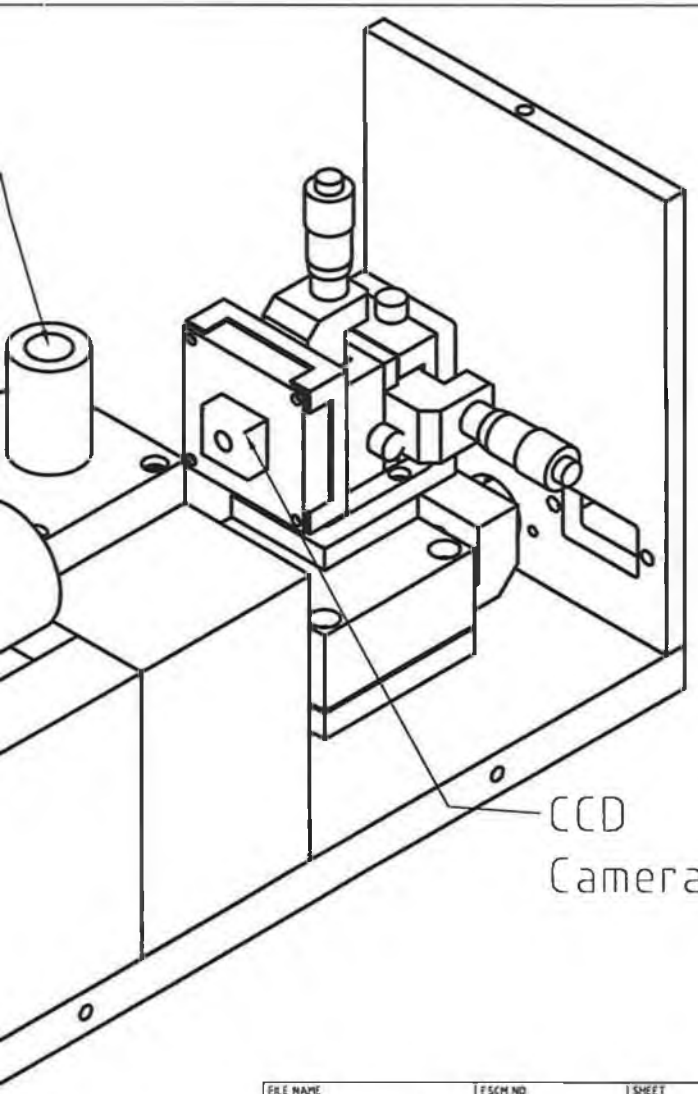

FILE NAME	FSCM NO	SHEET	SCALE
SIZE			
DRAWN			
CHECK			
APPR			
ISSUED			
REV		DWG NO	
CONTRACT NO		—	

3.3.4 Design Summary

In this chapter there has been a natural progression from concept 1 to concept 3. Concept 1 was designed with simplicity and cost in mind whereas concept 2 was complex and costly however it had excellent performance benefits. Concept 3 finds the middle ground between the initial two designs and takes the benefits of both the designs and integrates them into one design, this approach gives it superior cost and performance benefits over the other two devices. Therefore it was decided to pursue this design; the exact specifications for it are as follows:

- Imaging System:
    - ⅓ inch 6.5μm square pixel CCD camera
    - Automated three lens system
        - Low Magnification - 3X – 5X
        - Intermediate Magnification - 10X – 20X
        - High Magnification - 40X
- Illumination - Coaxial Illumination was found to be the most suitable method for illuminating the optical fibres
- Stepper motor autofocus system with single leadscrew guide
- Motorised lens exchange system with proximity sensor control
- X-Y-Z Axis Camera Adjustment for Optical Alignment
- Image Acquisition – USB 1.1 video acquisition
- Software Interface – Software interface that allows for direct access to image pixel values for analysis purposes.

The next chapter, *Chapter 4: Detail design* will discuss the implementation of this design into a working prototype based on the above specifications.

Chapter 4: Detail Design

This chapter discusses the detailed design and implementation of the optical fibre analysis system. The system design is discussed in two separate sections:

- System Hardware Design – The optical and mechanical design of the system
- System Implementation – Design of electronics, interfacing to PC and software interface coding

4.1 System Hardware Design

The primary hardware components that were required to be designed for proper implementation of the device are as follows:

- Imaging System
- Illumination System
- Autofocus System

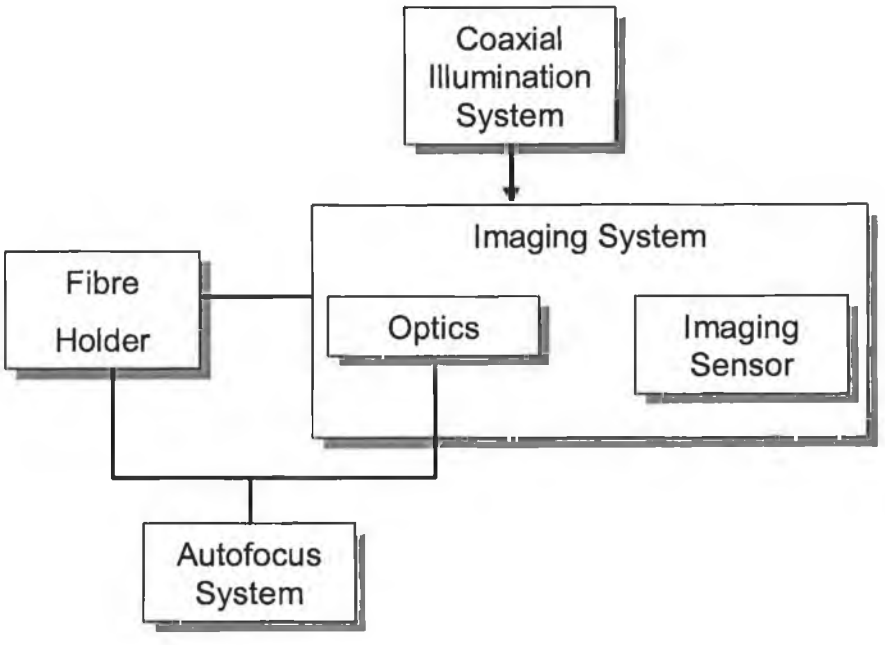

Figure 4-1 – Device Hardware Components

Figure 4-1 details the overall system flow between each component. The subsequent sections discuss in detail the mechanical design of each of these components.

4.1.1 Imaging System

The first stage of the hardware design was to design the optical system, as optical focal and image plane position, as well as the lens requirements, had to be known before mechanically designing the system. In order to determine the optical magnification requirements the field of view, resolution and sensor requirements must firstly be specified for the system.

Field of View: A maximum field of view of 0.9mm is required to image the complete diameter of the fibre connector.

Resolution: The resolution requirement of the system is determined by the size of the smallest detectable defect that needs to be detected. In this case defects as small as 2μm need to be detected on the fibre, so a system resolution of 500 l/p (line pair) per mm is required.

In specifying the optical system two factors will determine the resolution and field of view:

- The primary magnification of the lens - this is the ratio between the sensor size and the field of view. This is not the overall system magnification, as the image could still be magnified digitally.
- The sensor pixel size - in this case the pixel size used is 6.5μm squared (Figure 4-2).

The system resolution is therefore dependent on the primary magnification and sensor pixel size. Since the CCD pixel size remains constant, the only method of increasing the resolution is to change the optical magnification. In deciding what magnification to use a trade off has to be made between field of view and resolution, as the low magnification lenses will give a large field of view and a low resolution whereas as the high magnification lenses give a small field of view but a high resolution. To

overcome this problem, the proposal for the optical design was to use various magnification microscope objectives. Therefore for the outer fibre area a relatively large field of view, but a low resolution was required so a low magnification lens was used. For the inner areas a high-resolution image and a smaller field of view was required so a high magnification lens was used.

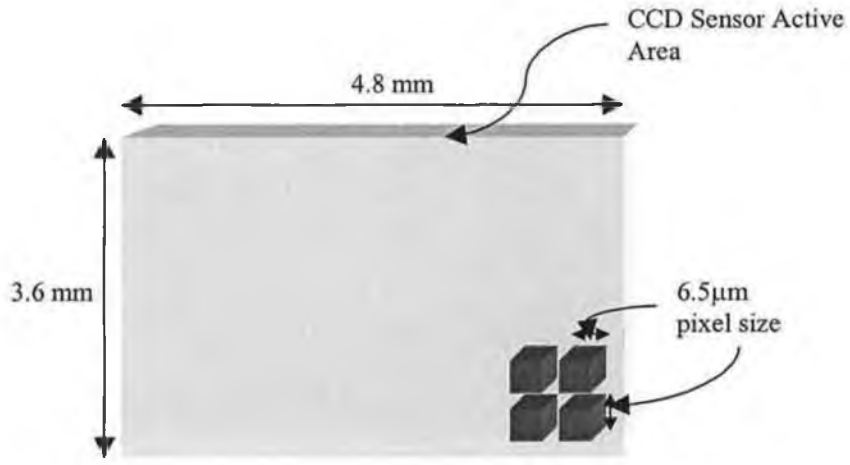

Figure 4-2 – CCD Sensor Dimensions

The approach taken to satisfy the optical requirements therefore was to segregate the fibre into three regions and view each region with a varying magnification lenses. The range of magnification for each of the lenses is shown is shown below:

- Low magnification (Range: 1X – 10X)
- Intermediate magnification (Range: 15X – 25X)
- High magnifications lens (Range: 30X – 40X)

The field of view and resolution requirements of the three lenses are as follows:

- Low Magnification
  - ⇒ Field of View = 0.9mm, as the overall surface of the optical fibre never exceeds 1mm (Figure 4-3)
  - ⇒ Resolution = 30µm, the smallest defect that needs to be detected in the outer fibre area is 30µm (Table 3-1)

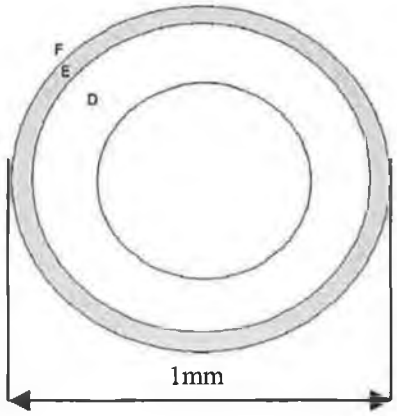

D = Ferrule Pedestal

E = Chamfer
D ≈ 0.9mm

F = Outside Cylindrical Surface
D ≈ 1mm

Figure 4-3 –The low magnification lens is used to view the outer area of the fibre which consists of the ferrule, chamfer and outside cylindrical surface

- Intermediate Magnification

  ⇒ Field of View = 200μm, as this is the maximum diameter of area C the ferrule surface (Figure 4-4)

  ⇒ Resolution = 2μm, the smallest defect that needs to be detected in the regions B and C is 2μm (Table 3-1)

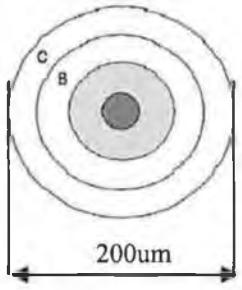

B = Fibre surface
Area outside fibre core to edge of fibre(125μm)

C = Ferrule Surface
Ferrule area covering area from 125 to 200 μm

Figure 4-4 –The intermediate magnification lens is used to view the central area of the fibre which consists of the fibre surface and the ferrule surface which holds the fibre in place

- High Magnification

  ⇒ Field of View = 95μm, the high magnification lens should be able to image the entire core. 95μm represents the maximum possible size of the fibre core for both multimode and single mode fibres (Figure 4-5)

  ⇒ Resolution = 2μm, defects as small as 2μm need to be detected in the central core of the fibre.

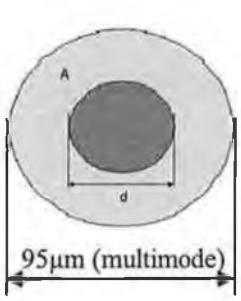

A = Restricted Area
'd' = core diameter of fibre
d for single mode = 8 µm
d for multimode = 62 µm
A = 66µm for single mode
A = 95µm for multimode

Figure 4-5 –The high magnification lens is used to view the fibre core

In order to achieve the field of view and resolution requirements, microscope objectives had to be chosen at a set magnification. In deciding what resolution and field of view can be achieved by an imaging system, a good starting point is to satisfy the field of view requirements by choosing a set magnification and then determine what resolution this magnification will yield.

4.1.1.1 Low Magnification Lens Calculations.

To image the entire area of the fibre a field of view of 0.9mm is required. Since the fibre is circular in cross-section, the limitation for the field of view is the shortest dimension of the imaging array. The ⅓" format CCD has a vertical dimension of 3.6mm and a sensing pixel size of 6.5µm. By applying equation 2-3 this field of view may be obtained using a ⅓-inch format CCD, together with an optical magnification of 3.6X:

⅓" CCD format $\Rightarrow SS = 3.6mm$

$FOV = 0.9mm$

$$M = \frac{SS}{FOV}$$

$\therefore$ **M = 3.6X**

At this optical magnification, the object resolution in the digitised image will be given by equation 2-8 as:

$PS = 6.5\mu m$

$$O.Res = \frac{2 * PS}{M} = 3.61 * 10^{-6}\, lpm$$

∴ Object Res = 3.61 lp per μm

Thus the smallest defect that can be detected is 3.61μm, this does not mean the defect can be resolved, as to resolve a defect it must contain a certain amount of information. According to Johnson's Criteria [44], the smallest resolvable object is:

$$SRO = O.Res * 7.5 \qquad \textbf{Equation 4-1}$$

∴ SRO = 27μm

SRO: Smallest resolvable object

Therefore the smallest object that can be detected at this optical magnification is 27μm (Equation 4-1).

4.1.1.2 Intermediate Magnification Lens calculations

The second area to be analysed covered the area from 94μm to 200μm so a field of view of 200μm was required. Again applying equation 2-3 this field of view may be obtained using a ⅓-inch format CCD, together with an optical magnification of 18X:

⅓" CCD format $\Rightarrow SS = 3.6mm$

$FOV = 200\mu m$

$$M = \frac{SS}{FOV}$$

∴ M = 18X

The object resolution at this magnification is 0.722 lp (line pair) (See below).

$$O.Res = \frac{2 * PS}{M} = 0.722 * 10^{-6}\, lpm$$

∴ Object Res.= 0.722 lp μm

At this object resolution, the minimum resolvable object size is 5.42μm (Equation 4-1).

$$SRO = O.Res * 7.5$$

$$\therefore \mathbf{SRO = 5.42\mu m}$$

The smallest detectable defect here was 10μm, with the exception of ferule scratches, which are 2μm. Using a magnification of 18X allows 36 pixels per 10μm defect and 7.2 pixels per 2μm defect. While 7.2 pixels per defect is less than the requirement of Johnson's criteria of 15 pixels, it was considered adequate, as due to the basic geometry of scratches very little information is required to detect them.

4.1.1.3 High Magnification Lens Calculations

The high magnification lens is necessary to achieve an adequate resolution to image the core of the fibre. Complex defects as small as 2μm need to be detected within this central core to a field of view of 95μm. To achieve this field of view an optical magnification of 38X is required (See below).

⅓" CCD format $\Rightarrow SS = 3.6mm$

$FOV = 95\mu m$

$$M = \frac{SS}{FOV}$$

$$\therefore \mathbf{M = 38X}$$

At this magnification, the object resolution is 0.34 lp (line pair) (See below).

$$O.Res = \frac{2 * PS}{M} = 0.34 * 10^{-6} lpm$$

$$\therefore \mathbf{Object\ Res. = 0.34\ lp\ \mu m}$$

This yields a minimum resolvable object size of 2.56μm (Equation 4-1); while this is outside the specifications of the system, in order to build a feasible system some trade-off has to be made between maximum field of view and minimum resolution. Alternatively a higher spec sensor could be employed to get the required specifications.

Table 4-1 below summarises the imaging system parameters for each optical magnification. In each case, the required field of view can be achieved at the given magnification; however, the required resolvable object size is not always achieved.

	FOV Required	MAG Required	Vertical Pixel Size	Object Resolution	Resolvable object size	Required Resolvable object size
Area 1	1mm	3.6X	6.5 μm	3.61 lp	27μm	30μm
Area 2	200μm	18X	6.5 μm	0.722 lp	5.42μm	10-2μm
Area 3	95μm	38X	6.5 μm	0.34 lp	2.56μm	2μm

Table 4-1 - Summary of required and theoretical imaging system parameters

In order to build the system to the required specifications, objective lenses of 3.6X, 18X and 38X are required. However, it was not possible to purchase off-the-shelf objectives at these magnifications. Therefore standard lenses had to be chosen with magnifications close to the values required. The final values chosen were:

- 4X - Low Magnification
- 20X – Intermediate Magnification
- 40X – High Magnification

As detailed in *appendix 2* there is a limited amount of standard lenses available and the magnifications were chosen so as to closely match the system requirements. Table

4-2 below details the field of view and object resolution achievable at these magnifications using a ⅓" CCD format.

	MAG	FOV	Object Resolution	Minimum Resolvable Object Size
Area 1	4X	0.9mm	3.25 lp	24.375 μm
Area 2	20X	180μm	0.65 lp	4.88 μm
Area 3	40X	90μm	0.325 lp	2.43 μm

Table 4-2 – Final Imaging System Parameters

The objective lenses chosen were Edmund optics DIN (Deutsche Industrie Norm) 45mm standard achromatic objective lenses, as they provided a good trade off between cost and performance (*Appendix 2*). These lenses had a standard tube length of 160mm; therefore the CCD had to be mounted 160mm from the objective-mounting flange. Having determined the optical specifications, the detailed mechanical design of the system can now be explained.

4.1.2 Detailed Mechanical Design

In designing the prototype system, the approach taken was to firstly design a skeleton imaging system and then design all the addition components around the imaging system. The mechanical requirements of the system were as follows:

- Three lens optical system with automated lens exchange
- Autofocus system with single leadscrew guide
- Coaxial illumination system
- X-Y-Z Axis camera adjustment for optical alignment

4.1.2.1 Imaging System

The imaging system consists of the following mechanical components:

- Three objective lenses with 0.8" *36 TPI mounting thread (*Appendix 2*)
- CCD sensor with X-Y-Z axis adjust

In addition to these components, the system must be automated and be able to accommodate an illumination system and autofocus system. The mechanical requirements of the optical system are:

- The distance from the lens mounting flange to CCD must be 160mm
- There must be one optical axis and it must be possible to rotate each lens into a position concentric with the optical axis via a fully automated system
- Each lens on rotation into position must be concentric with the optical axis

The optical system design consists of three objective lenses, a lens exchange system and a CCD sensor mounted on an X-Y-Z stage. The lens exchange system consists of a rotary holder that rotates on a DC motor armature, the three lenses are position 120^0 apart in the holder and can be position concentrically with the optical axis (Figure 4-6) The optical axis is positioned off axis to the DC motor axis, so as to maximise

the distance between the motor and the axis while minimising the overall size of the rotary holder (Figure 4-6).

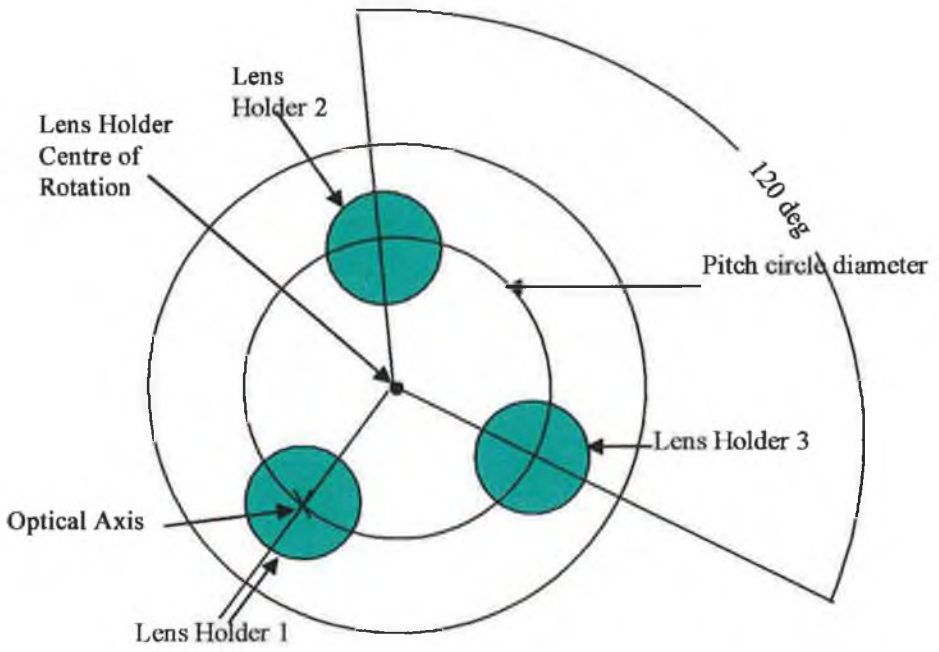

Figure 4-6 – Lens Exchange System

To locate each lens accurately on the optical axis, a ball bearing mechanism is used to ensure the mechanism stops at the same location each time. A spring-loaded ball bearing is located behind the lens holder (Figure 4-7). When a lens is rotated into position, a hole is also positioned in line with the ball bearing, which compensates for any error in the motor position. This mechanism is similar to the one employed in microscope systems to centre the lenses concentrically with the optical axis.

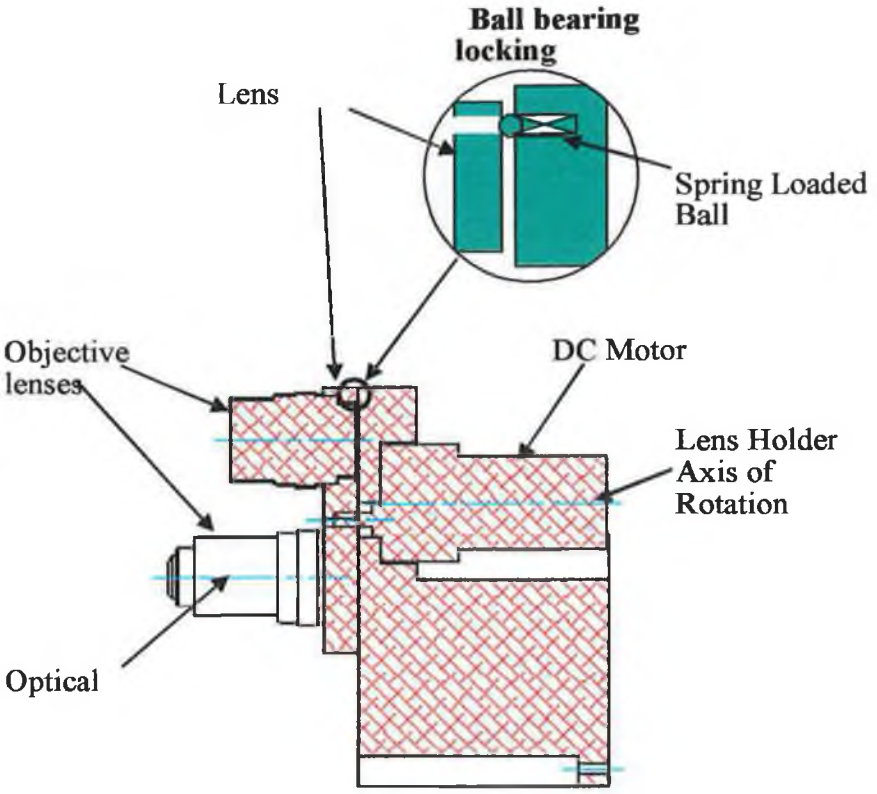

Figure 4-7 – Cross sectional drawing (Through optical axis) of lens rotation mechasism. Spring loaded ball bearing positioning system is used to position the lens concentric with the optical axis.

Figure 4-8 details a solid model of the final optical system design. The CCD sensor is mounted on an X-Y-Z micrometer stage to allow it to be aligned with the optical axis and also to precisely position it on the optical image plane.

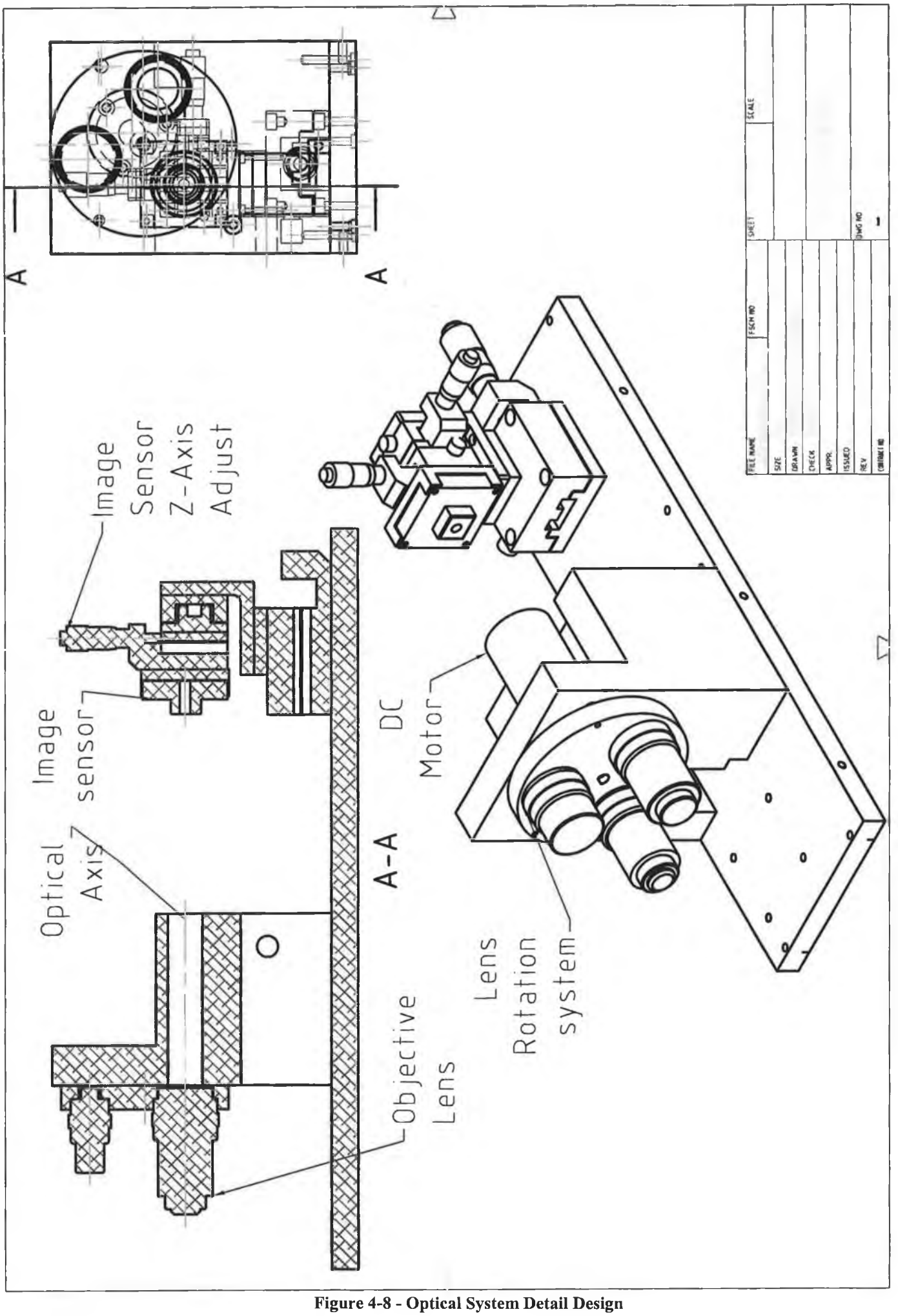

Figure 4-8 - Optical System Detail Design

4.1.2.2 Autofocus System

The autofocus system requires a mechanism to change the distance between the lens and CCD, or lens and object, in order to focus the system. Therefore some form of position control had to be designed into the device to provide this functionally. In designing the mechanical aspects of the autofocus system the minimum depth of focus of the optical system needs to be known, as the autofocus mechanical system must be able to achieve this precision in movement; otherwise the system will not focus correctly. In this case, the optical system's minimum depth of focus will occur when using the 40X lens, the theoretical depth of field can be calculated using equation 2-5:

$$\text{Depth of Field} = \frac{\lambda}{NA^2}$$

NA (40X lens) = 0.65

λ = 650nm (Approximate Wavelength of red light, red light was chosen as the CCD is more sensitive to this wavelength of light and thus produces a sharper image)

$\therefore$ Depth of field =1.53μm

Therefore a mechanical system that can achieve precision movement of 1.5μm is required to adequately implement the autofocus system. It was proposed to do this using a precision micrometer leadscrew coupled with a stepper motor (Figure 4-9). A stepper motor was chosen as it provides a lowest cost, high precision solution. The micrometer chosen was a 0.5mm per revolution Optosigma micrometer [45]. In order to achieve the required resolution with this micrometer, a 1.8^0 4-phase stepper motor was coupled with the micrometer. This system connected with a half stepping driver would allow for 400 steps per revolution. This would provide an overall resolution of

1.25μm, which is in excess of the minimum resolution requirement (Ref calculations below):

1.8^0 Stepper Motor gives 200 steps per revolution

Using a half-stepper driver $\Rightarrow$ 400 steps per revolution

Micrometer resolution = 500μm/rev

Therefore linear movement per step = 500/400 = 1.25μm

Figure 4-9 details a solid model of the final mechanical design of the autofocus system. It consists of a stepper motor coupled with the micrometer. A flexible coupling joins the two devices to compensate for any misalignment between them. The fibre will be mounted via a holder on the stage, which will provide linear movement parallel to the optical axis to focus the device.

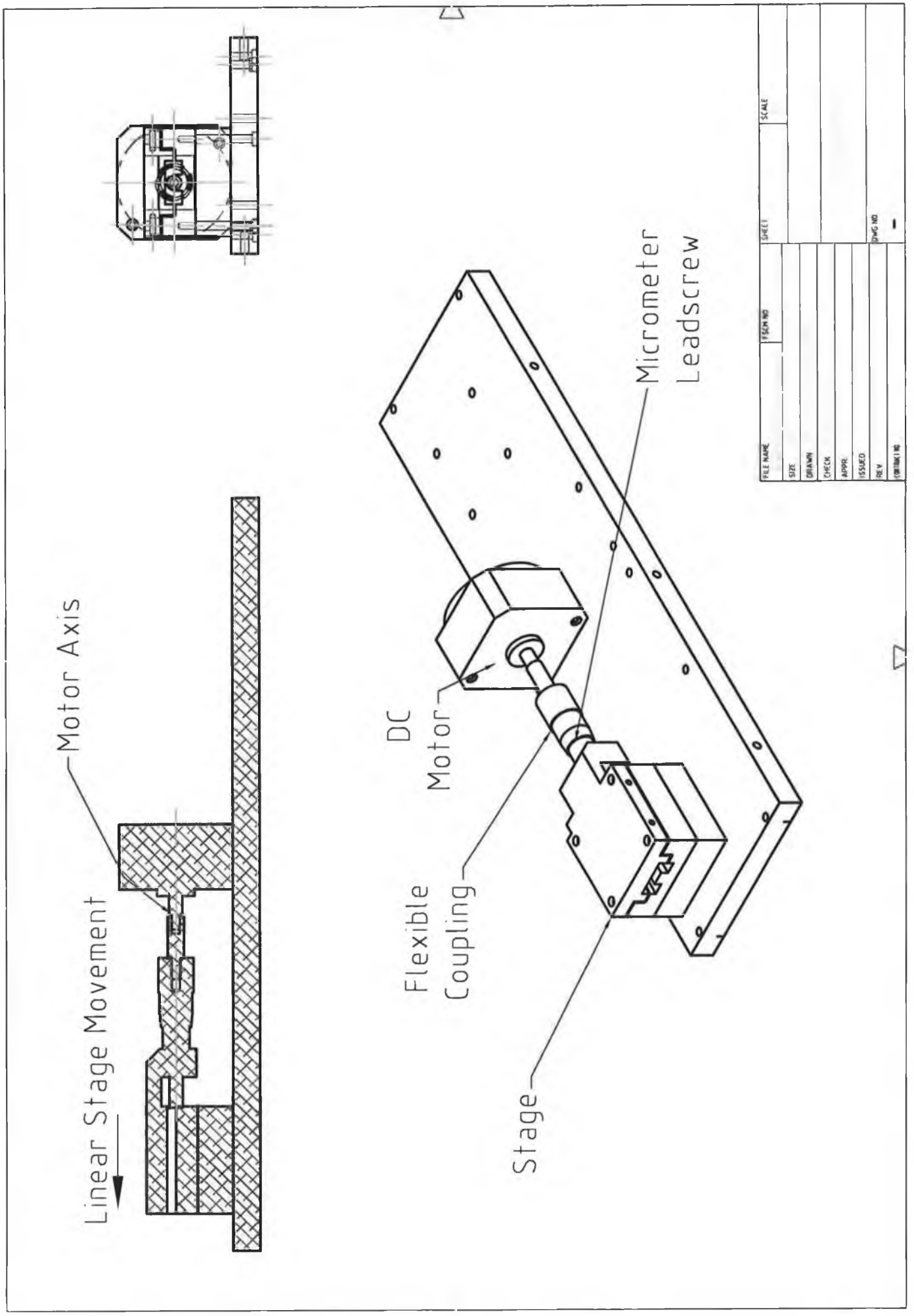

Figure 4-9 – Cross section solid model of Autofocus System

4.1.2.3 Illumination System

The lighting system used to illuminate the optical fibre was a diffused axial illumination system. Diffused axial illumination uses a half silvered mirror to illuminate the object from behind. Since the light is transmitted along the optical axis, it allows for shadow free illumination, which greatly improves the image quality and allows for increased measurement accuracy. The diagram below (Figure 4-10) details the main components of a diffused axial illumination system and how they relate to the position of the sensor lens and objects.

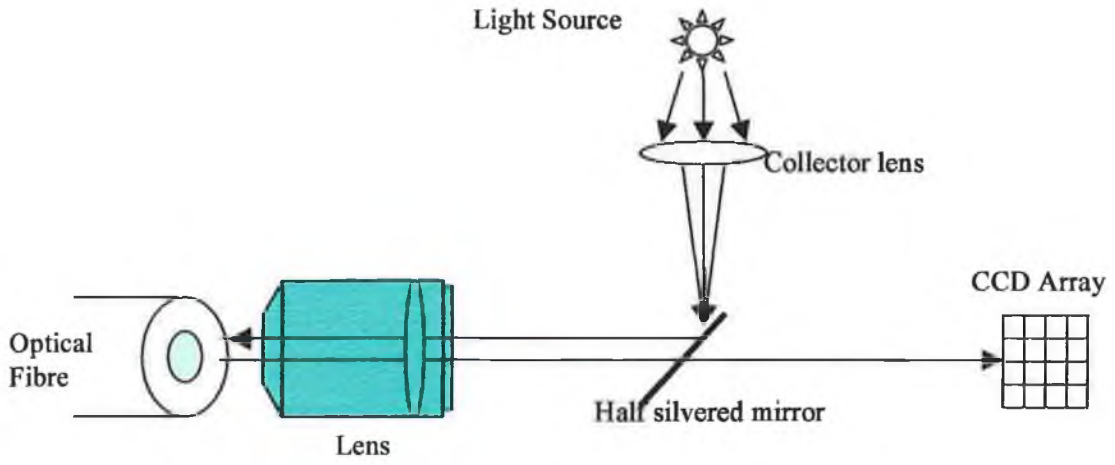

Figure 4-10 – Component layout of diffuse axial illumination system

The light source used to illuminate the object was a red LED, chosen as the CCD sensor is more sensitive to this wavelength of light and thus will form a clearer sharper image. Also, by keeping the wavelength of light within the confines of one colour spectrum, the occurrence of chromatic aberrations is prevented. Figure 4-11 details a cross section of the final design of the illumination system. The primary components of the system are a LED holder, light collimating tube and a holding block. The holding block has a face machined into it at a 45^0 angle, which holds the half silvered mirror in position. This set-up allows the light from the LED to be reflected along the optical axis to illuminate the fibre, and also light reflected from the fibre to travel through the mirror onto the CCD to form an image.

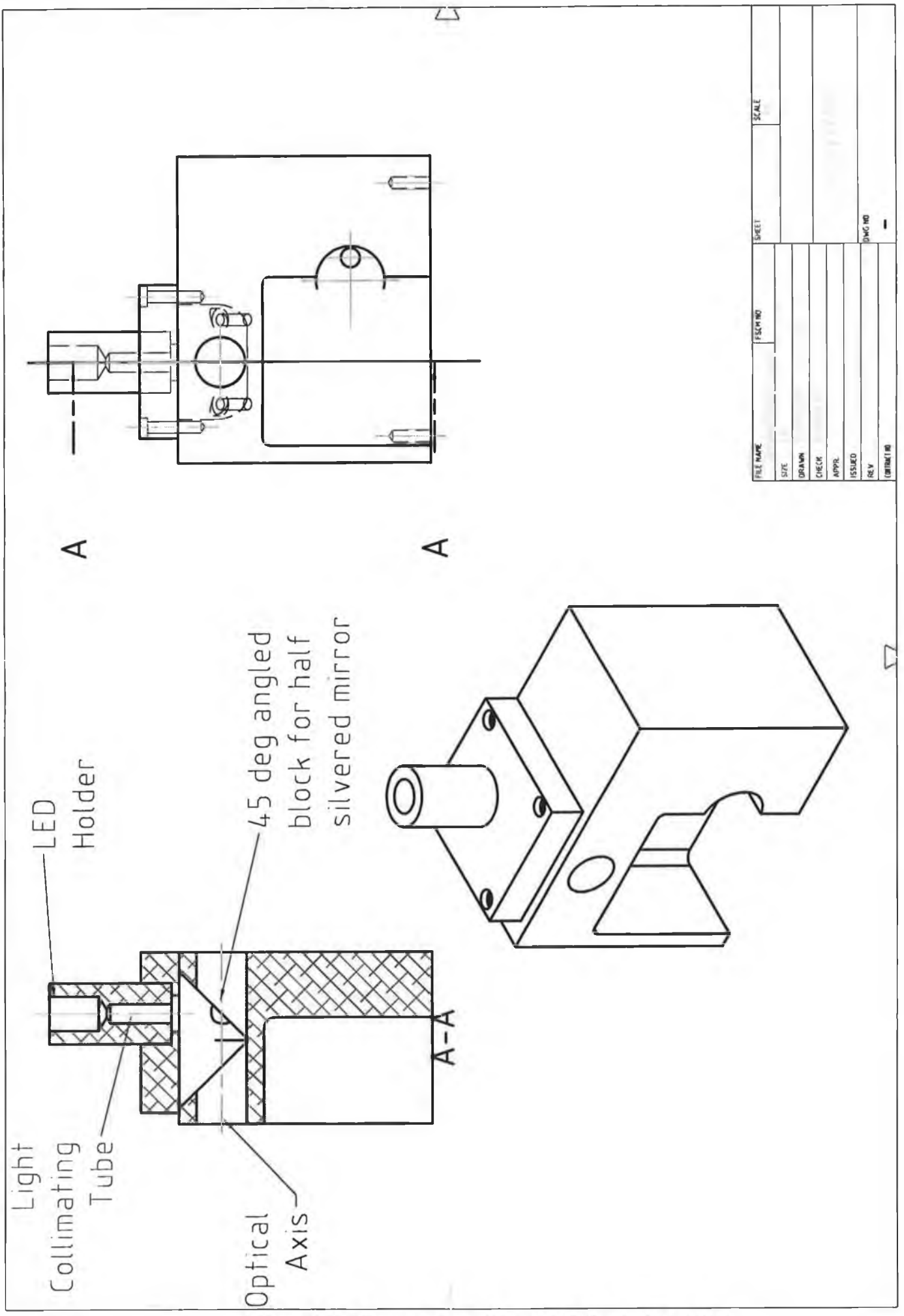

Figure 4-11 – Cross- section solid model of Illumination system

4.1.3 Final Assembly

On completion of the design the prototype was manufactured according to the drawings in *Appendix 5*. Figure 4-12 details an image of the final half assembled model that was manufactured. Isometric and exploded isometric drawings are detailed in Figure 4-13 and Figure 4-14. The components of the device and their applications are:

- Optical fibre holder
- Focusing system – An optical stage with 0.5mm leadscrew connected to a 1.8^0 stepper motor.
- Rotary lens holder – Rotate each lens as required into a position concentric with the optical axis
- Illumination system – Illuminate the fibre
- CCD Imaging sensor – Produces video output of fibre endface
- X-Y-Z axis CCD adjustment – Adjustment system for accurate positioning of CCD sensor

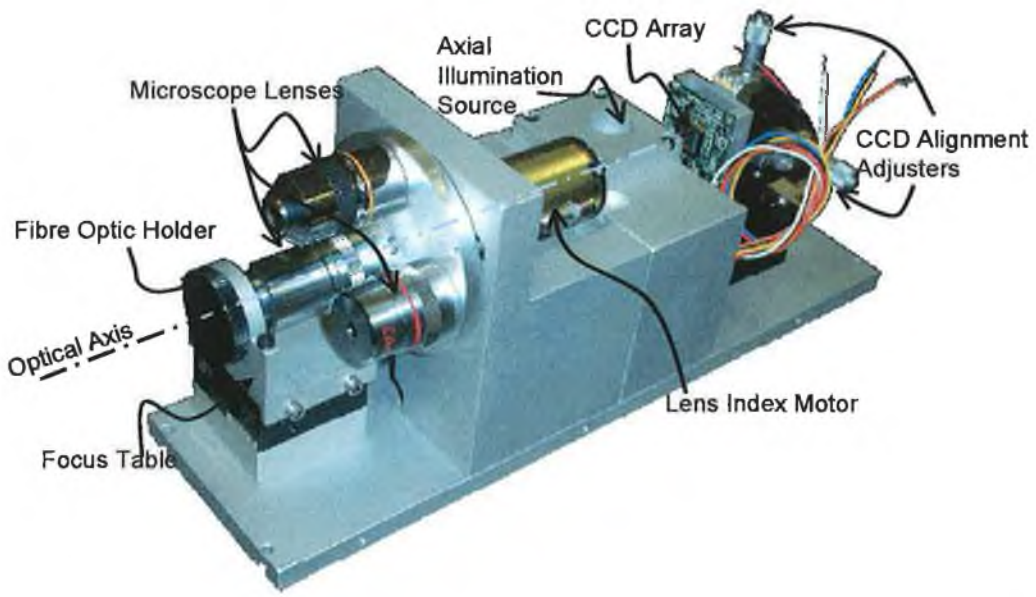

Figure 4-12 - Final partially assembled prototype, design was centred around the optical axis with the three microscope objectives rotated into position via rotary holder with its axis of rotation running parallel to the optical axis.

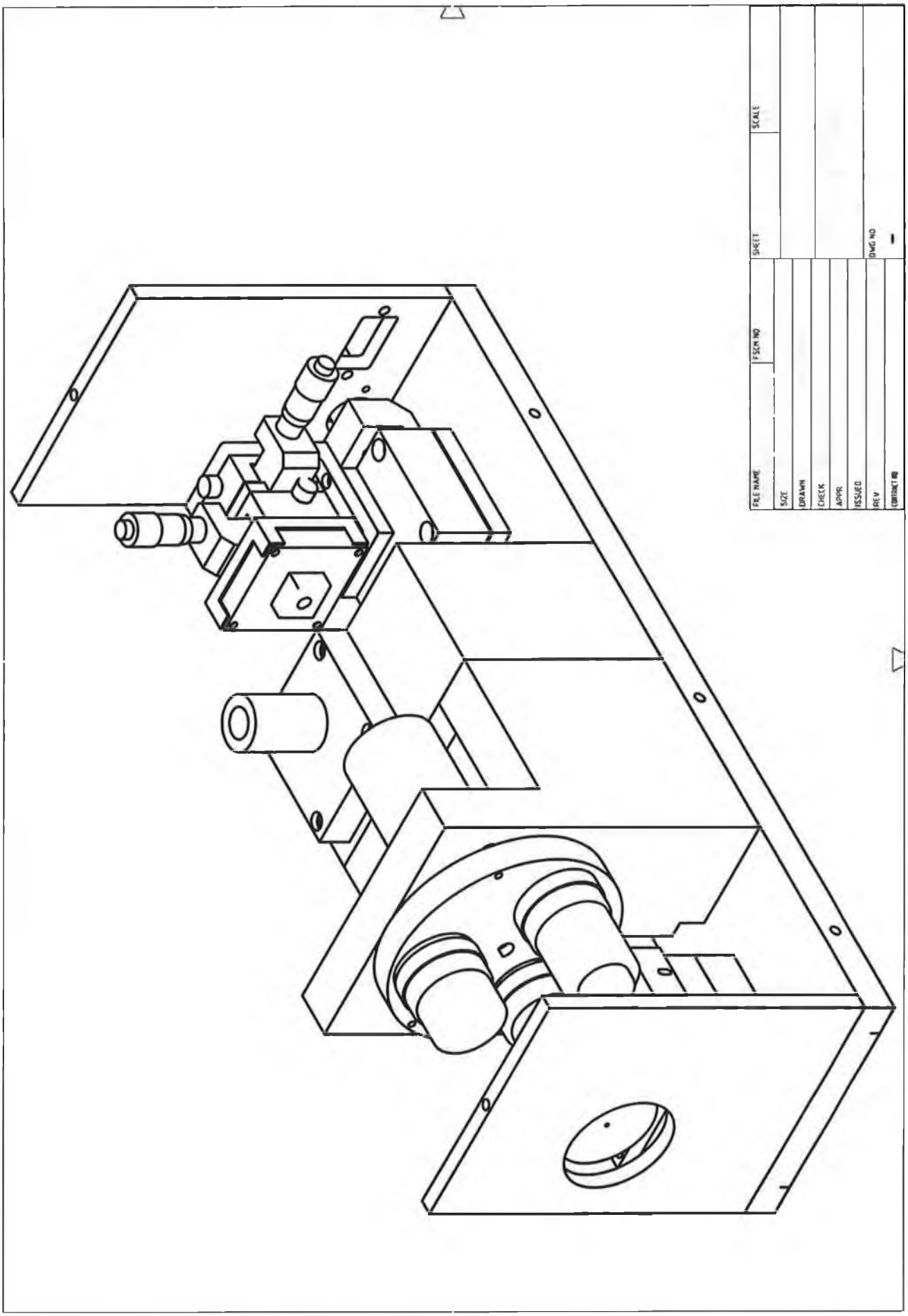

Figure 4-13 – Isometric view of final design

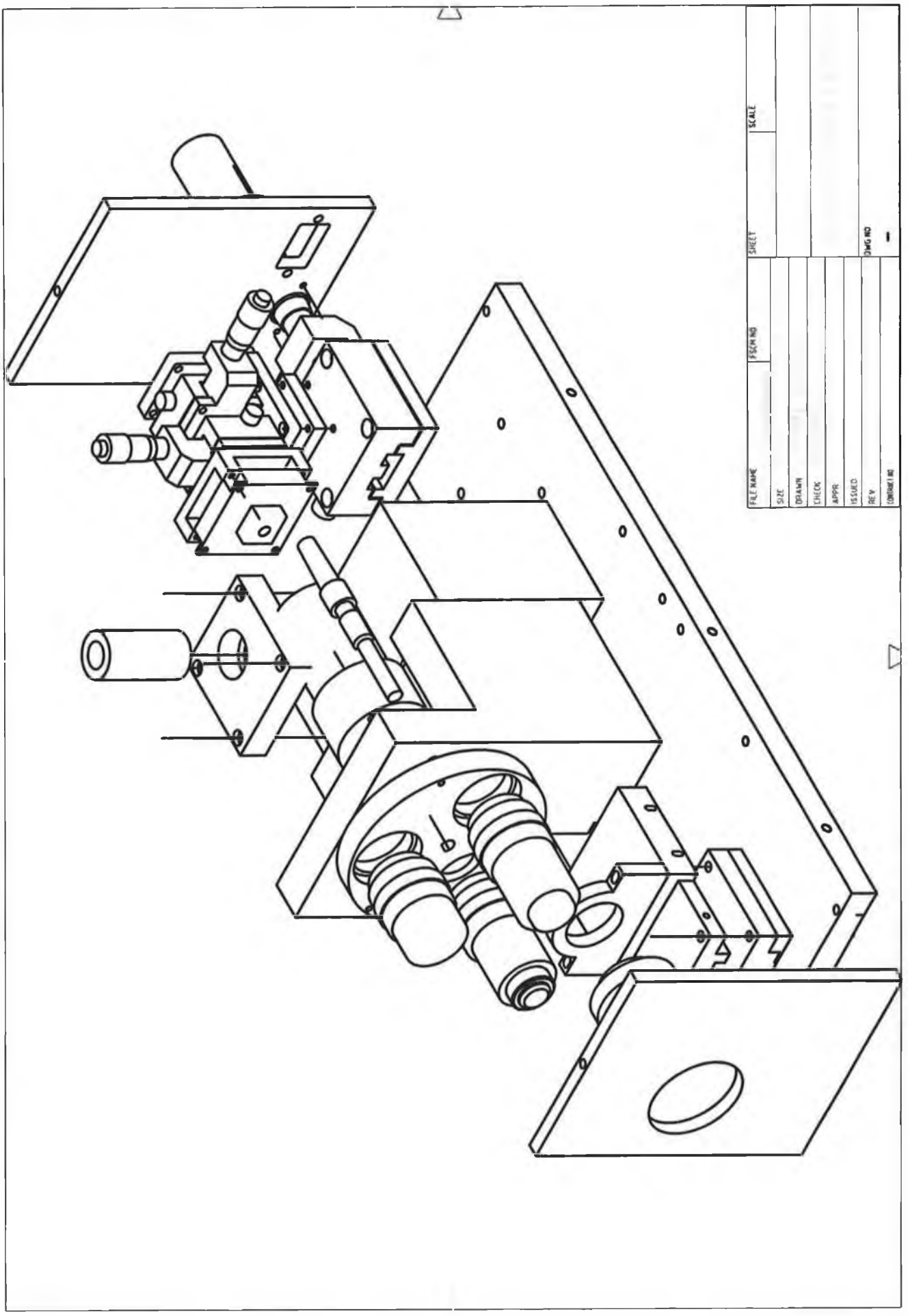

Figure 4-14 - Exploded Isometric view of final design

4.2 System Implementation

To implement automated control, system functions such as lens rotation, autofocus and image acquisition required a hardware and software interface. The hardware developed tried, where possible, to use external PC input ports. These made the system more flexible and also reduced the system cost, as expensive PCI cards were not required. The software is written in Visual C++, as this language allows easy design of graphical user interfaces, access to parallel and USB ports and an application-programming interface for playing and rendering video inputs. Figure 4-15 below illustrates the data flow and exchange between each system component.

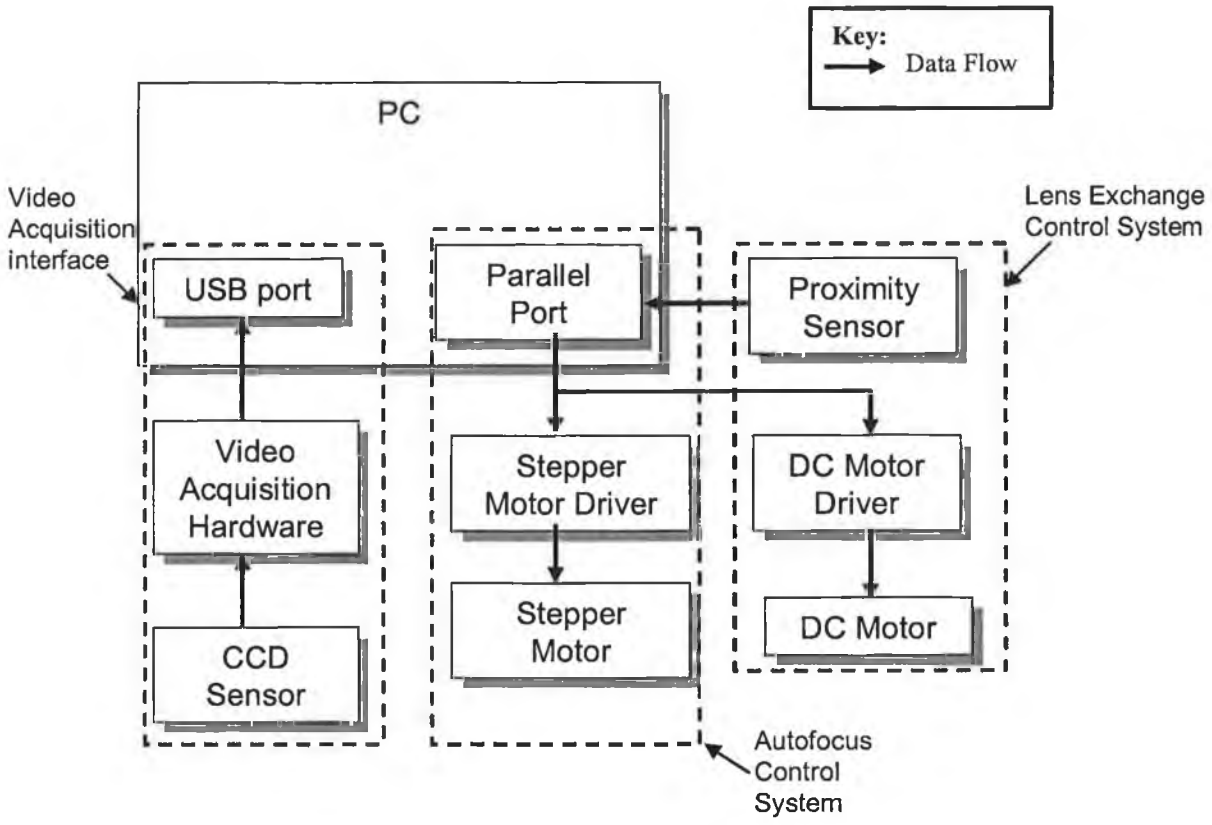

Figure 4-15 - System data flow and exchange

The subsequent sections discuss how both the hardware and software interface for each of these components were implemented.

4.2.1 Lens System Control

The rotation of the lenses into a position in line with the optical axis is controlled via a 12V DC motor and a proximity sensor. The motor used has gearing ratio of 50:1 and can achieve torques of up to 50mNm (*Appendix 2*). A proximity sensor is used in conjunction with the motor to give feedback as to the lens position in relation to the optical axis. The mechanical set-up of the system is such that when a lens is aligned with the systems optical axis, a corresponding hole in the lens holder is aligned with the proximity sensor (Figure 4-16)

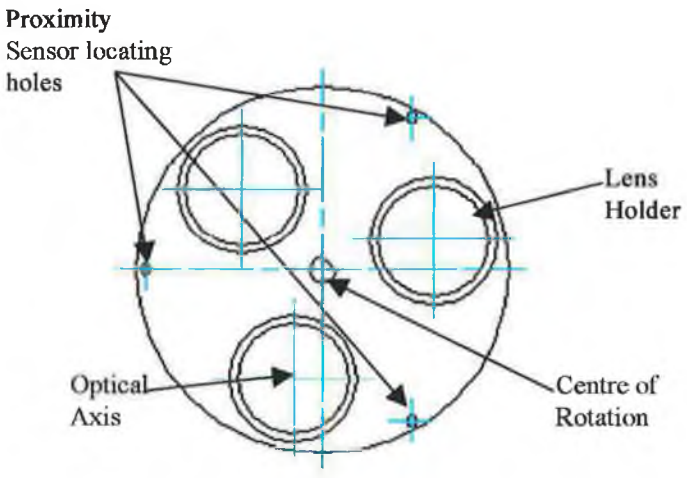

Figure 4-16 – Lens location feedback system

The proximity sensor is an inductive sensor that is active when metal is within 0.8mm±0.08mm of its sensing face (*Appendix 2*). So when the hole is aligned with the sensor's front face, it gives a low output signal, as no metal is present. Feedback from the proximity sensor is then used to control the motor positioning as when the proximity sensor is aligned with a hole, the lens is aligned with the optical axis.

4.2.1.1 DC Motor Control

To control the motor adequately, control is required over both the speed and the direction. The method used to control these variables is pulse width modulation (PWM) control for the speed and a H-bridge circuit to control the direction. Pulse width modulation works by driving the motor with short pulses to get varying degrees of torque and thus varying degrees of speed. These pulses vary in duration to change the speed of the motor; the longer the pulses, the faster the motor turns and vice versa. Incorporating a H-bridge circuit in this set-up allows both the direction and the speed to be controlled. H-bridges work by switching the polarity of the motor and thus control the motor direction. Relays are commonly used for high power motors, but for low power motors semiconductor H-bridges can be used. Semiconductor H-bridge systems use transistors to switch the polarity. A diagram of a standard semiconductor H-bridge circuit is detailed in Figure 4-17 [46].

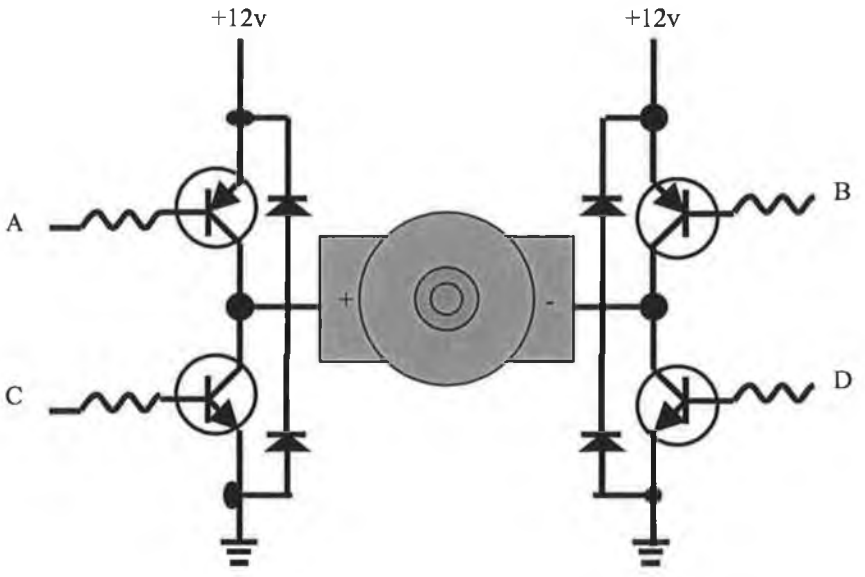

Figure 4-17 – H-bridge Motor Circuit

The transistors in the circuit control the power and ground connections to the motor terminals. The high side drivers use PNP transistors, as they act as good current sinks; the low side drivers use NPN transistors, as these are good current sources [46].

(Diodes are required in the circuit to prevent voltage that is generated by the motor coil when the power is switched on and off damaging control circuit). The truth table for the circuit is shown in Table 4-3.

A	B	C	D	Function
1	0	0	1	H (Forward)
0	1	1	0	L (Reverse)
1	1	0	0	Z (Brake)
0	0	1	1	Z (Brake)

Table 4-3 – Truth table for H-bridge circuit

Rather than build a H-bridge from the basic components, a standard H-bridge device circuit was used, the L293D (*Appendix 2*). The L293D is an integrated circuit motor driver that can be used for bi-directional control of up to two DC motors. The integrated circuit provides both direction and motor enable control. Table 4-4 details its one channel truth table.

Input	Enable	Output
H	H	H (Forward)
L	H	L (Reverse)
H	L	Z (Brake)
L	L	Z (Brake)

Table 4-4 – L293D one channel truth table

While the L293D provides directional and start stop control, in order to control the speed, a pulse width modulation control circuit had to be built in conjunction with the H-bridge driver. In order to implement this, a modulation system was built which allowed for control in the motor switching duration. This variation was achieved via an edge triggered D-flip-flop with an external clock signal supplied from a PC output port. By setting reset = 'low' and pulsing set on and off a square wave signal is generated at the Q_1 output pin (Figure 4-18). The pulse width of this signal can be controlled by changing the period of the clock signals, thereby controlling the speed of the motor. The longer the duration of the pulse, the faster the motor speed. The

reset signal allows the motor to be turned on and off - when it is low the clock signal pulses the motor on and off, when it is high the flip flop Q_1 pin outputs a low signal which disables the motor.

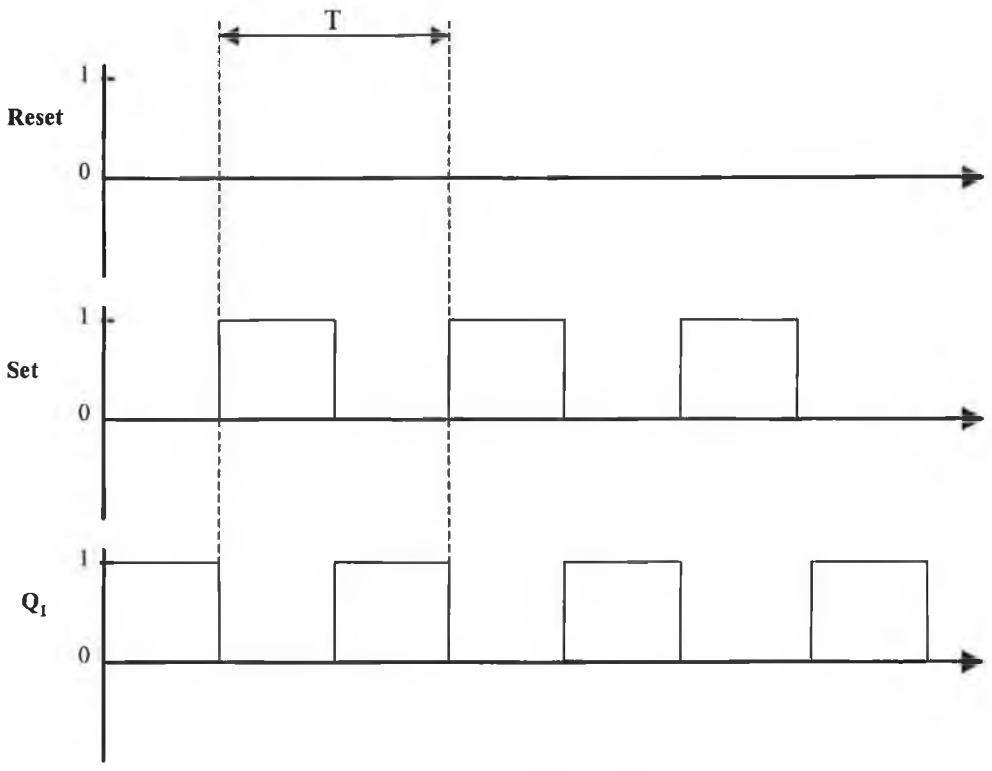

Figure 4-18 - Timing Diagrams for D-Flip flop

The complete circuit used to control the DC motor is shown in Figure 4-19. A 747D low power shottky IC was used to implement the PWM motor control (*Appendix 2*). The Q_1 output from this was connected to the motor enable signal of the L293D IC. This circuitry allowed for direction and speed control over the DC motor. These inputs were provided through a hardware interface to the PC. The PC parallel port provided this interface, as it was easy to access via software and required no communications protocol. Section 4.3.2.1 of this chapter explains the interface to the parallel port in detail.

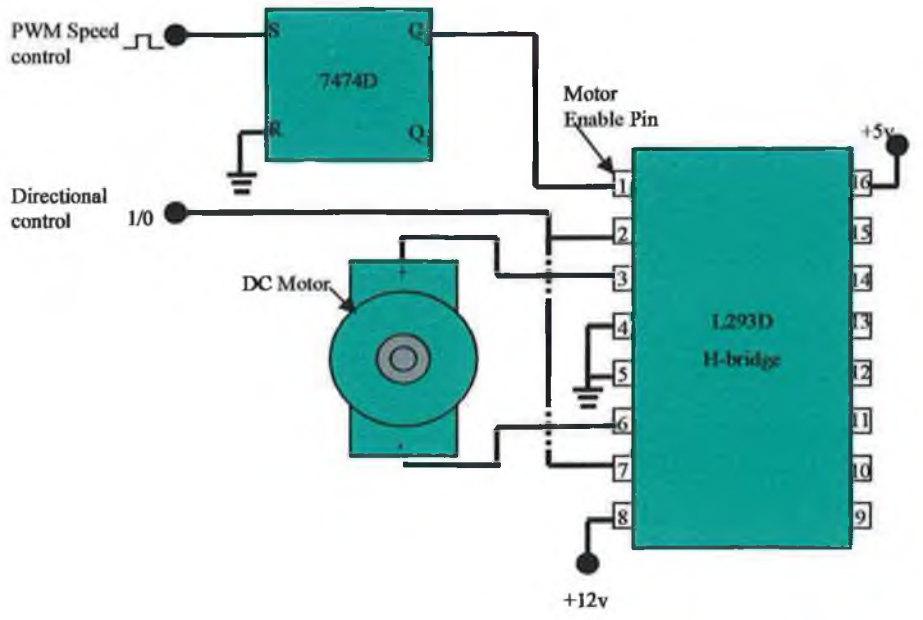

Figure 4-19 - DC motor control circuit

To control the lens system a software algorithm was required that took the hardware inputs from the proximity sensor and control flags from the software interface to determine the speed and direction signals to be sent to the PC parallel port (To drive DC motor). The basis of this control algorithm is outlined in Figure 4-20. The start point of the algorithm is a software flag called 'Lensmove' that requests the lens move and an input from the proximity sensor. On activation of the move algorithm the software reads predefined direction and speed inputs and sends control signals based on these to the motor driver circuitry. This causes the motor to rotate at the required speed which when in position triggers the proximity sensor that shuts off the motor by sending feedback signal back to the software which deactivates the 'lensmove' flag. When another lens change is required the flag is reset and the move algorithm is reactivated. Threaded programming is used to implement the algorithm as the proximity sensor input has to be read constantly and at a high frequency as if it is tripped the software will know instantaneously and will be able to react. The coding for this algorithm is detailed in *appendix 3*.

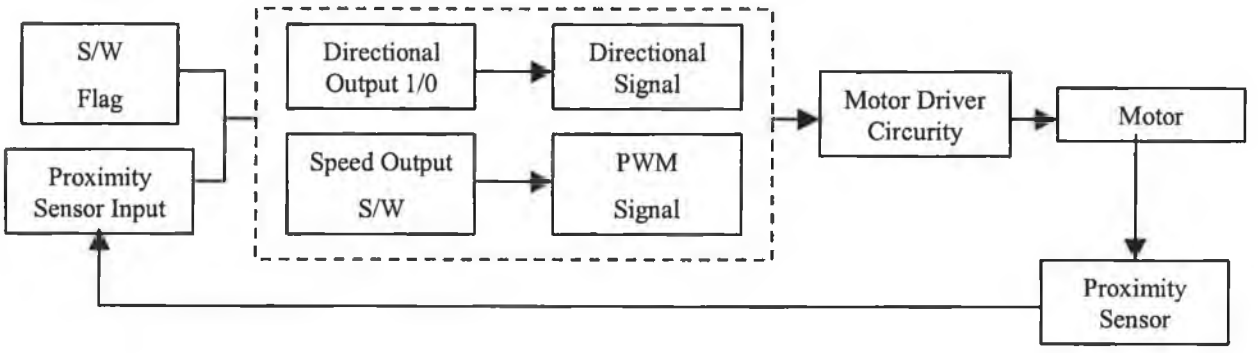

Figure 4-20 - Lens system control data flow

4.2.2 Autofocus System

To adequately implement an autofocus system it must be possible to achieve an acceptable focus feedback signal from the acquired image of the object. The definition of an acceptable feedback signal is one that contains the following characteristics [29]:

- Unimodality
- Accuracy
- Reproducibility
- Implementation
- Range

As discussed in *Chapter 2 Section 2.2.3* there are many methods available to achieve a feedback signal to autofocus an image. The majority of these are based on the same principle which is to determine when an image has the highest level of contrast. The method used to implement the autofocus algorithm is autofocus based on image statistical properties. This method is based on the statistical spread of the pixel values in an image. The standard deviation of an image details the spread of the pixel values. If the standard deviation is small the majority of the image pixels fall within a close range of each other. But as the standard deviation increases the pixels values will become more spread out from the mean, thus there will be more black and white

pixels in the image. This means there will be more areas of contrast in the image which implies the image is in focus. Before discussing the implementation of this method in detail the system used to drive the autofocus stepper motor is discussed.

4.2.2.1 Stepper Motor Controlling and Driving

In order to control the autofocus stepper motor a hardware interface is required between the host PC and the stepper motor. This interface must be set-up so as to receive digital motion data i.e. mode and direction from the PC convert it to analog signals, amplify them and provide them to the motor in the right sequence. This section discusses the driver circuits that best suit the motion requirements for the autofocus stepper motor, however, before discussing the driver the basis of stepper motors must be explained.

A stepper motor is an electromechanical device which converts electrical pulses into discrete mechanical movements. The spindle of a stepper motor rotates in discrete step increments when electrical commands are applied to it in the right sequence. The sequence of the applied pulses dictates the direction of motor shaft rotation. The speed of the motor shaft rotation is directly proportional to the frequency of the input pulses and the length of rotation is directly proportional to the number of input pulses applied. The applied torque versus angular displacement of the motor curve is approximately a sinusoid. As long as the torque remains below the holding torque of the motor, the rotor will remain within ¼ period of the equilibrium position. This implies that a stepper motor will be within one step of the equilibrium position. In order to achieve this equilibrium, every time an electrical pulse is sent to the motor, the motor steps once hence the name stepper motor.

To drive a stepper motor there are four possible modes:

- Wave drive (1 phase on),
- Full step drive (2 phases on),
- Half step drive (1 and 2 phases on),
- Microstepping (continuously varying).

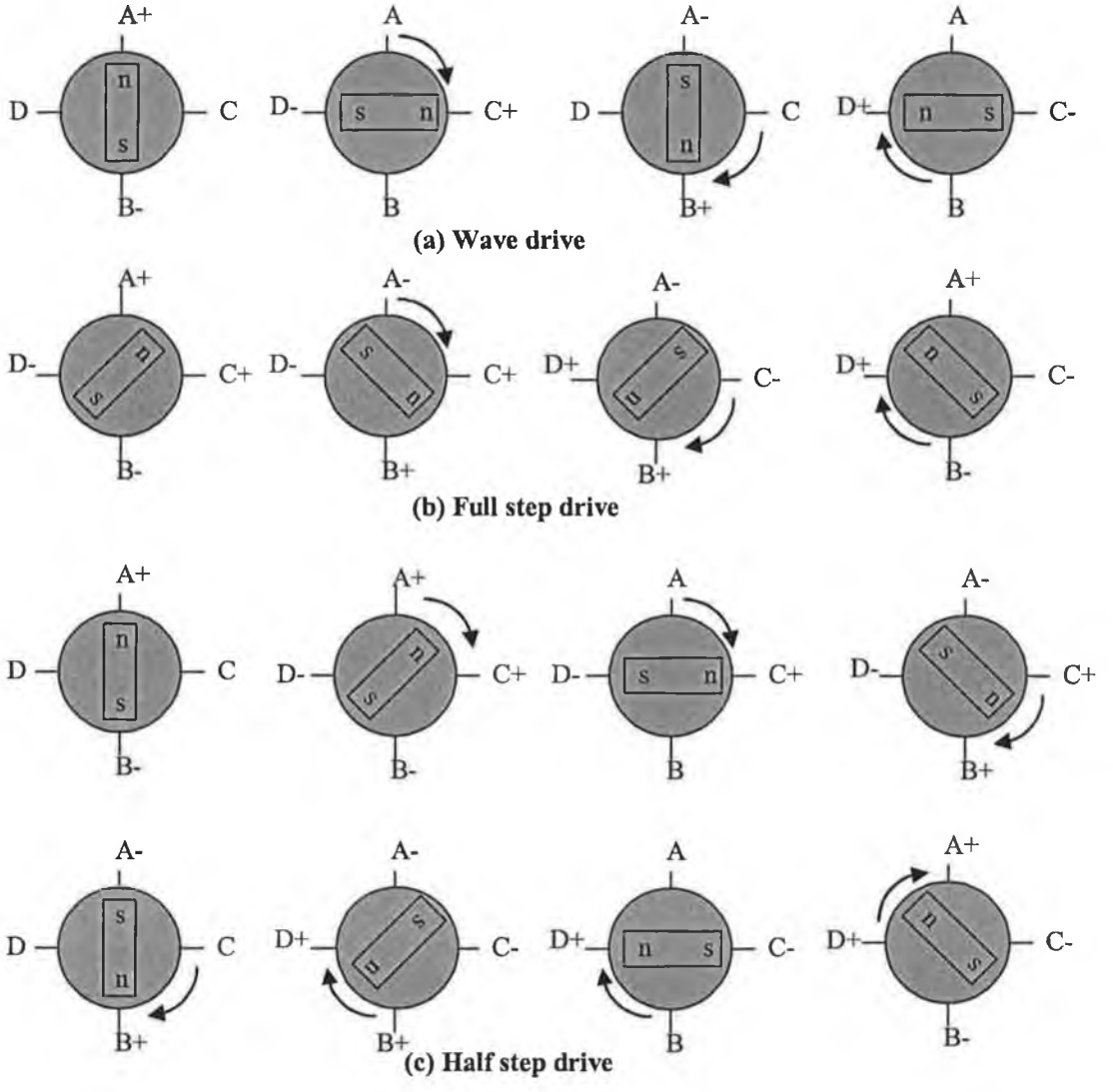

Figure 4-21 - Stepper Motor Driving Modes [49]

In wave drive, only one winding is energised at a given time (sequence A→C→B→D in Figure 4-21a). Hence, the system cannot use full motor torque (only 50% is used). Two phases are energised at any given time in full step drive (sequence AC→ CB→BD→DA (Figure 4-21b)). This driving mode suffers from the same problems as

wave-drive with the mechanical positions offset by half a step of wave drive. Half step drive combines both wave and full drives. Every second step, only one phase is energised and during the other steps one phase on each stator Figure 4-21c. This results in angular movements that are half wave or full drive.

A more precise method of driving the motor is microstepping. Microstepping is a way of moving the stator flux of a stepper motor more smoothly than in a full or half step drive modes by continuously varying currents in the windings to be able to break up one full step into many smaller discrete steps [48].

As discussed in *Section 4.1.2.1* of this chapter a half step driver is adequate to achieve the required step resolution for the autofocus system. However, due to issues with resonance when driving stepper motors in half step or full step mode it was decided to use a microstepping driver. The effect of microstepping is that the rotor will have a much smoother movement because the stator flux is moving in a continuous manner. This makes it possible to drive the motor at a low frequency with high step accuracy which reduces resonance and vibrations. This provides smooth noise free movement which is ideal for stage movements.

The microstepping driver used to control the stepper motor was the IM483 motion control system (*Appendix 2*). The IM483 provides up to 51000 steps per revolution for a 1.8^0 stepper motor in microstepping mode and directional and speed digital input controls. Figure 4-22 details the driver connections to the motor and PC. The interface to the host PC is provided via the parallel port which allows for the transmission of digital signals between the drive board and PC.

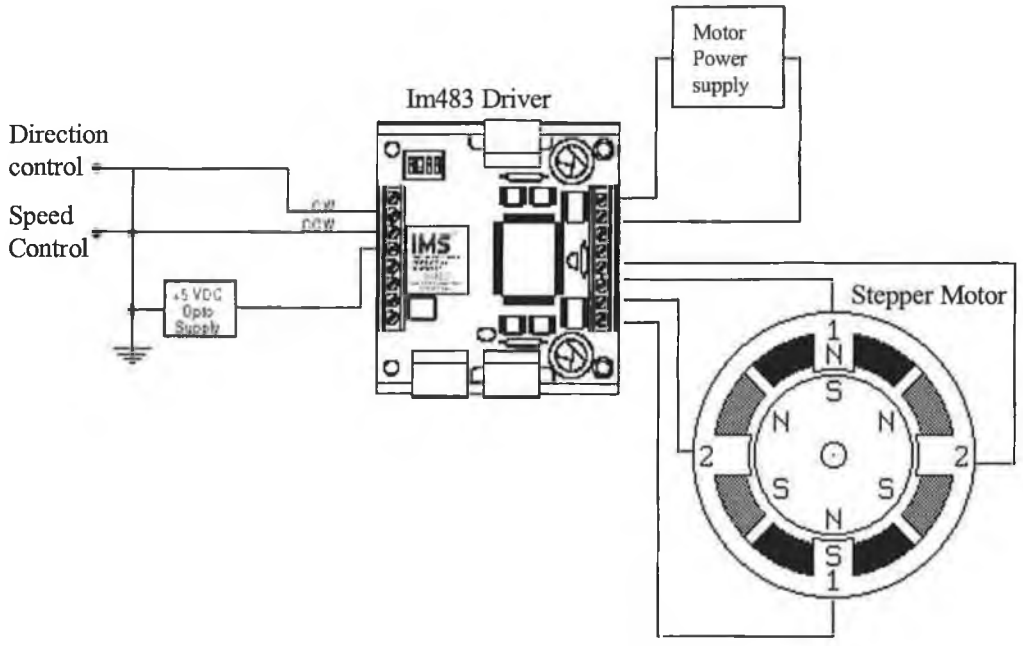

Figure 4-22 – Autofocus Stepper motor driver connections

4.2.2.2 Autofocus Algorithm Implementation

The basic strategy for autofocusing is to apply a focus function based on suitable algorithm at vertical positions of the image plane and thus find the global maximum or the best focus position. A focus function is a measure of the focus as a function of the axial (z) position and is sampled at different positions along the Z-axis. The method used to calculate the focus function is the standard deviation method (Equation 4-2).

$$f(z) = \sqrt{\sum_{i=1}^{n} \frac{(P_i - u)^2}{n}}$$ **Equation 4-2**

Where μ = Average Pixel intensity
P_i = Pixel intensity
n = Number of pixels in image

This algorithm works by calculating the standard deviation of an acquired image before movement and again after movement. By comparing the calculated standard deviation before movement (SD_1) and after movement (SD_2) the system can determine whether it's moving in or out of focus.

$SD_1 > SD_2 \Rightarrow$ *moving out of focus*

$SD_2 > SD_1 \Rightarrow$ *moving into focus*

After the system determines the direction of focus it moves in this direction and determines the location of the maximum standard deviation value. This position will be the position of best focus. Figure 4-23 shows the focus function curve achieved when focusing an optical fibre using this method. Due to the high acquisition rate of the camera there are high frequency components present in the focus function data. To eliminate these high frequency components a low pass filter is used to filter the acquired data. The filter employed is a 6th order Butterworth filter with a cutoff frequency of 6 Hz (Figure 4-23 - Dark line). This eliminates local maximum from the focus function and which makes the algorithm more robust. A complete evaluation of the autofocus system operation is given in chapter 5.

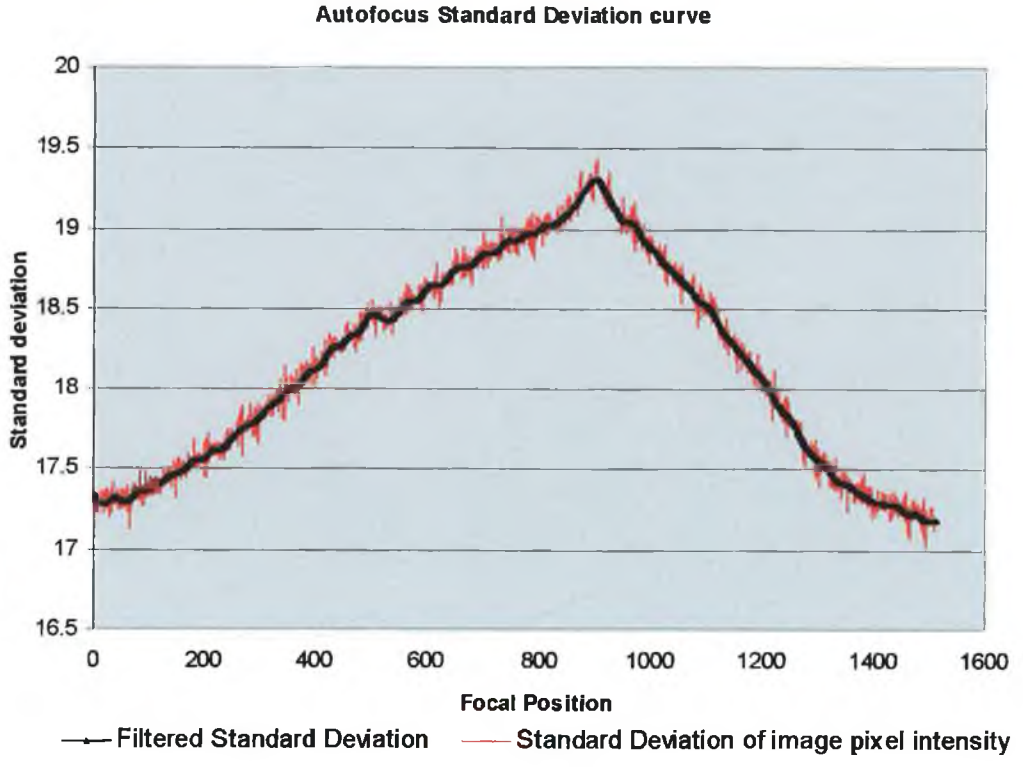

Figure 4-23 – Focus function with data passed through a 6th order Butterworth filter and without data passed through filter.

4.2.3 Hardware-Software Interface

To communicate with the device via a software GUI two hardware interfaces were required:

- Parallel port interface – To acquire inputs from sensors and send control signals to the autofocus system and lens exchange system.
- Video Acquisition Interface - To acquire video frames from the CCD camera via the PC USB port.

4.2.3.1 Parallel Port Interface

In order to acquire and send control signals between the device electronics and the software some form of hardware interface was required to form a communications bridge between these two components. To provide this hardware interface the parallel port was used as it incurred no significant costs to the project and operated at an adequate acquisition rate for interfacing with the device electronics. The parallel port also allowed for the input of up to 9 bits or the output of 12 bits at any given time, thus it requires minimal external circuitry to receive and transmit control signals [51]. The majority of parallel ports are standard 25 pin D-type connectors although there is a 30 pin centronics standard that will not be discussed. The pin assignment of a of a D-type parallel port connector are detailed in Table 4-5.

Pin No (D-Type 25)	Direction In/out	Register	Hardware Inverted
1	In/Out	Control	Yes
2	Out	Data	No
3	Out	Data	No
4	Out	Data	No
5	Out	Data	No
6	Out	Data	No
7	Out	Data	No
8	Out	Data	No
9	Out	Data	No
10	In	Status	No
11	In	Status	Yes
12	In	Status	No
13	In	Status	No
14	In/Out	Control	Yes
15	In	Status	No
16	In/Out	Control	No
17	In/Out	Control	Yes
18 - 25	Gnd	N/A	N/A

Table 4-5 – Pin assignment of the D-Type 25 pin parallel Port connector. Table also details register/pin assignment [50]

To read from and write to the parallel port the three status registers are used:

- Data
- Status
- Control

Each register is one byte large with each bit representing a pin on the parallel port.

Table 4-5 details the pin assignment for the data port.

Name	Read/Write	Bit No.	Properties (Pin)
Data port	Write	Bit7	Data 7 (Pin 9)
		Bit 6	Data 6 (Pin 8)
		Bit 5	Data 5 (Pin 7)
		Bit 4	Data 4 (Pin 6)
		Bit 3	Data 3 (Pin 5)
		Bit 2	Data 2 (Pin 4)
		Bit 1	Data 1 (Pin 3)
		Bit 0	Data 1 (Pin 2)

Table 4-6 – Data Register, pin assignment

So if a byte of information representing 128 is sent to the data register, bit 5 of the data register is set to 1 and pin 7 of the parallel port should read +5V. This is the basis for communicating with the parallel port. To communicate with the parallel port via the software two C++ functions were used.

Byte = _Inp(Register) – reads a byte of data from the specified register

_Outp(Register, Byte) – outputs a byte of data to the specified register

These allowed a byte of data to be sent or read from the specified status register. In this case the 'Data' register was used to send data to the parallel port and the 'status' register used to receive data from the port. The input and output requirements for the device electronics were 4 outputs and 1 input:

Outputs

- Clock signal to Autofocus stepper motor
- Direction signal to Autofocus stepper motor
- PWM signal to lens exchange system DC motor
- Direction signal to lens exchange system DC motor

Input

- Proximity Sensor status signal

The pin and registry assignment for each signal is detailed in Table 4-7

Control	Register	Bit No.	Pin
Outputs			
Direction signal to Autofocus stepper motor	Data	0	2
Clock to Autofocus stepper motor	Data	1	3
Direction to lens exchange DC motor	Data	2	4
Clock to lens exchange DC motor	Data	3	5
Inputs			
Proximity sensor input	Status	7	11

Table 4-7 – Pin and register assignment used to communicate between the device electronics and parallel port.

So if the direction of the DC motor is to be set to forward, pin 4 of the parallel port is set high. The following code executes this as it sends the binary representation of 8 to the data register which sets Bit 3 to '1'.

```
_outp(DATA ,8);
```

To read the status of the proximity sensor the code below is used.

```
int a = 0;
int b = 128;
int c = 0;

a = _inp(STATUS); // Read in a byte from status register
c = (a & b);  //Reads in MSB off parallel port and AND's  it with 128
```

If the status of C is '1' the proximity sensors is active, if its '0' the proximity sensor is not active. The above is just an overview of the methods used to communicate with the parallel port; the detailed coding to do this is detailed in *appendix 3*.

4.2.3.2 Video Acquisition Interface

In order to communicate with the video acquisition hardware, a software interface is required that allows for the acquisition of images and access to their pixel data for autofocusing and eventually image processing. To achieve this direct access is required to the PC hardware in this case the PC USB port. Due to the complexity of writing software functions to access PC hardware directly a pre-written software development kit (SDK) was used called 'Direct X'. Direct X is a set of application programming interfaces (API's) developed by Microsoft that provides direct access to hardware in the windows operating system environment [52]. Each API contains specific functions for accessing and controlling hardware. The API that Direct X supplies to interface with acquisition hardware is called 'DirectShow'. The DirectShow interface provides the programmer with a wide variety of functions to access media based hardware attached to a PC. For this reason and due to the fact that it is compatible with Visual C++ it was used for interfacing with the USB port.

In addition to using the DirectShow API, the Win32 API was also required in order to develop a GUI based application compatible with windows. Windows programming is mostly based on the WIN32 API which contains the original windows functions written in C [53]. In this case Microsoft Foundation class (MFC) was used which is the new definition and extension of WIN32 API which is a windows software library provided in C++ [53]. Therefore to create the software interface a combination of the MFC and DirectShow API's were used to allow for windows development and access to the capture device. The next section explains in detail the code written to communicate with the capture device to acquire media data from the acquisition hardware.

4.2.3.3 Software Interface

The aim of the software interface is to:

- Provide a windows based GUI for displaying media
- Provide preview window of media stream.
- Access the video capture device
- Determine if the capture device is capturing media data and if so access the media stream using an appropriate media format
- On user prompting capture the current frame from the media stream and store it in an array

To achieve this a program was written in visual C++ using functions from the DirectShow API and MFC API. The complete program code is detailed in *Appendix 3*. As outlined in the program function flow (Figure 4-24) the program used five functions to create the capture application:

- OnInitDialog
- InitDirectShow
- OnInitStillGraph
- GetDefaultCaptureDevice
- BufferCB

The first function 'OnInitDialog', like the 'main' function in dos based C and C++ is the starting point for windows based programs [54]. This function is derived from the CDialog class in the MFC library. When the program is executed, this is the first function visible to the programmer that is called. Its purpose is to directly initialise the dialogs variables and functions and also indirectly initialise the DirectShow interfaces by calling a separate function 'InitDirectShow'.

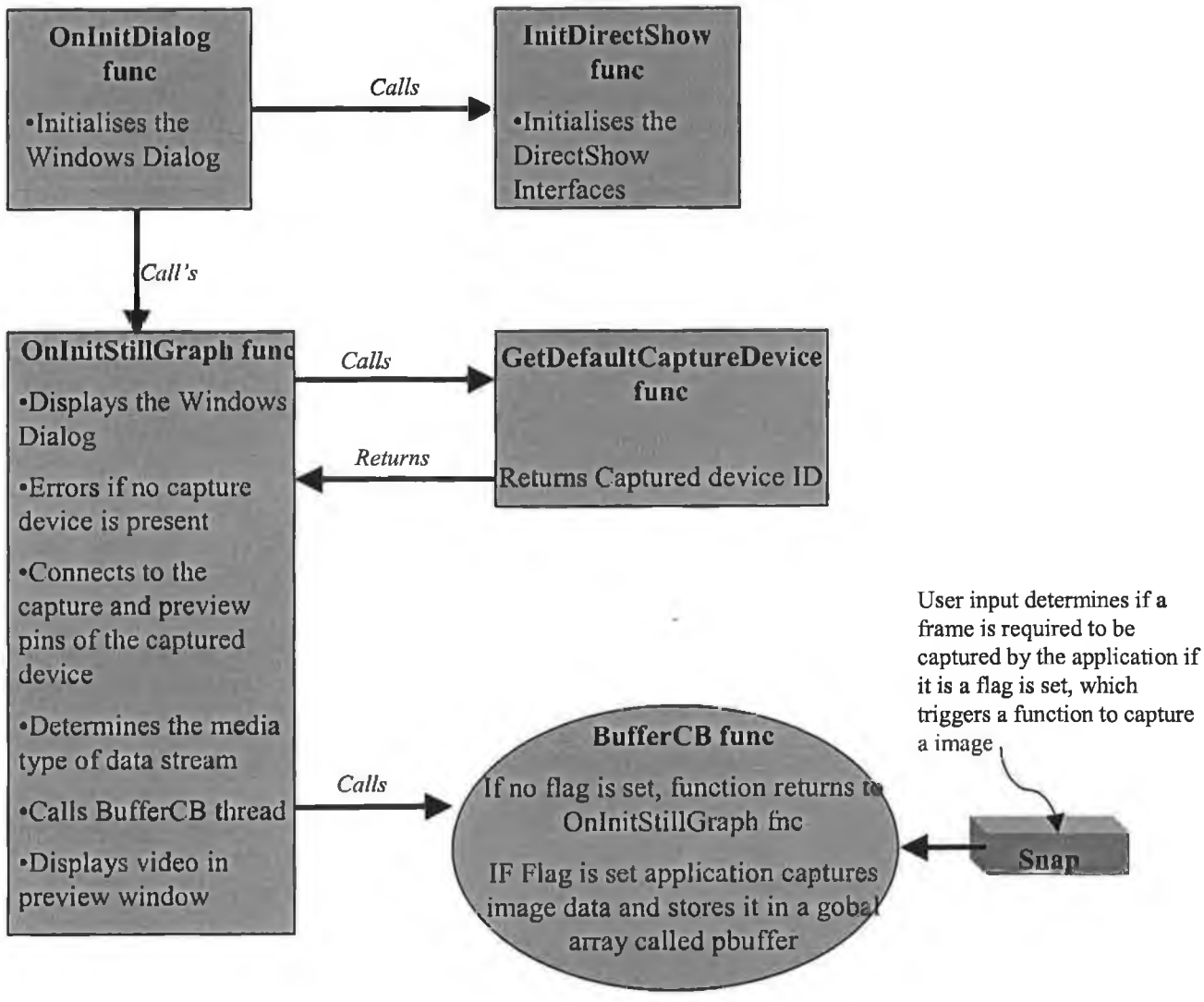

Figure 4-24 - Function flow of program created to access video aquistion hardware

The "InitDirectShow" function sets up capture graphs which are the interfaces DirectShow uses to communicate with hardware devices (Figure 4-25). Each capture graph represents a hardware device and is made up of subsets called filters, the filters handle components like capture, audio preview and render [55].

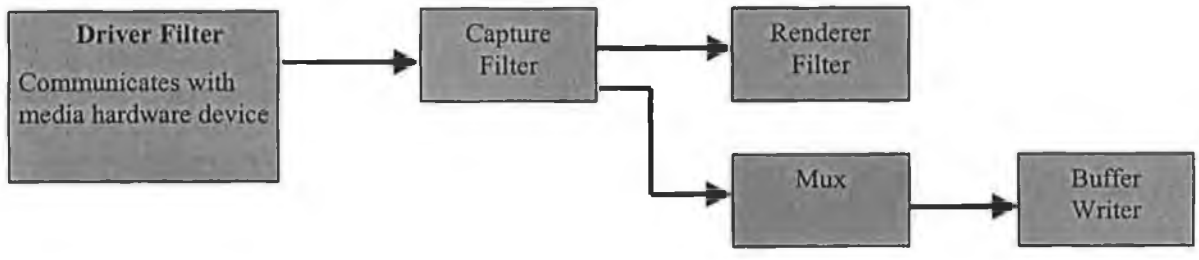

Figure 4-25 - Capture Graphs Architecture, detailed a typical capture graph filter that is used to acquire data from a hardware device. [55]

After setting up the direct show interfaces, the 'OnInitDialog' function then calls the 'InitlialiseStillGraph' function. The first purpose of this function is to determine a pointer to the default capture device attached to the PC. It accomplishes this by calling a function called 'GetDefaultCaptureDevice'. This function determines all the video hardware devices attached to the PC by using the system device enumerator [55]. The system device enumerator is accessed by calling the DirectShow method:

CreateClassEnumerator(CLSID_VideoInputDeviceCategory, &pEm, 0)

This method retrieves a list of all the video input devices present on the PC. The program then determines the first item on the list by using a while loop and returns a pointer to the first hardware device present on the PC. This pointer is then returned to the 'OnInitStillGraph' function. If no device is present the software returns an error. If a device is present the 'OnInitStillGraph' function creates a 'capture filter' with the capture device as the source and a 'graph filter' with the capture graph as the base. It then connects the 'output pin of the Capture filter and the 'input pin' of the graph filter to start acquiring the data. While this system might seem complicated for a relatively simple task, using filters graph makes it easier in the long term as each filter represents a logical function and it's only possible to connect certain filters to each other. Once the pins are connected it is possible to access each individual video frame. However, it's important to have the functionality to capture select frames otherwise the PC hard drive would become overloaded with data. For this reason the program is constructed in such a way so as to call a thread every time a video frame is captured. The thread called "BufferCB" which is called by the code:

m_pGrabber→SetCallback(&mcb,1);

A global flag determines if the frame is stored or not, if it's set to "True" the frame is stored and visa versa if its set to 'False'. Pressing the 'Snap' button on the application

window sets this flag. The 'buffer CB' thread then stores the image data in a array called "Pbuffer[]" by calling the function:

Memcpy(Cb.pbuffer,pbuffer,lbuffersize);

This buffer contains the red, green and blue pixel intensity values for the image. By using a nested "for" loop the data can be split into individual data buffers to represent each primary colour. Having done this anyone of the colour arrays can be used for autofocusing or processing of the image. Since the illumination type used is red light it would be best to use the red pixel array as this would form the highest contrast image.

4.3 Detail Design Summary

This chapter has outlined the detailed mechanical and system design of the optical fibre analysis system. The initial design requirements of the system were as follows:

- Imaging System:
    - ⅓ inch 6.5μm square pixel CCD camera
    - Automated three lens system
        - Low Magnification - 4X optical magnification
        - Intermediate Magnification - 20X optical magnification
        - High Magnification - 40X optical magnification
- Illumination - Coaxial Illumination system
- Stepper motor autofocus system
- Motorised lens exchange system with proximity sensor control
- X-Y-Z Axis Camera Adjustment for Optical Alignment
- Software Interface –
    - Allows for direct access to image pixel values for analysis purposes.
    - Provides control over the autofocus and lens exchange system via then parallel port

The mechanical, electronic and software aspects for each requirement has been satisfied and a final prototype realised. The next chapter will evaluate the functionality of this prototype in detail.

Chapter 5: Evaluation of Working Prototype

Having designed and assembled the system the next phase of development was to evaluate the system functionality. The system functionality was assessed under three categories.

- Imaging system mechanical alignment
- Image Quality
- Autofocus Operation

Imaging system mechanical alignment assessed the overall mechanical functionality and manufacturing tolerance of the system. The image quality determined the ability of the system to produce an adequate image for analysis purposes. The functionality of the autofocus system was also examined to determine if it operated as required.

5.1 Imaging system mechanical alignment

In an optical system it is important to have the optical axis of the lens centred with respect to each component of the optical system. Any misalignment of the optical axis will cause degradation of the image quality due to aberrations inherent in optical lenses [56]. Therefore when assembling the system it is important to get the illumination system and sensor aligned with respect to the lens optical axis (Figure 5-1).

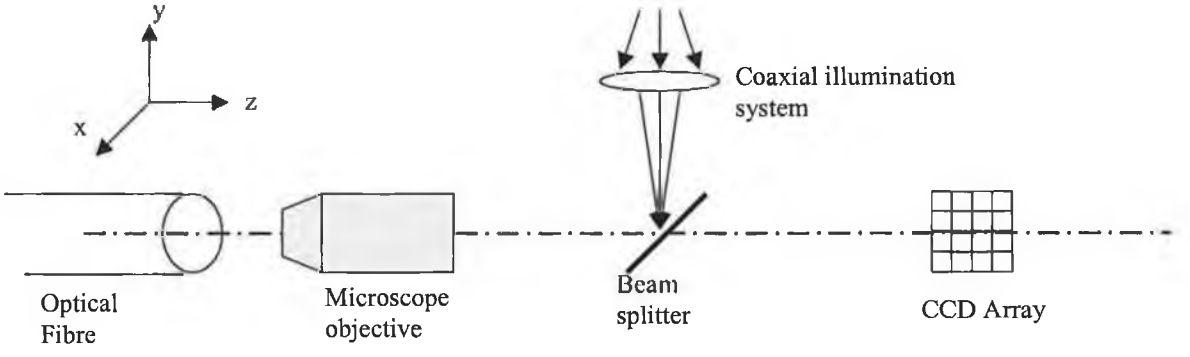

Figure 5-1 - Optical System Alignment

The illumination system position has a greater margin of error when compared with the other components, as its only requirement is to provide even illumination across the surface of the fibre. The other components (object/lens/CCD) need to be aligned precisely with each other otherwise the image quality and field of view will be reduced. To allow the system to be aligned correctly the sensor is placed on a three axis linear stage. The fibre holder could also be adjusted by means of oversized slots which allowed its position to be changed in the X and Y-axis. Using these adjustments, the fibre holder and the CCD sensor could be aligned to the lens optical axis. However, while this system will allow one lens to be aligned correctly with the optical axis the overall system accuracy depends on the accuracy of the lens holder system in terms of its ability to place each of the three lenses concentrically in relation to the optical axis (Figure 5-2).

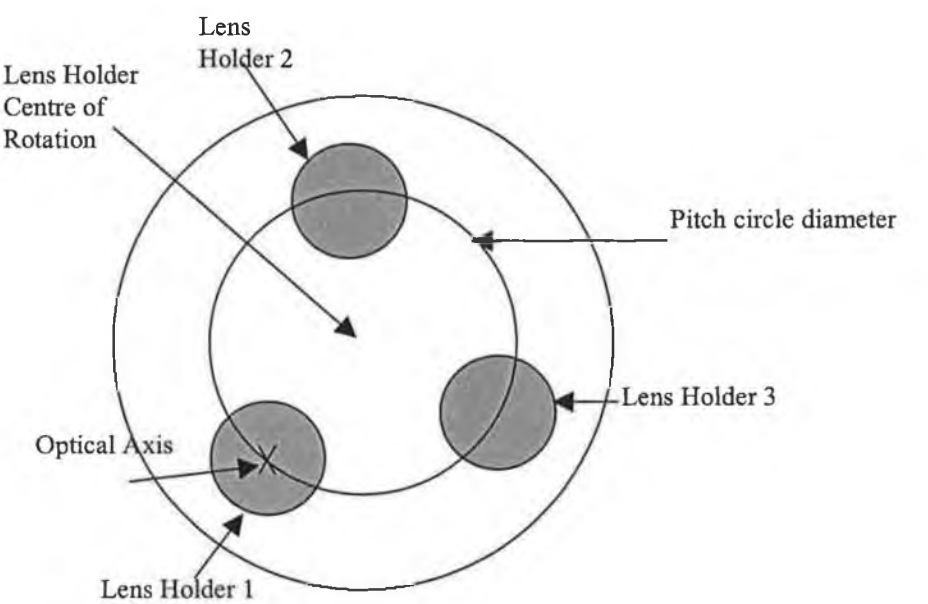

Figure 5-2 - Lens Holder Assembly

On investigation it was found that if the system was aligned correctly for one of the lenses, once the other lenses were rotated into position they were found to be misaligned, as the fibre-CCD optical axis did not line up in the lens optical axis (Figure 5-3).

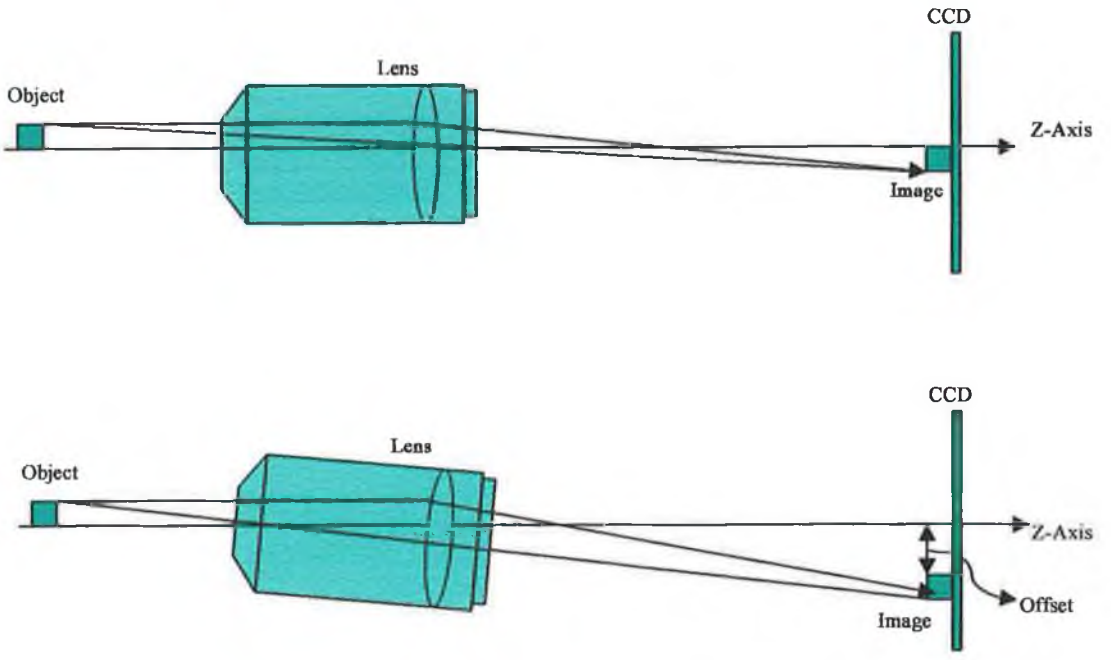

Figure 5-3 – Position of image formation when lens is aligned with optical axis and position of image when lens is positioned at an exaggerated angle to the optical axis

To determine the extent of the misalignment the position of each lens was measured in relation to each other using the sensor micrometer adjusts. This was carried out by centring the 40X lens in the CCDs FOV, then the other two lenses were rotated into position and the distance the sensor had to be moved to re-centre the lenses was measured in both axes. The average distance (10 samples) the sensor had to be moved in the X and Y-Axis is shown in Table 5.1.

	X Axis	Y axis
40X → 20X	-2.1mm	2.2mm
40X → 5X	0.15mm	-0.55mm

Table 5-1 –Lens Misalignment, these distances represents the average distance the CCD sensor has to be moved in the X and Y axes to re-centre the image after the lenses were exchanged

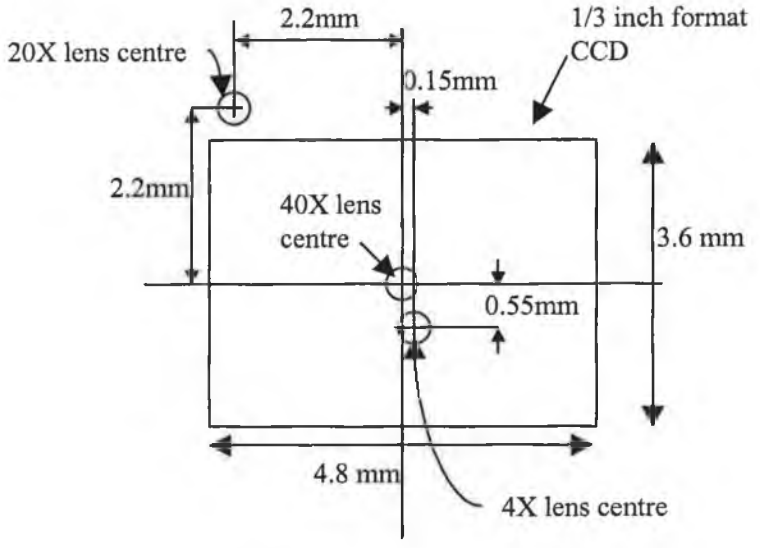

Figure 5-4 - Lens Positioning is relation to CCD

Figure 5-4 shows the position of the optical axis of the 20X and 4X lens relative to the 40X lens position. As can be seen from the diagram the total misalignment is quite significant, although it should be considered that these measurements are translational so any variations in position of the lens will be amplified when the image is projected onto the sensor. To determine the cause of the misalignment each possible source of misalignment in the system was examined.

5.1.1 Sources of Optical Misalignment

The first possible source of misalignment investigated was if the lens holder was rotating centrally on it axis of rotation. If due to inaccuracies or errors in the manufacturing process, the axis of rotation of the lens holder was not positioned centrally, the lenses would rotate along different pitch circle diameters. Thus there position in relation to the optical axis would vary. To determine if this source of misalignment was present a dial gauge was placed on the circumference of the lens holder disk and it was rotated through 360^0 to measure its centring (Figure 5-5).

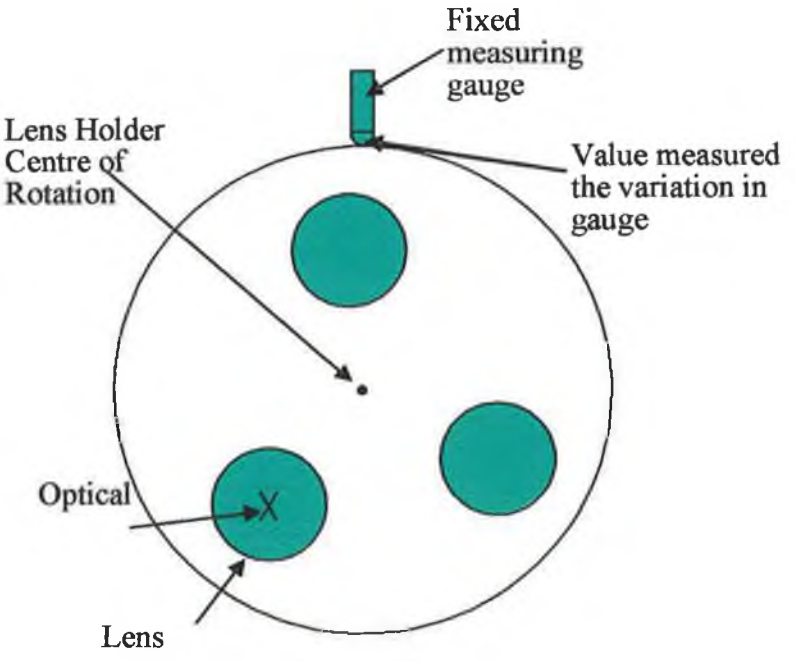

Figure 5-5 - System used to measure lens holder centring

The value measured for the lens holder centring accuracy was 0.01mm. This value is negligible is relation the actual offsets measured in the system and can be attributed to the surface roughness of the material. Therefore it was decided that the lens holder centring was not the cause of the misalignment in the system.

The final possible source of error in the system was if the lenses were not on the same pitch circle diameter. The method used to determine if the lenses lay on the same pitch circle diameter was to measure the distance between the lens holder upper quadrant and the lens upper quadrant for each lens slot as illustrated in Figure 5-6. The same lens was used to measure each distance so variations in the lens diameter can be eliminated as a source of error.

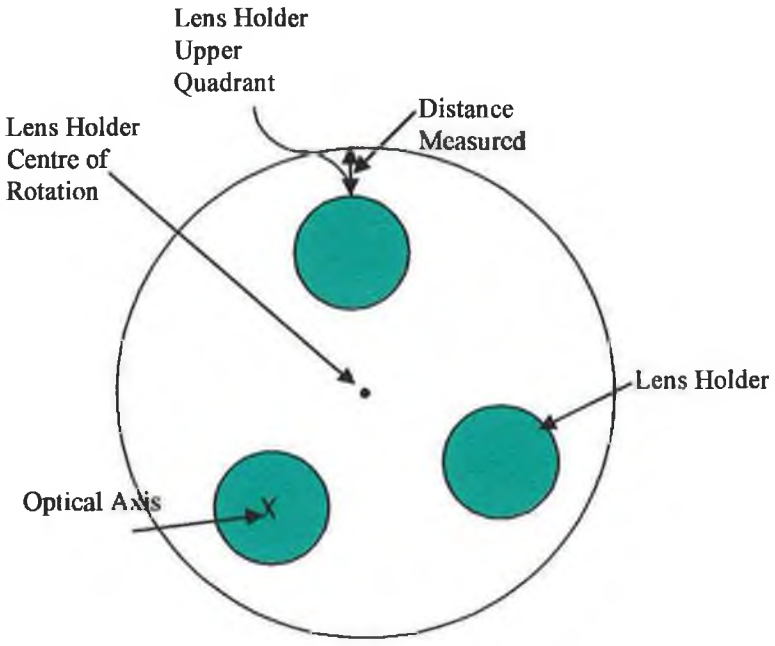

Figure 5-6 – Pitch Circle Diameter Centring

Using an identical lens for each slot the following distances were recorded.

Lens Holder 1: 2.26mm

Lens Holder 2: 2.3mm

Lens Holder 3: 2.17mm

Since the circumference of the disk only deviates by 0.01 mm and the same lens was used to measure the distance each time suggests that the lenses are positioned on different radiuses with respect to the centre of the lens holder. The values measured also correlate proportionately to the offsets measure at the CCD sensor. Therefore it was deduced that machining inaccuracies in the manufacture of the lens holder caused the positioning error.

5.2 Image Quality of Prototype

The goal of the system is to produce an image to a required standard for image analysis purposes. Within a machine vision system the quality of an image will vary depending on certain factors such as:

- Lens Magnification
- Lens Quality
- Lighting
- Imaging Sensor

How each of the above parameters individually affects the image quality has been previously explained in *Chapter 2*. What this section discusses is the overall image quality achievable for the optical fibre analysis system and how factors such as illumination, lens magnification, and CCD acquisition parameters affect the overall image quality. It also suggests methods to improve the image quality and overcome optical anomalies inherent in the system.

5.2.1 Illumination

Illumination affects the final image quality more that any other parameter in an imaging system, after all the light reflected off the object is what forms an image. Consequently the type of illumination used can have a significant bearing on what can be viewed in an image. Different illumination techniques can highlight different characteristics of an image, although certain types of illumination can have a detrimental effect on the image quality if used incorrectly.

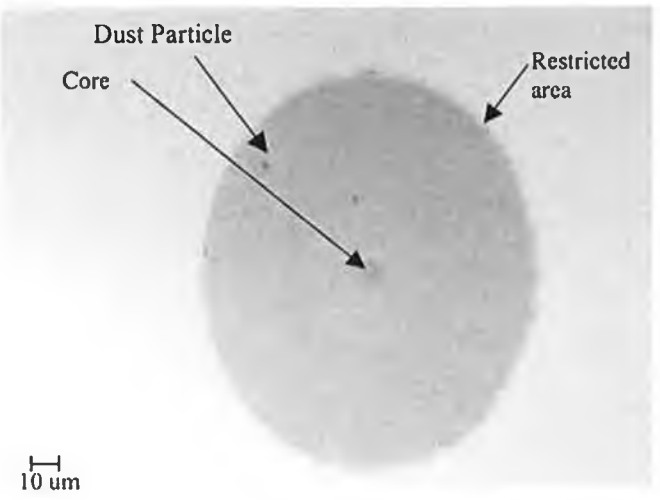

Figure 5-7 –Directional Illumination (20X). Due to the nature of the illumination used features such as the core and voids can be seen, as directional illumination produces shadowing that allow recessed features to be viewed.

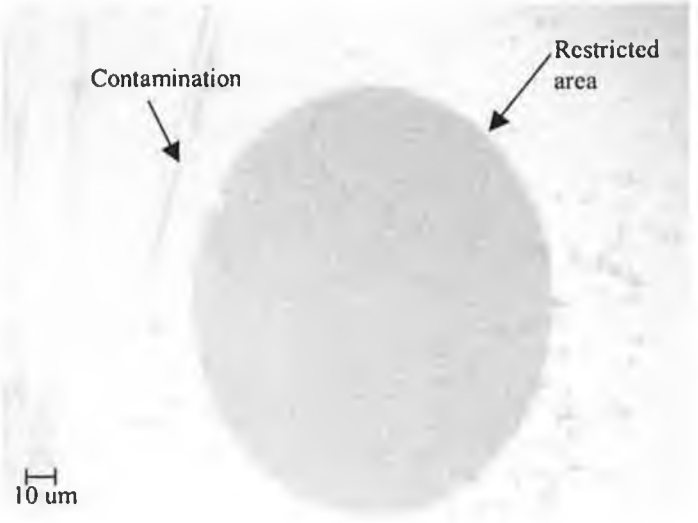

Figure 5-8 –Diffuse Axial Illumination (20X). This type of illumination produces a higher contrast image a thus certain defects that can not be seen using side illumination can be detected using this type of illumination.

The above images (Figure 5-7 & Figure 5-8) contrast the effect different illumination techniques have when viewing the surface of an optical fibre and the range of defects that can be detected. Both images are viewed using a 20X magnification objective lens. Figure 5-7 is illuminated from the side using a fibre optic light source. What can be detected quite clearly is the core and to a lesser extent the restricted area. Despite polishing the core is often recessed from the rest of the fibre, so when the fibre is illuminated from the side less light falls into the core and causes it to appear as a dark

spot. Therefore this method of illumination can be used to distinguish between different regions of the optical fibre.

Figure 5-8 is the same fibre illuminated using the diffuse axial method. This illumination method produces an evenly illuminated image with no glare or shadows. Due to the higher contrast of the image it is easier to view defects as can clearly be seen in the image. While both illumination techniques have their advantages in terms of defect detection and area location, in order to obtain the necessary information to adquately analyse the fibre the use of both illumination methods is necessary.

5.2.2 Lens Magnification

The limitation of both these types of illumination methods becomes apparent when the object is viewed at a different magnification. Figure 5-9 and Figure 5-10 show the images produced when using a 4X magnification lens with the object illuminated using directional illumination and diffuse axial illumination respectively.

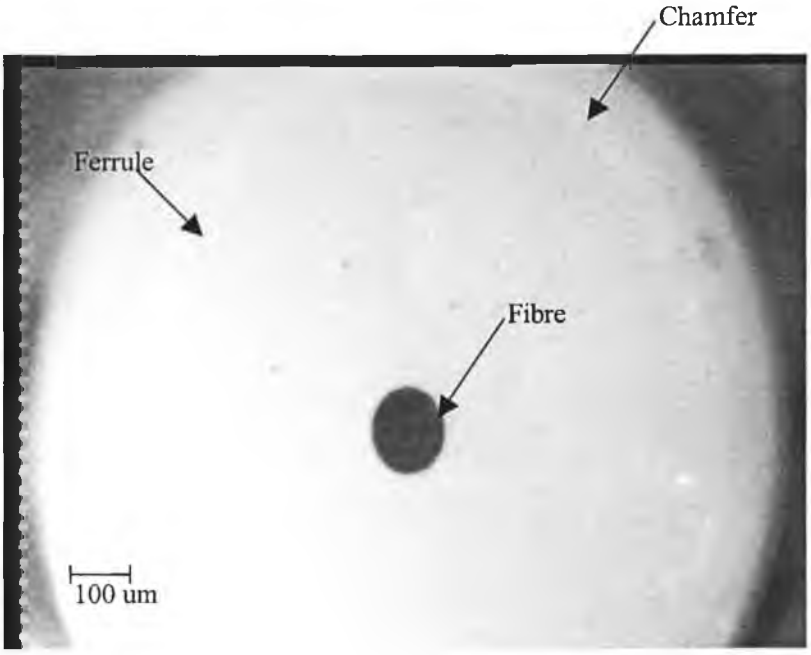

Figure 5-9 – Directional Illumination (4X)

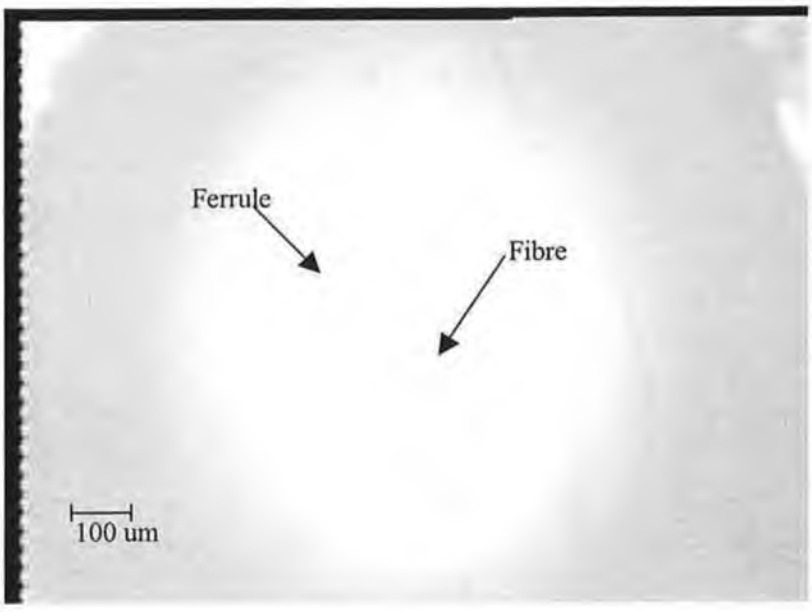

Figure 5-10 - Diffuse Axial Illumination (4X)

In this case the best quality images are produced using side illumination. The images produced using the diffuse axial method are over-exposed and the edges of the image are cut off. The overexposure of the image stems from an oversight when integrating the CCD sensor into the system. All the necessary components were specified to fit one optical magnification including the CCD sensor. There was no variability designed into the initial prototype to suit the use of variable magnification lenses. A method for overcoming this problem is discussed in *Section 5.2.3*.

The diffused axial illuminated image (Figure 5-10) suffers from an optical aberration called vignetting. Vignetting is when the image quality at the periphery of an image degrades due to uneven illumination intensity [57]. This may be attributed to various factors, the illumination source, the design of the light path between the sensor and the lens or the behaviour of the imaging device. In this case there is a gradual transition from a bright-overexposed image centre to dark-underexposed edges. Therefore it can be concluded that the vignetting is not caused by a mechanical stop,

as there would be an abrupt transition between the image edge and the vignetted area. A more likely source of the vignetting is the illumination source. Since only the diffuse axial illuminated image suffers from vignetting the issue is obviously linked to this type of illumination method.

Due to the implementation of diffused axial illumination the illumination source is focused by the imaging lens onto the object. Therefore the light exiting the lens forms a spot. In this case the spot formed is less than the total field of view that is required to be viewed thus vignetting occurs (Figure 5-11).

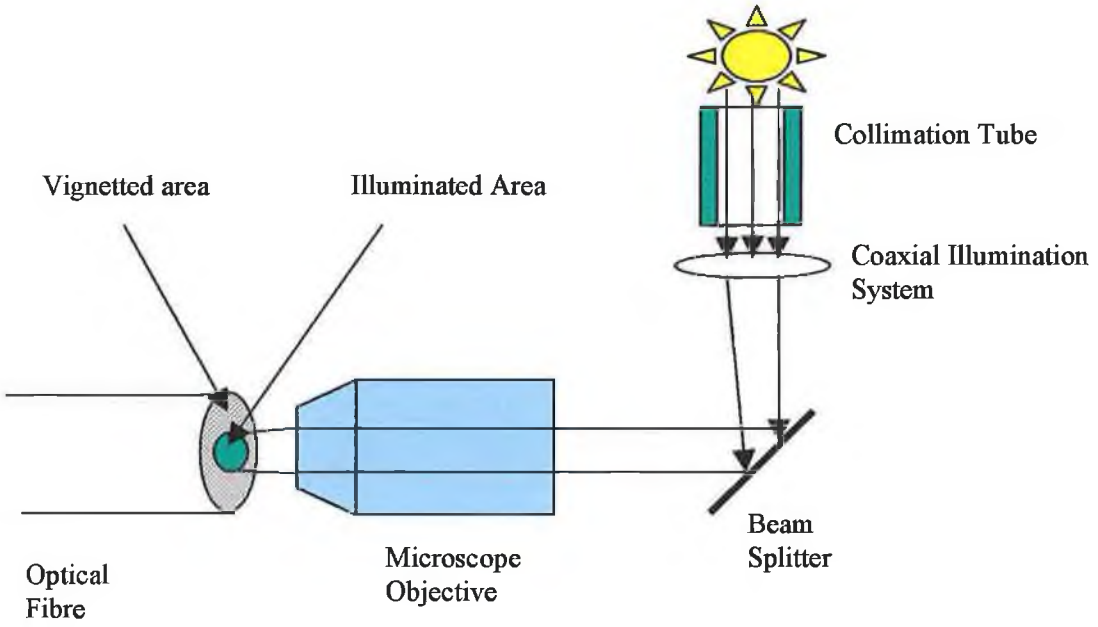

Figure 5-11 - Illustration of spot size formed by diffused axial illumination method

A means of overcoming the vignetting is to increase the illumination spot formed by the illumination beam. This can be done by increasing the aperture opening or in this case the width of the collimation tube. However, increasing the size of the aperture only serves to slightly increase the overall size of the illumination cone and thus the spot size formed [58](Figure 5-12).

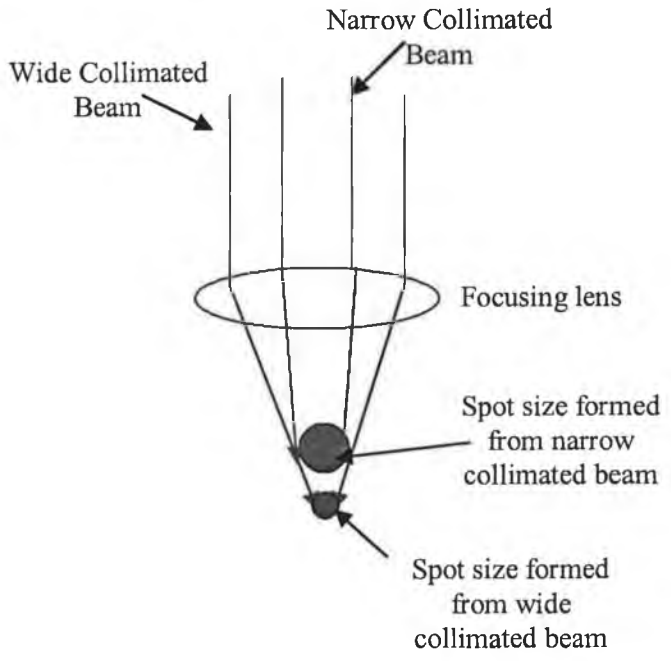

Figure 5-12 - Illumination spot size variation with beam collimation

In most microscope systems the illumination spot is controlled by use of an aperture. However, the main purpose of the aperture is not to vary the spot size but to control the depth of field of the image. An alternative but more complicated solution is to adopt the solution used in microscopy. In microscopy the condenser lens focuses the light onto the object in question (Figure 5-13). Again the use of this illumination method causes vignetting issues at lower magnification factors due to the spot size formed. To overcome this, many microscope systems are adapted with specialised substage condensers that have a swing out top lens that can be removed from the optical path for use with low power objectives (2X to 5X) [59]. This action changes the direction of the light path to form a wider spot size.

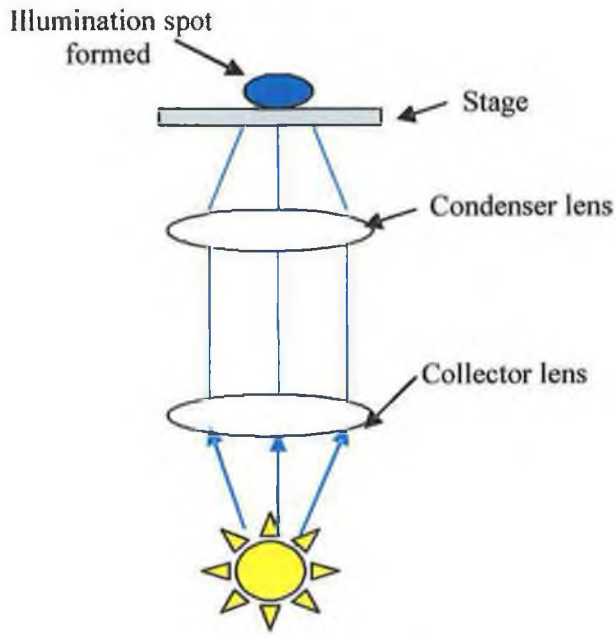

Figure 5-13 – Light Path formed in Backlit Microscopy System [59]

However, this system is only adequate for a back illuminated system, as the condenser lens does not interfere with the image forming light path. For coaxial illuminated systems the objective lens acts as the condenser lens. Therefore removing the illumination condenser lens is not feasible as it also acts as the image-forming lens. An alternative is to insert an optical beam expander into the light-forming path (Figure 5-14).

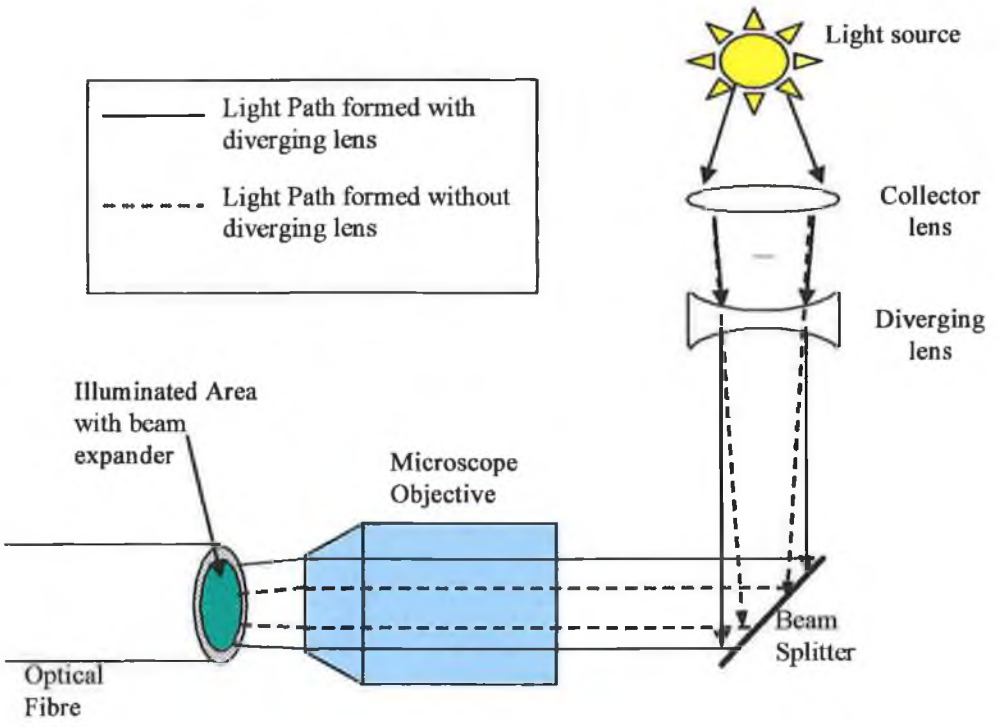

Figure 5-14 -- Diffused axial illumination system with beam expander

A diverging lens in series with the collector lens will have the effect of producing an expanded beam, which in turn will produce a larger spot size when focused by the objective lens (Figure 5-14). This apparatus set-up in combination with the illumination source will increase the illumination spot size and thus eliminate the vignetting (Figure 5-14).

5.2.3 CCD Acquisition Parameters

The CCD sensor has an important bearing on the quality of the final image produced. CCD sensor variables such as exposure time and gain determine the brightness and contrast of the image produced. The images detailed in Figure 5-15 and Figure 5-16 show the optical fibre endface at two different magnification settings - 4X and 20X respectively. As can be seen from the images Figure 5-16 is over-exposed whereas Figure 5-15 is acquired at the correct sensor exposure setting.

Figure 5-15 – Diffused Axial illumination (20X)

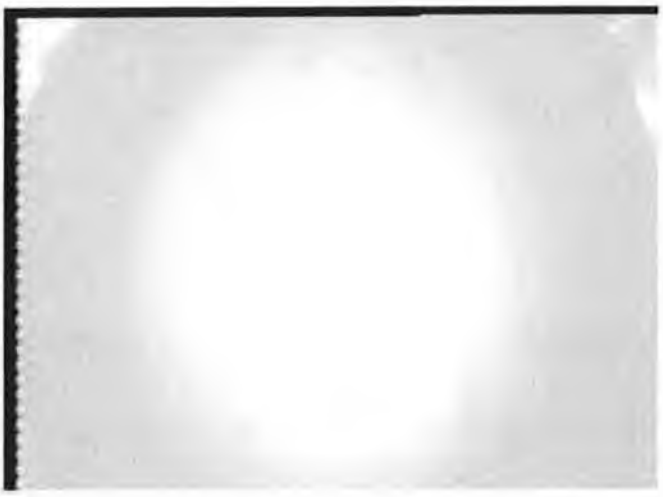

Figure 5-16 – Directional illuminated fibre (4X)

The CCD sensor used in the initial prototype design was set up for a single magnification system and did not allow for the acquisition parameters to be changed in real time via software. When using variable magnification lenses with one CCD it is important to be able to change the exposure time of the sensor. For low magnification lenses the amount of light reaching the CCD is high as the aperture is large. Therefore the exposure time of the sensor must be low otherwise the image will become saturated. The opposite is true for high magnification lenses. The amount light reaching the CCD is less as the aperture is smaller, thus the exposure time must be increased or the image will be to dim. To overcome this problem a new camera was sourced that allowed the acquisitions parameters to be changed in real time. This camera is integrated into the proposed alternative design. The use of this camera permits the exposure time setting to be changed in tandem with changes to the systems magnification thus allowing for consistent image brightness across the range of magnifications. The proposed alternative design is discussed in detail in the final section of this chapter.

5.3 Evaluation of autofocus system

As explained previously the autofocus system works by calculating the standard deviation of an image pixel intensities at various focal position and from this determines the focus position. Figure 5-17 shows an example of a focus function curve achieved when focusing an optical fibre using the standard deviation method. A data point is acquired for every frame captured by the acquisition device which is equivalent to every 0.33sec. Since there is no focal position sensor present on the device the standard deviation is plotted against time, since the motor is moving constantly time is proportional to distance.

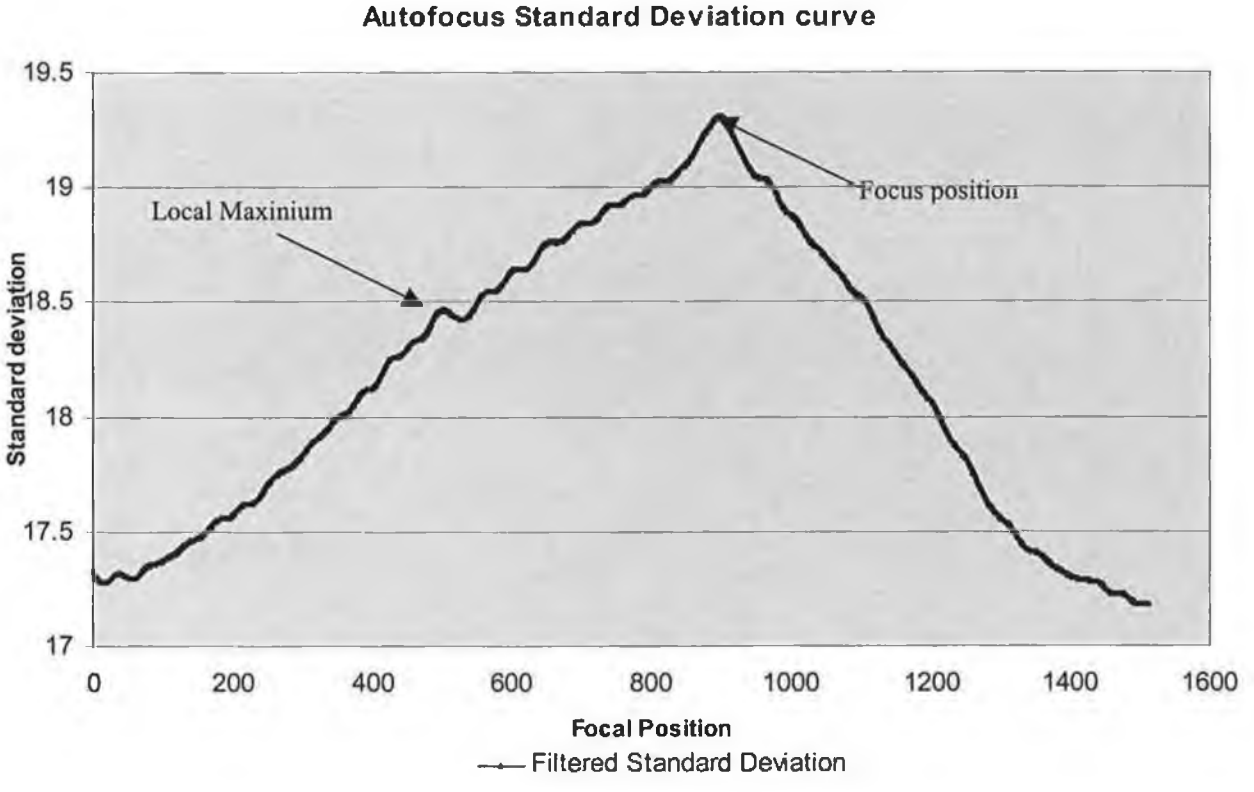

Figure 5-17 - Focus function curve achieved when focusing the optical fibre under 20X optical magnification

As can be seen from the graph it exhibits all the characteristics of a useful focus function [29].

- Unimodality – Only one peak

- Accuracy – The focus position is at the maximum value
- Reproducibility – The curve peaks sharply
- Implementation – The focus measurement is computed in real time
- Range –Provides focus information over the desired range

Therefore it can be concluded that the standard deviation autofocus algorithm demonstrates excellent focusing accuracy and produces a focus function with all the necessary characteristics to implement a robust autofocus system. However, certain issues were encountered when implementing the system. There were as follows:

- The ability of the algorithm to deal with local maximum in the focus function curve (Figure 5-17)
- The illumination method used.

While the use of the low pass filter eliminates the majority of local maximum, certain local maximum still remain which causes issues when autofocusing. To eliminate these the autofocus algorithm could be altered to average the local maximum by using multiple focus passes; the initial pass would be coarse ($\Delta Z_{coarse} \cong 10\mu m$), thus eliminating the possibility of determining the focus position to be at a local maximum. The latter passes would then use a fraction of ΔZ_{coarse}, ΔZ_{fine} to determine the focus position to the required accuracy. This system would also eliminate the number of image acquisitions required thus speeding up the total autofocusing process time.

The other issue that was encountered with the autofocus system was the effect the illumination method had on the system. Figure 5-18 compares the two focus function curves acquired when using side and back illumination. If side illumination is used a flat focus function results, which has none of the characteristics of useful focus function. This is due the reflection caused when using this type of illumination that

create areas in the image of high intensity level which remain constant as the focus changes, therefore the standard deviation of the image remains the same as the object in moved in and out of focus. With back illumination the light is evenly spread across the image, as the light source is coaxial with the optical axis thus when the image is moved in and out of focus the image contrast changes according to the focus position. Consequently it is essential to use an illumination technique that results in a high contrast image when autofocusing the image.

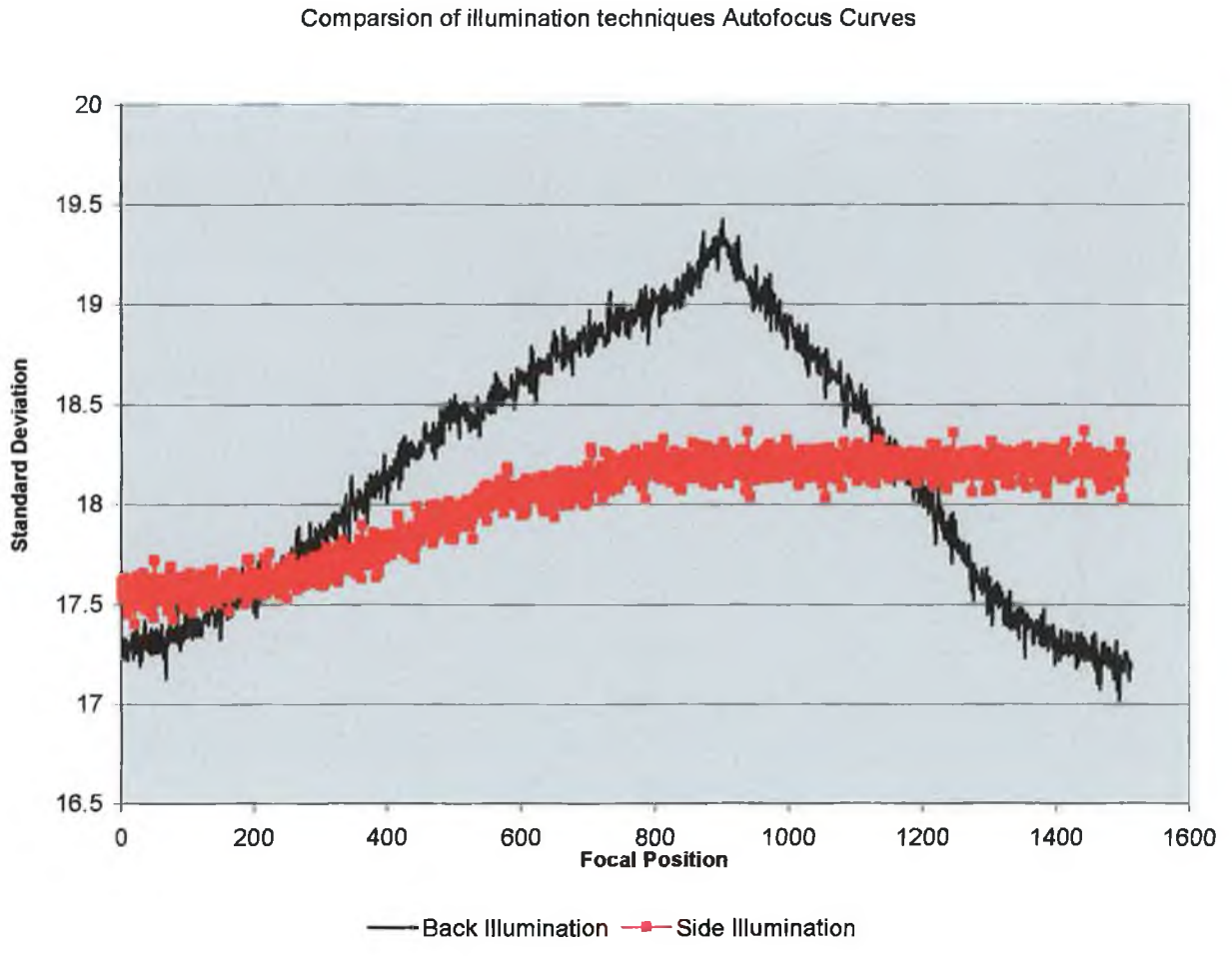

Figure 5-18 - Comparison of Standard Deviation for Different Illumination Techniques

5.4 Proposed Alternative Design

Having evaluated the final design it was decided to completely redesign the system to overcome the problems with optical alignment and image quality, as to alter the final design wouldn't adequately overcome the issues with it. A summary of the fundamental issues with the final design are shown below:

1. The lens holder did not position the lenses concentrically with respect to the optical axis.
2. The lens holder was held on the DC motor bearings and positioned using a ball bearing that sat into circular groves positioned along its circumference. This system was found to be unreliable and not repeatable for positioning the lens accurately each time.
3. The method employed to position the optical fibre holder used oversized holes. This was found to be cumbersome and awkward when aligning the fibre holder with the optical axis and thus not very accurate.
4. The system used to hold the stepper motor in place made it difficult to align it with the micrometer it was rotating to autofocus the system. Any modifications to the motor position meant the entire assemble would have to be completely disassembled and reassembled.
5. The camera used did not allow for real time control of the image acquisition parameters.
6. The illumination system did not completely illuminate the fibre at low magnifications.

As well as the fundamental issues with the design, within the overall design the device was designed with industrial use in mind. Therefore the device was designed taking scale and ergonomics into consideration. A better approach would be to design

a more cumbersome prototype which could be used to prove the principle of operation of the device. Figure 5-19 details the final design and highlights the issues with it.

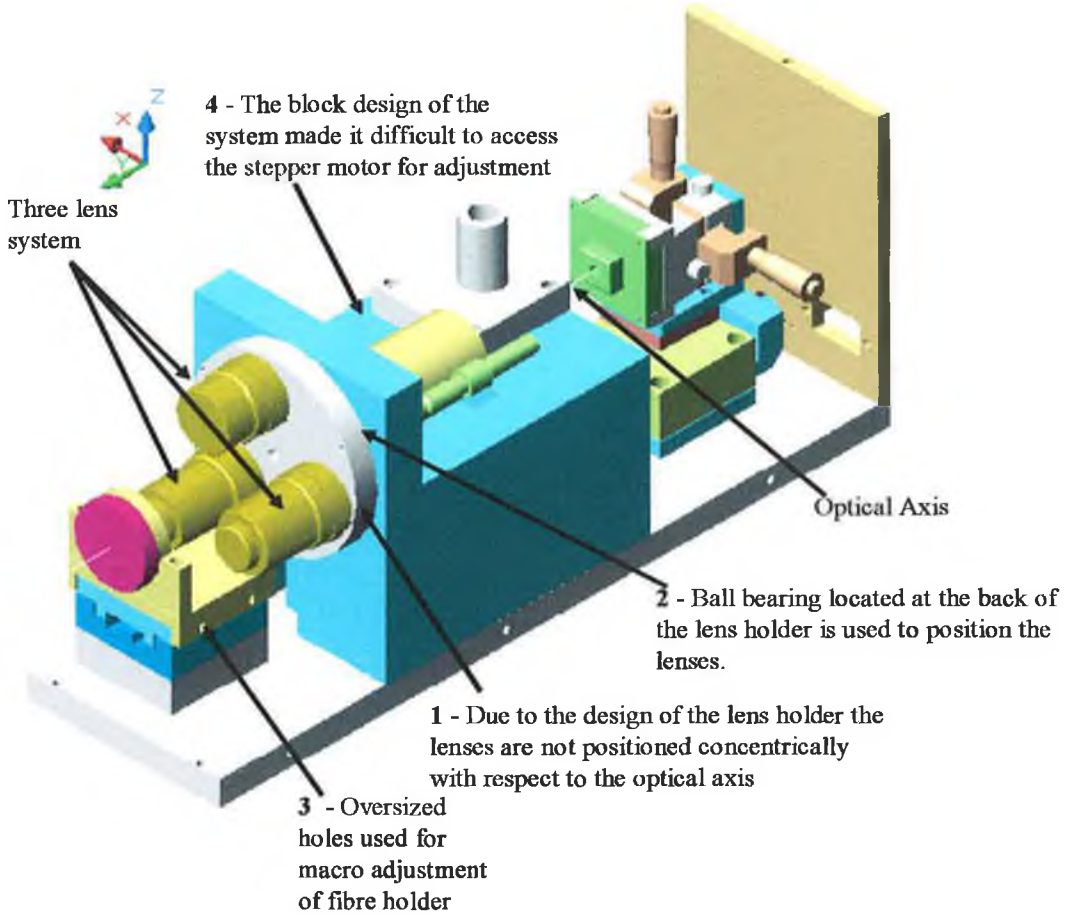

Figure 5-19 - Final Design, the mechanical issues with the design of the device are highlighted

To overcome the shortcomings with the final design two concepts were proposed and the most feasible one chosen. Overviews of the two design concepts are given below.

5.4.1 Alternative Design Concepts

The main issue with the original design was the systems inability to align the three lenses with respect to the optical axis. This was due to the scheme used to interchange the lenses that consisted of moving parts which had a certain degree of error associated with them. The approach taken with both these design concepts was to eliminate or minimise the number of moving parts in the designs and thus reduce the amount of error associated with theses.

5.4.1.1 Alternative Design Concept 1

The basis of this concept was to use a larger area CCD with only one lens (Figure 5-20). Using a 20X lens with a CCD of vertical sensor size 20mm will yield the required field of view of 1mm to view the entire fibre area. If the sensor had a 3μm pixel size it would adequately detect defects as small as 2μm. Any magnification required could be done digitally using software. This would make redundant the need for the extra lenses and the DC motor to rotate them into the required position. It would also solve any misalignment problems involved with rotating the lenses into position. However, the issue with fulfilling this design was to get a CCD sensor with both a 20mm*20mm sensing area and a 3μm pixel size. While it is possible manufacture a CCD sensor of these dimensions they are not commercially available so an alternative design had to be conceived.

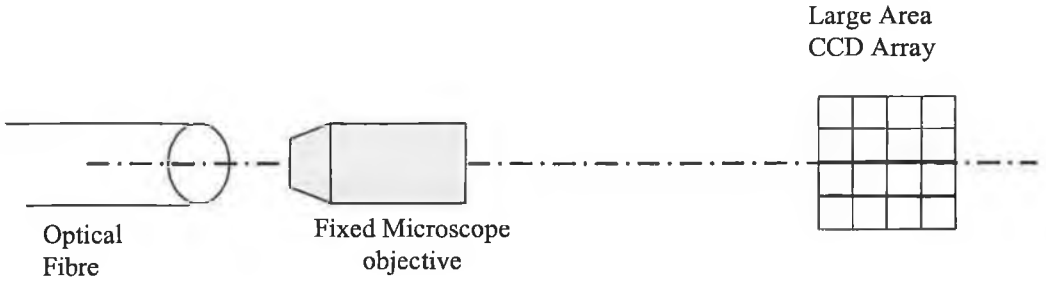

Figure 5-20 - Alternative Design Concept 1

5.4.1.2 Alternative Design Concept 2

The second design option was basically a trade off between concept 1 and the final design built. This concept proposes a two-lens system to be used in conjunction with a larger area, higher resolution CMOS sensor. While this re-introduces the problem of lens changing, the extra lens is necessary to allow for a standard camera to be incorporated into the system. Also incorporated in the design is the following:

- Adjustment of the fibre holder and the camera holder so the system can be aligned correctly and accurately.
- Lens exchange and guide system – The lens index system will contain a two tier linear slideway to allow for accurate movement of the lenses into position.
- Easier assembly of the stepper motor for autofocus control
- Enhanced illumination system

The approach taken in designing the new system was to make a prototype more suitable for research work. In order to achieve this aim, the system was designed for easier access and simpler assembly. Also incorporated in the system was greater adjustment of the imaging and optical devices to allow the device to be more easily aligned.

The new design was designed around a ½" format CMOS sensor with a 3μm square pixel size. The complete camera specification is show in *appendix 2*. Due to the size of the CMOS sensor area and pixels, only two lenses were required to provide adequate resolution and field of view. (Calculations shown in *Appendix 1*)

- 20X Lens - FOV = .24mm
  - Smallest Detectable defect = 2.1μm(13 pixels)
- 4X lens - FOV = 1.2mm

- Smallest Detectable defect = 10.75μm(13 pixels)

Figure 5-21 details a solid model of the final design.

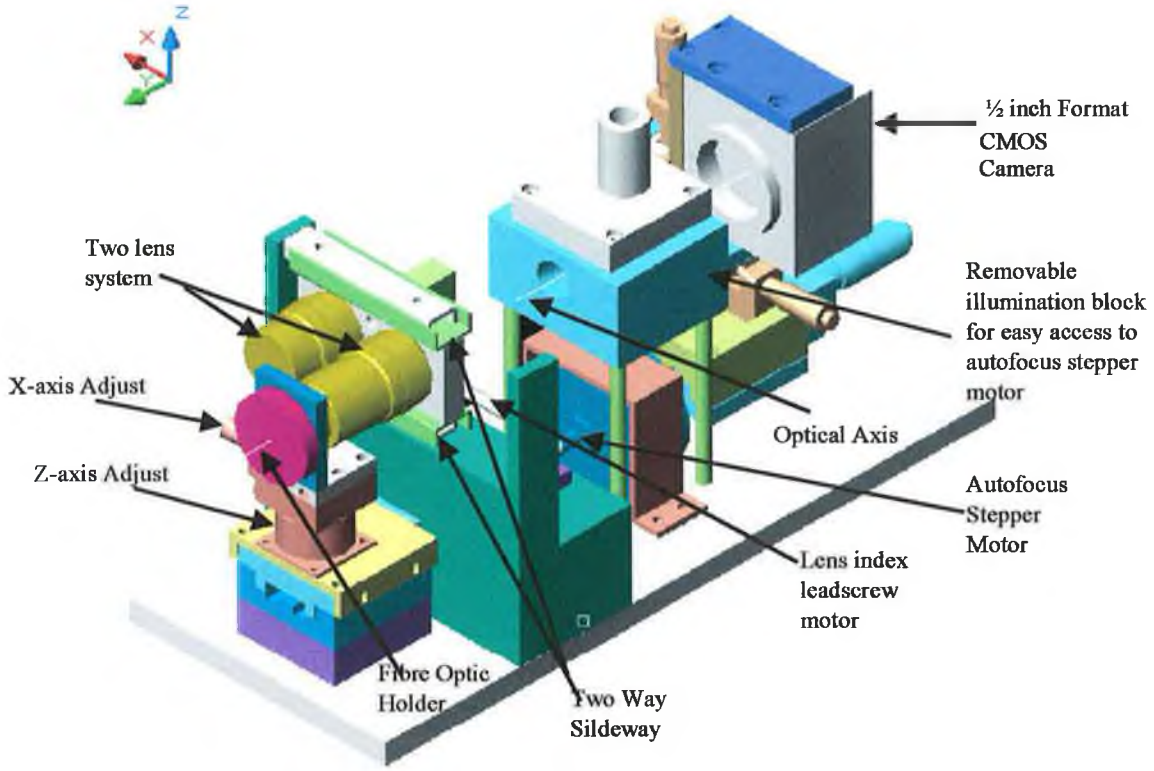

Figure 5-21 - Solid model of proposed alternative design

The main features of the new design are:

- Manual movement of the fibre holder in the X and Z-axis
- Automated movement of the fibre holder's Y-axis by means of a stepper motor.
- Two Microscope objectives
    - 4X
    - 20X
- Two tier linear slideway with movement in the Y-Axis for the interchange of lenses
- Leadscrew with 80μm stroke for movement of slideway

- ½" format COMS sensor with 3 μm pixel size which allows for real time camera control via USB port (*Appendix 2*)
- Camera is attached to stage with movement in X-Y-Z axis for accurate alignment of the system
- Enhanced illumination system which can achieve a larger spot size at lower magnifications
- Beam expanding optics in the illumination system optical path to eliminate the occurrence of vignetting when using the 4X lens.

More detailed drawings of this design are illustrated in Figure 5-22 and Figure 5-23.

Any future attempts to implement an optical fibre analysis system should adopt the proposed design as it improves the old design in the following aspects.

- More adjustment of the optics allows for easier device alignment
- Easier assembly
- More repeatable and accurate positioning of the lenses
- Improved imaging system with the integration of the CMOS sensor which allows for real time adjustment of the sensor parameters

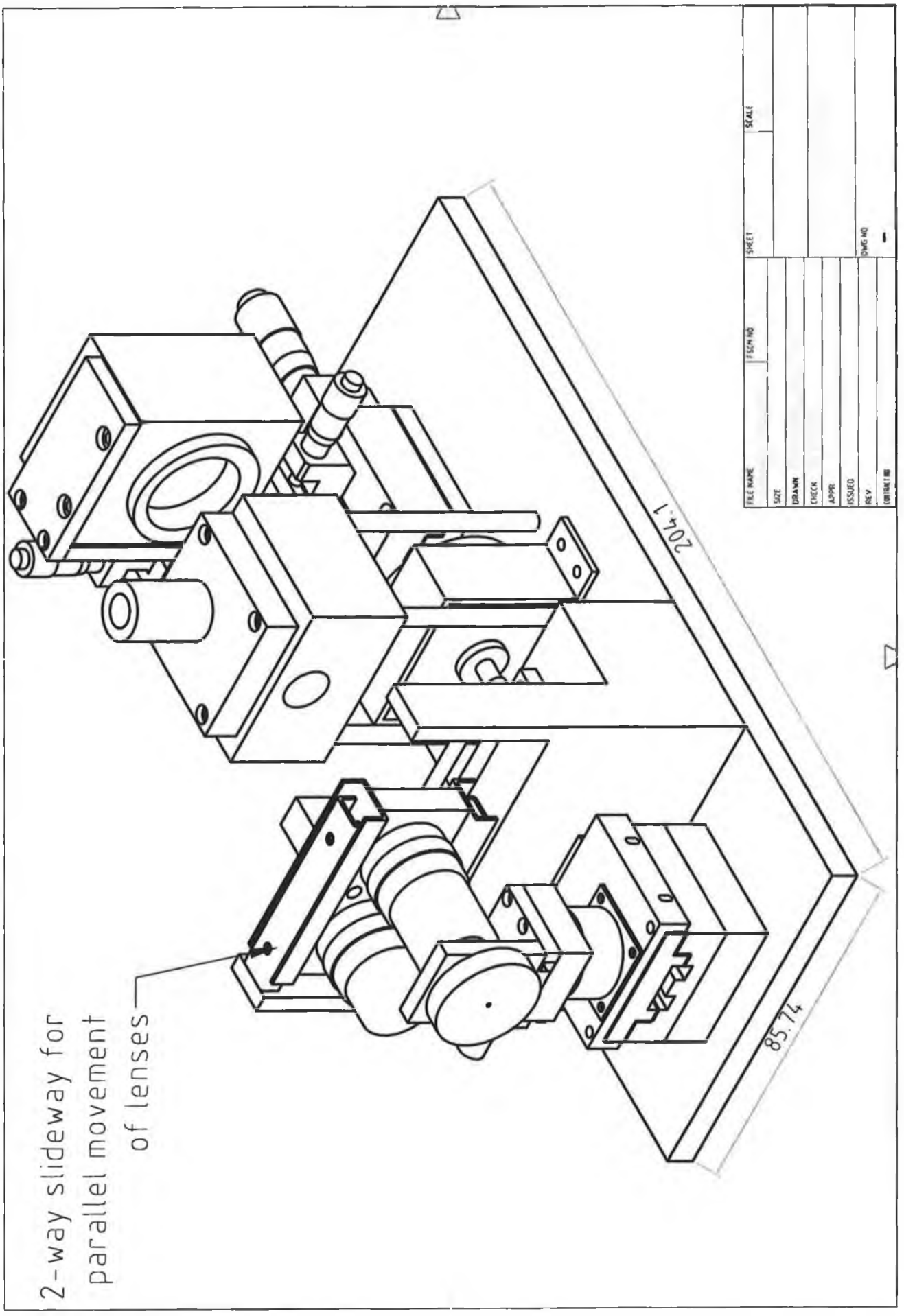

Figure 5-22 - Isometric view of final proposed design

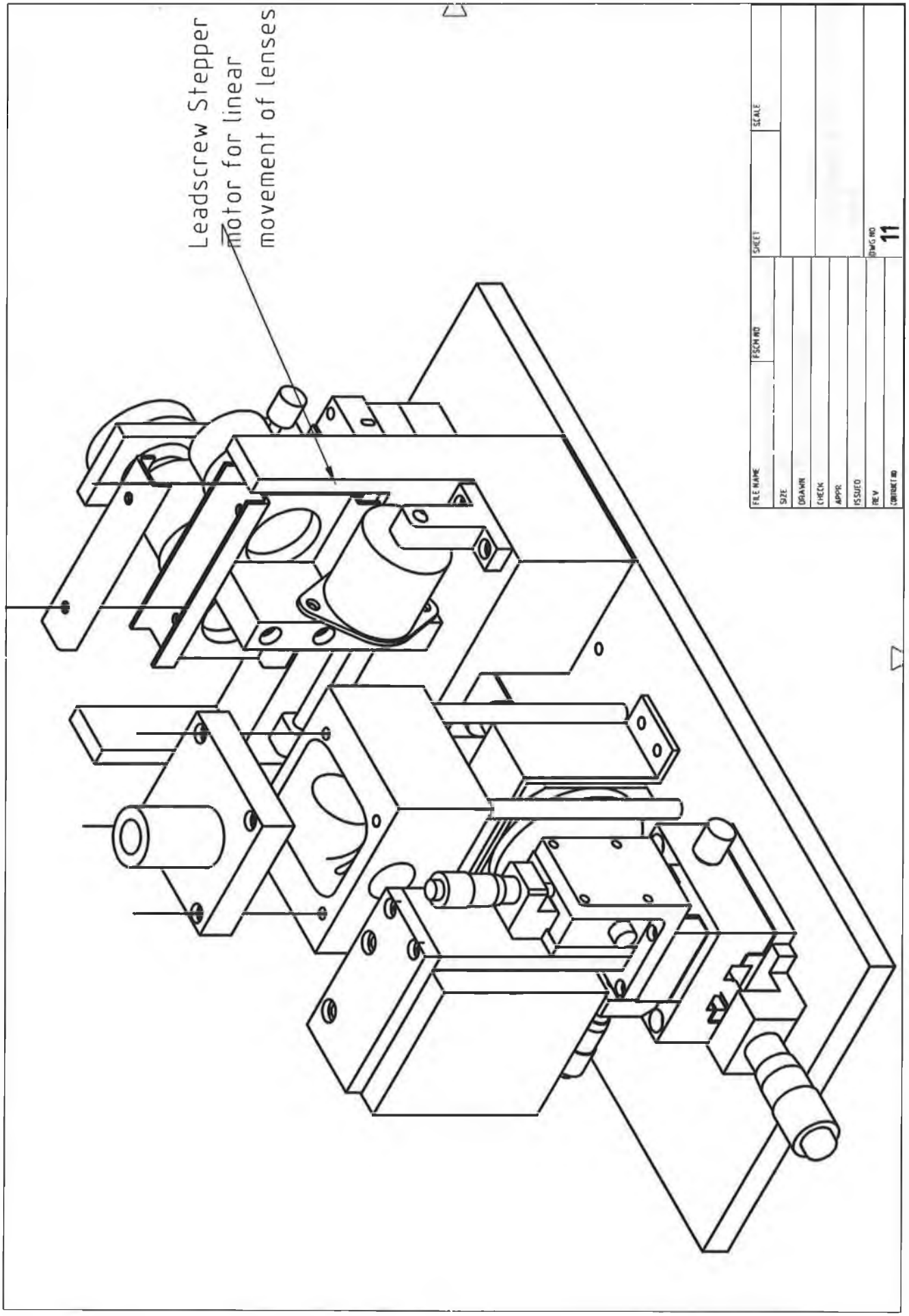

Figure 5-23 – Parially Exploded back view of final proposed design

Chapter 6: Conclusions

The necessity and technical challenges involved in the design of an automated inspection system for the analysis of optical fibre endfaces has been outlined in this thesis. The final proposed design, detailed in *chapter 4, section 4.1.3,* realises all the mechanical and electronic requirements of an automated inspection system. The primary achievements of the project are as follows:

- An imaging system has been designed and built that has the ability to identify macro and micro defects through use of a three lens optical system. The imaging system has the ability to detect defects as small as 2.43μm and can view objects as large as 0.9mm.
- A successful image acquisition module has been designed that allows scaled microscopic images to be acquired from the device. This system can achieve acquisition rates of approximately 25 fps.
- A robust autofocus system with depth of focus resolution <1.25μm has been designed, built and implemented successfully.
- A software interface that communicates with the acquisition module and allows direct access to image pixel values has been coded.
- Software has been written that provides fully automated control of the device.

From an evaluation of the final design certain limitations of the device have been realised, these are as follows:

- The lens exchange system does not align the lens concentrically with the optical axis.
- Adequate images for analysis purposes can't be acquired at 4X or 40X magnifications due to limitations with the imaging sensor control.

- The illumination system requires enhanced optics to prevent vignetting occurring at low magnifications.

Based on these limitations stricter design criteria have been set out and an alternative design realised which overcomes these. The final proposed design, detailed in *Section 5.4,* realises all the mechanical and electronic requirements of an automated inspection system. This design is a hybrid of the first design built and has been designed in such a way so as to overcome the shortcomings of the initial design.

What remains to be completed for any future project is the software component of the project. Currently the software can control the device and acquire scaled microscopic images of a fibre endface. From the acquired image the software can directly access the individual pixel values. In order to complete the software component of the project, analysis of the image, through this pixel array would have to be carried out. Two approaches can be taken for the analysis of the fibre, 2D analysis or 3D analysis. 2-D analysis is the more traditional approach and involves analysing 2D images of the object, 3-D analysis is much more complex and requires the determination of a mathematical model for both the light sources and the surface reflectance of the fibre surface. From these models a 3-D map of the fibre surface can be constructed. A detailed explanation of this analysis method is outline in *appendix 4*.

To conclude what has been achieved from the project is the design of a tool for the inspection of fibre surfaces. Also a methodology for the inspection of fibres has being thoroughly researched and presented. Hence the foundations have been laid for a future project to complete the development of a software algorithm for the analysis of the fibre surfaces.

Bibliography

1. Fibrepulse Technical Article Endface inspection Available From: http://www.fibrepulse.com/html/technical.html [Accessed 10th February 2003]
2. David R. Goff, Fibre Optic Reference Guide.621.3692 Gof : Focal Press
3. Dr Gerald Farrell, Cleaning and inspecting optical fibre connectors,Available from: http://www.pxit.com/pdf/Cleaning%20&%20Inspecting.PDF, [Accessed 7th November 2002]
4. Dr Fred Logue Lucent Technologies Europe
5. Paul F. Whelan &Derek Molloy, Machine Vision Algorithms in Java, 006.37whe, ISBN: 1852332182, Springer 2000.
6. John Stack, Sensors Online Magazine Available from: http://www.sensorsmag.com/articles/0400/34/main.shtml , [Accessed 10th February 2003]
7. Edmund Industrial Optics technical article, available from: http://www.edmundoptics.com/TechSupport/DisplayArticle.cfm?articleid=287 [Accessed 25th February 2002]
8. Phontonics website, available from: http://www.photonics.com/dictionary [Accessed 28th February 2002]
9. Imaging source website, available from: http://www.imagingsource.com , [Accessed 10th March 2002]
10. UCLA Website, available from: http://www.btrip.mednet.ucla.edu/bri/lenes.htm, [Accessed 23rd November 2002]
11. Melles Groit Website, available from: http://http://www.mellesgriot.com/products/machinevision/lef_6.htm [Accessed 15th November 2002]
12. Edmund Industrial Optics technical article, available from: http://www.edmundoptics.com/Techsupport/Displayarticle.cfm?articleid=256, [Accessed 10th November 2003]
13. Technical article, available from: http://www.cartgae.org.lb/en/themes/sciences/physics/optics/optical/lens/lens.htm,[Accessed 10th November 2003]
14. Melles Groit Website, available from: http://www.mellesgriot.com/products/machinevision/cl_1.htm ,[Accessed 15th November 2002
15. Technical article, available from: http://hyperphysics.phy-astr.gsu.edu/hbase/geoopt/telep.html
16. R G Bower Zoom Lens, Available from: http://www.dur.ac.uk/~dphorg/OpticsI/optlec/node38.html,[Accessed 13th Febuary 2002]
17. Technical article, available from: http://www.dalsa.com/shared/content/Photonics_Spectra_CCDvsCMOS_Litwiller.pdf, [Accessed 13th March 2002]
18. How stuff works website technical article, available from: http://www.howstuffworks.com/digital-camera4.htm,[Accessed 23rd February 2002]

19. Edmund Industrial Optics technical article, available from: http://www.edmundoptics.com/TechSupport/DisplayArticle.cfm?articleid=290 [Accessed 20th February 2002]
20. Technical article, available from: http://www.lrc.rpi.edu/programs/nlpip/tutorials/photosensors/spectral.asp , [Accessed 16th November 2003]
21. Imaging Source website, technical article available from: http://www.theimagingsource.com/prod/cam/camintro_2.htm, [Accessed 17th November 2002]
22. Richard Berry, Veikko Kanto, John Munger, The CCD Camera Cookbook, 622.367ber, ISBN: 0943396417, William Bell 1994
23. Technical Article, available from: http://www.astrosurf.com/re/ccdrev.html [Accessed 10 November 2003]
24. Edmund Industrial Optics Website Available from: http://www.edmundoptics.com/techSupport/DisplayArticle.cfm?articleid=289 [Accessed 20 February 2002]
25. Nello Zuech, Understanding and Applying Machine Vision , 006.37 zue , ISBN: 0824789296, Marcel Dekker Inc December 1999
26. Edmund Industrial Optics Website Available from: http://www.edmundoptics.com/TechSupport/DisplayArticle.cfm?articleid=291 [Accessed 20 February 2002]
27. The imaging source website, available from: http://www.theimagingsource.com/prod/ill/Illintro_2.htm [Accessed 15th April 2002]
28. Edmund Industrial Optics technical article, available from: http://www.edmundoptics.com/techSupport/DisplayArticle.cfm?articleid=256 [Accessed November 2002]
29. Zanoguera, MB. Massenbach, B. Kellner, A. Price, J.1998. "High-performance autofocus circuit for biological microscopy", Review of Scientific instruments November 1998. pp3966-3977.
30. Xiao Tang, Pierre L'Hostis and Yu Xiao, 2000 "An Auto-focusing Method in a microscopic Testbed for Optical Disks", July –August 2000, Journal of Research of National Institute of Standards Technology November 2000. pp565-569.
31. F. R. Boddeke, L.J. Van Vliet, H. Netten, and I.T. Young, "Autofocusing in microscopy based on the OTF and sampling", Bioimaging, Vol 2, 1994, pp. 193-203.
32. Technical article, available from: http://www.pcguide.com/ref/mbsys/buses/funcBandwidth-c.html, [Accessed 10th March 2003]
33. The imaging source website, Technical article, available from: http://www.theimagingsource.com/prod/grab/grabintro_2.htm, [Accessed 15th April 2003]
34. Technical article, available from: http://compnetworking.about.com/library/glossary/bldef-firewire.htm, [Accessed 17th March 2003]
35. Technical article, available from: http://searchnetworking.techtarget.com/sDefinition/0,,sid7_gci212126,00.html [Accessed 17th March 2003]
36. Supplier website, http://www.silicon imaging.com [Accessed 15 March 2003]

37. Beyond logic website, technical article, available from: http://www.beyondlogic.org/usbnutshell/usb1.htm [Accessed 15th March 2003]
38. John Hyde, USB Design by Example, a practical guide to building I/O devices, ISBN 0471-37048-7, Intel University Press 1999
39. Technical article, available from: http://computer.howstuffworks.com/usb1.htm, [Accessed October 2003]
40. Technical article, available from: http://www.taurusstudio.net/research/texture/ps/, [Accessed July 2003]
41. Berthold K. P Horn and Robert W. Sjoberg, Calculating the Reflectance Map, October 1978, Applied Optics, Volume 18, Issue 11, June 1, 1979, pp.1770-1779
42. Milan Sonka, Image Processing and Analysis, and Machine vision 2nd edition ISBN 0-534-95393 PWS Publishing
43. Lu, J. Mei, X. Gunaratne, M 2000. Development of automatic crack detection system fro measuring cracks
44. J. Johnson, "Analysis of Image Forming Systems," Proc. Image Intensifier Symposium, US Army Engineer Research and Development Laboratories, Fort Belvoir, Va., 6-7 Oct. 1958 (AD220160).
45. Technical article, available from: http://www.optosigma.com [Accessed 10th November 2003]
46. Technical article, available from: http://www.dprg.org/tutorials/1998-04a/ [Accessed 10th December 2003]
47. Tom Duncan, Success in Electronics 2nd Edition, ISBN 0-7195-7105-3, John Murray 1997
48. Technical article, available from: http://www.cs.uiowa.edu/~jones/step/physics.html [Accessed 10th August 2002]
49. Technical article, available from: http://www.st.com/stonline/books/ascii/docs/1679.htm, [Accessed 5th June 2002]
50. "IEEE Standard for Interface and Protocol Extensions to IEEE 1284-Compliant Peripherals and Host Adapters" Available From: http://standards.ieee.org/catalog/olis/busarch.html,[Accessed 10 August 2004]
51. http://www.beyondlogic.org/spp/parallel.htm, [Accessed 9 August 2004]
52. Technical article titled: "What is direct X ", available from: http://www.programmersheaven.com/2/FAQ-DirectX-what-IS-DirectX [Accessed 15th August, 2002]
53. Microsoft, "MSDN developer's library", available from: http://www.msdn.microsoft.com/library/default.asp [Accessed 20th September, 2002]
54. David J Kruglinski, Programming Microsoft Visual C++, ISBN 1572318570, Microsoft Press
55. Technical article titled:"How to write a capture application" available from: http://msdn.microsoft.com/archive/default.asp?url=/archive/en-us/dx81_c/directx_cpp/htm/howtowriteacaptureapplication.asp [Accessed 15th August 2002]
56. M Fancon, Optical Image Formation and Processes,535.2,
57. Warren J. Smith, Modern Optical Engineering 3rd edition, McGraw-Hill, 2000

58. Optical Microscopy, Michael w. Davidson & Mortimer Abramowitz December 1999, Downloadable from: http://micro.magnet.fsu.edu/primer/pdfs/microscopy.pdf, [Accessed 10 October 2003]
59. Technical article, available from: http://www.microscopyu.com/articles/optics/components.html [Accessed 21st October 2003]
60. Allen Stimson, Photometry and Radiometry for Engineers, ISBN: 047182531X, John Wiley & Sons Inc December 1974
61. Berthold K. P Horn, Robot Vision (MIT Electrical Engineering and Computer Science), ISBN: 0262081598, The MIT Press, March 1986
62. Radiometry, BRDF and Photometric stereo EE7730 – Computer vision notes series 4 available from: http://www.ece.lsu.edu/gunturk/EE4780/Lecture%20-%20Radiometry2.ppt, [Accessed 11th June 2003]
63. R. J. Woodham, Photometric Method for Determining Surface Orientation from Multiple Images, Journal of Optical Engineering, Vol. 19, No. 1, 1980, pp. 138-144.

Appendices

Appendix 1 – Imaging System Calculations

Concept 1 Calculations:

Pixel Size = 6.5μm square

CCD Dimensions = 3.6mm X 4.6mm

Magnification = 20X

Camera Res. (μm) = 2*Pixel Size (μm)

Object Res. (μm) = Camera Res. (μm)/Optical Magnification

⇒Camera Resolution = 13μm

$$\Rightarrow \text{Object Resolution} = \frac{13}{20} = 0.65$$

⇒Maximum Feature size detectable: 0.625μm

$$\text{Field of View} = \frac{SS}{M}$$

$$\text{Field of View} = \frac{3.6}{20}$$

⇒Maximum FOV achievable: 0.18mm

Concept 2 Zoom Lens – Calculations:

Pixel Size = 6.5μm square

CCD Dimensions = 3.6mm X 4.6mm

Minimum Zoom Magnification = 1X

Maximum Zoom Magnification = 20X

Camera Res. (μm) = 2*Pixel Size (μm)

Object Res. (μm) = Camera Res. (μm)/Optical Magnification

⇒Camera Resolution = 13μm

Highest resolution will occur at 20X magnification

$$\Rightarrow \text{Object Resolution} = \frac{13}{20} = 0.65$$

⇒Maximum Feature size detectable: 0.625μm at 20X optical magnification

$$\text{Field of View} = \frac{SS}{M}$$

Largest Field of view will occur at 1X Magnification

$$\text{Field of View} = \frac{3.6}{1}$$

⇒Maximum FOV achievable: 3.6mm at 1X optical zoom

Alternative Design Concept 2 Calculations:

- 20X Lens - FOV = .24mm

  Smallest Detectable defect = 2.1μm(13 pixels)

- 4X lens - FOV = 1.2mm

  Smallest Detectable defect = 10.75μm(13 pixels)

Pixel Size = 3 μm square

CCD Dimensions = 4.8mm X 6.4mm

Two Lens System:

- 20X
- 4X

With 20X lens:

$$\text{Field of View} = \frac{SS}{M}$$

$$\text{Field of View} = \frac{4.8}{20}$$

⇒ FOV at 20X magnification: 0.24mm

Camera Res. (μm) = 2*Pixel Size (μm)

Object Res. (μm) = Camera Res. (μm)/Optical Magnification

⇒Camera Resolution = 6μm

$$\Rightarrow \text{Object Resolution} = \frac{6}{20} = 0.3\mu m$$

Smallest detectable defect = 0.3*7 = 2.1μm

⇒Smallest Detectable Defect at 20X = 2.1μm

With 4X lens:

$$\text{Field of View} = \frac{SS}{M}$$

$$\text{Field of View} = \frac{4.8}{4}$$

⇒ FOV at 4X magnification: 1.2mm

Camera Res. (μm) = 2*Pixel Size (μm)

Object Res. (μm) = Camera Res. (μm)/Optical Magnification

⇒Camera Resolution = 6μm

$$\Rightarrow \text{Object Resolution} = \frac{6}{4} = 1.5\ \mu m$$

Smallest detectable defect = 1.5*7 = 10.75μm

⇒Smallest Detectable Defect at 4X = 10.75μm

Appendix 2 – Important Datasheet Extracts

International Standard Microscope Objectives

[Specification Table | Related Products | Helpful Literature | Product Matrix | Technical Images]

Our full selection of objectives can be used with all major brands of microscopes. Our matrix includes both DIN (Deutsche Industrie Norm) 45mm standard and JIS (Japan Industrial Standards) 36mm standard objectives. All optics are AR coated. DIN microscopes are configured for a 160mm tube length, and JIS microscopes for a 170mm tube length. DIN and JIS objectives can be interchanged, although the powers will not be equivalent (approximately 10% difference). All 20X to 100X objectives have spring-loaded (retractable) front ends in order to prevent slide damage. Oil immersion is recommended for all 100X objectives in order to achieve an NA higher than 1.0 (for typical use: low viscosity 150 cps, 0.5 oz. tube with nd=1.515).

Specification Table

DIN Objectives (dimensions in mm)					
Power	**A**	**B**	**C**	**D**	
4X	28.7	11.0	18.0	—	
10X	38.5	19.5	17.7	11.0	
20X	41.8	21.0	17.7	15.3	
40X	44.4	20.4	17.7	15.3	
60X	44.7	22.5	17.7	15.3	
100X	44.8	22.5	17.7	15.3	
JIS Objectives (dimensions in mm)					
Power	**A**	**B**	**C**	**D**	**E**
10X	31.0	20.0	8.5	11.0	15.3
20X	33.3	18.0	10.7	15.3	21.0
40X	36.0	18.0	10.7	15.3	21.0
60X	36.3	21.0	11.0	15.3	21.0
100X	36.4	21.0	10.8	15.3	21.0

Products

[Quotation Request]

Description	Type	Magnification	E.F.L. (mm)	Field of View (mm)	Working Distance (mm)	N.A.	Stock Number	Price *		
• IMMERSION OIL							NT38-502	$8.95	in stock	BUY
• OBJECTIVE MICRO 100X DIN	Semi-Plan	100X Spring Loaded	1.86	0.18	0.13	1.25	NT38-344	$256.50	in stock	BUY
• OBJECTIVE MICRO 100X DIN	Achromatic	100X Spring Loaded	1.90	0.18	0.13	1.25	NT36-134	$211.50	in stock	BUY
• OBJECTIVE MICRO 100X JIS	Achromatic	100X Spring Loaded	1.82	0.18	0.14	1.25	NT41-670	$191.50	in stock	BUY
• OBJECTIVE MICRO 10X DIN	Semi-Plan	10X	16.60	1.80	6.5	0.25	NT38-342	$136.50	in stock	BUY
• OBJECTIVE MICRO 10X DIN	Achromatic	10X	16.6	1.80	6.5	0.25	NT36-132	$76.50	in stock	BUY
• OBJECTIVE MICRO 10X JIS	Achromatic	10X	16.76	1.80	6.5	0.25	NT30-046	$59.50	in stock	BUY
• OBJECTIVE MICRO 20X DIN	Achromatic	20X Spring Loaded	8.55	0.90	3.30	0.40	NT38-339	$86.50	in stock	BUY
• OBJECTIVE MICRO 20X JIS	Achromatic	20X Spring Loaded	8.55	0.90	3.3	0.40	NT30-047	$84.00	in stock	BUY
• OBJECTIVE MICRO 40X DIN	Achromatic	40X Spring Loaded	4.48	0.45	0.57	0.65	NT36-133	$96.50	in stock	BUY
• OBJECTIVE MICRO 40X DIN	Semi-Plan	40X Spring Loaded	4.50	0.45	0.6	0.65	NT38-343	$156.50	in stock	BUY
• OBJECTIVE MICRO 40X JIS	Achromatic	40X Spring Loaded	4.48	0.45	0.57	0.65	NT30-048	$84.00	in stock	BUY
• OBJECTIVE MICRO 4X DIN	Achromatic	4X	31.00	4.50	16.7	0.10	NT36-131	$53.50	in stock	BUY
• OBJECTIVE MICRO 4X DIN	Semi-Plan	4X	30.60	4.50	15.8	0.10	NT38-341	$96.50	in stock	BUY
• OBJECTIVE MICRO 60X DIN	Achromatic	60X Spring Loaded	3.09	0.30	0.28	0.85	NT38-340	$161.50	in stock	BUY
• OBJECTIVE MICRO 60X JIS	Achromatic	60X Spring Loaded	3.08	0.30	0.28	0.85	NT30-049	$136.50	in stock	BUY

* Highlighted item price indicates quantity pricing available. Click price to view details.

in stock — This icon represents an item that is **in stock** and **ready to ship**.

e-mail — **Click this icon** to receive an e-mail with **delivery information**.

Technical Images

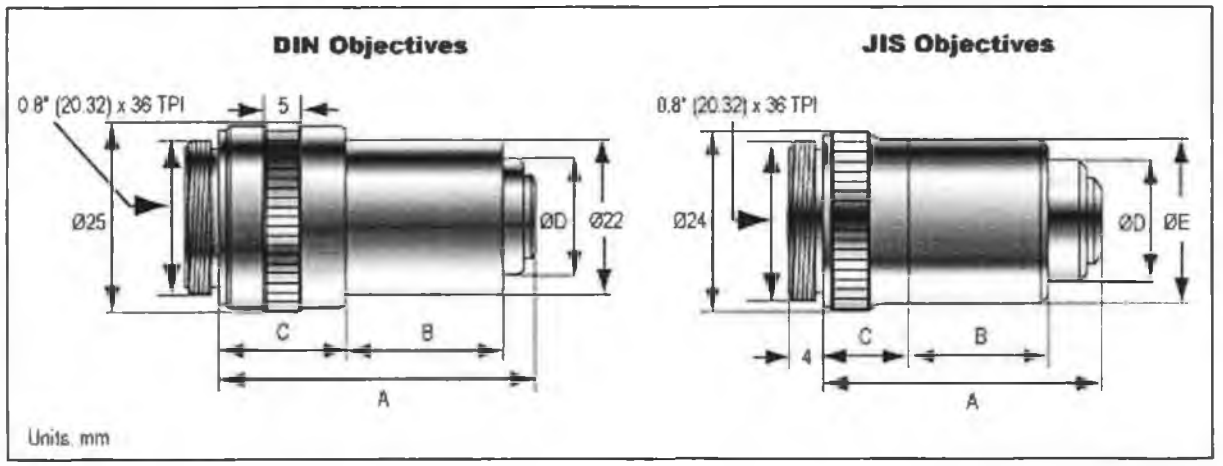

TRIDENT IG33 low cost DC Motor Gearhead

The Igarashi IG33 range is designed for low cost, high volume applications such as vending machines, magnetic card readers, printer mechanisms, actuators and all types of coin control systems.

The IG33 is fitted with an all metal gearhead with sintered iron gears running on hardened steel shafts. The output shaft runs in sintered bronze bearings.

The permanent magnet motors are wound for different speeds for each voltage to give a wide choice of final speeds when matched to the seven gearheads.

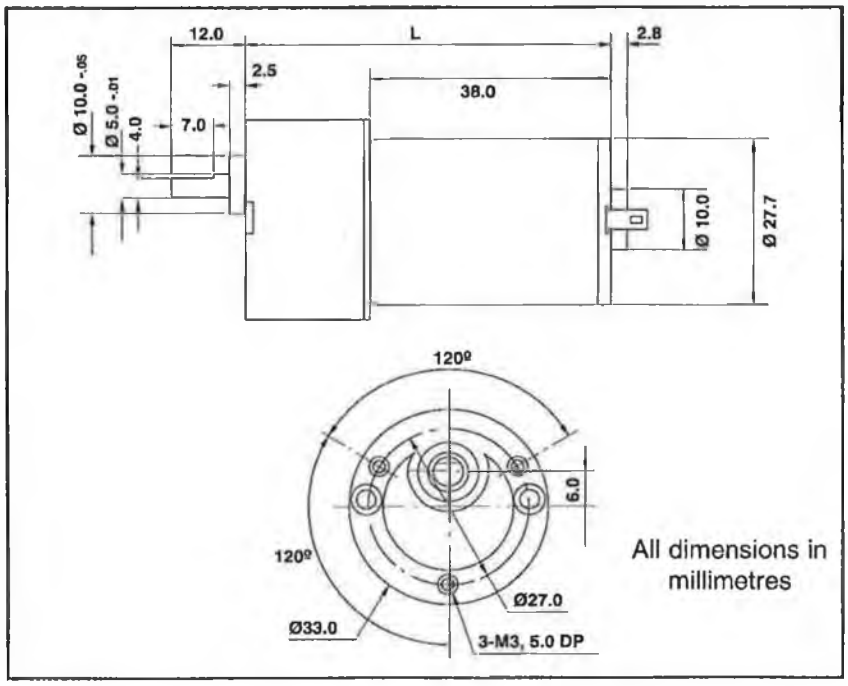

Weight 115 - 140 gms according to ratio
Max. radial load: 50N (8mm from mounting face)
Max. axial load: 33N (at shaft centre)
Max. radial play: 0.08mm
Max. axial play: 0.50mm

Type	Voltage(V.)	Ratio	*Output Rotation	Length (L) (mm)	Maximum Torque (mNm)	Nominal No load speed rev/min	Nominal No load current mA
0132-0008	12	8:1	CCW	57.8	50	700	70
0196-0008	12					460	50
0267-0008	24					680	50
0380-0008	24					475	30
0132-0020	12	20:1	CW	57.8	100	280	70
0196-0020	12					180	50
0267-0020	24					270	50
0380-0020	24					190	30
0132-0050	12	50:1	CCW	57.8	200	110	70
0196-0050	12					70	50
0267-0050	24					105	50
0380-0050	24					75	30
0132-0125	12	125:1	CW	62.3	300	44	70
0196-0125	12					29	50
0267-0125	24					43	50
0380-0125	24					30	30
0132-0312	12	312:1	CCW	62.3	300	18	70
0196-0312	12					11	50
0267-0312	24					17	50
0380-0312	24					12	30
0132-0781	12	781:1	CW	66.8	300	7	70
0196-0781	12					5	50
0267-0781	24					7	50
0380-0781	24					5	30
0132-1953	12	1953:1	CCW	66.8	300	3	70
0196-1953	12					2	50
0267-1953	24					3	50
0380-1953	24					2	30

* The motors are bidirectional; the rotation listed is achieved with positive supply connected to +ve terminal on motor.

Detail view

Proximity Sensor
150371
SIEN-M5B-PS-S-L

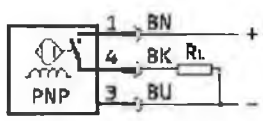

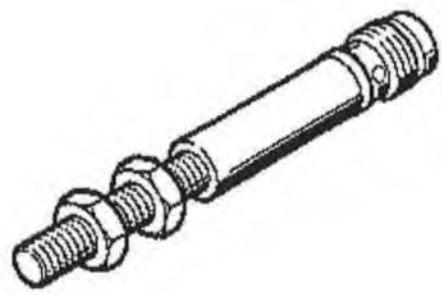

(PDF) Catalog page

Criterion	Feature
Design	Round
Type of installation	flush
Conforms to standard	DIN EN 60947-5-2
Short circuit strength	Pulsing
Switching element function	Normally open contact
Polarity protected	for all electrical connections
Operating status display	Yellow LED
Max. switching frequency	3,000 Hz
Max. switching frequency, DC	3,000 Hz
Operating voltage DC	10 - 30 V
Idle current	<= 10 mA
Max. output current	200 mA
Residual ripple	10 %
Switch output	PNP
Voltage drop	2 V
CE Symbol	In compliance with EU directive 89/336/EWG (EMV)

Protection class	IP67
Ambient temperature	-25 - 70 °C
Tightening torque	2 Nm
Product weight	9 g
Nominal switching distance	0.8 mm
Guaranteed switching distance	0.64 mm
Reduction factors	Aluminium = 0.4
	Stainless steel, St 18/8 = 0.7
	Copper = 0.3
	Brass = 0.4
	Steel, St 37 = 1.0
Reproducibility of switching value	+/- 0.04 mm
Repetition accuracy	0.04 mm
Electrical connection	M8x1
	Plug
	3-pin
Mounting type	with lock nut
Materials note	Copper and Teflon-free
Materials information, housing	High alloy steel, non-corrosive

SGS-THOMSON MICROELECTRONICS

L293D

PUSH-PULL FOUR CHANNEL DRIVER WITH DIODES

PRELIMINARY DATA

- 600mA. OUTPUT CURRENT CAPABILITY PER CHANNEL
- 1.2A PEAK OUTPUT CURRENT (NON REPETITIVE) PER CHANNEL
- ENABLE FACILITY
- OVERTEMPERATURE PROTECTION
- LOGICAL "0" INPUT VOLTAGE UP TO 1.5v (HIGH NOISE IMMUNITY
- INTERNAL CLAMPS DIODES

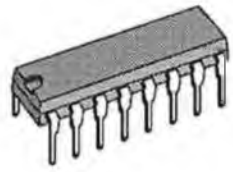

Powerdip 12+2+2

ORDERING NUMBER : L293D

DESCRIPTION

The L293D is a monolithic integrated high voltage, high current four channel vriver designed to accept standard DTL or TTL logic levels and drive inductive loads (such as relays solenoides, DC and stepping motors) and switching power transistors.

To simplify use as two bridges is pair of channels is equiped with an enable input. A separate supply innput is provited formthe logic, allowing operation at a low voltage and internal clamp diodes are included.

This device is suitable for use in switching applications at frequencies up to 5 KHz.

The L293D is assembled in a 16 lead plastic packege which has 4 center pins connected together and used for heatsinking.

BLOCK DIAGRAM

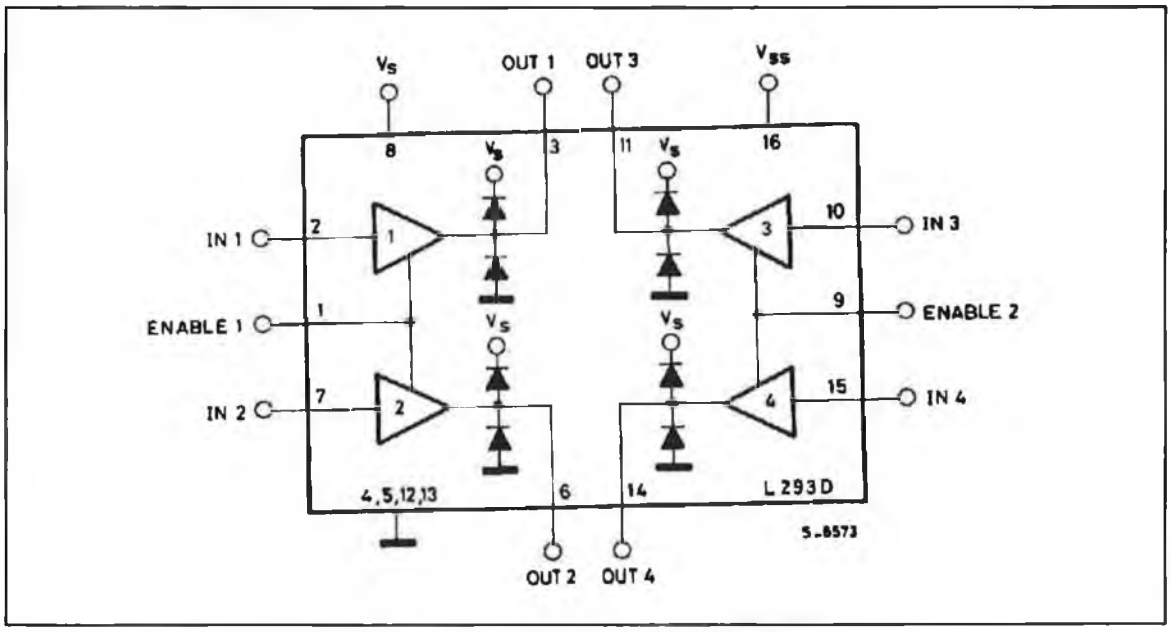

ABSOLUTE MAXIMUM RATINGS

Symbol	Parameter	Value	Unit
V_S	Supply Voltage	36	V
V_{SS}	Logic Supply voltage	36	V
V_i	Input voltage	7	V
V_{en}	Enable voltage	7	V
I_o	Peak output current (100µs non repetitive)	1.2	A
P_{tot}	Total power dissipation at $T_{ground\text{-}pins}$ = 80°C	5	W
T_{stg}, Tj	Storage and junction temperature	-40 to 150	°C

CONNECTION DIAGRAM

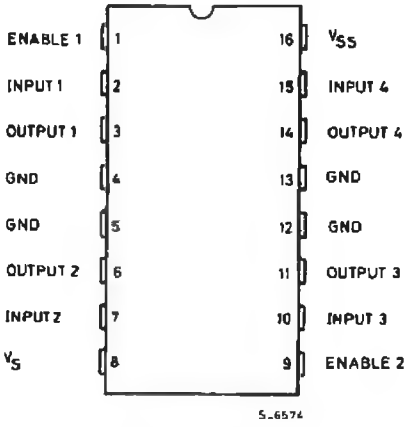

THERMAL DATA

Symbol	Parameter		Value	Unit
Rth-j-case	Thermal resistance junction-case	max	14	°C/W
Rth j-case	Thermal resistance junction-ambient	max	80	°C/W

ELECTRICAL CHARACTERISTICS (For each channel, V_s = 24V, V_{ss} = 5V, T_{amb} = 25 °C, unless otherwise specified)

Symbol	Parameter	Test conditions	Min.	Typ.	Max.	Unit
V_s	Supply voltage		V_{ss}		36	V
V_{ss}	Logic supply voltage (pin 16)		4.5		36	V
I_s	Total quiescent supply current (pin 8)	V_i = L I_o = 0 V_{en} = H		2	6	mA
		V_i = H I_o = 0 V_{en} = H		16	24	
		V_{en} = L			4	
I_{ss}	Total quiescent logic supply current (pin 16)	V_i = L I_o = 0 V_{en} = H		44	60	mA
		V_i = H I_o = 0 V_{en} = H		16	22	
		V_{en} = L		16	24	
V_{IL}	Input low voltage (pin 2, 7, 10, 15)		-0.3		1.5	V
V_{IH}	Input high voltage (pin 2, 7, 10, 15)	$V_{ss} \leq 7V$	2.3		V_{ss}	V
		$V_{ss} > 7V$	2.3		7	
I_{IL}	Low voltage input current (pin 2, 7, 10, 15)	V_{IL} = 1.5V			-10	µA
I_{IH}	High voltage input current (pin 2, 7, 10, 15)	$2.3 \leq V_{IH} \leq V_{ss}$ -0.6V		30	100	µA
V_{enL}	Enable low voltage (pin 1, 9)		-0.3		1.5	V
V_{enH}	Enable high voltage (pin 1, 9)	$V_{ss} \leq 7V$	2.3		V_{ss}	V
		V_{ss} 7V	2.3		7	
I_{enL}	Low voltage enable current (pin 1, 9)	V_{enL} = 1.5V		-30	-100	µA
i_{enH}	High voltage enable current (pin 1, 9)	$2.3V \leq V_{enH} \leq V_{ss}$ -0.6V			± 10	µA
V_{CEsatH}	Source output saturation voltage (pin 3, 6, 11, 14)	I_o = -0.6A		1.4	1.8	V
V_{CEsatL}	Sink output saturation voltage (pins 3, 6, 11, 14)	I_o +0.6A			1.2	1.8
V_F	Clamp diode forward voltage	I_o = 600 mA		1.3		V
t_r	Rise time (*)	0.1 to 0.9 V_o		250		ns
t_f	Fall time (*)	0.9 to 0.1 V_o		250		ns
t_{on}	Turn-on delay (*)	0.5 V_i to 0.5 V_o		750		ns
t_{off}	Turn-off delay (*)	0.5 V_i to 0.5 V_o		200		ns

(*) See fig.1

TRUTH TABLE (One channel)

INPUT	ENABLE (*)	OUTPUT
H	H	H
L	H	L
H	L	Z
L	L	Z

Z = High output impedance

(*) Relative to the considered channel

Figure 1. Switching Times

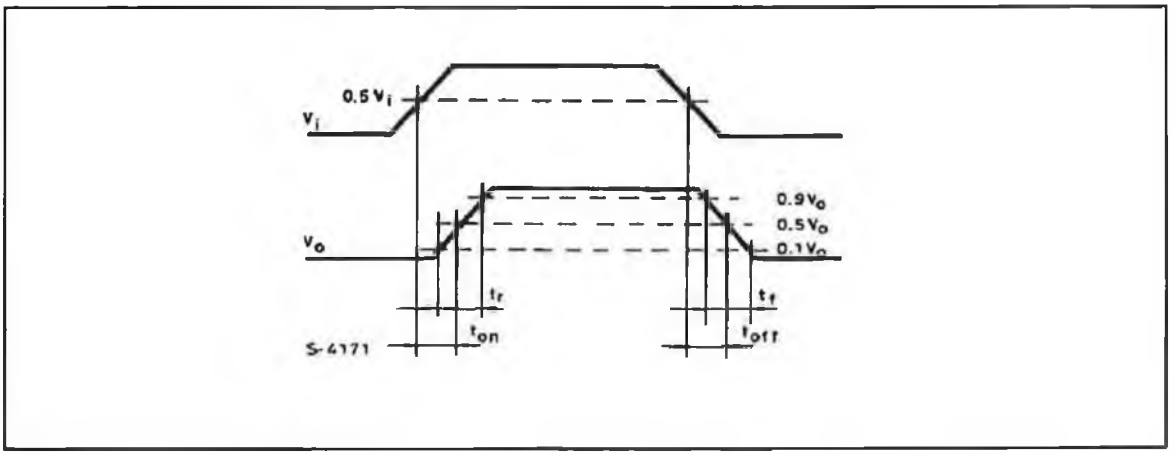

FAIRCHILD SEMICONDUCTOR™

March 1998

DM7474
Dual Positive-Edge-Triggered D Flip-Flops with Preset, Clear and Complementary Outputs

General Description

This device contains two independent positive-edge-triggered D flip-flops with complementary outputs. The information on the D input is accepted by the flip-flops on the positive going edge of the clock pulse. The triggering occurs at a voltage level and is not directly related to the transition time of the rising edge of the clock. The data on the D input may be changed while the clock is low or high without affecting the outputs as long as the data setup and hold times are not violated. A low logic level on the preset or clear inputs will set or reset the outputs regardless of the logic levels of the other inputs.

Features

- Alternate Military/Aerospace device (5474) is available. Contact a Fairchild Semiconductor Sales Office/Distributor for specifications.

Connection Diagram

Dual-In-Line Package

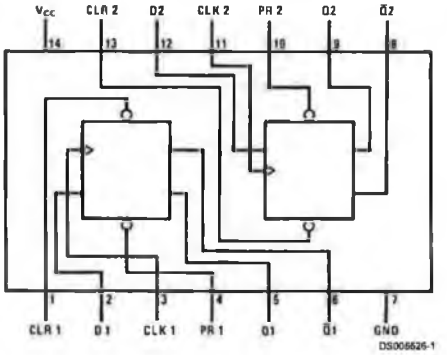

Order Number 5474DMQB, 5474FMQB, DM5474J, DM5474W, DM7474M or DM7474N
See Package Number J14A, M14A, N14A or W14B

Function Table

Inputs				Outputs	
PR	CLR	CLK	D	Q	$\overline{Q}$
L	H	X	X	H	L
H	L	X	X	L	H
L	L	X	X	H (Note 1)	H (Note 1)
H	H	↑	H	H	L
H	H	↑	L	L	H
H	H	L	X	Q_0	$\overline{Q}_0$

H = High Logic Level
X = Either Low or High Logic Level
L = Low Logic Level
↑ = Positive-going transition of the clock.

Note 1: This configuration is nonstable; that is, it will not persist when either the preset and/or clear inputs return to their inactive (high) level.
Q_0 = The output logic level of Q before the indicated input conditions were established.

 DS006526

IM483

HIGH PERFORMANCE MICROSTEPPING DRIVER

FEATURES

- Low Cost
- Extremely Small (2.7 x 3.0 x 1.2 inches) (70 x 69 x 31 mm)
- High Input Voltage (48V)
- High Output Current (3 Amps RMS, 4 Amps Peak)
- Advanced Surface Mount and ASIC Technology
- No Minimum Inductance
- Single Supply
- Up to 10 MHz Step Clock Rate
- Opto-Isolated Inputs
- Fault Output
- Short Circuit and Over Temperature Protection
- Up to 51,200 Steps/Rev
- Microstep Resolutions Can Be Changed On-The-Fly without Loss of Motor Position
- 20 kHz Chopping Rate
- Automatically Switches Between Slow and Fast Decay for Unmatched Performance
- 14 Selectable Resolutions Both in Decimal and Binary
- Adjustable Automatic Current Reduction
- At Full Step Output
- Optional On-board Indexer and Encoder Feedback

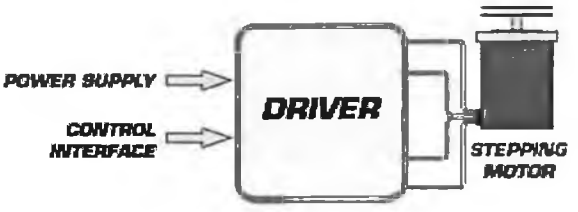

BLOCK DIAGRAM

DESCRIPTION

The IM483 is a high performance, low cost microstepping driver that incorporates advanced surface mount and ASIC technology. The IM483 is small, easy to interface and use, yet powerful enough to handle the most demanding applications.

The IM483 has 14 different resolutions (both in binary and decimal) built into the driver. These resolutions can be changed at any time. There is no need to reset the driver.

This feature allows the user to rapidly move long distances, yet precisely position the motor at the end of travel without the expense of high performance controllers.

The development of proprietary circuits has minimized ripple current while maintaining a 20 kHz chopping rate. This prevents additional motor heating that is common with drivers requiring higher chopping rates. Now low inductance stepper motors can be used to improve high speed performance and system efficiency. The IM483 also comes with an optional on-board indexer to provide design engineers with versatility and power unmatched in today's industry.

The IM483 is priced lower to provide customers with affordable state-of-the-art technology for that competitive edge needed in today's market.

SPECIFICATIONS

ELECTRICAL — IM483

Input Voltage	+12 to 48 Volts*
Drive Current (Per Phase)	0.4 to 4 Amps Peak (Max 3 Amps RMS)
Isolated Inputs	Step Clock, Direction, Enable & Reset
Step Frequency (Max)	10 MHz (1.8 MHz –NR Option)
Steps per Revolution (1.8° Motor)	400, 800, 1000, 1600, 2000, 3200, 5000, 6400, 10000, 12800, 25000, 25600, 50000, 51200
Protection	Thermal and All Way Short Circuit

*Includes Motor Back EMF, Power Supply Ripple and High Line Conditions. Recommended Power Supply: ISP200-4

MECHANICAL

Dimensions in Inches (mm)

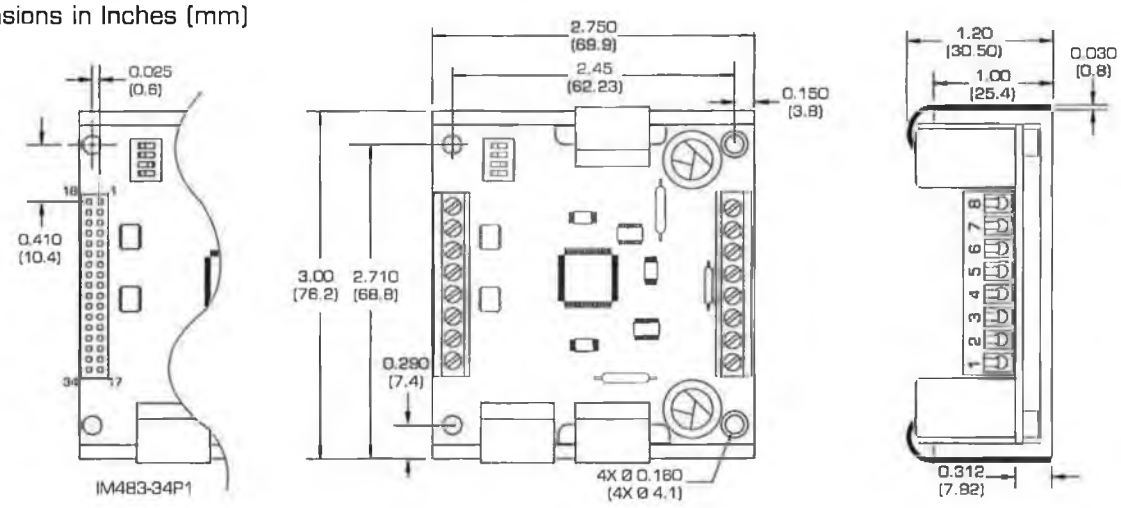

TEMPERATURE

Storage	–40 to +125° C
Case* (Max)	0 to +70° C

*External heat sink may be required to maintain case temperature.

OPTIONS

–NR	Noise Reduction Inputs (1.8 MHz)
H–4X	Heat Sink
TN–48	Thermal Pad
–8P2	8 Position 0.045" sq Pin P2 Connector with 8 Position 0.025" sq Pin P1 Connector
–34P1	34 Position 0.025" sq Pin P1 Connector
–PLG	Plug Type Terminal Strip for P1 and P2 Connectors
PLG-R1/2	Mating Connectors for the -PLG Option
U3-CLP	Side Mounting Clip Set

PIN FUNCTIONS

Connector P1 (8 Pin)

1. No Connection
2. Step Clock
3. Direction
4. Opto Supply
5. Enable
6. Reset
7. Fault
8. On Full Step

Connector P1* (34 Pin)

3.	Resolution Select 3	16, 26.	On Full Step
4.	Step Clock In	21.	Step Clock Out
6.	Direction In	22.	Direction Out
8.	Opto Supply	23.	Resolution Select 0
10.	Enable	24.	Resolution Select 2
12.	Reset	25.	Resolution Select 1
14.	Fault	27.	Ground

*Pins not shown are no connections.

Connector P2

8. Phase $\overline{A}$
7. Phase A
6. Phase $\overline{B}$
5. Phase B
4. V+ (12V to 48V)
3. Ground
2. Current Adjust
1. Reduction Adjust

REV102204

SI-1280F Sensor Specifications

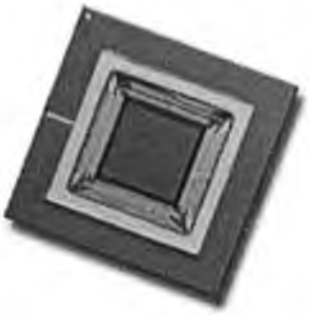

	Value	Units	Remarks
Resolution	1280 x 1024	pixels	-
Pixel pitch	6.7	µm	
Pixel type	4 transistor		
Optical format	2/3	"	8.6 x 6.9mm
Sensitivity	2.7 -	V per lx s V per Ws/m2	at focal plane
QE x FF	> 30	%	peak
noise	20-30 40-60	e- e-	rolling shutter snapshot shutter
Full well capacity	60,000	e-	
Dynamic range	60-66	dB	
dual-slope dynamic range expansion	yes	multiple slopes	
pixel rate	40	MHz	Nominal
shutter	rolling, snapshot		
color	B&W, RGB Bayer		
double sampling	yes		
fixed pattern noise	< 0.5	% RMS	
dark current	750	e-/s	

Appendix 3 - Important Program Sections

DC Motor Control Program and Parallel Port Interfacing

Detailed in this appendix is the software coding used to interface between the PC and the lens control system. Shown below is the coding for the primary thread used to control the DC motor and three interface functions used to start, stop and control the direction of the program. Parallel port calls were used to communicate between software interface and device.

```
UINT DCMotorThread(LPVOID pParam)
{
        PARLLIOINFO         Info; //Structure that holds the parallel port info
        int nLpt = 1; //Port number N.B must be set to one or program will give
                                //Runtime error
        int LoopSpeed = 600000;
        CMotorControllerDlg ParOut;

        EnableIOPortRange(0, 0x300, 0x10);
        Info.dwParllIoInfoSize = sizeof(PARLLIOINFO);

        GetParallelPortInfo(nLpt, &Info);
        ClaimParallelPort(nLpt, 50);
        char String[55];

        int a = 0;
        int b = 128;
        int c = 0;

        Data = fopen( "Data1", "w" );
        while(stop) //Stop is controlled by signal from proximity sensor
        {
                a = _inp(STATUS); // Read in a byte (Proximity sensor signal)
                c = (a & b);  //Reads in MSB off parallel port and AND it with 128 to
get the input bit
                if(c == 128)
                        stop = 0; // MSB of parallel port is hardware inverted
                else if(c == 0)
                        stop = 1;
                if(Direction == 1)
                {
                        _outp(DATA ,12);
                        ParOut.MicroSecondDelay(LoopSpeed);      //duty cycle delay
                        _outp(DATA ,8);
```

```
                ParOut.MicroSecondDelay(LoopSpeed);     //duty cycle delay
            }
            if(Direction == 0)
            {
                _outp(DATA ,4);
             //output a 1 to the 3rd pin of the parallel port & a 0 to the 4th pin
                ParOut.MicroSecondDelay(LoopSpeed);     //duty cycle delay
                _outp(DATA ,0);
                ParOut.MicroSecondDelay(LoopSpeed);     //duty cycle delay
            }
        }
        ReleaseParallelPort(nLpt); //Free's the parallel port for use by other programs


        return 0; //End of Thread terminate
}

void CMotorControllerDlg::OnStart()
{
        stop = 1;
        AfxBeginThread(DCMotorThread,(LPVOID)this);
}

void CMotorControllerDlg::OnDirection()
{
        Direction =! Direction;

}

void CMotorControllerDlg::OnStop()
{
        stop = 0;
}
```

Program for Capturing Video from USB port

Detailed in this appendix is the coding used to acquire video from a USB acquisition device, extract a frame from it and finally get access to the image pixel data.

```
// CaptureBitmapDlg.cpp : implementation file
//
#include "stdafx.h"
#include "CaptureBitmap.h"
#include "CaptureBitmapDlg.h"
#include "SampleGrabber.h"

#include

"d:\directx\dxf\dxsdk\samples\multimedia\directshow\common\dshowutil.cpp"


#ifdef _DEBUG
#define new DEBUG_NEW
#undef THIS_FILE
static char THIS_FILE[] = __FILE__;
#endif

// Constants
#define  WM_CAPTURE_BITMAP     WM_APP + 1 //Defines Window Message

WM_CAPTURE_BITMAP

// Global data
BOOL g_bOneShot = FALSE;          //Flag for getting a taking a shot of the video.
DWORD g_dwGraphRegister=0;  // For running object table
HWND g_hwnd;

//Motor Commands
bool stop = 1;

// Structures
typedef struct _callbackinfo
{
   double dblSampleTime;
   long lBufferSize;
   BYTE *pBuffer;
   BITMAPINFOHEADER bih;

} CALLBACKINFO;
//Initlize the CallBackInfo Structure
CALLBACKINFO cb={0};

//Declare class object
```

```
CSampleGrabberCB mCB;

class CAboutDlg : public CDialog
{
public:
	CAboutDlg();

	// Dialog Data
	//{{AFX_DATA(CAboutDlg)
	enum { IDD = IDD_ABOUTBOX };
	//}}AFX_DATA

	// ClassWizard generated virtual function overrides
	//{{AFX_VIRTUAL(CAboutDlg)
	protected:
	virtual void DoDataExchange(CDataExchange* pDX);    // DDX/DDV
support
	//}}AFX_VIRTUAL

// Implementation
protected:
	//{{AFX_MSG(CAboutDlg)
	//}}AFX_MSG
	DECLARE_MESSAGE_MAP()
};

CAboutDlg::CAboutDlg() : CDialog(CAboutDlg::IDD)
{
	//{{AFX_DATA_INIT(CAboutDlg)
	//}}AFX_DATA_INIT
}

void CAboutDlg::DoDataExchange(CDataExchange* pDX)
{
	CDialog::DoDataExchange(pDX);
	//{{AFX_DATA_MAP(CAboutDlg)
	//}}AFX_DATA_MAP
}

BEGIN_MESSAGE_MAP(CAboutDlg, CDialog)
	//{{AFX_MSG_MAP(CAboutDlg)
		// No message handlers
	//}}AFX_MSG_MAP
END_MESSAGE_MAP()

/////////////////////////////////////////////////////////////////////////////
// CCaptureBitmapDlg dialog

CCaptureBitmapDlg::CCaptureBitmapDlg(CWnd* pParent /*=NULL*/)
	: CDialog(CCaptureBitmapDlg::IDD, pParent)
```

```
{
	//{{AFX_DATA_INIT(CCaptureBitmapDlg)
	//}}AFX_DATA_INIT
	// Note that LoadIcon does not require a subsequent DestroyIcon in Win32
	m_hIcon = AfxGetApp()->LoadIcon(IDR_MAINFRAME);
}

void CCaptureBitmapDlg::DoDataExchange(CDataExchange* pDX)
{
	CDialog::DoDataExchange(pDX);
	//{{AFX_DATA_MAP(CCaptureBitmapDlg)
	DDX_Control(pDX, IDC_STILL, m_Still);
	DDX_Control(pDX, IDC_PREVIEW, m_Preview);
	//}}AFX_DATA_MAP
}

BEGIN_MESSAGE_MAP(CCaptureBitmapDlg, CDialog)
	//{{AFX_MSG_MAP(CCaptureBitmapDlg)
	ON_WM_SYSCOMMAND()
	ON_WM_PAINT()
	ON_WM_QUERYDRAGICON()
	ON_BN_CLICKED(IDC_SNAP, OnSnap)
	ON_WM_CLOSE()
	ON_BN_CLICKED(IDC_BACK, OnBack)
	ON_BN_CLICKED(IDC_FORWARD, OnForward)
	ON_BN_CLICKED(IDC_STOP, OnStop)
	//}}AFX_MSG_MAP
END_MESSAGE_MAP()

/////////////////////////////////////////////////////////////////////////////
// CCaptureBitmapDlg message handlers

BOOL CCaptureBitmapDlg::OnInitDialog()
{
	CDialog::OnInitDialog();

	// Add "About..." menu item to system menu.

	// IDM_ABOUTBOX must be in the system command range.
	ASSERT((IDM_ABOUTBOX & 0xFFF0) == IDM_ABOUTBOX);
	ASSERT(IDM_ABOUTBOX < 0xF000);

	CMenu* pSysMenu = GetSystemMenu(FALSE);
	if (pSysMenu != NULL)
	{
		CString strAboutMenu;
		strAboutMenu.LoadString(IDS_ABOUTBOX);
		if (!strAboutMenu.IsEmpty())
		{
			pSysMenu->AppendMenu(MF_SEPARATOR);
```

```
                    pSysMenu->AppendMenu(MF_STRING, IDM_ABOUTBOX,
strAboutMenu);
                }
        }

        // Set the icon for this dialog.  The framework does this automatically
        // when the application's main window is not a dialog
        SetIcon(m_hIcon, TRUE);                 // Set big icon
        SetIcon(m_hIcon, FALSE);        // Set small icon

        // StillCap-specific initialization
    CoInitialize( NULL );
        InitDirectShow();

        //GetSafeHwnd() return a window handle to a window
        g_hwnd = GetSafeHwnd();

    // start up the still image capture graph
    //
    HRESULT hr = InitStillGraph();
    if (FAILED(hr))
       Error( TEXT("Failed to initialize StillGraph!"));

    // Modify the window style of the capture and still windows
    // to prevent excessive repainting
    m_Preview.ModifyStyle(0, WS_CLIPCHILDREN);
    m_Still.ModifyStyle(0, WS_CLIPCHILDREN);

        return TRUE;  // return TRUE  unless you set the focus to a control
}

void CCaptureBitmapDlg::OnSysCommand(UINT nID, LPARAM lParam)
{
        if ((nID & 0xFFF0) == IDM_ABOUTBOX)
        {
                CAboutDlg dlgAbout;
                dlgAbout.DoModal();
        }
        else
        {
                CDialog::OnSysCommand(nID, lParam);
        }
}
// If you add a minimize button to your dialog, you will need the code below
// to draw the icon.  For MFC applications using the document/view model,
// this is automatically done for you by the framework.

void CCaptureBitmapDlg::OnPaint()
{
        if (IsIconic())
```

```
        {
                CPaintDC dc(this); // device context for painting

                SendMessage(WM_ICONERASEBKGND, (WPARAM)
dc.GetSafeHdc(), 0);

                // Centre icon in client rectangle
                int cxIcon = GetSystemMetrics(SM_CXICON);
                int cyIcon = GetSystemMetrics(SM_CYICON);
                CRect rect;
                GetClientRect(&rect);
                int x = (rect.Width() - cxIcon + 1) / 2;
                int y = (rect.Height() - cyIcon + 1) / 2;

                // Draw the icon
                dc.DrawIcon(x, y, m_hIcon);
        }
        else
        {
                CDialog::OnPaint();

        // Update the bitmap preview window, if we have
        // already captured bitmap data
                mCB.DisplayCapturedBits(cb.pBuffer, &(cb.bih));
        }
}

// The system calls this to obtain the cursor to display while the user drags
// the minimized window.
HCURSOR CCaptureBitmapDlg::OnQueryDragIcon()
{
        return (HCURSOR) m_hIcon;
}

HRESULT CCaptureBitmapDlg::InitDirectShow()
{
  HRESULT hr = S_OK;
        // create a filter graph
  //
  hr = CoCreateInstance(CLSID_FilterGraph, NULL, CLSCTX_INPROC,
                IID_IGraphBuilder, (void **)&m_pGraph);
  if( !m_pGraph )
  {
    Error( TEXT("Could not create filter graph") );
    return E_FAIL;
  }
        // create a sample grabber
  //
        hr = CoCreateInstance(CLSID_SampleGrabber, NULL, CLSCTX_INPROC,
                        IID_ISampleGrabber, (void **)&m_pGrabber);
```

```
    if( !m_pGrabber )
    {
        Error( TEXT("Could not create SampleGrabber (is qedit.dll registered?)"));
        return hr;
    }


        m_pGraph->QueryInterface(IID_IMediaControl, (void **)&pControl);
        m_pGraph->QueryInterface(IID_IVideoWindow, (void **)&pWindow);
        m_pGrabber->QueryInterface(IID_IBaseFilter,  (void **)&pGrabBase);

    return S_OK;
}


HRESULT CCaptureBitmapDlg::InitStillGraph( )
{
    HRESULT hr;

    // get whatever capture device exists
    //

    IBaseFilter  *pCap;
    GetDefaultCapDevice( &pCap );
    if( !pCap )
    {
        Error( TEXT("No video capture device was detected on your system.\r\n\r\n")
            TEXT("This sample requires a functional video capture device, such\r\n")
            TEXT("as a USB web camera.") );
        return E_FAIL;
    }

    // add the capture filter to the graph
    //
    hr = m_pGraph->AddFilter( pCap, L"Cap" );
    if( FAILED( hr ) )
    {
        Error( TEXT("Could not put capture device in graph"));
        return E_FAIL;
    }


    // add the grabber to the graph
    //
    hr = m_pGraph->AddFilter( pGrabBase, L"Grabber" );
    if( FAILED( hr ) )
    {
        Error( TEXT("Could not put sample grabber in graph"));
        return hr;
    }
```

```
// find the two pins and connect them
//
IPin * pCapOut = GetOutPin( pCap, 0 );
IPin * pGrabIn = GetInPin( pGrabBase, 0 );
hr = m_pGraph->Connect( pCapOut, pGrabIn );
if( FAILED( hr ) )
{
   Error( TEXT("Could not connect capture pin #0 to grabber.\r\n")
        TEXT("Is the capture device being used by another application?"));
   return hr;
}

// render the sample grabber output pin, so we get a preview window
//
IPin * pGrabOut = GetOutPin( pGrabBase, 0 );
hr = m_pGraph->Render( pGrabOut );
if( FAILED( hr ) )
{
   Error( TEXT("Could not render sample grabber output pin"));
   return hr;
}

// ask for the connection media type so we know how big
// it is, so we can write out bitmaps
//

AM_MEDIA_TYPE mt;
hr = m_pGrabber->GetConnectedMediaType( &mt );
if ( FAILED( hr) )
{
   Error( TEXT("Could not read the connected media type"));
   return hr;
}

VIDEOINFOHEADER * vih = (VIDEOINFOHEADER*) mt.pbFormat;
mCB.pOwner = this;
mCB.lWidth  = vih->bmiHeader.biWidth;
mCB.lHeight = vih->bmiHeader.biHeight;
FreeMediaType( mt );

// don't buffer(Store)the samples as they pass through
//
m_pGrabber->SetBufferSamples( FALSE );

// only grab one at a time, stop stream after
// grabbing one sample
//
      m_pGrabber->SetOneShot( FALSE );

/* SetCallback calls back the ISampleGrabber interface it takes a pointer
```

```
        to the object and either calls back the SampleCB(0) or the BufferCB (1). In
        this case the Buffer CB is called back.*/

    m_pGrabber->SetCallback( &mCB, 1 );

    // find the video window and stuff it in our window
    //
    if( !pWindow )
    {
        Error( TEXT("Could not get video window interface"));
        return E_FAIL;
    }

    // set up the preview window to be in our dialog
    // instead of floating popup
    //
    HWND hwndPreview = NULL;
    GetDlgItem( IDC_PREVIEW, &hwndPreview );
    RECT rc;
    ::GetWindowRect( hwndPreview, &rc );
    pWindow->put_Owner( (OAHWND) hwndPreview );
    pWindow->put_Left( 0 );
    pWindow->put_Top( 0 );
    pWindow->put_Width( rc.right - rc.left );
    pWindow->put_Height( rc.bottom - rc.top );
    pWindow->put_Visible( OATRUE );
    pWindow->put_WindowStyle( WS_CHILD | WS_CLIPSIBLINGS );

    // run the graph
    //

    hr = pControl->Run( );
    if( FAILED( hr ) )
    {
        Error( TEXT("Could not run graph"));
        return hr;
    }
    return 0;
}


void CCaptureBitmapDlg::GetDefaultCapDevice( IBaseFilter ** ppCap )
{
    HRESULT hr;

    *ppCap = NULL;

    // create an enumerator
    //
    CComPtr< ICreateDevEnum > pCreateDevEnum;
```

```
    pCreateDevEnum.CoCreateInstance( CLSID_SystemDeviceEnum );
    if( !pCreateDevEnum )
        return;

    // enumerate video capture devices
    //
    CComPtr< IEnumMoniker > pEm;
    pCreateDevEnum->CreateClassEnumerator( CLSID_VideoInputDeviceCategory,
&pEm, 0 );
    if( !pEm )
        return;

    pEm->Reset( );

    // go through and find first video capture device
    //
    while( 1 )
    {
        ULONG ulFetched = 0;
        CComPtr< IMoniker > pM;
        hr = pEm->Next( 1, &pM, &ulFetched );
        if( hr != S_OK )
            break;

        // get the property bag interface from the moniker
        //
        CComPtr< IPropertyBag > pBag;
        hr = pM->BindToStorage( 0, 0, IID_IPropertyBag, (void**) &pBag );
        if( hr != S_OK )
            continue;


        // ask for the actual filter
        //
        hr = pM->BindToObject( 0, 0, IID_IBaseFilter, (void**) ppCap );
        if( *ppCap )
            break;
    }

    return;
}

// Snap a still picture
void CCaptureBitmapDlg::OnSnap()
{
        g_bOneShot = TRUE; //Set capture flag.
}

void CCaptureBitmapDlg::Error( TCHAR * pText )
{
```

```
   ::MessageBox( NULL, pText, TEXT("Error!"), MB_OK | MB_TASKMODAL |
MB_SETFOREGROUND );
}


void CCaptureBitmapDlg::OnClose()
{
        // Free the memory allocated for our bitmap data buffer
   if (cb.pBuffer != 0)
   {
      delete cb.pBuffer;
      cb.pBuffer = 0;
   }

        CDialog::OnClose();
}
//The function processes any Posted or Sent message depending on there position in

the queue


LRESULT CCaptureBitmapDlg::WindowProc(UINT message, WPARAM wParam,
LPARAM lParam)
{
        // Field the message posted by our SampleGrabber callback function.
   if (message == WM_CAPTURE_BITMAP)
      mCB.CopyBitmap(cb.dblSampleTime, cb.pBuffer, cb.lBufferSize);

        return CDialog::WindowProc(message, wParam, lParam);
}

// fake out any COM ref counting
//
STDMETHODIMP_(ULONG) CSampleGrabberCB::AddRef() { return 2; }
STDMETHODIMP_(ULONG) CSampleGrabberCB::Release() { return 1; }

// fake out any COM QI'ing
//
STDMETHODIMP CSampleGrabberCB::QueryInterface(REFIID riid, void ** ppv)
{
   if( riid == IID_ISampleGrabberCB || riid == IID_IUnknown )
   {
      *ppv = (void *) static_cast<ISampleGrabberCB*> ( this );
      return NOERROR;
   }
   return E_NOINTERFACE;
}

// we don't implement this interface for this example
//
```

```
STDMETHODIMP CSampleGrabberCB::SampleCB( double SampleTime,
IMediaSample * pSample )
{
    return 0;
}

// The sample grabber is calling us back on its deliver thread.
// This is NOT the main app thread!
// On Windows 9x systems, you are not allowed to call most of the
// Windows API functions in this callback because the
// video renderer might hold the global Win16 lock so that the video
// surface can be locked while you copy its data.  This is not an
// issue on Windows 2000, but is a limitation on Win95,98,98SE, and ME.
// Calling a 16-bit legacy function could lock the system, because
// it would wait forever for the Win16 lock, which would be forever
// held by the video renderer.
// As a workaround, copy the bitmap data during the callback,
// post a message to our app, and write the data later.
//This method will be called for every incoming video frame
STDMETHODIMP CSampleGrabberCB::BufferCB( double dblSampleTime, BYTE
* pBuffer, long lBufferSize )
{
   // this flag will get set to true in order to take a picture

   if( !g_bOneShot )
      return 0;

   // Since we can't access Windows API functions in this callback, just
   // copy the bitmap data to a global structure for later reference.
   cb.dblSampleTime = dblSampleTime; /*Store the sample time, this value is in
seconds*/
   cb.lBufferSize   = lBufferSize;

   // If we haven't yet allocated the data buffer, do it now.
   // Just allocate what we need to store the new bitmap.
   if (!cb.pBuffer)
      cb.pBuffer = new BYTE[lBufferSize];

         char String[100];
         sprintf(String, "The buffer is %d", lBufferSize);
         //AfxMessageBox(String);

   // Copy the bitmap data into our global buffer
   if (cb.pBuffer)
      memcpy(cb.pBuffer, pBuffer, lBufferSize);
         // Post a message to our application, telling it to come back
   // and write the saved data to a bitmap file on the user's disk.
   PostMessage(g_hwnd, WM_CAPTURE_BITMAP, 0, 0L);
   return 0;
}
```

Appendix 4 – Photometric Stereo Reconstruction

The aim of photometric stereo is to determine the surface gradients of an object by using several images of the object taken from the same viewpoint but under illumination from different directions. The theory of photometric stereo can be more easily understood by examining the image produced of a sphere illuminated from one side (Figure 2-35).

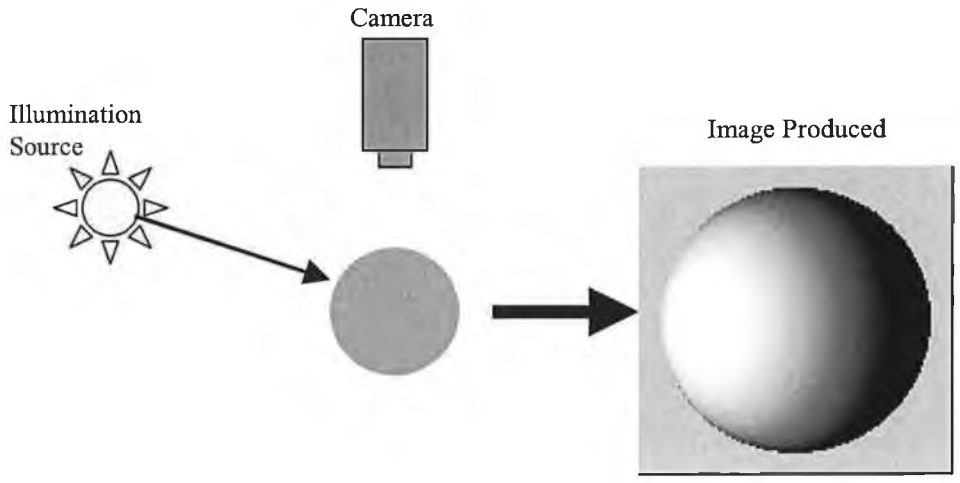

Figure 7-1 – Image produced when sphere is illuminated using directional illumination

While the image of the object produced is essentially 2-D, 3-D information can be extracted from it by examining the variations in surface brightness as the brightness of an object surface depends on two factors [41]:

- The surface orientation with respect to the camera
- The illumination intensity and orientation of the illumination relative to the surface being illuminated

This can be clearly seen in the image produced of the sphere. Where the surface is at right angles to the illumination source, the image intensity is highest. As the surface orientation changes, the image intensity reduces. Therefore it can be concluded that the image intensity will depend on two factors:

- The surface geometry relative to the camera and illumination source

- The amount of light that falls on the object being viewed

So if the position of the camera and illumination source is known relative to the object, the surface orientation can be extracted from a 2-D image of the object, this is the basis of photometric stereo. Before explaining photometric stereo in detail, it is first necessary to have some knowledge of radiometry, as it will define theoretically and mathematically the term of brightness, which is the basis for extraction of 3-D information in photometric stereo.

6.1.1.1 Radiometry

Radiometry is the discipline concerned with measurements of radiant energy within the optical spectrum [41]. Within the visible spectrum, radiant energy can be defined as brightness. In mathematical terms, radiometry defines brightness as a factor of:

1. The amount of light falling on a surface
2. The amount of light a surface reflects

Both of these factors will determine how bright an object is when viewed. The first factor is called the *irradiance* and is more strictly defined as the amount of light radiant on a surface patch per unit area [61]. The second term is *radiance* and is defined as the amount of light/power emitted by a surface patch into a cone of directions having a unit solid angle [61]. To relate this to an imaging system, radiance and irradiance occur wherever light is collected or emitted as illustrated in Figure 7-2.

- Light originates at a source – *radiance*
- Object is illuminated by source – *irradiance*
- Object reflects light – *radiance (Scene)*
- Light collected by camera lens and focused onto a sensor to form an image – *irradiance*

It is important to understand the relationship in terms of irradiance and radiance in a vision system, as what is measured by the camera is the image radiance but what is required to recreate the object surface is the scene radiance. Provided there is one source of illumination, the radiance from this should be proportional to the irradiance values measured by the image sensor. This constant of proportionality can be easily measured experimentally, although it will vary depending on the type of imaging system, i.e. focal length, lens aperture.

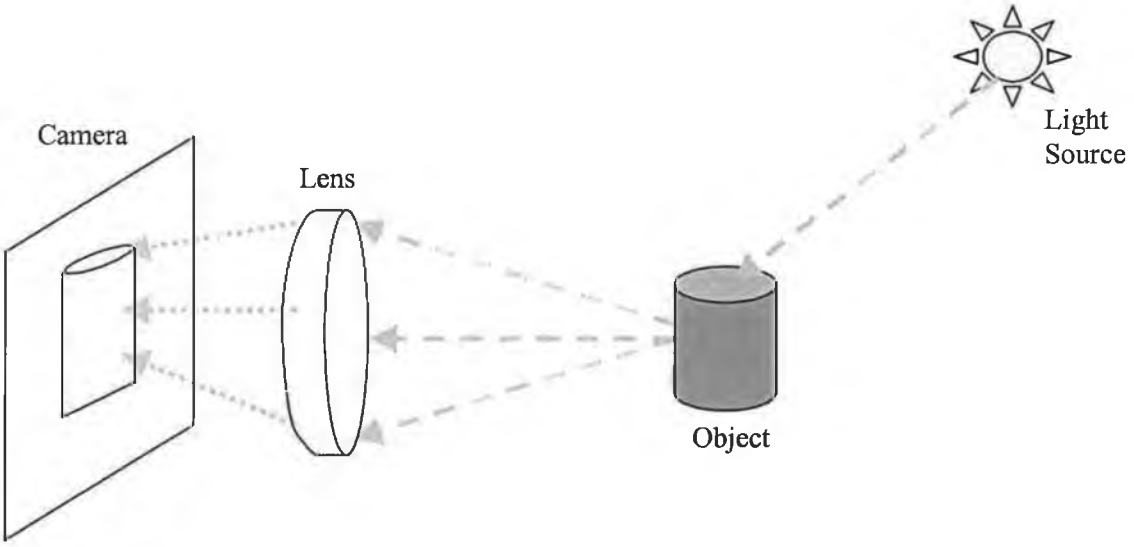

Figure 7-2 - Image formation, radiance occurs when an object emits light, irradiance is the amount of light incident on an object

Equation 7-1 and Equation 7-2 present irradiance and radiance in mathematical terms:

$$\textbf{Equation 7-1 - Irradiance} \rightarrow E = \frac{\delta P}{\delta A} \Rightarrow \frac{Power}{Area}$$

$$\textbf{Equation 7-2 - Radiance} \rightarrow L = \frac{\delta P^2}{\delta A \delta w} \Rightarrow \frac{Power}{Area * SolidAngle}$$

In the definition of radiance we have identified a new term: *solid angle*. This term is necessary to measure the amount of light reflected from a surface patch or emmitted from a source. Solid angle is defined as the projected area of a surface patch onto a unit sphere of a point [62]. Thus a solid angle is subtended by a point and a surface

patch. The point in question is where the object is being viewed. Figure 7-3 and Figure 7-4 illustrate this.

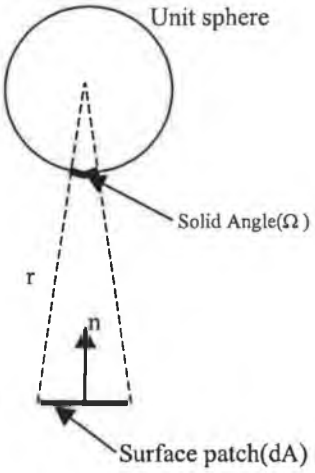

Figure 7-3

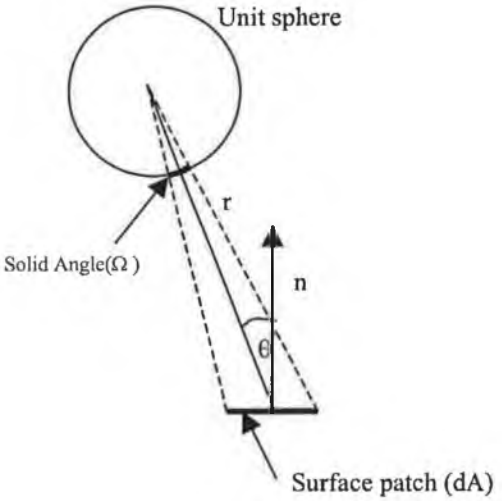

Figure 7-4

In Figure 7-3 the surface patch is located directly below the point in question. Thus the area the surface patch projects onto the sphere is directly proportional to the surface patch. The constant of proportionality is the inverse squared of the distance of the surface patch to the point. Therefore the solid angle is:

$$\textbf{Equation 7-3 - } \Omega = \frac{dA}{r^2}$$

However, when the point in question is located at an angle θ with respect to the surface patch normal there, is a foreshortening of the area. In other words, when an object is viewed from an angle, it appears smaller than when viewed directly from above. The foreshortened area of a surface patch is illustrated in Figure 7-5.

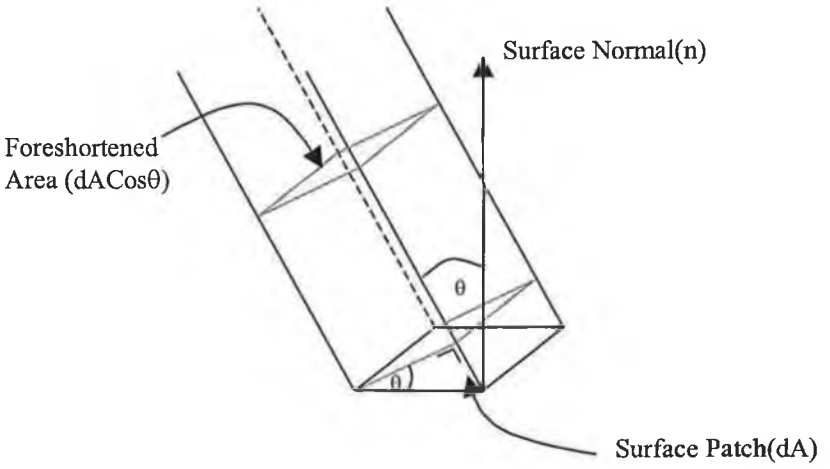

Figure 7-5 – Illustration of foreshortened area

The foreshortened area is dACosθ. Therefore, a small planar patch of area dA at distance r from the origin with an angle θ between the surface normals and the line connecting the point source subtends a solid angle [61]:

$$\textbf{Equation 7-4 - } \Omega = \frac{dACos\theta}{r^2}$$

The solid angle is an important concept, as brightness is determined by the amount of energy an imaging system receives per unit apparent area. All the above assumes a point light source. In reality, light sources cannot be modelled as point sources, but need to be modelled as area patches.

6.1.1.2 Bi-Directional Reflectance distribution function (BRDF)

To determine the surface orientation of an object, the relationship between the object brightness with respect to the angle it is viewed and illuminated from must be known. As mentioned previously, scene radiance depends on the amount of light that falls on a surface and the fraction of incident light that is reflected [41]. It also depends on the geometry of light reflection. An example of how the object geometry effects light reflection is a freshly cut soccer pitch. When mowed in different directions, the pitch will appear to have varying brightness intensities. This is because the grass is oriented

differently depending on the direction in which it is cut. Therefore the amount of light the surface emits, 'scene radiance' will vary even though the viewing position is constant and the amount of light incident on the surface remains the same. The BRDF is a method of characterising the reflection properties of a surface, in terms of its orientation and illumination direction.

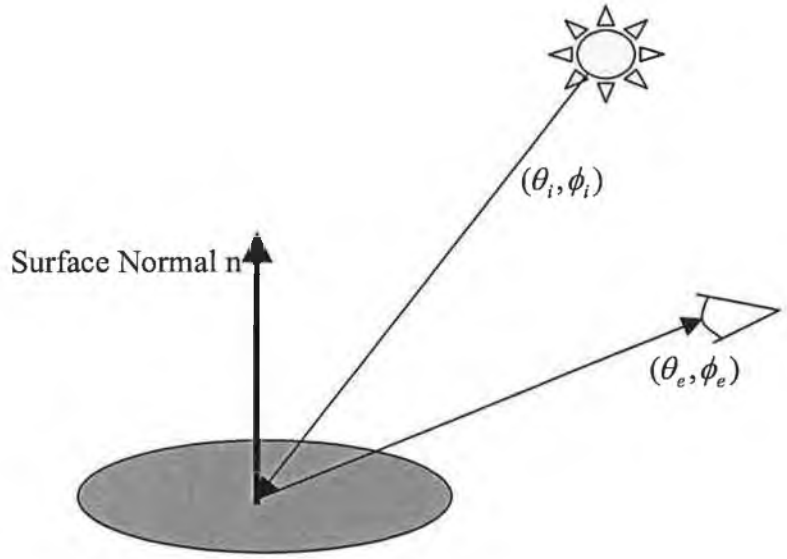

Figure 7-6 - The bi-directional reflectance distribution function is the ratio of the radiance of the surface patch as viewed from the direction (θ_e,ϕ_e) to the irradiance resulting from illumination from the direction (θ_i,ϕ_i).

The BRDF is defined as the ratio of radiance to irradiance:

$$\textbf{Equation 7-5 - } f(\theta_i\phi_i, \theta_e\phi_e) = \frac{\delta L(\theta_e\phi_e)}{\delta E(\theta_i\phi_i)}$$

So the BRDF is simply a mathematical expression stating the relationship between radiance and irradiance in terms of the viewing and illumination directions. To determine BRDF for a particular surface, the surface reflection properties must examined.

6.1.1.3 Surface reflection properties.

The basic principle behind determining a surface's orientation is to understand how it will reflect light. As discussed previously, two factors affect how the surface will reflect light:

- Surface orientation
- The amount of light that falls on a surface

The BRDF combines these two factors to determine how a surface will reflect light. The BRDF is then determined by approximating mathematically the surface reflectance properties. An ideal Lambertian surface is the most common approximation for surface reflectance. It is defined as a surface that appears equally bright from all viewing directions and reflects all incident light absorbing none [41]. Mathematically it is defined as a surface source that manifests luminous intensity in any direction proportional to the cosine of the angle between that direction and the normal to the surface at the point in question [62].

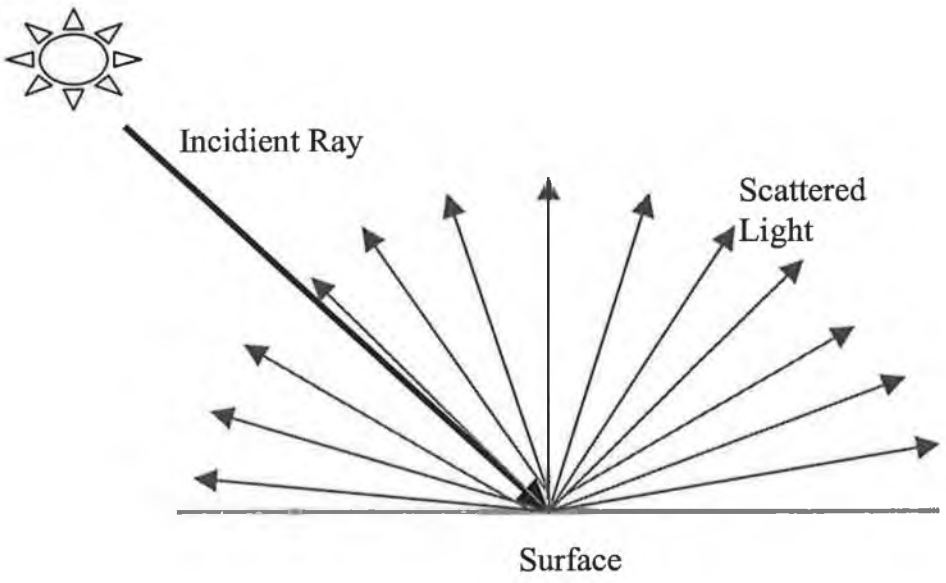

Figure 7-7 – A Lambertian surface is one where the incident light is reflected in a hemisphere of possible directions relative to the surface and with intensity proportional to the cosine of the angle between that direction and the normal to the surface at the point in question

Even though there are no truly Lambertian surfaces or sources many surfaces approximate closely enough to use this assumption. Examples are snow, paper and

matte paint [41], or any material that appears equally bright no matter what direction it is viewed from.

Another common surface approximation is that of a specular surface. A specular surface reflects light at the same angle but in the opposite direction, as the light is incident on the surface.

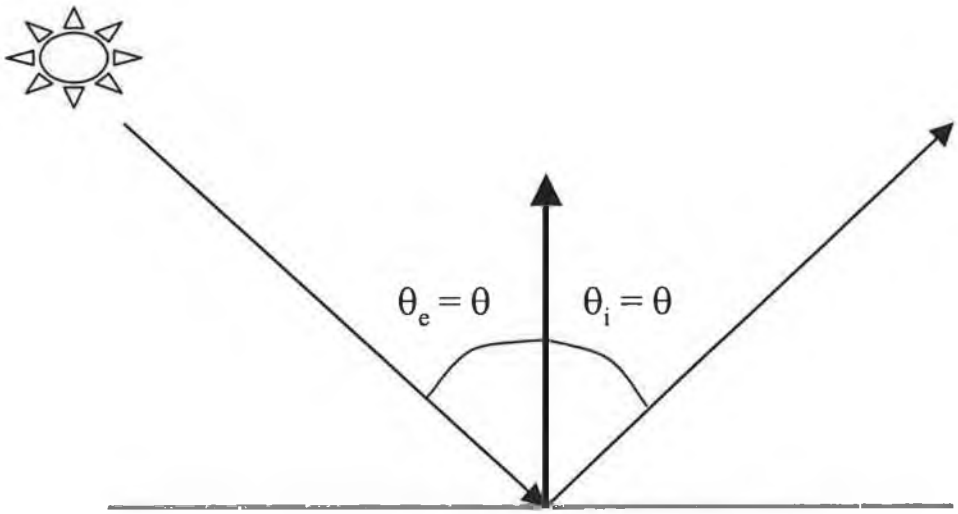

Figure 7-8 A Specular Surface reflects all incident light in a direction that lies in the same plane as the incident ray and the surface normal. The emittance and incident angles with respect to the surface normal are the same.

An example of a specular surface is a mirror as it reflects all the light falling on it from surrounding objects and thus reforms an image of them. However, both of the above examples are simple approximations that are inadequate for most commonly found materials.

An alternative to approximating the BRDF is to determine it experimentally by illuminating a flat sample of the material of interest with a lamp mounted on a goniometer (a device with two axes of rotation) and measuring its irradiance using a sensor mounted on another goniometer. Alternatively, a method to determine how light is reflected from a surface can be devised, and the reflection properties can be found analytically or by numerical simulation [41]. This method, however, is quite

complex and is based on analysing the surface microstructure. It also only produces a closed form solution, which will only work if the material reflectance properties are uniform across its surface.

Often a surface is not uniform in its reflectance properties. The BRDF does not account for when surface reflectance properties are not uniform and only a fraction of the incident light is reflected. It only considers the geometry of the surface and the radiance incident on the surface. This situation can be dealt with by introducing a term to define the fraction of the incident light reemitted by the surface. This term is called the *Albedo*. The albedo is mathematically defined as a constant of proportionality between all the imaged pixels in an object. So, for example, it can be defined as a number between zero and one that indicates how much light the surface reflects relative to some ideal surface with the same geometric dependence on the BRDF [63]. So where two imaged pixels of an object have the same orientation and incident light falling on them, the shading might be different due to the material properties. In this case they will have different albedo values.

6.1.1.4 Surface Orientation

In order to retrieve the 3-D coordinates of a surface for its simulated reconstruction, one must first understand how 3-D surfaces are represented mathematically. A 3-D surface can be described in terms of its perpendicular distance z from a reference plane parallel to the image plane [41].

Equation 7-6 - $z = f(x, y)$

Figure 7-9 illustrates an example of a parabola where the z coordinates are written as a function of the x, y coordinates of the image plane, i.e. $z = x^2 + y^2$, where the x and y coordinates lie on the image plane and the surface height can be described by its perpendicular distance 'z' from the image plane.

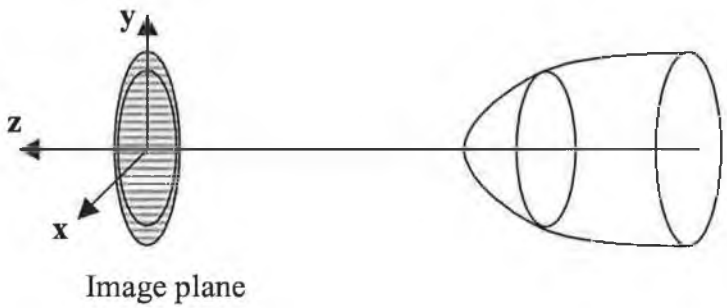

Figure 7-9 – Any 3-D surface can be described in terms of any 2-D reference plane parallel to it

A smooth surface will have a tangent plane at every point. The orientation of the tangent plane will represent the orientation of the surface at that point. The surface normal, a unit vector perpendicular to the tangent plane, is appropriate for specifying the orientation of the plane. Next, one must specify the surface normal in terms of the slopes of the x and y directions. The slopes of the x and y plane are called p and q respectively and are represented by the partial derivatives of z with respect to x and y, i.e.

Equation 7-7 - $p = \frac{\delta z}{\delta x}$ **And** $q = \frac{\delta z}{\delta y}$

The quantity (p,q) is called the gradient of $f(x,y)$ and gradient space is the two dimensional space of all such points (p,q) of a surface [41]. Figure 7-10 illustrates how the gradients in the x and y directions, p and q, can define a surface orientation. If a small step is taken in the x direction of δx, the height changes by pδx. Similarly, if a small step is taken in the y direction, the height will change by qδy. Two perpendicular vectors r_x and r_y define the surface patch where

$$r_x = [\delta x \quad 0 \quad p\delta x]^T$$

$$r_y = [0 \quad \delta y \quad q\delta x]^T$$

Both these values can be normalised to give two vectors parallel to them:

$$R_x = [1 \quad 0 \quad p]^T$$

$$R_y = [0 \quad 1 \quad q]^T$$

These vectors represent the exact same surface orientation as r_x and r_y, except they are at different locations.

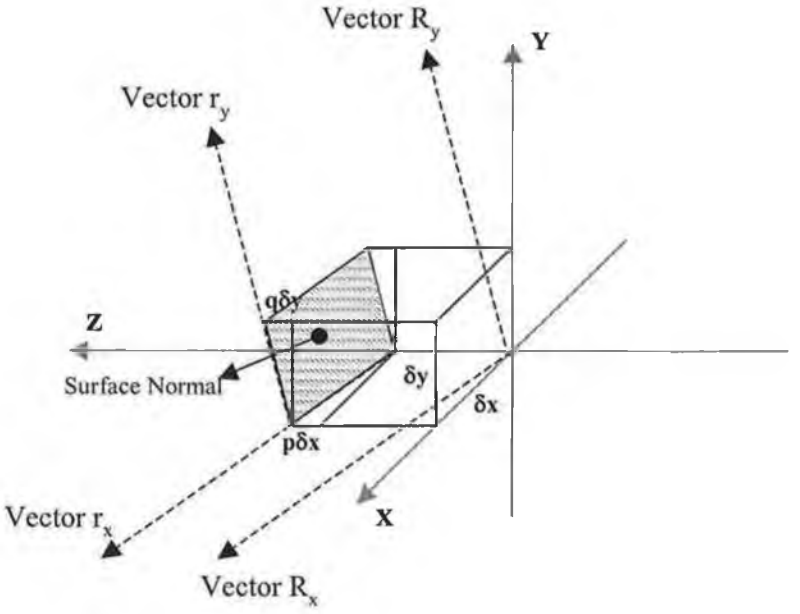

Figure 7-10 – How the gradients in the x and y directions, p and q can define a surface orientation

The surface normal can be computed by taking the cross product of the two vectors.

$$n = R_x \text{ X } R_y$$

$$\text{Rx X Ry} = \begin{bmatrix} i & j & k \\ 1 & 0 & p \\ 0 & 1 & q \end{bmatrix}$$

Equation 7-8 - $\therefore n = \begin{bmatrix} -p & -q & 1 \end{bmatrix}^T$

And the unit surface normal is:

Equation 7-9 - $\hat{n} = \frac{n}{|n|} = \frac{(-p \quad -q \quad 1)}{\sqrt{1+p^2+q^2}}$

So if the surface normal can be ascertained, the surface orientation can subsequently be computed, as they will be at right angles to each other.

6.1.1.5 3-D Surface Reconstruction

So now that an understanding of how 3-D surfaces are represented mathematically has been established, the next step is to determine an object's 3-D surface orientation. The first step in finding the surface orientation is to establish the reflectance map for an image of a surface. A reflectance map is a convenient way to incorporate a fixed scene illumination, surface reflectance and imaging geometry into a single model that allows image intensity to be written as a function of surface orientation [41]. The reflectance map is usually depicted as a series of contours of constant scene radiance. It can be measured directly using a goinometer-mounted sample, or indirectly from an image of an object of known shape. But establishing the reflectance map by the latter method would make redundant the original goal, to establish surface orientation. An alternative is to use an approximation of the reflectance properties of a surface material and the distribution of light sources to ascertain the reflectance map.

Consider a surface illuminated by a single light source of radiance E. Assuming the surface is lambertian, the irradiance L will depend on the incident angle θ_i.

Equation 7-10 - $$L = \frac{1}{\pi} E Cos\theta_i$$

As shown previously the surface normal vector is:

Equation 7-11 - $$n = \begin{bmatrix} -p & -q & 1 \end{bmatrix}^T$$

The vector that points towards the light source can easily be found if it is assumed that the source is far away from the object. There exists a surface orientation that corresponds to this vector, that is, a surface orientated perpendicular to the ray arrived from the source. If a normal to the source is $\begin{bmatrix} -p_s & -q_s & 1 \end{bmatrix}^T$ then the gradient $(p_s q_s)$ can be used to specify the direction of the source (Figure 7-11).

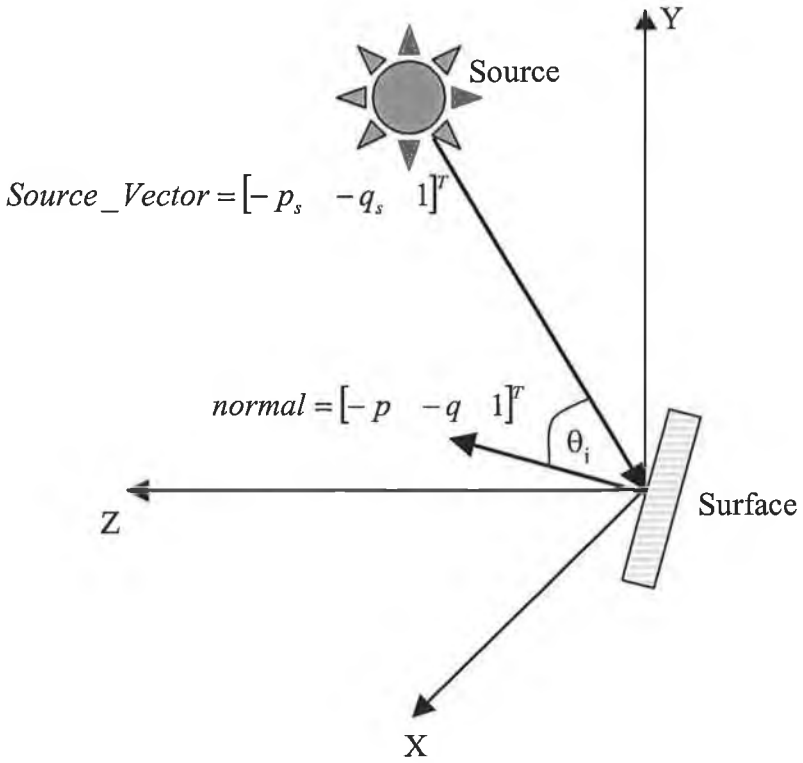

Figure 7-11 – Vector Representation of surface normal and illumination source

Taking the dot product of these two vectors, an expression for $Cos\theta_i$ can be established.

Equation 7-12 - $$Cos\theta_i = \frac{1 + pp_s + qq_s}{\sqrt{1 + p^2 + q^2}\sqrt{1 + {p_s}^2 + q_s^2}}$$

Image irradiance is proportional to a number of constants such as the focal length of the lens and the radiance of the source. So the reflectance map is a constant times the surface orientation.

Equation 7-13 - $$R(p,q) = K\left[\frac{1 + pp_s + qq_s}{\sqrt{1 + p^2 + q^2}\sqrt{1 + {p_s}^2 + q_s^2}}\right]$$

The reflectance map can be plotted as a series of iso-brightness contours in gradient space. Each contour represents a different intensity value. Using the reflectance map, the basic equation describing the image forming process can be expressed as:

Equation 7-14 - $I(x,y) = R(p,q)$ **[63]**

Where $I(x,y)$ is the intensity of an image pixel. So given a reflectance map, a unique value of image intensity can be determined from a known surface orientation. This is quite useful for computer graphics and computer simulation. However, retrieving surface orientation from a single irradiance value is not as simple. Since irradiance only has one degree of freedom and surface orientation has two (p,q), surface orientations can only be determined in unique cases, e.g. $R(p,q) = 1$ and $(p,q) = (p_s,q_s)$ for a Lambertian surface. For this reason, two images are required in order to find a particular orientation at a point.

With two images there will be two different reflectance maps obtained:

Equation 7-15 - $R_1(p,q) = E_1$

Equation 7-16 - $R_2(p,q) = E_2$

Since there are two different light sources there will be two different vectors:

Equation 7-17 - $s_1 = \begin{pmatrix} p_1 & q_1 & -1 \end{pmatrix}^T$

Equation 7-18 - $s_2 = \begin{pmatrix} p_2 & q_2 & -1 \end{pmatrix}^T$

If the reflectance map equations are linear and independent, there will be a unique solution for p and q; however, if they are quadratic or cubic there will be more that one solution, as is the case with a Lambertian surface. For the sake of simplicity the reflectance maps are assumed to be:

$$R_1(p,q) = \sqrt{\frac{1 + p_1 p + q_1 q}{r_1}} \quad \text{And} \quad R_2(p,q) = \sqrt{\frac{1 + p_2 p + q_2 q}{r_2}}$$

Where:

$$r_1 = \sqrt{1 + p_1^2 + q_1^2} \quad \text{And} \quad r_2 = \sqrt{1 + p_2^2 + q_2^2}$$

Combining the two-reflectance map functions yields a unique value for the surface gradients across the entire wafer.

$$p = \frac{\left(E_1^2 r_1 - 1\right)q_2 - \left(E_1^2 r_2 - 1\right)q_1}{p_1 q_2 - q_1 p_2} \;,\; q = \frac{\left(E_2^2 r_2 - 1\right)p_1 - \left(E_2^2 r_1 - 1\right)p_2}{p_1 q_2 - q_1 p_2}$$

It has been shown that the light collected at the camera, the irradiance, can be related to the scene radiance. So since the scene radiance and the vector to the light source are known, the surface gradients can be calculated for each point in an image. If the surface gradients can be determined, the 3-D surface orientation can then also be determined.

Appendix 5 –Detailed drawings of final design

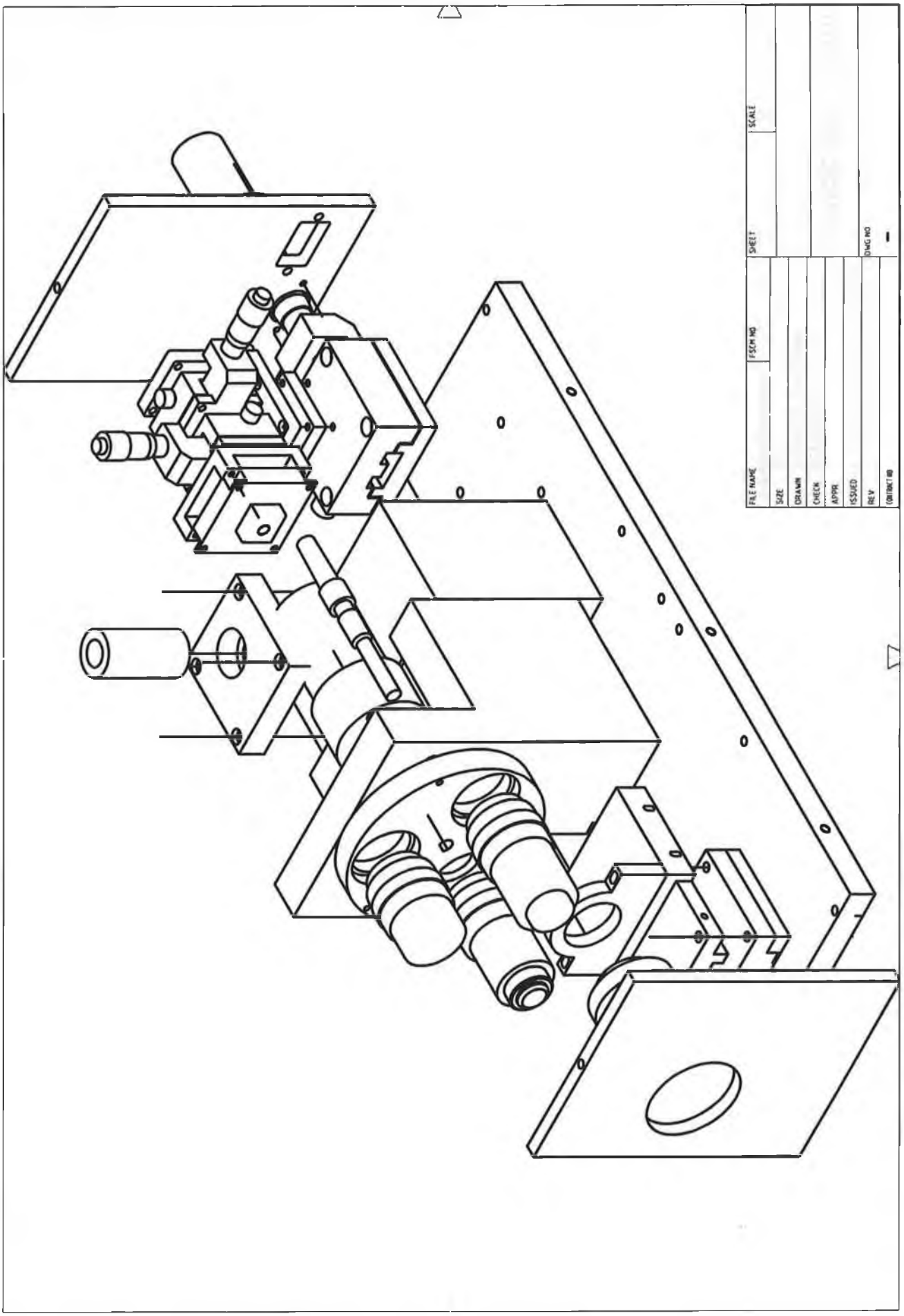

Figure 7-1 - Front left exploded view of final design

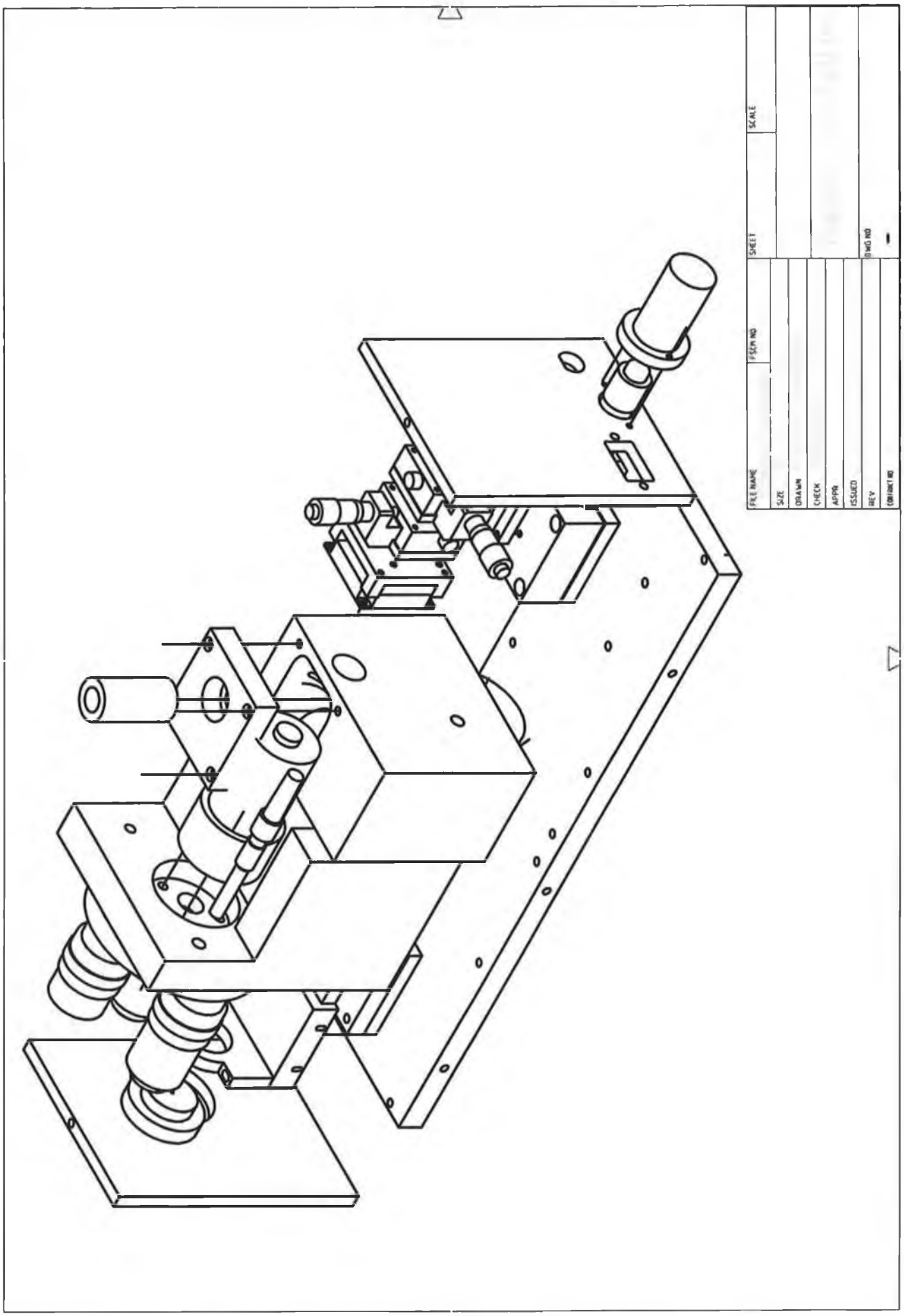

Figure 7-2 - Back left exploded view of final design

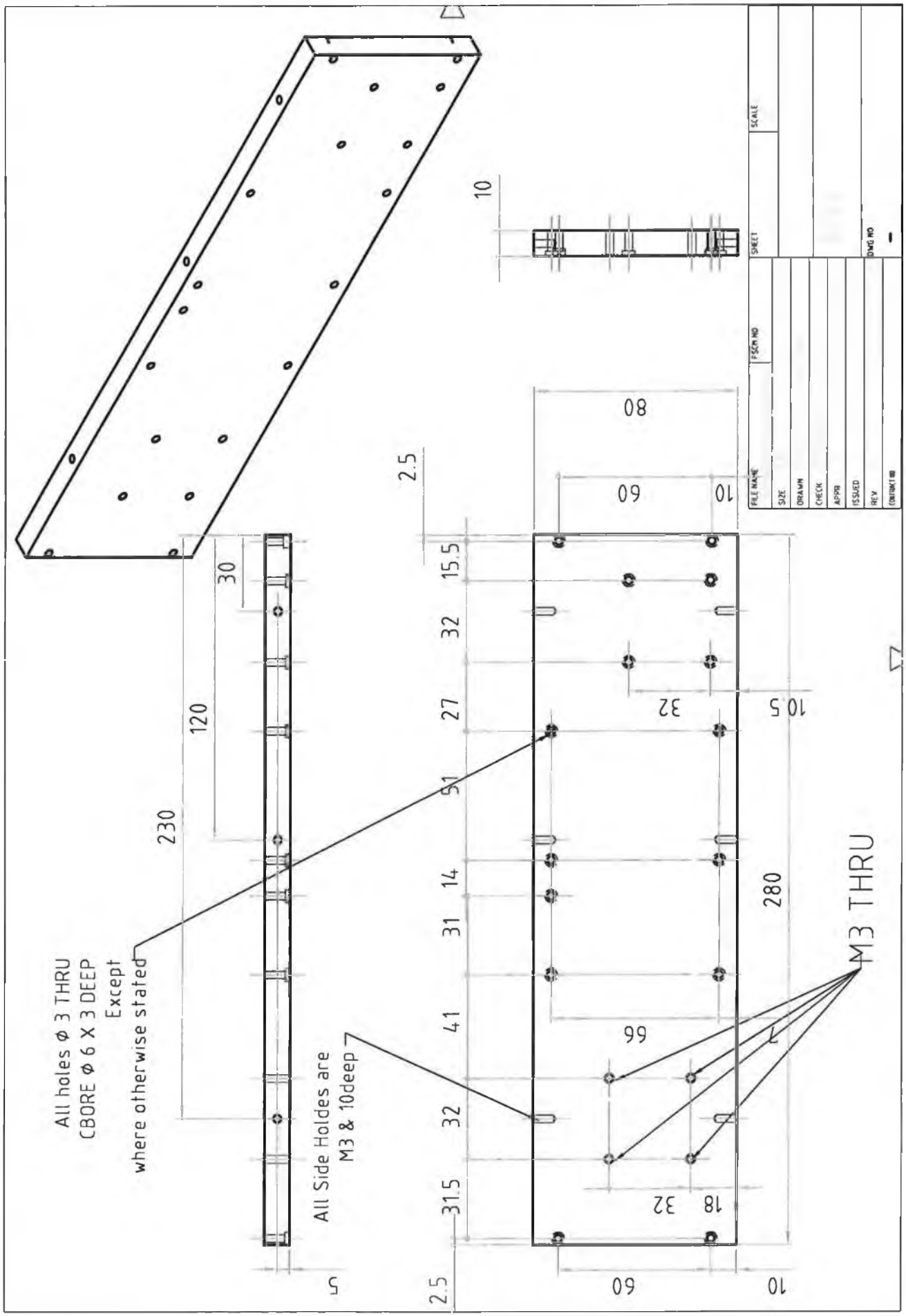

Figure 7-3 – Detailed drawing of Base

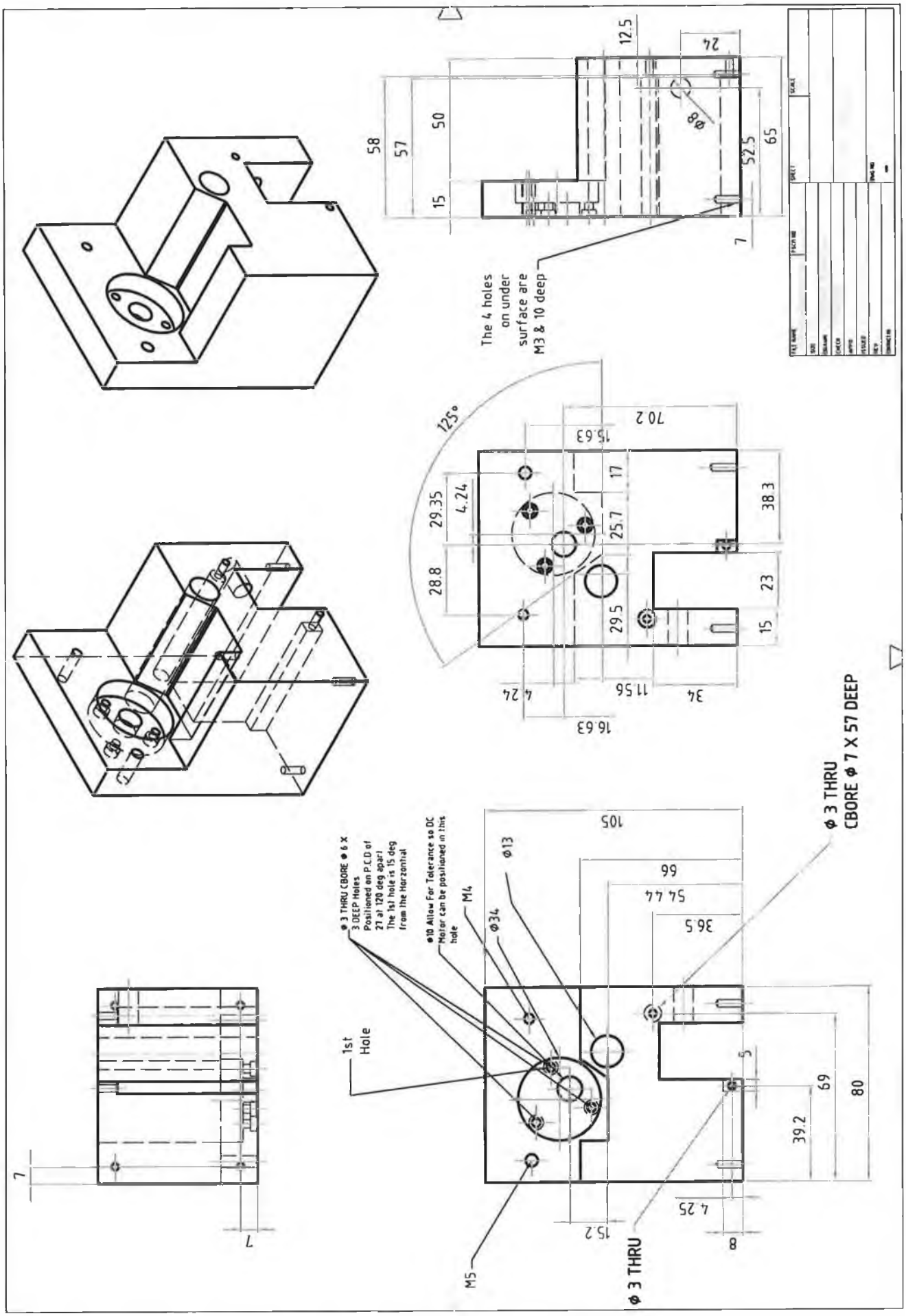

Figure 7-4 – Detailed drawing of Front optical system block

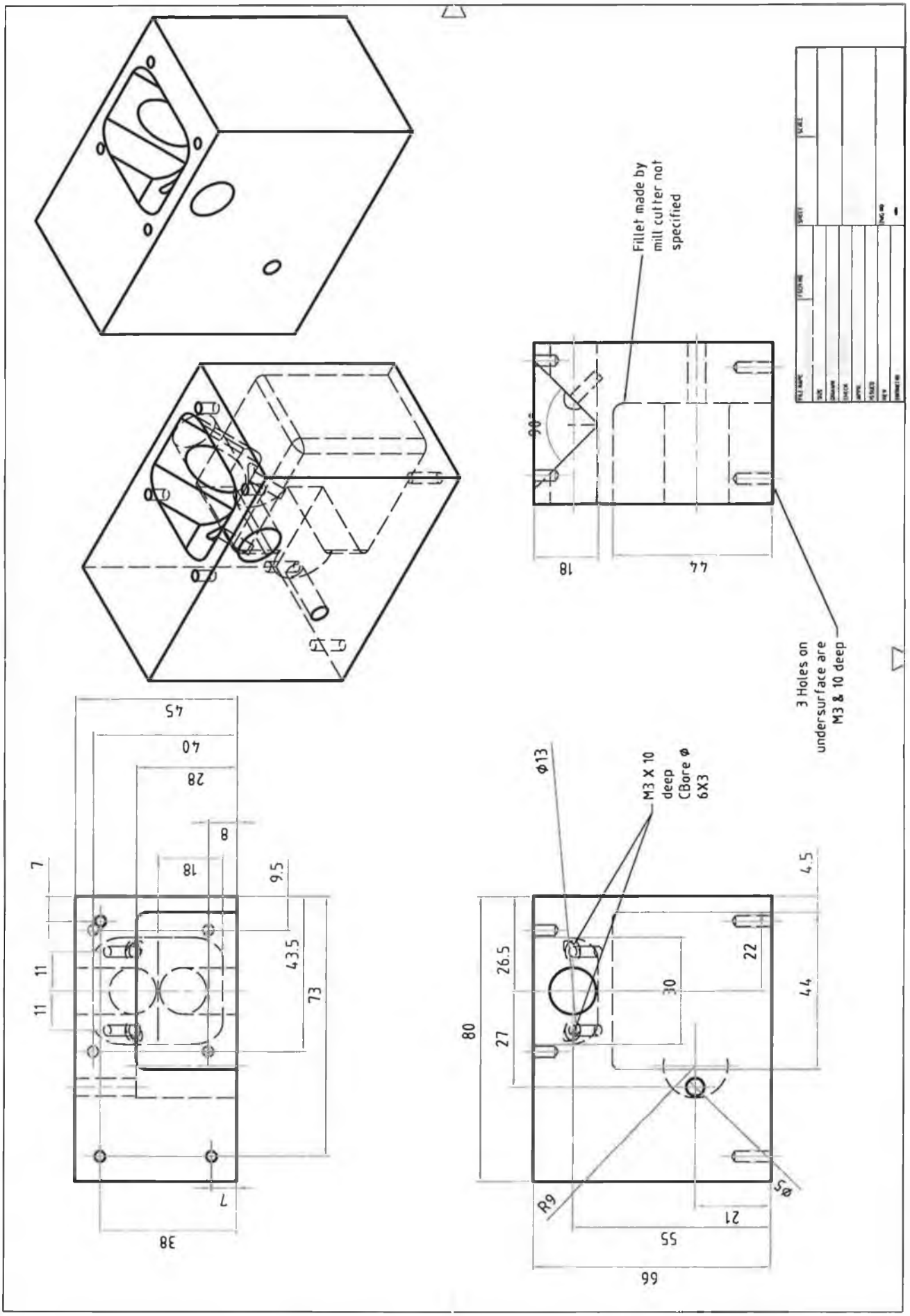

Figure 7-5 – Detailed drawing of back illumination system block

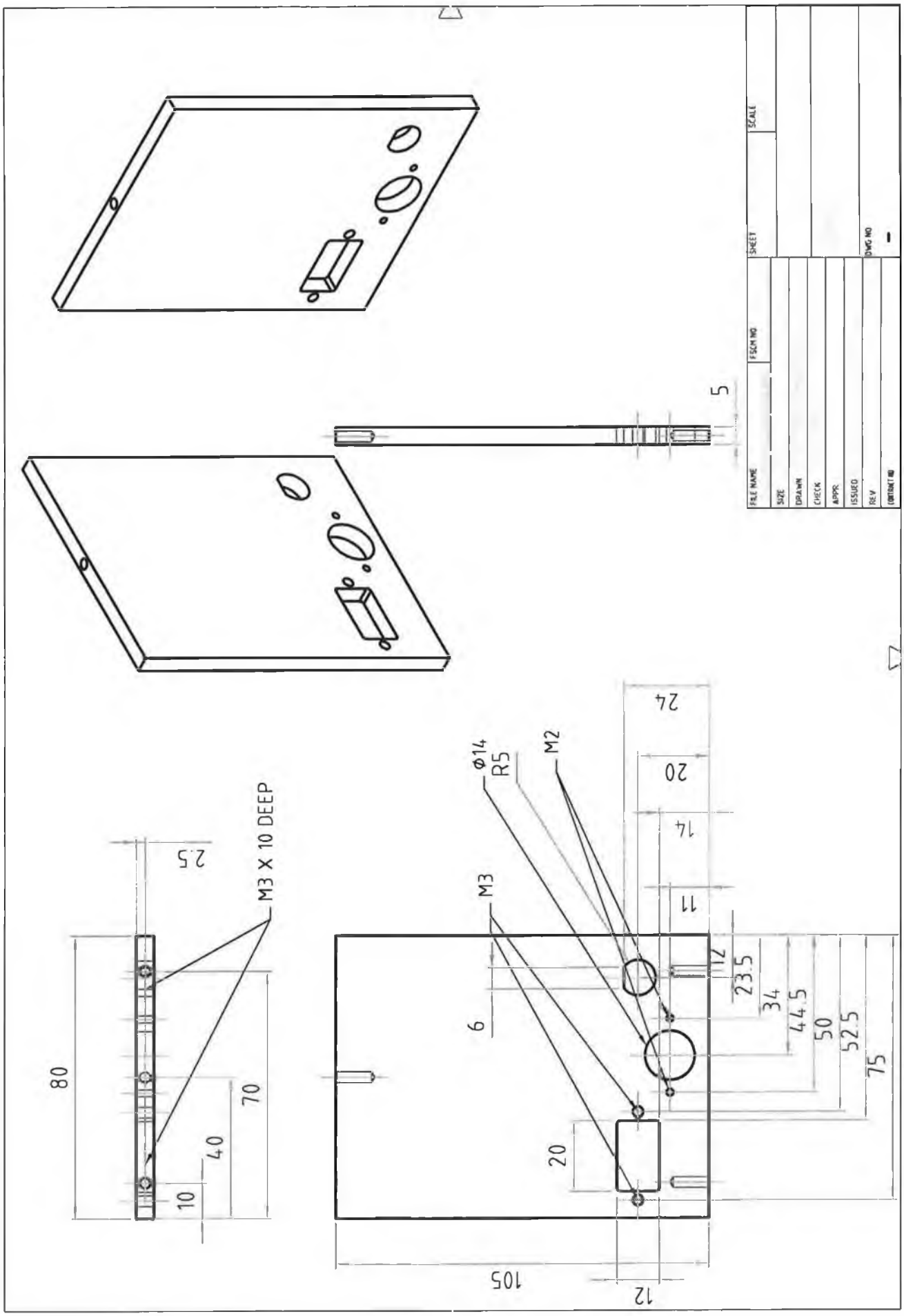

Figure 7-6 – Detailed drawing of back frame

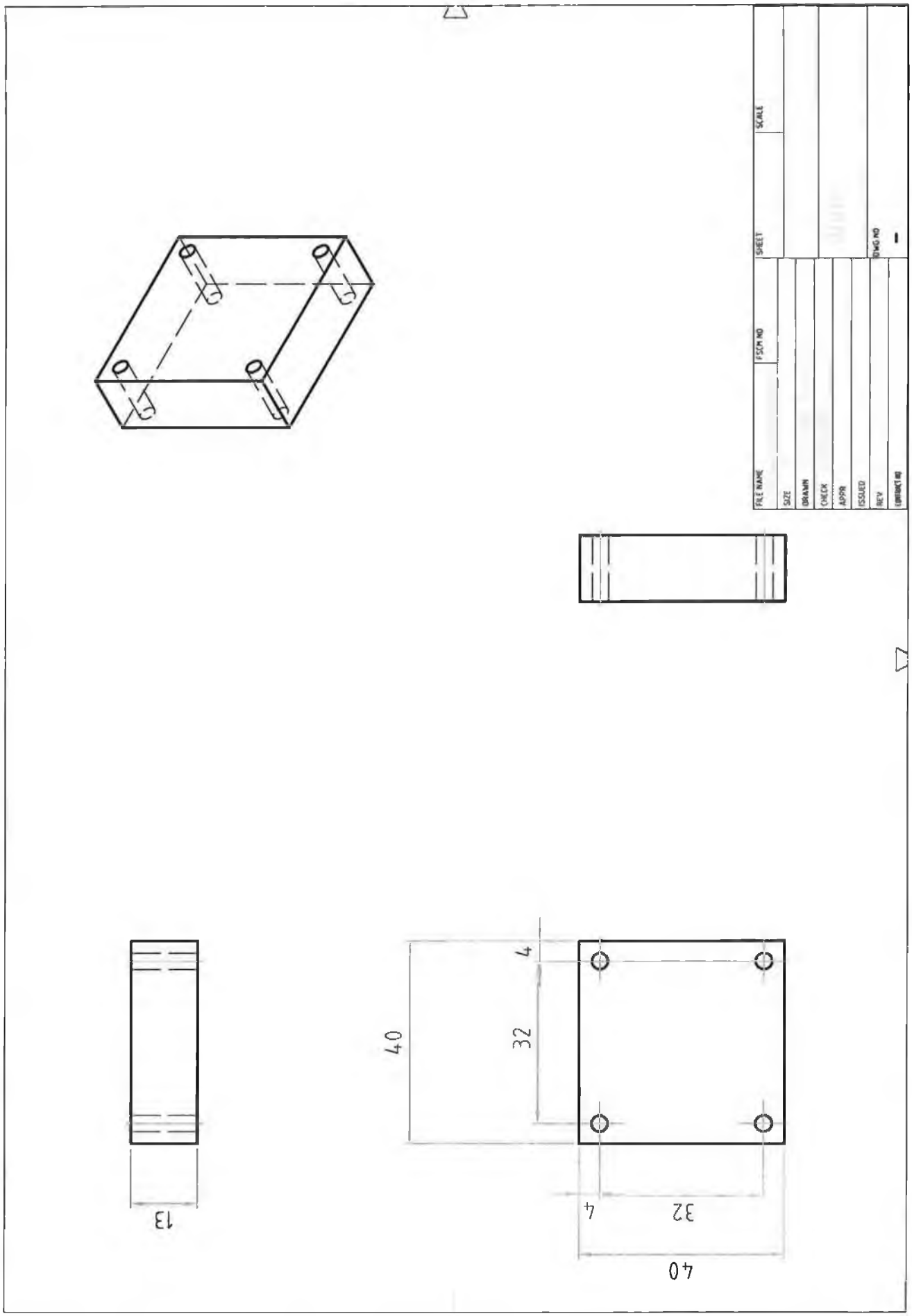

Figure 7-7 – Detailed drawing of Focusing Stage mounting block

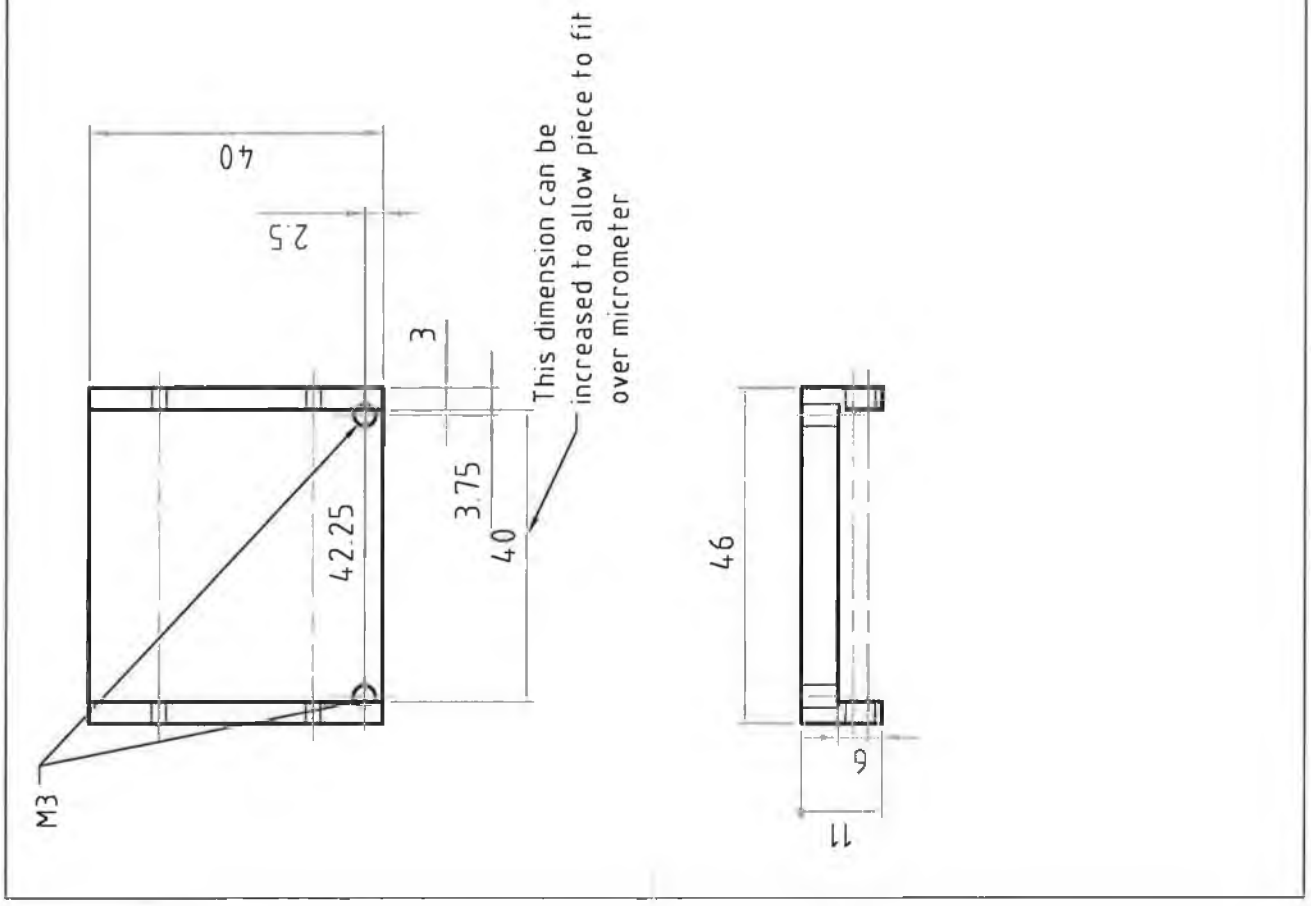

Figure 7-8 – Detailed drawing of Fibre connector holder base

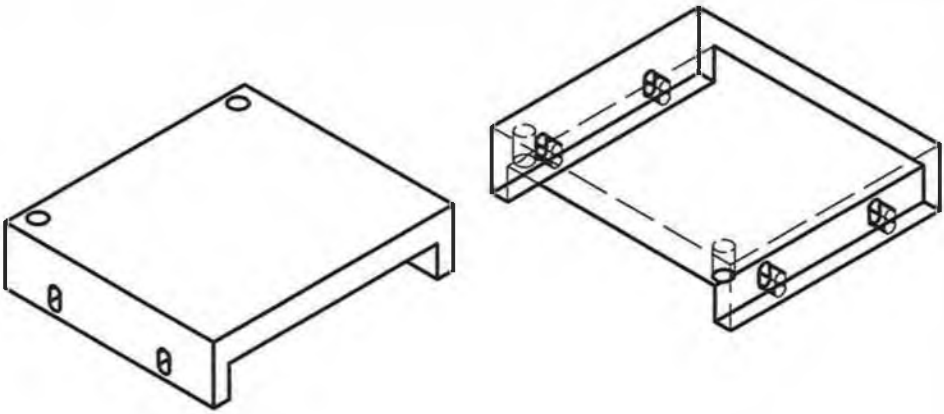

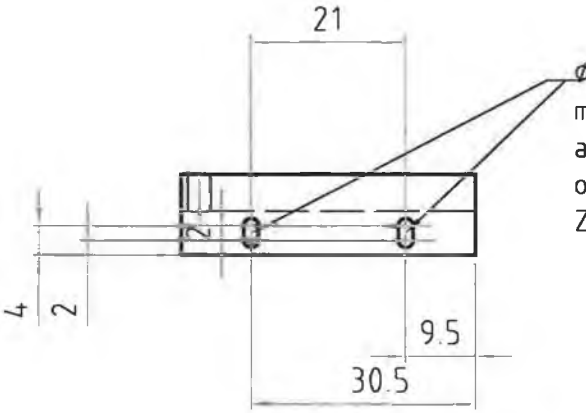

Ø2. Holes to be made oversized to allow for alignment of connector in the Z-Axis

FILE NAME	FSCM NO	SHEET	SCALE
SIZE			
DRAWN			
CHECK			
APPR.			
ISSUED			
REV		DWG NO	
CONTRACT NO		–	

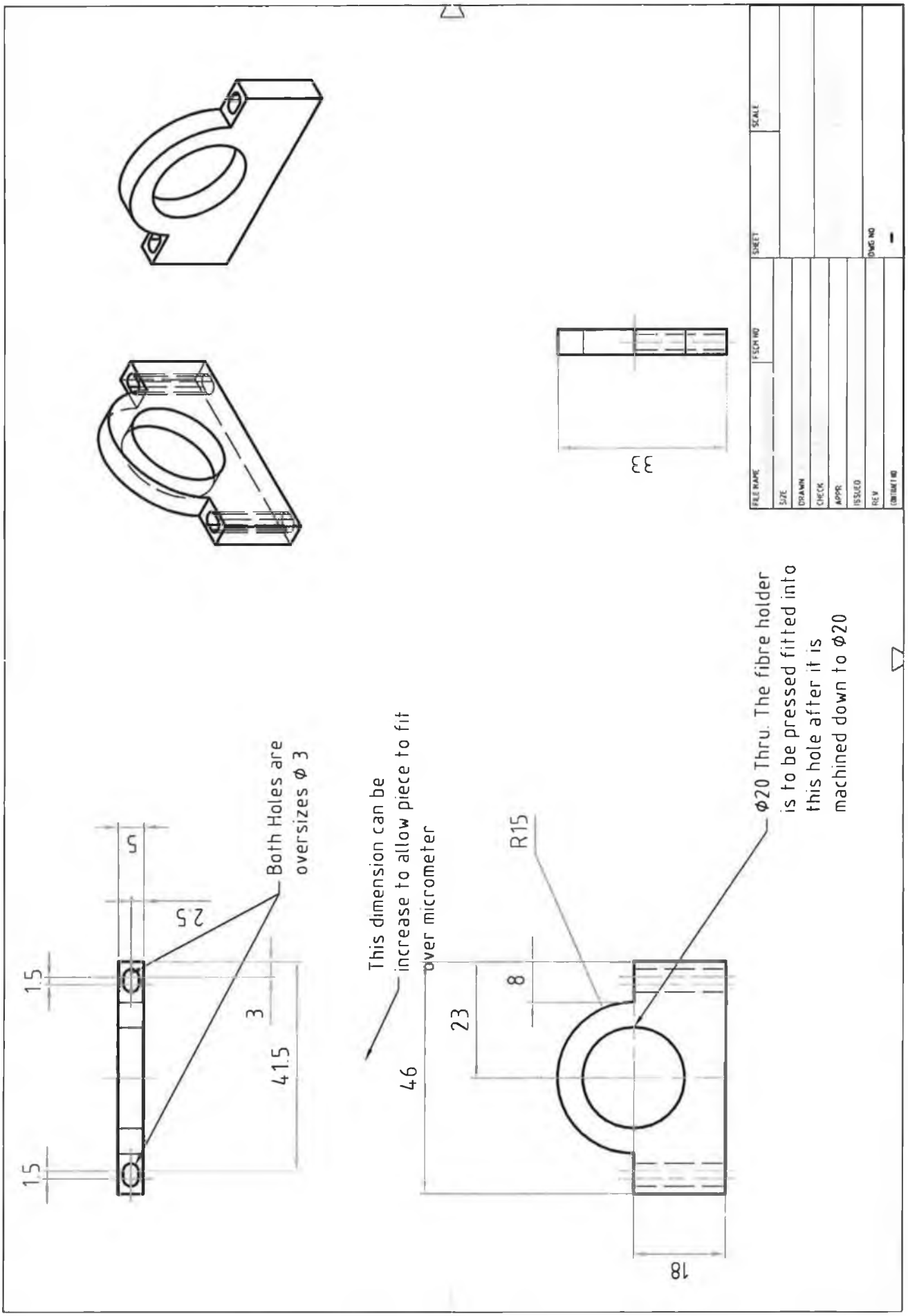

Figure 7-9 – Detailed drawing of fibre connector holder

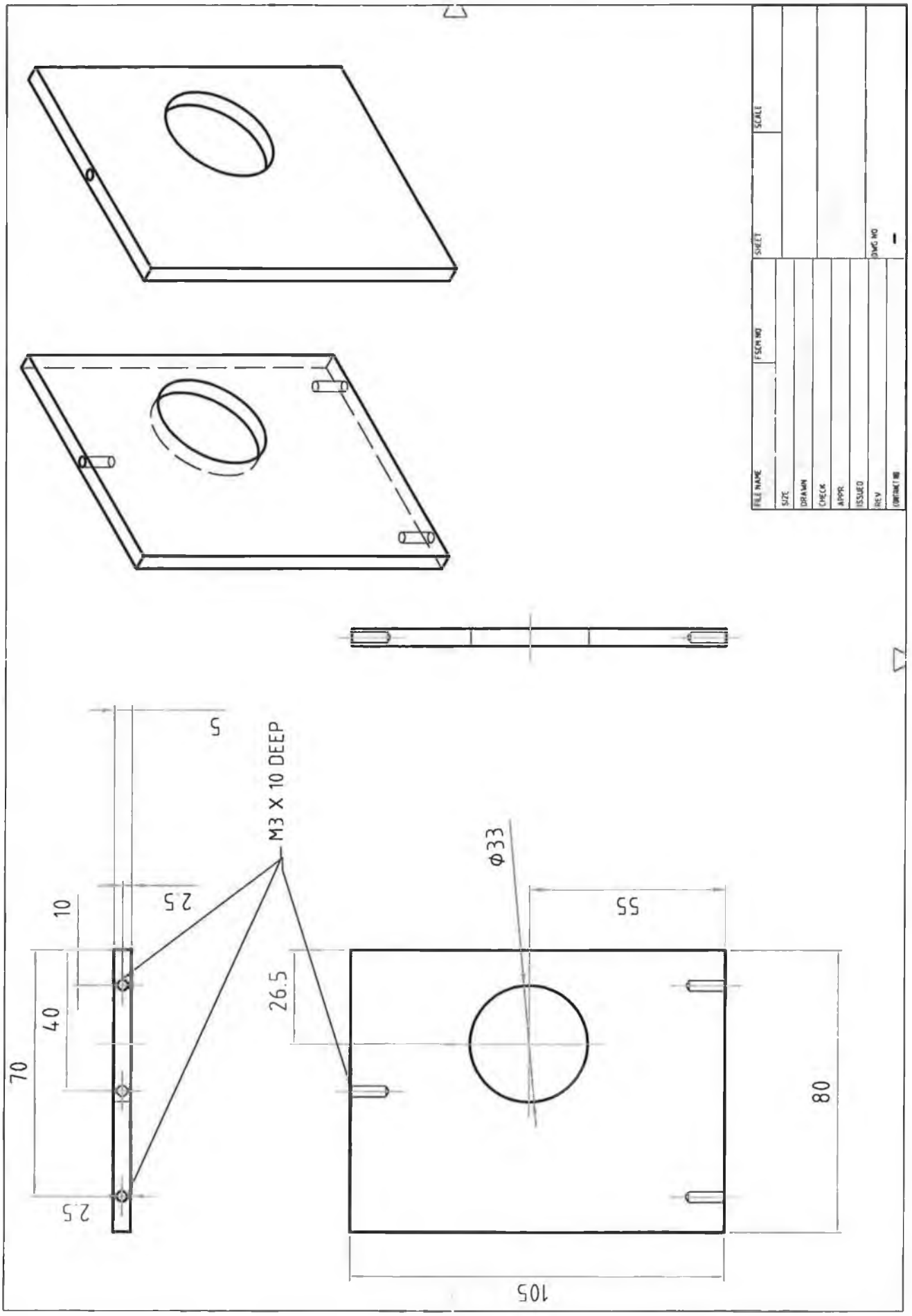

Figure 7-10 – Detailed drawing of Front frame

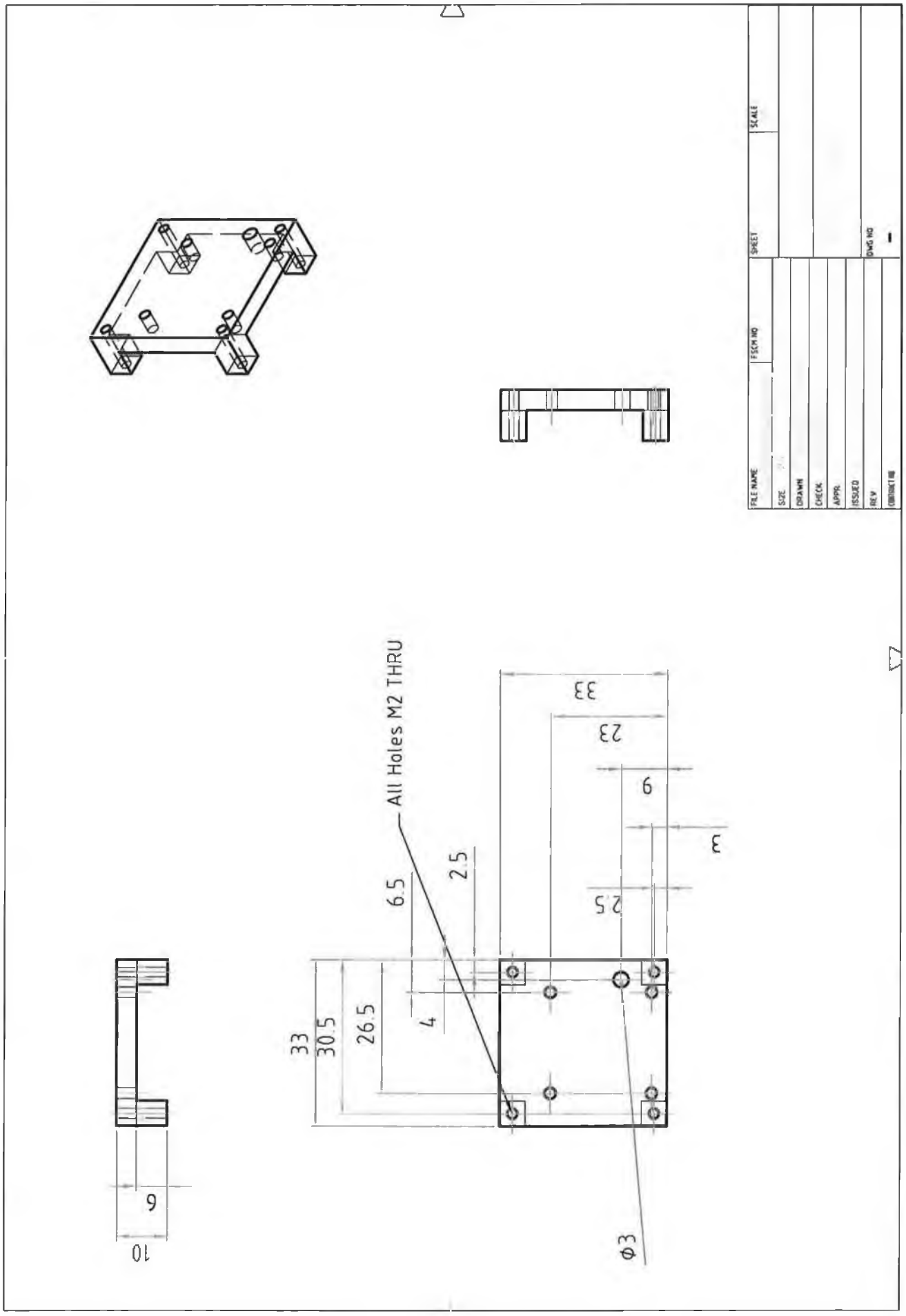

Figure 7-11 – Detailed drawing of CCD Holder

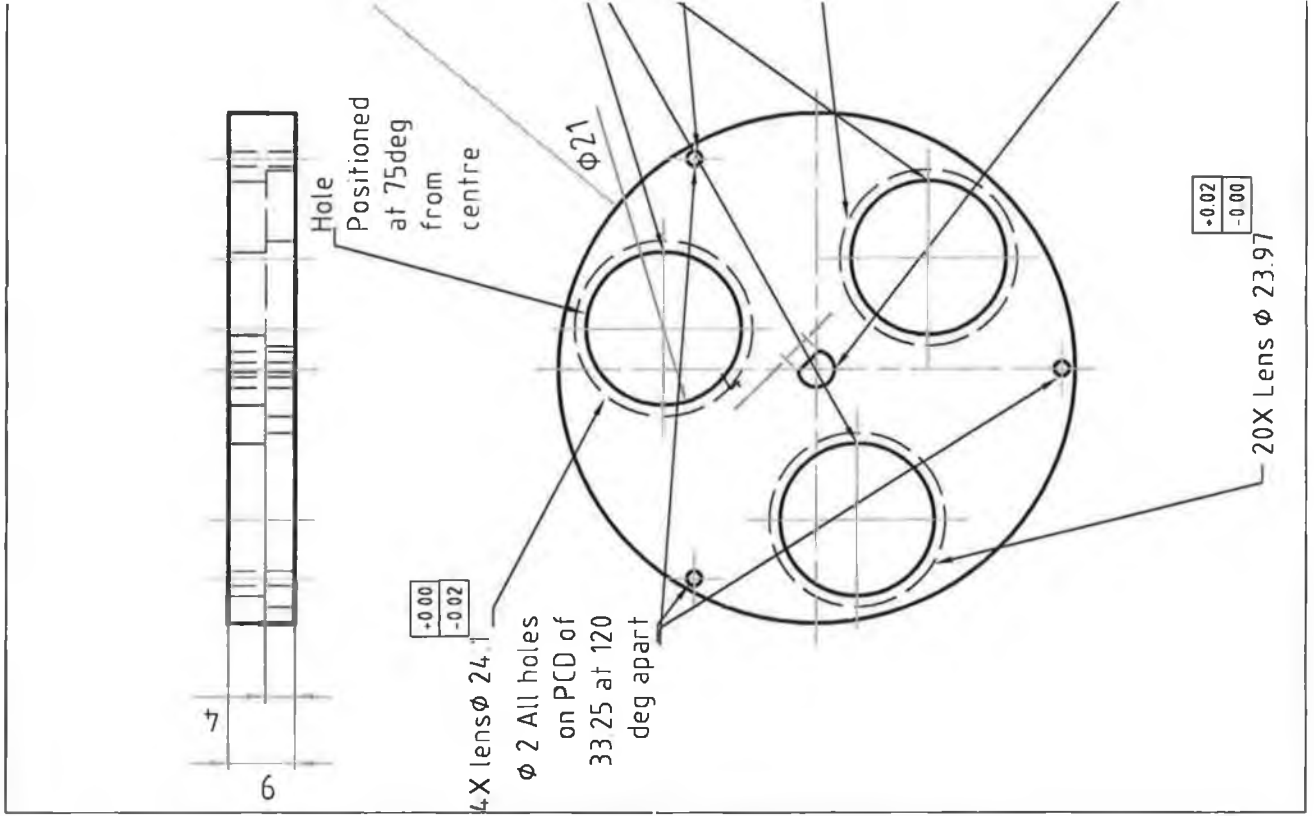

Figure 7-12 – Detailed drawing of Lens holder and exchange system

Φ70

Φ21.6X36TPI Holes on PCD of 21.5 at 120 deg apart

Hole Positioned at 30 deg from centre

+0.02
-0.00

40X lens Φ 24.02

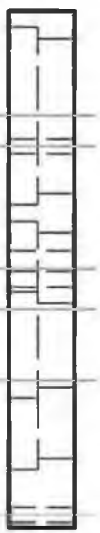

Φ 5 toleranced so DC motor can be pressed fitted on

FILE NAME	FSCM NO	SHEET	SCALE
SIZE			
DRAWN			
CHECK			
APPR			
ISSUED			
REV		DWG NO	
CONTRACT NO		—	

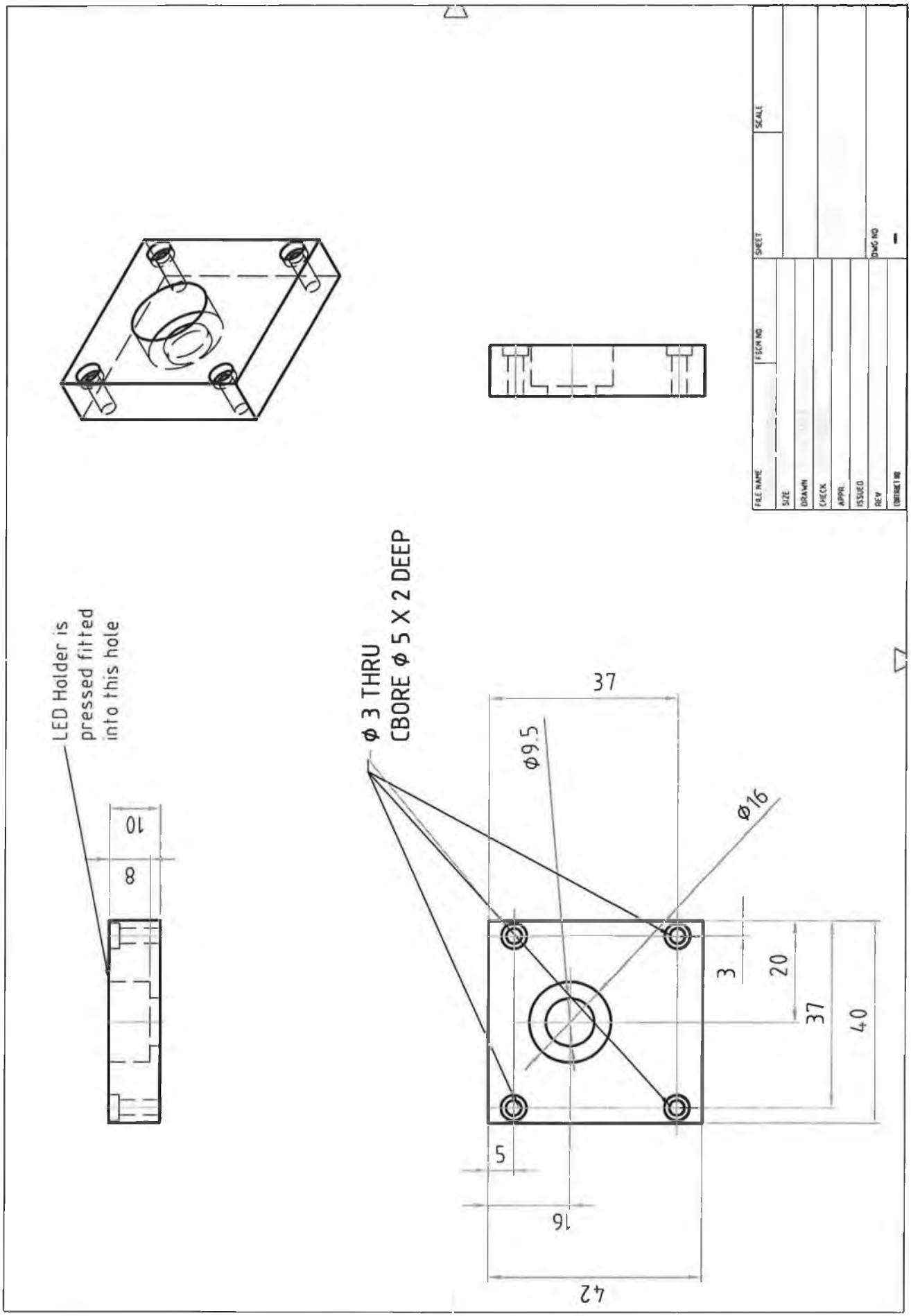

Figure 7-13 – Detailed drawing of LED Holder

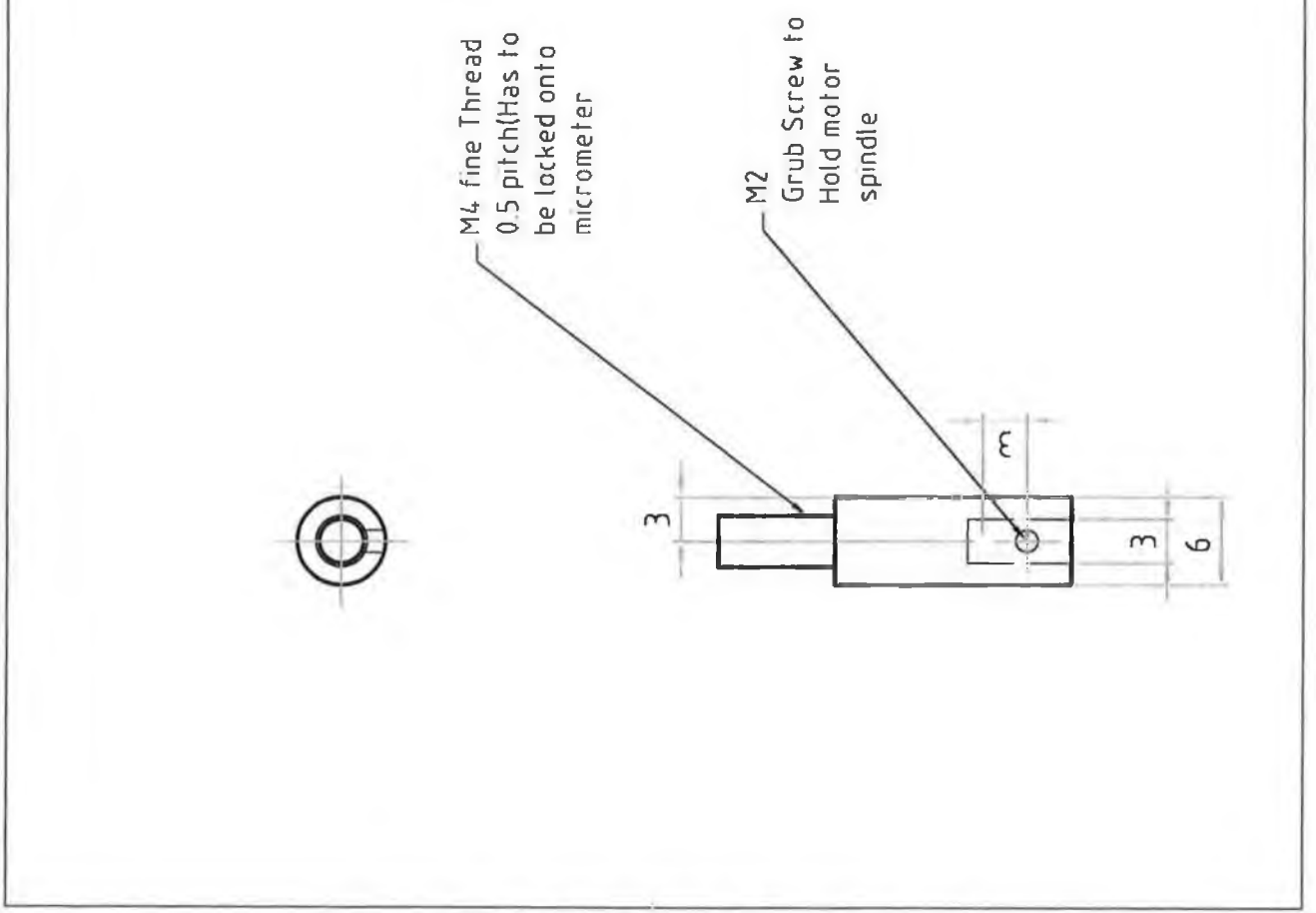

Figure 7-14 – Detailed drawing of Motor Connector

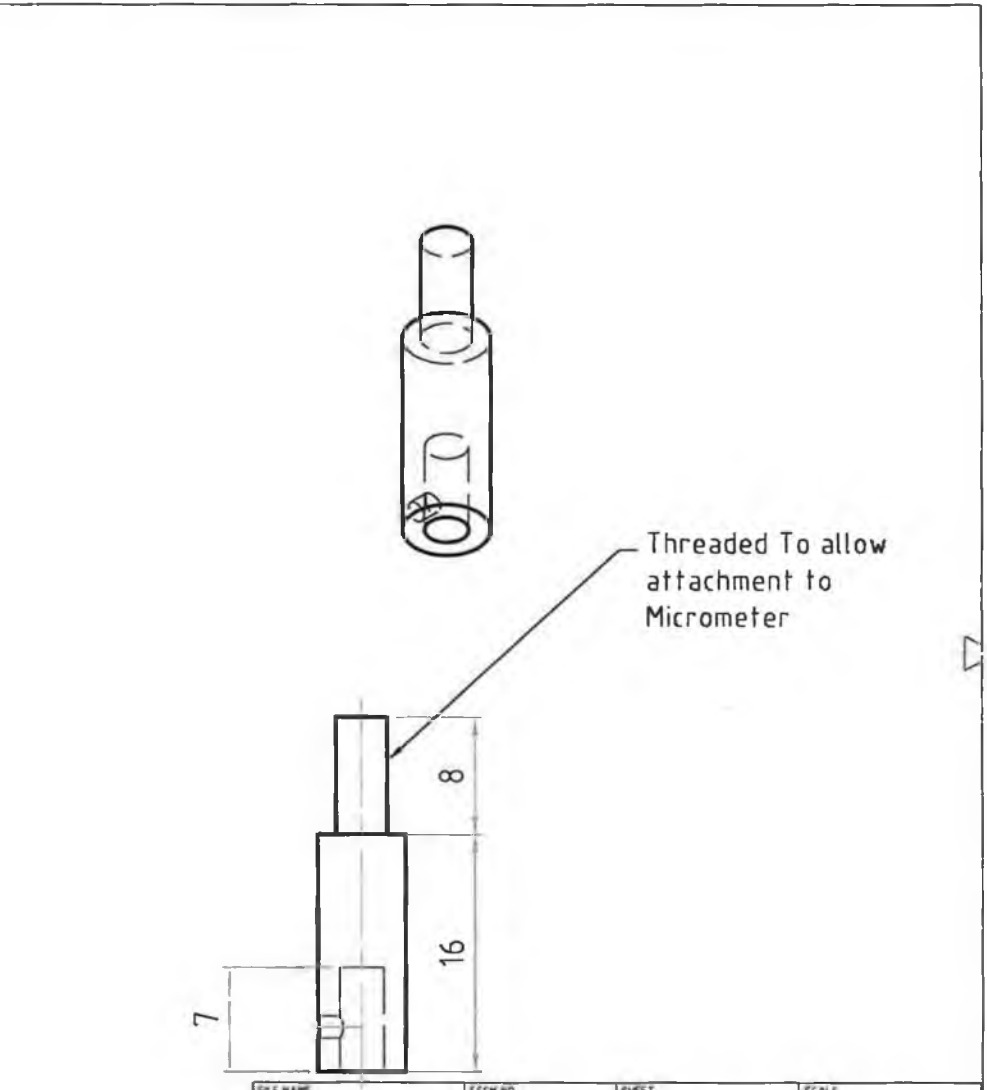

FILE NAME	FSCM NO	SHEET	SCALE
SIZE			
DRAWN			
CHECK			
APPR			
ISSUED			
REV		DWG NO	
CONTRACT NO		–	

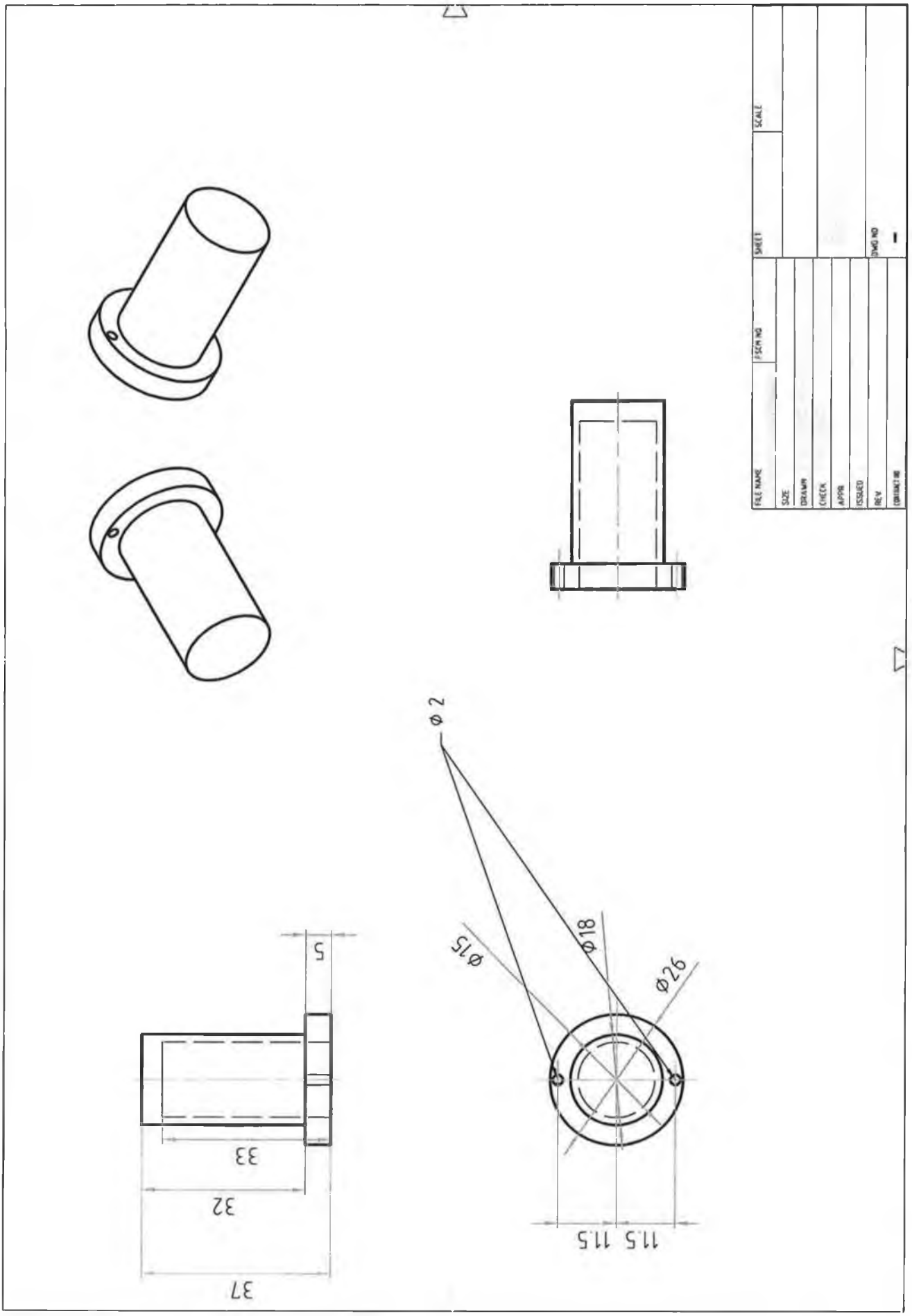

Figure 7-15 – Detailed drawing of back cover